

# Climate change projections and impacts for the Bay of Plenty Region

*Prepared for Bay of Plenty Regional Council*

*October 2019*

Prepared by:

Petra Pearce  
Nava Fedaeff  
Brett Mullan  
Stephen Stuart  
Abha Sood  
Gregor Macara




For any information regarding this report please contact:

Petra Pearce  
Manager – Climate, Atmosphere and Hazards  
+64-9-375 2052  
petra.pearce@niwa.co.nz

National Institute of Water & Atmospheric Research Ltd  
Private Bag 99940  
Viaduct Harbour  
Auckland 1010

Phone +64 9 375 2050

NIWA CLIENT REPORT No: 2019218AK  
Report date: October 2019  
NIWA Project: BOP19101

Quality Assurance Statement		
	Reviewed by:	Dr Sam Dean Principal Scientist – Climate NIWA Wellington
	Formatting checked by:	Petra Pearce
	Approved for release by:	Dr Andrew Tait Chief Scientist – Climate, Atmosphere and Hazards NIWA Wellington

© All rights reserved. This publication may not be reproduced or copied in any form without the permission of the copyright owner(s). Such permission is only to be given in accordance with the terms of the client's contract with NIWA. This copyright extends to all forms of copying and any storage of material in any kind of information retrieval system.

Whilst NIWA has used all reasonable endeavours to ensure that the information contained in this document is accurate, NIWA does not give any express or implied warranty as to the completeness of the information contained herein, or that it will be suitable for any purpose(s) other than those specifically contemplated during the Project or agreed by NIWA and the Client.

# Contents

- Executive summary ..... 11**
- 1 Introduction ..... 13**
  - 1.1 Global and New Zealand climate change..... 15
  - 1.2 Year to year climate variability and climate change..... 17
  - 1.3 Representative Concentration Pathways ..... 21
  - 1.4 Climate modelling methodology ..... 23
- 2 Current and future climate of the Bay of Plenty Region..... 24**
- 3 Temperature ..... 24**
  - 3.1 Mean temperature ..... 24
  - 3.2 Maximum temperature ..... 30
  - 3.3 Minimum temperature ..... 36
  - 3.4 Diurnal temperature range..... 42
  - 3.5 Hot days ..... 48
  - 3.6 Extreme hot days ..... 52
  - 3.7 Heatwave days..... 54
  - 3.8 Frost days..... 56
  - 3.9 Growing degree days ..... 60
- 4 Rainfall and Drought ..... 63**
  - 4.1 Rainfall ..... 63
  - 4.2 Wet days ..... 69
  - 4.3 Heavy rain days..... 76
  - 4.4 99<sup>th</sup> percentile of daily rainfall..... 82
  - 4.5 Maximum 1-day rainfall..... 84
  - 4.6 Maximum 5-day rainfall..... 86
  - 4.7 Extreme, rare rainfall events (HIRDS v4) ..... 89
  - 4.8 Dry days ..... 90
  - 4.9 Potential Evapotranspiration Deficit ..... 97
  - 4.10 Soil moisture deficit ..... 99
- 5 Wind and other variables ..... 106**
  - 5.1 Mean wind speed ..... 106

5.2	Windy days.....	110
5.3	99 <sup>th</sup> percentile of mean wind speed .....	111
5.4	Surface solar radiation.....	112
5.5	Relative humidity .....	116
<b>6</b>	<b>Projections for storms affecting the Bay of Plenty.....</b>	<b>122</b>
6.1	Model simulations .....	122
6.2	Identifying storm tracks.....	124
6.3	Characteristics of storm track changes.....	127
6.4	Changes in Wet Spell Rainfalls.....	134
6.5	Conclusions .....	137
<b>7</b>	<b>Climate change impacts for the Bay of Plenty Region .....</b>	<b>139</b>
<b>8</b>	<b>Impacts of sea-level rise .....</b>	<b>139</b>
8.1	Ministry for the Environment coastal hazards and climate change guidance .....	139
8.2	Bay of Plenty sea-level rise, coastal erosion and inundation .....	148
8.3	More extreme SLR projections - Hansen et al. (2016).....	151
<b>9</b>	<b>Impacts on biosecurity and pests.....</b>	<b>152</b>
9.1	Terrestrial biosecurity.....	152
9.2	Aquatic biosecurity .....	154
<b>10</b>	<b>Impacts of drought and future pasture growth .....</b>	<b>155</b>
<b>11</b>	<b>Impacts on horticulture.....</b>	<b>156</b>
<b>12</b>	<b>Impacts on forestry.....</b>	<b>159</b>
<b>13</b>	<b>Impacts on health .....</b>	<b>160</b>
13.1	Direct health impacts.....	161
13.2	Indirect health impacts .....	161
<b>14</b>	<b>Summary and conclusions .....</b>	<b>163</b>
<b>15</b>	<b>Glossary of abbreviations and terms .....</b>	<b>167</b>
<b>Appendix A</b>	<b>Climate modelling methodology .....</b>	<b>170</b>
<b>16</b>	<b>References.....</b>	<b>172</b>

## Tables

Table 1-1:	Projected change in global mean surface air temperature for the mid- and late-21st century relative to the reference period of 1986-2005 for different RCPs.	22
Table 3-1:	Modelled annual average number of hot days (maximum temperature >25°C) for the historic period and two climate change scenarios (RCP4.5 and RCP8.5) at two future time periods.	51
Table 3-2:	Modelled annual average number of frost days (minimum temperature <0°C) for historic and two climate change scenarios (RCP4.5 and RCP8.5) at two future time periods.	59
Table 4-1:	Modelled annual average rainfall for historic and two climate change scenarios (RCP4.5 and RCP8.5) at two future time periods.	69
Table 4-2:	Modelled annual average number of heavy rain days (>25 mm) for historic and two climate change scenarios (RCP4.5 and RCP8.5) at two future time periods.	82
Table 4-3:	Historic rainfall depths for a 1:50 year return period, 24 hour duration event (millimetres) and projected changes to the return period of this size event under two climate change scenarios at two future time periods. Data source: HIRDS v4 ( <a href="http://www.hirds.niwa.co.nz">www.hirds.niwa.co.nz</a> )	90
Table 4-4:	Historic rainfall depths for a 1:100 year return period, 24 hour duration event (millimetres) and projected changes to the return period of this size event under two climate change scenarios at two future time periods. Data source: HIRDS v4 ( <a href="http://www.hirds.niwa.co.nz">www.hirds.niwa.co.nz</a> )	90
Table 6-1:	Total number of identified Wet Spells (25mm or more on “Day 0”) over a 20-year period, per model and scenario/period.	127
Table 6-3:	Numbers of ex-tropical storms summed over all six GCMs, by month and scenario/period, producing heavy rainfall in the Bay of Plenty region.	131
Table 8-1:	Approximate years, from possible earliest to latest, when specific SLR increments (metres above 1986-2005 baseline) could be reached for various projection scenarios of SLR for the wider New Zealand region.	148
Table 8-2:	SLR projections (metres above 1986–2005 baseline MSL) in 2070 and 2130 for the wider New Zealand region.	149
Table 8-3:	SLR projections (metres above MVD–53) in 2070 and 2130 for the Bay of Plenty region.	149

## Figures

Figure 1-1:	The Bay of Plenty Region administered by the Bay of Plenty Regional Council.	14
Figure 1-2:	New Zealand national temperature series, 1909-2018.	16
Figure 1-3:	Average summer percentage of normal rainfall during El Niño (left) and La Niña (right).	18
Figure 1-4:	New Zealand Temperature - historical record and an illustrative schematic projection illustrating future year-to-year variability.	20
Figure 1-5:	CMIP5 multi-model simulated time series from 1950-2100 for change in global annual mean surface temperature relative to 1986-2005.	22
Figure 3-1:	Modelled annual and seasonal mean temperature, average over 1986-2005.	25

Figure 3-2:	Projected annual and seasonal mean temperature changes by 2040 for RCP4.5.	26
Figure 3-3:	Projected annual and seasonal mean temperature changes by 2040 for RCP8.5.	27
Figure 3-4:	Projected annual and seasonal mean temperature changes by 2090 for RCP4.5.	28
Figure 3-5:	Projected annual and seasonal mean temperature changes by 2090 for RCP8.5.	29
Figure 3-6:	Modelled annual and seasonal mean maximum temperature, average over 1986-2005.	31
Figure 3-7:	Projected annual and seasonal mean maximum temperature changes by 2040 for RCP4.5.	32
Figure 3-8:	Projected annual and seasonal mean maximum temperature changes by 2040 for RCP8.5.	33
Figure 3-9:	Projected annual and seasonal mean maximum temperature changes by 2090 for RCP4.5.	34
Figure 3-10:	Projected annual and seasonal mean maximum temperature changes by 2090 for RCP8.5.	35
Figure 3-11:	Modelled annual and seasonal mean minimum temperature, average over 1986-2005.	37
Figure 3-12:	Projected annual and seasonal mean minimum temperature changes by 2040 for RCP4.5.	38
Figure 3-13:	Projected annual and seasonal mean minimum temperature changes by 2040 for RCP8.5.	39
Figure 3-14:	Projected annual and seasonal mean minimum temperature changes by 2090 for RCP4.5.	40
Figure 3-15:	Projected annual and seasonal mean minimum temperature changes by 2090 for RCP8.5.	41
Figure 3-16:	Modelled annual and seasonal mean diurnal temperature range, average over 1986-2005.	43
Figure 3-17:	Projected annual and seasonal diurnal temperature range changes by 2040 for RCP4.5.	44
Figure 3-18:	Projected annual and seasonal diurnal temperature range changes by 2040 for RCP8.5.	45
Figure 3-19:	Projected annual and seasonal diurnal temperature range changes by 2090 for RCP4.5.	46
Figure 3-20:	Projected annual and seasonal diurnal temperature range changes by 2090 for RCP8.5.	47
Figure 3-21:	Modelled annual number of hot days (days with maximum temperature >25°C), average over 1986-2005.	49
Figure 3-22:	Projected annual hot day (maximum temperature >25°C) changes for RCP4.5 and RCP8.5, by 2040 and 2090.	50
Figure 3-23:	Historic and future projected numbers of hot days for locations in the Bay of Plenty.	52
Figure 3-24:	Modelled annual number of extreme hot days (days with maximum temperature >30°C), average over 1986-2005.	53

Figure 3-25:	Projected annual extreme hot day (maximum temperature >30°C) changes for RCP4.5 and RCP8.5, by 2040 and 2090.	54
Figure 3-26:	Modelled annual number of heatwave days (≥ three consecutive days with maximum temperatures > 25°C), average over 1986-2005.	55
Figure 3-27:	Projected annual heatwave day (≥ three consecutive days with maximum temperatures > 25°C) changes for RCP4.5 and RCP8.5, by 2040 and 2090.	56
Figure 3-28:	Modelled annual number of frost days (daily minimum temperature <0°C), average over 1986-2005.	57
Figure 3-29:	Projected annual frost day (minimum temperature <0°C) changes for RCP4.5 and RCP8.5, by 2040 and 2090.	58
Figure 3-30:	Historic and future projected numbers of frost days for locations in the Bay of Plenty.	60
Figure 3-31:	Modelled annual number of growing degree days (base 10°C), average over 1986-2005.	61
Figure 3-32:	Projected annual growing degree-day (base 10°C) changes for RCP4.5 and RCP8.5, by 2040 and 2090.	62
Figure 4-1:	Modelled annual and seasonal rainfall (mm), average over 1986-2005.	64
Figure 4-2:	Projected annual and seasonal mean rainfall changes by 2040 for RCP4.5.	65
Figure 4-3:	Projected annual and seasonal mean rainfall changes by 2040 for RCP8.5.	66
Figure 4-4:	Projected annual and seasonal mean rainfall changes by 2090 for RCP4.5.	67
Figure 4-5:	Projected annual and seasonal mean rainfall changes by 2090 for RCP8.5.	68
Figure 4-6:	Modelled annual and seasonal number of wet days (daily rainfall >1mm), average over 1986-2005.	71
Figure 4-7:	Projected annual and seasonal wet day (>1mm rain) changes by 2040 for RCP4.5.	72
Figure 4-8:	Projected annual and seasonal wet day (>1mm rain) changes by 2040 for RCP8.5.	73
Figure 4-9:	Projected annual and seasonal wet day (>1mm rain) changes by 2090 for RCP4.5.	74
Figure 4-10:	Projected annual and seasonal wet day (>1mm rain) changes by 2090 for RCP8.5.	75
Figure 4-11:	Modelled annual and seasonal number of heavy rain days (daily rainfall >25mm), average over 1986-2005.	77
Figure 4-12:	Projected annual and seasonal number of heavy rain day (>25mm) changes by 2040 for RCP4.5.	78
Figure 4-13:	Projected annual and seasonal number of heavy rain day (>25mm) changes by 2040 for RCP8.5.	79
Figure 4-14:	Projected annual and seasonal number of heavy rain day (>25mm) changes by 2090 for RCP4.5.	80
Figure 4-15:	Projected annual and seasonal number of heavy rain day (>25mm) changes by 2090 for RCP8.5.	81
Figure 4-16:	Modelled annual 99 <sup>th</sup> percentile daily rainfall (approx. the wettest day of the year), average over 1986-2005.	83
Figure 4-17:	Projected annual 99 <sup>th</sup> percentile daily rainfall (approx. the wettest wet day of the year) changes for RCP4.5 and RCP8.5, by 2040 and 2090.	84
Figure 4-18:	Modelled annual maximum daily rainfall (Rx1day), average over 1986-2005.	85

Figure 4-19:	Projected annual mean maximum 1-day rainfall (Rx1day) changes for RCP4.5 and RCP8.5, by 2040 and 2090.	86
Figure 4-20:	Modelled annual maximum 5-day rainfall (Rx5day), average over 1986-2005.	87
Figure 4-21:	Projected annual mean maximum 5-day rainfall (Rx5day) changes for RCP4.5 and RCP8.5, by 2040 and 2090.	88
Figure 4-22:	Modelled annual and seasonal number of dry days (daily rainfall <1mm), average over 1986-2005.	92
Figure 4-23:	Projected annual and seasonal number of dry day (<1mm rainfall) changes by 2040 for RCP4.5.	93
Figure 4-24:	Projected annual and seasonal number of dry day (<1mm rainfall) changes by 2040 for RCP8.5.	94
Figure 4-25:	Projected annual and seasonal number of dry day (<1mm rainfall) changes by 2090 for RCP4.5.	95
Figure 4-26:	Projected annual and seasonal number of dry day (<1mm rainfall) changes by 2090 for RCP8.5.	96
Figure 4-27:	Modelled annual potential evapotranspiration deficit accumulation (mm), average over 1986-2005.	98
Figure 4-28:	Projected annual potential evapotranspiration deficit (PED) accumulation changes for RCP4.5 and RCP8.5, by 2040 and 2090.	99
Figure 4-29:	Modelled annual and seasonal number of days of soil moisture deficit, average over 1986-2005.	101
Figure 4-30:	Projected change in the number of annual and seasonal soil moisture deficit days by 2040 for RCP4.5.	102
Figure 4-31:	Projected change in the number of annual and seasonal soil moisture deficit days by 2040 for RCP8.5.	103
Figure 4-32:	Projected change in the number of annual and seasonal soil moisture deficit days by 2090 for RCP4.5.	104
Figure 4-33:	Projected change in the number of annual and seasonal soil moisture deficit days by 2090 for RCP8.5.	105
Figure 5-1:	Projected annual and seasonal mean wind speed changes by 2040 for RCP4.5.	107
Figure 5-2:	Projected annual and seasonal mean wind speed changes by 2040 for RCP8.5.	108
Figure 5-3:	Projected annual and seasonal mean wind speed changes by 2090 for RCP4.5.	109
Figure 5-4:	Projected annual and seasonal mean wind speed changes by 2090 for RCP8.5.	110
Figure 5-5:	Projected change in the annual number of windy days (>10 m/s) by 2040 and 2090, for RCP4.5 and RCP8.5.	111
Figure 5-6:	Projected annual 99 <sup>th</sup> percentile daily mean wind speed changes for RCP4.5 and RCP8.5, by 2040 and 2090.	112
Figure 5-7:	Projected annual and seasonal mean surface solar radiation changes by 2040 for RCP4.5.	113
Figure 5-8:	Projected annual and seasonal mean surface solar radiation changes by 2040 for RCP8.5.	114
Figure 5-9:	Projected annual and seasonal mean surface solar radiation changes by 2090 for RCP4.5.	115



Figure 5-10:	Projected annual and seasonal mean surface solar radiation changes by 2090 for RCP8.5.	116
Figure 5-11:	Projected annual and seasonal mean relative humidity changes by 2040 for RCP4.5.	118
Figure 5-12:	Projected annual and seasonal mean relative humidity changes by 2040 for RCP8.5.	119
Figure 5-13:	Projected annual and seasonal mean relative humidity changes by 2090 for RCP4.5.	120
Figure 5-14:	Projected annual and seasonal mean relative humidity changes by 2090 for RCP8.5.	121
Figure 6-1:	Example maps of weather and circulation for 6 <sup>th</sup> January 1986, according to the NIWA global climate model simulation driven by sea surface temperatures taken from the UK MetOffice Hadley model (HadGEM2-ES).	123
Figure 6-2:	Mean sea-level pressure map on 16 <sup>th</sup> June 1988 of the HadGEM2-ES simulation.	125
Figure 6-3:	Track of low-pressure weather system producing heavy rainfall in Bay of Plenty on 8 <sup>th</sup> January 1986, according to the HadGEM2-ES GCM simulation.	126
Figure 6-4:	All cyclone tracks producing more than 25mm of daily rainfall over the Bay of Plenty region, for all six GCM simulations and all years 1986-2005.	126
Figure 6-5:	(Next page) Change in track statistics between 1986-2005 (RCPpast) and 2081-2100 (RCP4.5) per 5°x5° square, for summer months (left) and winter months (right): number of lows over 20 years and 6 models (top row), average mean sea-level pressure (centre row), average vorticity (bottom row).	128
Figure 6-6:	All tracks of ex-tropical storms producing more than 25mm of daily rainfall over the Bay of Plenty region, for all six GCM simulations, for the historical 1986-2005 period (left) and 2081-2100 period under RCP4.5 (right).	130
Figure 6-7:	Change in track statistics for ex-tropical storms, between 1986-2005 (RCPpast) and 2081-2100 (RCP4.5) per 5°x5° square: number of lows over 20 years and 6 models (top), average mean sea-level pressure (centre), average vorticity (bottom).	132
Figure 6-8:	Ensemble-average change in sea-surface temperature (in °C) for the summer season between the historical 1986-2005 period and 2081-2100 under RCP8.5.	134
Figure 6-9:	(Next page) Bay of Plenty rainfall statistics, by season, for RCPpast 1986-2005, RCP 4.5 and RCP8.5 at mid-century (2031-2050), and RCP4.5 and RCP8.5 at end-of-century (2081-2100). Panels show (from top left): number of wet spells, number of wet days, cumulative rainfall over the wet spells, length of wet spell, seasonal rainfall, number of extremely-wet spells.	134
Figure 6-10:	Comparison of seasonal GCM wet-spell statistics with those from NIWA's VCSN data set (interpolated observations): number of wet spells (top) and cumulative rainfall over the wet spells (bottom).	136
Figure 6-11:	Ensemble-average summary of Bay of Plenty rainfall statistics, by season, for the percentage change between RCPpast 1986-2005 and RCP 4.5 2081-2100 (top), or between RCPpast and RCP8.5 2081-2100 (bottom).	137
Figure 8-1:	Difference in mean sea level (MSL) shoreline between absolute and local (relative) SLR where land subsidence occurs.	140

Figure 8-2:	Cumulative changes in global mean sea level (MSL) since 1880, based on a reconstruction of long-term tide gauge measurements to end of 2013 (black) and recent satellite measurements to end 2015 (red).	141
Figure 8-3:	Time series and trend in global average sea level over the satellite era from January 1993 to July 2017.	142
Figure 8-4:	Change in annual local MSL for the four main ports from 1900–2015, and initial global-mean SLR projections for RCP2.6 and RCP8.5 to 2020 (dashed lines).	143
Figure 8-5:	Historic long-term RSLR rates for the 20 <sup>th</sup> century up to and including 2015 (excluding Whangarei), determined from longer sea-level gauge records at the four main ports.	144
Figure 8-6:	Average vertical land movements (mm/yr) for near-coastal continuous GPS sites across central New Zealand regions.	145
Figure 8-7:	IPCC AR5 projections of global-average MSL rise (metres, relative to a base MSL of 1986-2005) covering the range of scenarios from RCP2.6 to RCP8.5.	146
Figure 8-8:	SLR scenarios for New Zealand seas, based on a set of median projections for all four RCPs (based on Church et al., 2013b) plus a higher 83rd percentile RCP8.5 projection (based on (Kopp et al., 2014)).	147
Figure 8-9:	Coastal sensitivity index for erosion for the Bay of Plenty Region. After Goodhue et al. (2012).	151
Figure 8-10:	Coastal sensitivity index for climate change-induced inundation (flooding by the sea) for the Bay of Plenty Region. After Goodhue et al. (2012).	151
Figure 9-1:	Change in climate suitability from 2015 to 2090 for 17 different fruit fly species.	153
Figure 11-1:	Screenshot of Kiwifruit climate suitability web application.	157
Figure 15-1:	Schematic showing dynamical downscaling method used in this report.	171

## Executive summary

The Bay of Plenty's climate is changing, and these changes will continue for the foreseeable future. It is internationally accepted that human greenhouse gas emissions are the dominant cause of recent global climate change, and that further changes will result from increasing amounts of greenhouse gases in the atmosphere. The rate of future climate change depends on how fast greenhouse gases increase.

Bay of Plenty Regional Council commissioned NIWA to analyse projected climate changes for the Bay of Plenty Region and potential impacts of climate change on some of Bay of Plenty's environments and sectors. This report addresses expected changes for 24 different climate variables out to 2100 and draws heavily on climate model simulations from the Intergovernmental Panel on Climate Change (IPCC) Fifth Assessment Report. The following bullet points outline some key findings of this report:

- The projected Bay of Plenty temperature changes increase with time and emission scenario. Future annual average warming spans a wide range: 0.5-1.0°C by 2040, and 1.0-3.5°C by 2090. Diurnal temperature range (i.e., difference between minimum and maximum temperature of a given day) is expected to increase with time and emission scenarios.
- The average number of hot days (days >25°C) and extreme hot days (days >30°C) is expected to increase with time and scenario, with the largest increases in the central part of the region and the least in the eastern hill country. The area between Maketu, Whakatāne, and Murupara may observe 20-25 more hot days per year by 2040 (both scenarios) and 70-80 more hot days per year by 2090 (RCP8.5). Extreme hot days for this area may increase by 1-2 days per year by 2040 (both scenarios), and 10-14 more days per year by 2090 (RCP8.5).
- Projected changes in rainfall show variability across the Bay of Plenty region. By 2040 under both scenarios, annual rainfall is not expected to change much, but the seasonality of rainfall is expected to change with spring and summer generally becoming drier and winter and autumn becoming wetter than the historic period. By 2090, annual rainfall totals are projected to decline under both scenarios. Similar to 2040, summer and spring rainfall is projected to decline, and winter and autumn rainfall is projected to increase.
- Extreme, rare rainfall events are projected to become more severe in the future. Short duration rainfall events have the largest relative increases compared with longer duration rainfall events. The depth currently projected for a 1-in-100-year rainfall event (e.g. 248 mm in Tauranga) is projected to become a 1-in-34-year event by 2090 under RCP8.5, i.e. a rainfall event of this magnitude may occur three times as often under this scenario.
- Drought potential is projected to increase across the Bay of Plenty, with increasing accumulated Potential Evapotranspiration Deficit totals with time and increasing greenhouse gas concentrations. The coastal areas around Tauranga and Te Puke are expected to observe the largest increases in PED, and the hill country areas of the Urewera and Raukumara Ranges the smallest increases in PED.

- There is good evidence that storms originating from the sub-tropics in the summer that impact on the Bay of Plenty have more intense circulation that is likely to lead to stronger winds, greater storm surge and higher rainfall accumulations. Evidence for such changes in other seasons is less clear. However, there is also good evidence that heavy rainfall intensity associated with storms increases in all seasons with global warming, particularly in winter, likely associated with the increased moisture carrying capacity of a warmer atmosphere.

A changing climate will have impacts on different sectors and environments in the Bay of Plenty.

- Sea-level rise information from Ministry for the Environment (2017) is presented, as well as sea-level rise projections for the Bay of Plenty, which is rising slightly faster than the New Zealand average. Overall, the Bay of Plenty coastline has moderate-high sensitivity to erosion and inundation.
- Increasing temperatures are likely to result in higher biosecurity risks in the Bay of Plenty, through pest incursions (both animal and plant pests). This is because pests that cannot survive in the region over winter currently (because it is too cold) may be able to survive year-round in the future. This may have implications for the primary sector and the natural environment.
- It is likely that the region will experience more drought conditions in the future, with implications for pasture growth and crops.
- Hayward kiwifruit is particularly dependent on winter chilling. As air temperatures in the region continue to rise, the potential for years with marginal or poor winter chilling conditions steadily increases. This could make kiwifruit production marginal or unviable in parts of the Bay of Plenty (this is assuming no use of chemical agents to break dormancy).
- There may be opportunities for diversification of crop type in the Bay of Plenty, where new varieties that are unviable in the current climate may be able to be grown in the region in the future.
- Exotic forestry (*Pinus radiata*) is projected to increase in productivity in the future due to increasing temperatures and increased CO<sub>2</sub>. However, increased fire risk may cause issues in the forestry industry.
- Human health is likely to be impacted by a changing climate, through both direct and indirect impacts. Direct impacts include injury from floods, extreme heat, and storms, and indirect effects include microbial contamination, mosquito-borne diseases, algal blooms, mental health, and air quality.

# 1 Introduction

Climate change is already affecting New Zealand and the Bay of Plenty with downstream effects on our natural environment, the economy, and communities. In the coming decades, climate change is highly likely to increasingly pose challenges to New Zealanders' way of life.

Bay of Plenty Regional Council commissioned the National Institute of Water and Atmospheric Research (NIWA) to undertake a review of climate change projections and impacts for the Bay of Plenty Region (Figure 1-1). This work follows the publication of the Intergovernmental Panel on Climate Change (IPCC) Fifth Assessment Report in 2013 and 2014, and the New Zealand climate change projections report published by the Ministry for the Environment (updated 2018) (Ministry for the Environment, 2018). The contents of this technical report include analysis of climate projections for the Bay of Plenty Region in greater detail than the national-scale analysis. Regional-scale climate projection maps have been provided for 24 different climate variables, and GIS data files have been provided to the Council.

This technical report describes changes which may occur over the 21<sup>st</sup> century to the climate of the Bay of Plenty Region. Consideration about future change incorporates knowledge of both natural variations in the climate and changes that may result from increasing global concentrations of greenhouse gases that are contributed to by human activities. Climatic variables discussed in this report include temperature, rainfall, potential evapotranspiration deficit (a measure of drought potential), soil moisture, storminess, wind, solar radiation, and humidity. Projections for sea-level rise are also discussed. Commentary on climate change impacts and implications for some of the Bay of Plenty's different environments and sectors are provided, including biosecurity, horticulture, agriculture, forestry, and health.

Some of the information that underpins portions of this report resulted from academic studies based on the latest assessments of the Intergovernmental Panel on Climate Change (IPCC, 2013, IPCC, 2014c, IPCC, 2014a, IPCC, 2014b). Details specific to Bay of Plenty were based on scenarios for New Zealand that were generated by NIWA from downscaling of global climate model simulations. This effort utilised several IPCC representative concentration pathways for the future and this was achieved through NIWA's core-funded Regional Modelling Programme. The climate change information presented in this report is consistent with recently-updated national-scale climate change guidance produced for the Ministry for the Environment (2018), and sea-level rise information is consistent with the coastal hazards guidance manual published by Ministry for the Environment (2017).

The remainder of this chapter includes a brief introduction of global and New Zealand climate change, based on the IPCC Fifth Assessment Report. It includes an introduction to the climate change scenarios used in this report, and the methodology that explains the modelling approach for the climate change projections that are presented for Bay of Plenty.

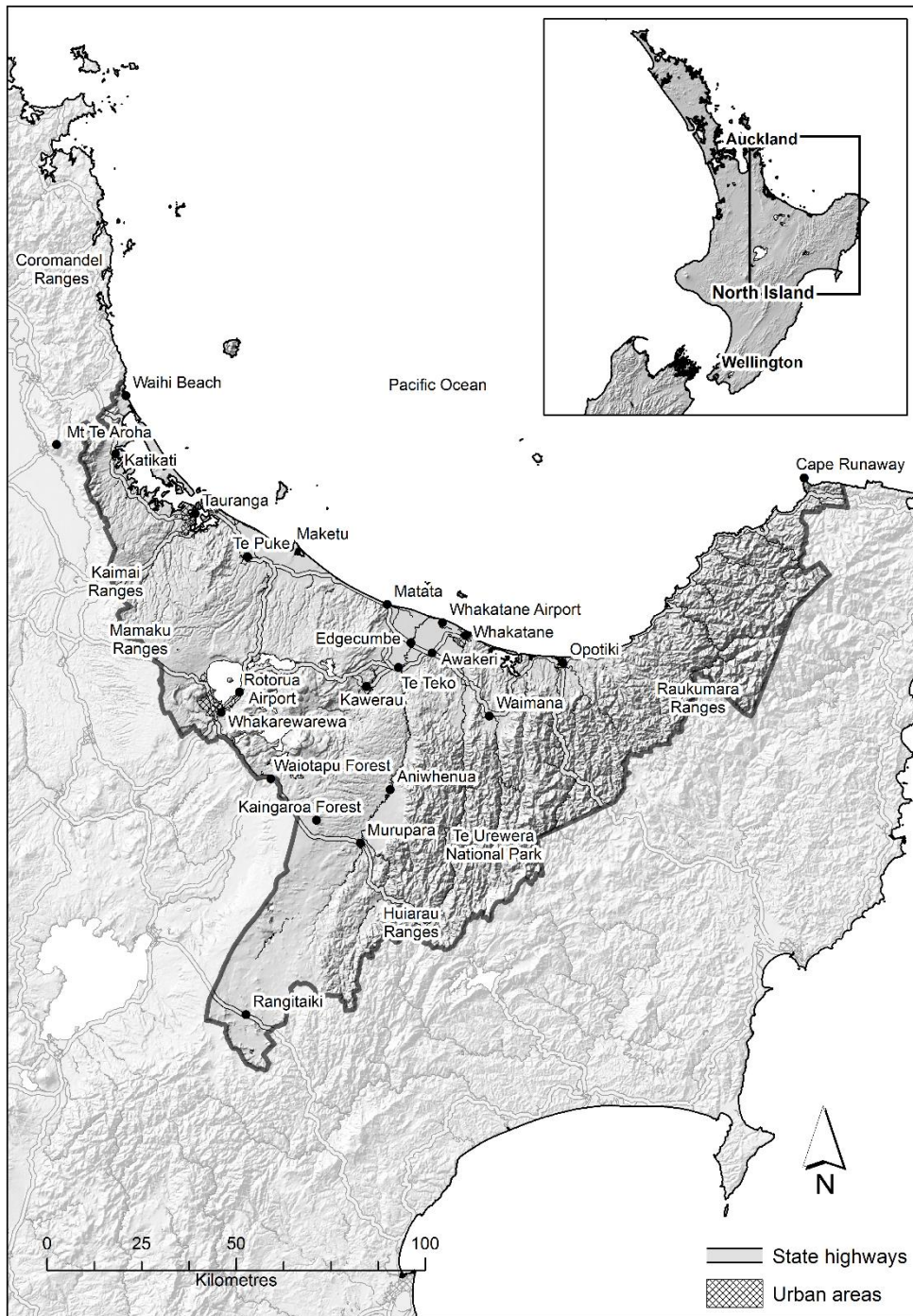


**Figure 1-1: The Bay of Plenty Region administered by the Bay of Plenty Regional Council.**

## 1.1 Global and New Zealand climate change

### Key messages

- The global climate system is warming and many of the recently observed climate changes are unprecedented.
- Global mean sea level has risen over the past century at a rate of about 1.7 mm/year and has very likely accelerated to 3.2 mm/year since 1993.
- Human activities (and associated greenhouse gas emissions) are estimated to have caused approximately 1.0°C of global warming above pre-industrial levels.
- Estimated human-induced global warming is currently increasing at 0.2°C per decade due to past and ongoing emissions.
- Continued increases in greenhouse gas emissions will cause further warming and impacts on all parts of the global climate system.

Warming of the global climate system is unequivocal, and since the 1950s, many of the observed climate changes are unprecedented over short and long timescales (decades to millennia) (IPCC, 2013). These changes include warming of the atmosphere and ocean, diminishing of ice and snow, sea-level rise, and increases in the concentration of greenhouse gases in the atmosphere. Climate change is already influencing the intensity and frequency of many extreme weather and climate events globally. Shifts in average temperatures will result in proportionally large increases in the occurrence of extreme temperatures. The Earth's atmosphere has warmed by 0.85°C on average over the period 1880-2012. The rate of sea-level rise since the mid-19<sup>th</sup> century has been larger than the mean rate of change during the previous two millennia. Over the period 1901-2010, global mean sea level rose by 0.19 m.

The atmospheric concentrations of carbon dioxide have increased to levels unprecedented in at least the last 3 million years (Willeit et al., 2019). Carbon dioxide concentrations have increased by at least 40% since pre-industrial times, primarily from fossil fuel emissions and secondarily from net land use change emissions (IPCC, 2013). In May 2019, the carbon dioxide concentration of the atmosphere reached 415 parts per million. The ocean has absorbed about 30% of the emitted anthropogenic carbon dioxide, causing ocean acidification. Due to the influence of greenhouse gases on the global climate system, it is extremely likely that human influence has been the dominant cause of the observed warming since the mid-20<sup>th</sup> century (IPCC, 2013, IPCC, 2018).

Published information about the expected impacts of climate change on New Zealand is summarised and assessed in the Australasia chapter of the IPCC Working Group II assessment report (Reisinger et al., 2014) as well as a report published by the Royal Society of New Zealand (Royal Society of New Zealand, 2016). Key findings from these publications include:

**The regional climate is changing.** The Australasia region continues to demonstrate long-term trends toward higher surface air and sea surface temperatures, more hot extremes and fewer cold extremes, and changed rainfall patterns. Over the past 50 years, increasing greenhouse gas concentrations have contributed to rising average temperatures in New Zealand. Changing precipitation patterns have resulted in increases in rainfall for the south and west of the South Island

and west of the North Island and decreases in the northeast of the South Island and the east and north of the North Island. Some heavy rainfall events already carry the fingerprint of a changed climate, in that they have become more intense due to higher temperatures allowing the atmosphere to carry more moisture (Dean et al., 2013). Cold extremes have become rarer and hot extremes have become more common.

The region has exhibited warming to the present and is virtually certain to continue to do so. New Zealand’s mean annual temperature has increased, on average, by 1.00°C (± 0.25°C) per century since 1909 (Figure 1-2).

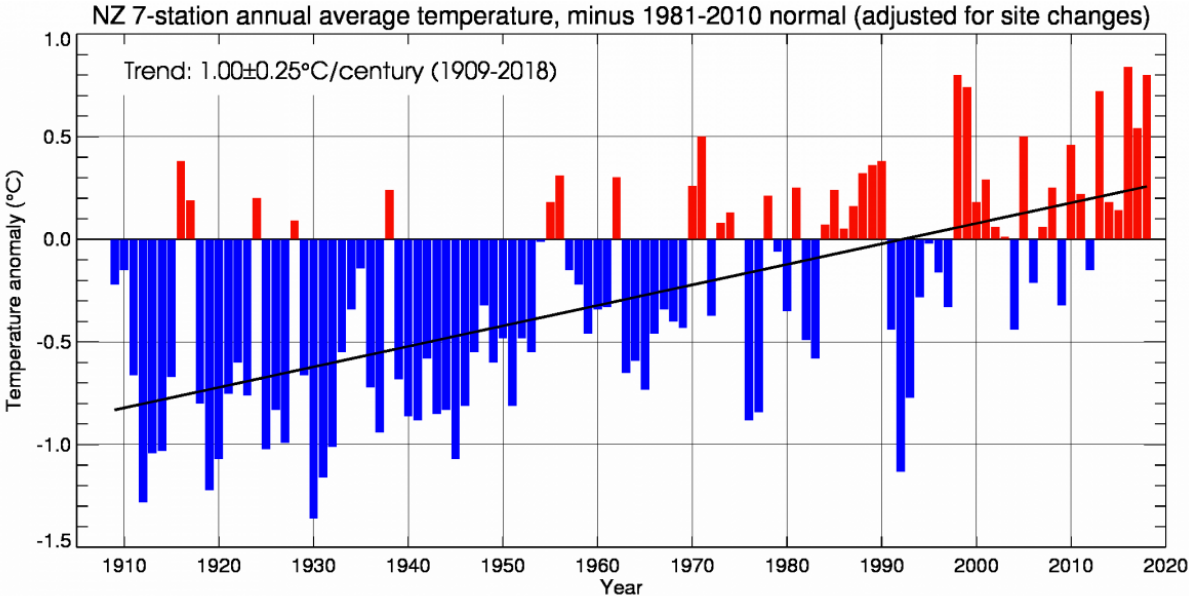


**Figure 1-2: New Zealand national temperature series, 1909-2018.** More information about the New Zealand seven-station temperature series can be found at <https://www.niwa.co.nz/our-science/climate/information-and-resources/nz-temp-record/seven-station-series-temperature-data>

**Warming is projected to continue through the 21<sup>st</sup> century along with other changes in climate.**

Warming is expected to be associated with rising snow lines, more frequent hot extremes, less frequent cold extremes, and increasing extreme rainfall related to flood risk in many locations. Annual average rainfall is expected to decrease in the northeast South Island and north and east of the North Island, and to increase in other parts of New Zealand. Fire hazard is projected to increase in many parts of New Zealand. Regional sea level rise will very likely exceed the historical rate, consistent with global mean trends.

**Impacts and vulnerability:** Without adaptation, further climate-related changes are projected to have substantial impacts on water resources, coastal ecosystems, infrastructure, health, agriculture, and biodiversity. However, uncertainty in projected rainfall changes and other climate-related changes remains large for many parts of New Zealand, which creates significant challenges for adaptation.

Additional information about recent New Zealand climate change can be found in Ministry for the Environment (2018).



## 1.2 Year to year climate variability and climate change

### Key messages

- Natural variability is an important consideration in addition to the underlying climate change signal.
- El Niño-Southern Oscillation is the most dominant mode of inter-annual climate variability and it impacts New Zealand primarily through changing wind, temperature and rainfall patterns.
- The Interdecadal Pacific Oscillation affects New Zealand through drier conditions in the east and wetter conditions in the west during the positive phase the opposite in the negative phase.
- The Southern Annular Mode affects New Zealand through higher temperatures and settled weather during the positive phase and lower temperatures and unsettled weather during the negative phase.
- Natural variability will continue to affect the year-to-year climate of New Zealand into the future.

Much of the material in this report focuses on the projected impact on the climate of the Bay of Plenty over the coming century due to increases in global anthropogenic greenhouse gas concentrations. However, natural variations will also continue to occur. Much of the variation in New Zealand's climate is random and lasts for only a short period, but longer term, quasi-cyclic variations in climate can be attributed to different factors. Three large-scale oscillations that influence climate in New Zealand are the El Niño-Southern Oscillation, the Interdecadal Pacific Oscillation, and the Southern Annular Mode (Ministry for the Environment, 2008). Those involved in (or planning for) climate-sensitive activities in the Bay of Plenty Region will need to cope with the sum of both anthropogenic change and natural variability.

### 1.2.1 The effect of El Niño and La Niña

El Niño-Southern Oscillation (ENSO) is a natural mode of climate variability that has wide-ranging impacts around the Pacific Basin (Ministry for the Environment, 2008). ENSO involves a movement of warm ocean water from one side of the equatorial Pacific to the other, changing atmospheric circulation patterns in the tropics and subtropics, with corresponding shifts for rainfall across the Pacific.

During El Niño, easterly trade winds weaken and warm water 'spills' eastward across the equatorial Pacific, accompanied by higher rainfall than normal in the central-east Pacific. La Niña produces opposite effects and is typified by an intensification of easterly trade winds, retention of warm ocean waters over the western Pacific. ENSO events occur on average 3 to 7 years apart, typically becoming established in April or May and persisting for about a year thereafter.

During El Niño events, the weakened trade winds cause New Zealand to experience a stronger than normal south-westerly airflow. This generally brings lower seasonal temperatures to the country and drier than normal conditions to the north and east of New Zealand, including the Bay of Plenty (Salinger and Mullan, 1999) (Figure 1-3). During La Niña conditions, the strengthened trade winds cause New Zealand to experience more north-easterly airflow than normal, higher-than-normal

temperatures (especially during summer), and wetter conditions in the north and east of the North Island, including the Bay of Plenty (Figure 1-3).

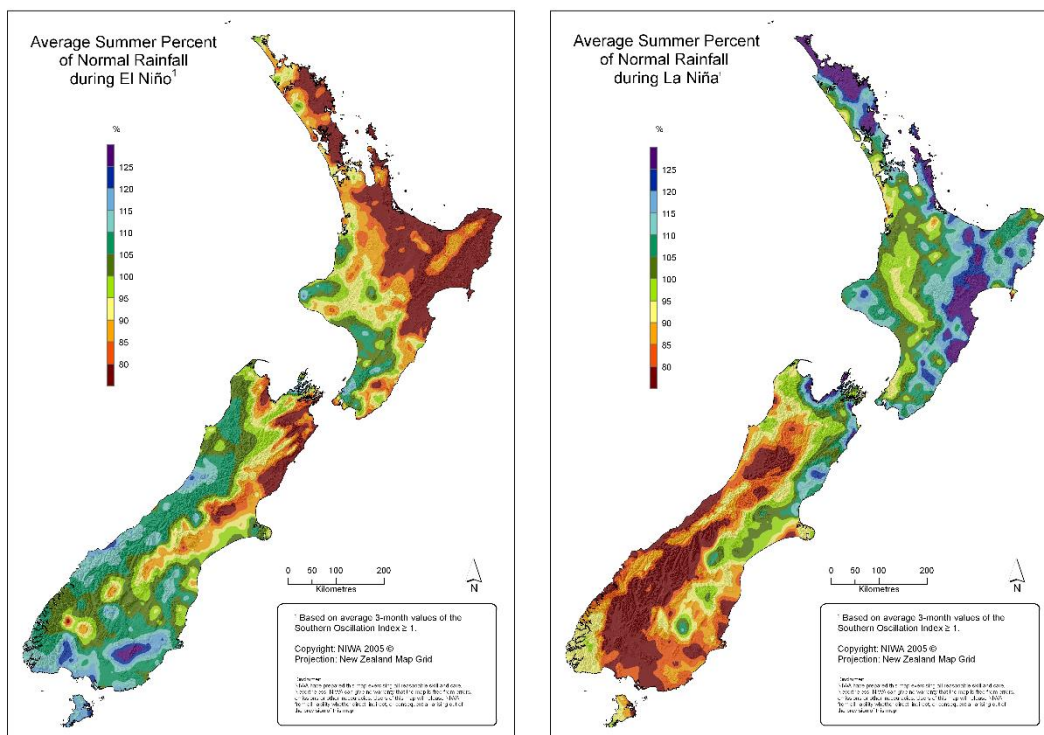


**Figure 1-3: Average summer percentage of normal rainfall during El Niño (left) and La Niña (right).** El Niño composite uses the following summers: 1963/64, 1965/66, 1968/69, 1969/70, 1972/73, 1976/77, 1977/78, 1982/83, 1986/87, 1987/88, 1991/92, 1994/95, 1997/98, 2002/03. La Niña composite uses the following summers: 1964/65, 1970/71, 1973/74, 1975/76, 1983/84, 1984/85, 1988/89, 1995/96, 1998/99, 1999/2000, 2000/01. This figure was last updated in 2005. © NIWA.

According to IPCC (2013), ENSO is highly likely to remain the dominant mode of natural climate variability in the 21<sup>st</sup> century, and that rainfall variability relating to ENSO is likely to increase. However, there is uncertainty about future changes to the amplitude and spatial pattern of ENSO.

### 1.2.2 The effect of the Interdecadal Pacific Oscillation

The Interdecadal Pacific Oscillation (IPO) is a large-scale, long-period oscillation that influences climate variability over the Pacific Basin including New Zealand (Salinger et al., 2001). The IPO operates at a multi-decadal scale, with phases lasting around 20 to 30 years. During the positive phase of the IPO, sea surface temperatures around New Zealand tend to be lower, and westerly winds stronger, resulting in drier conditions for eastern areas of both North and South Islands (including the Bay of Plenty). The opposite occurs in the negative phase. The IPO can modify New Zealand's connection to ENSO, and it also positively reinforces the impacts of El Niño (during IPO+ phases) and La Niña (during IPO- phases).

### 1.2.3 The effect of the Southern Annular Mode

The Southern Annular Mode (SAM) represents the variability of circumpolar atmospheric jets that encircle the Southern Hemisphere that extend out to the latitudes of New Zealand. The SAM is often coupled with ENSO, and both phenomena affect New Zealand's climate in terms of westerly wind strength and storm occurrence (Renwick and Thompson, 2006). In its positive phase, the SAM is

associated with relatively light winds and more settled weather over New Zealand, with stronger westerly winds further south towards Antarctica. In contrast, the negative phase of the SAM is associated with unsettled weather and stronger westerly winds over New Zealand, whereas wind and storms decrease towards Antarctica.

The phase and strength of the SAM is influenced by the size of the ozone hole, giving rise to positive trends in the past during spring and summer. In the future other drivers are likely to have an impact on SAM behaviour, for example changing temperature gradients between the equator and the high southern latitudes would have an impact on westerly wind strength in the mid-high latitudes.

#### 1.2.4 The influence of natural variability on climate change projections

It is important to consider human-induced climate change in the context of natural climate variability. An example of this for temperature is shown in Figure 1-4. The solid black line on the left-hand side represents the observed annual average temperature for New Zealand<sup>1</sup>, and the dashed black line represents the 1909-2014 trend of 0.92 °C/century extrapolated to 2100. All the other line plots and shading refer to the modelled air temperature averaged over the New Zealand region. Post-2014, the two line plots show the annual temperature changes for the New Zealand region under RCP8.5 (orange) and RCP2.6 (blue); a single model is selected to illustrate the inter-annual variability. The shading shows the range across all IPCC AR5 models for both historical and future periods.

Over the 1900-2014 historical period, the New Zealand observed temperature curve lies within the simulations of all models (purple shading). For the future 2015-2100 period, the RCP2.6 models (blue shading) show very little warming trend after about 2030, whereas the RCP8.5 models (orange shading) 'take off' to be anywhere between +2°C and +5°C by 2100.

Figure 1-4 should not be interpreted as a set of specific predictions for individual years. However, it illustrates that although we expect a long term overall upward trend in temperatures (at least for RCP8.5), there will still be some relatively cool years. For this particular example, a year which is unusually warm under our present climate could become the norm by about 2050, and an "unusually warm" year in 30-50 years' time (under the higher emission scenarios) is likely to be warmer than anything we currently experience.

---

<sup>1</sup> <https://www.niwa.co.nz/our-science/climate/information-and-resources/nz-temp-record/seven-station-series-temperature-data>

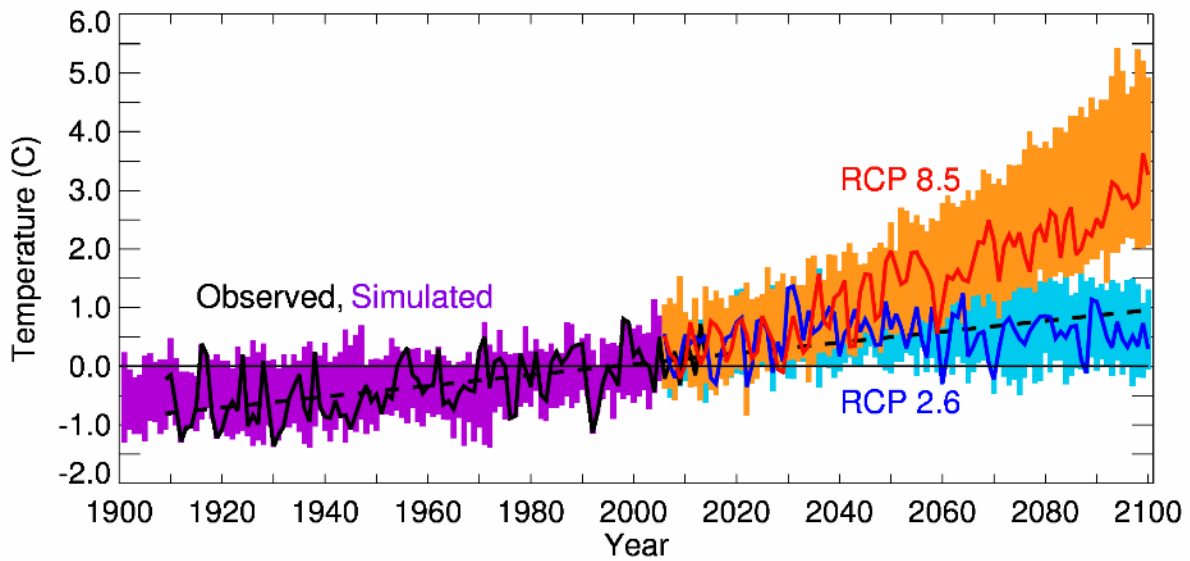


**Figure 1-4: New Zealand Temperature - historical record and an illustrative schematic projection illustrating future year-to-year variability.** (See text for full explanation). From Ministry for the Environment (2018).

For rainfall, multi-decadal variability associated with the IPO can enhance or counter the impacts of anthropogenic climate change. This influence may generate either slightly above normal or below normal rainfall for parts of New Zealand during summer. For the historic period, IPO-negative conditions coupled with more frequent La Niña episodes could increase rainfall during spring and summer, essentially in the opposite direction as expected from anthropogenic factors (i.e. a potential reduction in spring and summer rainfall). A subsequent further reversal of the IPO in 10-20 years' time could have the opposite effect, enhancing part of the anthropogenic (drying) trend in rainfall for a few decades. The message from the section is *not* that anthropogenic trends in climate can be ignored because of natural variability. In the projections, we have discussed these anthropogenic trends because they become the dominant factor locally as the century progresses. Nevertheless, we need to bear in mind that at some times natural variability will be adding to the human-induced trends, while at others it may be offsetting part of the anthropogenic effect.

## 1.3 Representative Concentration Pathways

### Key messages

- Future climate change projections are considered under four emission scenarios, called Representative Concentration Pathways (RCPs) by the IPCC.
- The four RCPs project different climate futures based on future greenhouse gas concentrations, determined by economic, political and social developments during the 21<sup>st</sup> century.
- RCP2.6 is a mitigation scenario requiring significant reduction in greenhouse gas emissions, RCP4.5 and RCP6.0 are mid-range scenarios where greenhouse gas concentrations stabilise by 2100, and RCP8.5 is a 'business as usual' scenario with greenhouse gas emissions continuing at current rates.
- Projections for the future climate in the Bay of Plenty are presented for RCP4.5 and RCP8.5 in this report.

Assessing possible changes for our future climate due to human activity is difficult because climate projections depend strongly on estimates for future greenhouse gas concentrations. Those concentrations depend on global greenhouse gas emissions that are driven by factors such as economic activity, population changes, technological advances and policies for sustainable resource use. In addition, for a specific future trajectory of global greenhouse gas emissions, different climate model simulations produced somewhat different results for future climate change.

This range of uncertainty has been dealt with by the IPCC through consideration of 'scenarios' that describe concentrations of greenhouse gases in the atmosphere. The wide range of scenarios are associated with possible economic, political, and social developments during the 21<sup>st</sup> century, and via consideration of results from several different climate models for any given scenario. In the 2013 IPCC Fifth Assessment Report, the atmospheric greenhouse gas concentration components of these scenarios are called Representative Concentration Pathways (RCPs). These are abbreviated as RCP2.6, RCP4.5, RCP6.0, and RCP8.5, in order of increasing radiative forcing by greenhouse gases (i.e. the change in energy in the atmosphere due to greenhouse gas emissions). RCP2.6 leads to low anthropogenic greenhouse gas concentrations (requiring removal of CO<sub>2</sub> from the atmosphere, also called the 'mitigation' scenario), RCP4.5 and RCP6.0 are two 'stabilisation' scenarios (where greenhouse gas concentrations and therefore radiative forcing stabilises by 2100) and RCP8.5 has very high greenhouse gas concentrations (the 'business as usual' scenario). Therefore, the RCPs represent a range of 21<sup>st</sup> century climate policies. Table 1-1 shows the projected global mean surface air temperature for each RCP.

**Table 1-1: Projected change in global mean surface air temperature for the mid- and late- 21st century relative to the reference period of 1986-2005 for different RCPs. After IPCC (2013).**

Scenario	Alternative name	2046-2065 (mid-century)		2081-2100 (end-century)	
		Mean (°C)	Likely range (°C)	Mean (°C)	Likely range (°C)
RCP2.6	Mitigation scenario	1.0	0.4 to 1.6	1.0	0.3 to 1.7
RCP4.5	Stabilisation scenario	1.4	0.9 to 2.0	1.8	1.1 to 2.6
RCP6.0	Stabilisation scenario	1.3	0.8 to 1.8	2.2	1.4 to 3.1
RCP8.5	Business as usual scenario	2.0	1.4 to 2.6	3.7	2.6 to 4.8

The full range of projected globally-averaged temperature increases for all scenarios for 2081-2100 (relative to 1986-2005) is 0.3 to 4.8°C (Figure 1-5). Warming will continue beyond 2100 under all RCP scenarios except RCP2.6. Warming will continue to exhibit inter-annual-to-decadal variability and will not be regionally uniform.

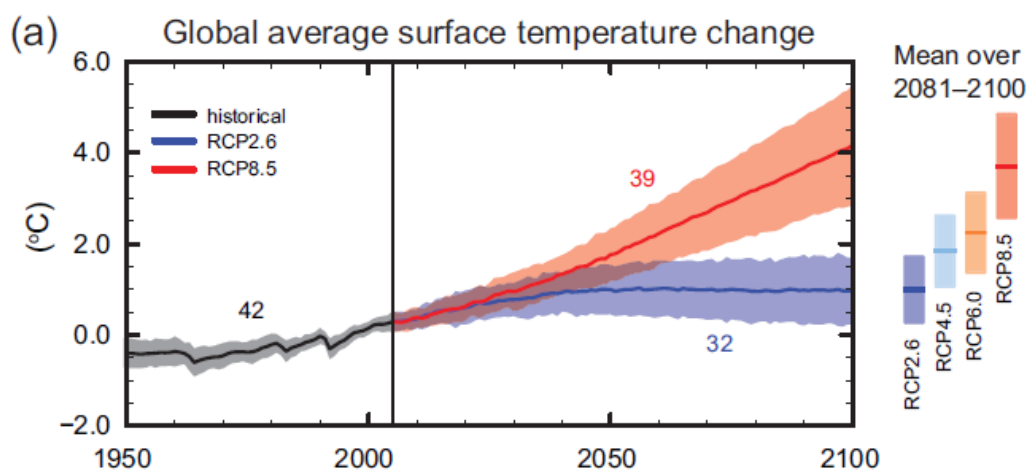


**Figure 1-5: CMIP5 multi-model simulated time series from 1950-2100 for change in global annual mean surface temperature relative to 1986-2005.** Time series of projections and a measure of uncertainty (shading) are shown for scenarios RCP2.6 (blue) and RCP8.5 (red). Black (grey shading) is the modelled historical evolution using historical reconstructed forcings. The mean and associated uncertainties averaged over 2081-2100 are given for all RCP scenarios as coloured vertical bars to the right of the graph (the mean projection is the solid line in the middle of the bars). The numbers of CMIP5 models used to calculate the multi-model mean is indicated on the graph. From IPCC (2013).

As global temperatures increase, it is virtually certain that there will be more hot and fewer cold temperature extremes over most land areas. It is very likely that heat waves will occur with a higher

frequency and duration. Furthermore, the contrast in rainfall between wet and dry regions and wet and dry seasons will increase. Along with increases in global mean temperature, mid-latitude and wet tropical regions will experience more intense and more frequent extreme rainfall events by the end of the 21<sup>st</sup> century. The global ocean will continue to warm during the 21<sup>st</sup> century, influencing ocean circulation and sea ice extent.

Cumulative CO<sub>2</sub> emissions will largely determine global mean surface warming by the late 21<sup>st</sup> century and beyond. Even if emissions are stopped, the inertia of many global climate changes will continue for many centuries to come. This represents a substantial multi-century climate change commitment created by past, present, and future emissions of CO<sub>2</sub>.

In this report, global climate model outputs based on two RCPs (RCP4.5 and RCP8.5) have been downscaled to produce future climate projections for the Bay of Plenty Region. The rationale for choosing these two scenarios was to present a ‘business-as-usual’ scenario if greenhouse gas emissions continue at current rates (RCP8.5) and a scenario which could be realistic if global action is taken towards mitigating climate change, for example the Paris climate change agreement (RCP4.5).

## 1.4 Climate modelling methodology

The following bullet points summarise the methodology used by NIWA for modelling New Zealand’s future climate.

- Climate model simulation data from the IPCC Fifth Assessment has been used to produce climate projections for New Zealand.
- Six climate models were chosen by NIWA for dynamical downscaling. These models were chosen because they produced the most accurate results when compared to historical climate and circulation patterns in the New Zealand and southwest Pacific region.
- Downscaled climate change projections are at a 5 km x 5 km resolution over New Zealand.
- Climate projection and historic baseline maps and tables present the average of the six downscaled models.
- Climate projections are presented as a 20-year average for two future periods: 2031-2050 (termed ‘2040’) and 2081-2100 (termed ‘2090’). All maps show changes relative to the baseline historic climate of 1986-2005 (termed ‘1995’).

More details about the methods used in climate change modelling are found in Appendix A.

## 2 Current and future climate of the Bay of Plenty Region

The topography of the North Island has a profound effect on the weather of the Bay of Plenty Region. The sheltering provided by high country on three sides produces a climate that is one of the sunniest and least windy in New Zealand. The annual rainfall is quite plentiful compared with some eastern parts of the country, although there is considerable rainfall variability. Most of the rainfall in the region, and especially heavy rain, occurs when northerly airstreams of tropical origin are forced to ascend over the land. Temperatures too are subject to considerable variability. The seas in the Bay of Plenty, because of the presence of a warm ocean current and sheltering provided by the North Island, are among the calmest and warmest in New Zealand. More information about the historic climate of the Bay of Plenty, outside of the information in this report, can be found in Chappell (2013).

The following sections (3-6) present climate change projections for the Bay of Plenty Region.

## 3 Temperature

### 3.1 Mean temperature

Historic (average over 1986-2005) and future (average over 2031-2050 and 2081-2100) maps for mean temperature are shown in this section. The historic maps show annual and seasonal mean temperature in units of degrees Celsius (°C) and the future projection maps show the change in mean temperature compared with the present day, in units of °C. Note that the historic maps are on a different colour scale to the future projection maps.

For the historic period, the coastal Bay of Plenty has the warmest annual and seasonal mean temperatures in the region (Figure 3-1), with 14-15°C mean annual temperature, 18-19°C in summer and 9-11°C in winter. The areas furthest inland have the coolest mean temperatures, with 10-11°C mean annual temperature, 15-16°C in summer and 5-6°C in winter.

In the future, mean temperature is projected to increase by 0.5-1.0°C for all seasons (and annual) by 2040 under RCP4.5 (Figure 3-2). The same is projected for 2040 under RCP8.5, except autumn is projected to warm by 1.0-1.5°C (Figure 3-3). By 2090, most of the region is projected to warm by 1.0-1.5°C under RCP4.5 for all seasons and at the annual scale (Figure 3-4). Under RCP8.5 (Figure 3-5), warming is projected to be around 2.5-3.0°C for most of the region at the annual scale (with some isolated areas projecting 3.0-3.5°C of warming, and eastern areas projecting 1.5-2.5°C of warming). At the seasonal scale, widespread warming of 3.0-3.5°C is projected for autumn, with the least warming projected in winter (2.0-3.0°C for most of the region).

The area closest to East Cape warms the least (e.g. annual warming of 1.5-2.0°C compared with 2.5-3.5°C for most of the region under RCP8.5 by 2090). This is an area with complex topography close to the coastline with changes modulated by maritime influences. As such, the magnitude of temperature and precipitation changes are more uncertain.



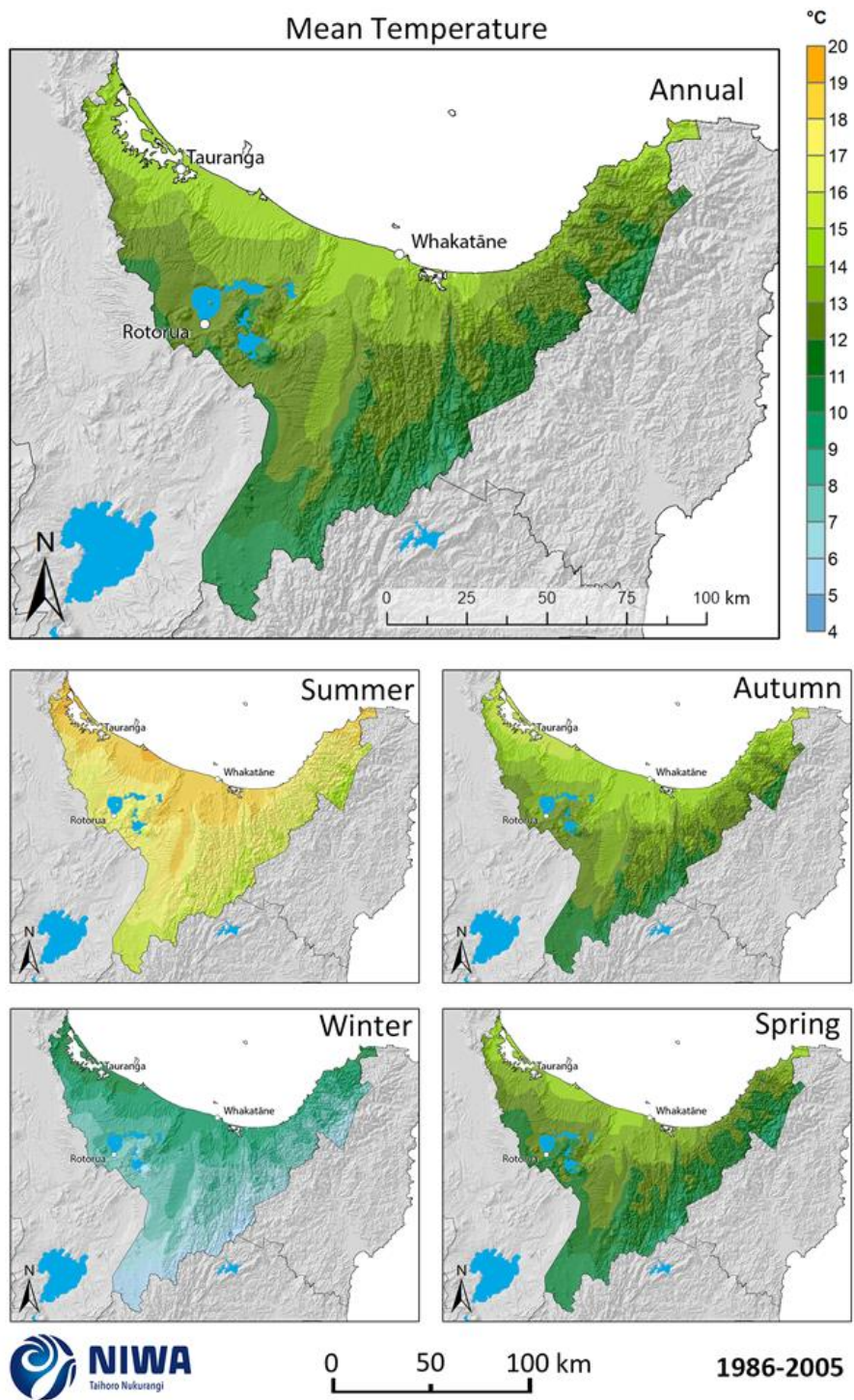


**Figure 3-1: Modelled annual and seasonal mean temperature, average over 1986-2005.** Results are based on dynamical downscaled projections using NIWA's Regional Climate Model. Resolution of projection is 5km x 5km.

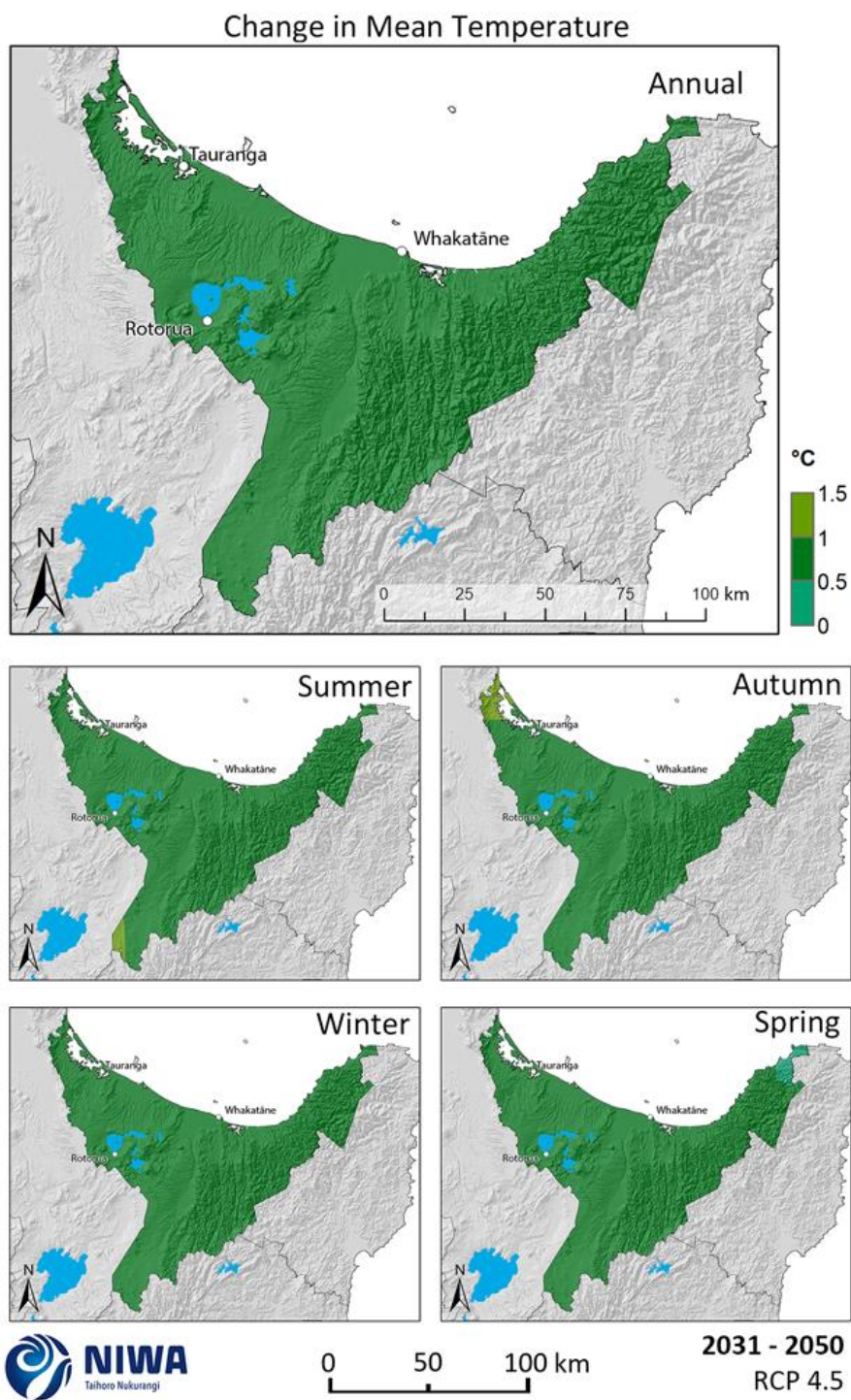


**Figure 3-2: Projected annual and seasonal mean temperature changes by 2040 for RCP4.5.** Relative to 1986-2005 average, based on the average of six global climate models. Results are based on dynamical downscaled projections using NIWA's Regional Climate Model. Resolution of projection is 5km x 5km.

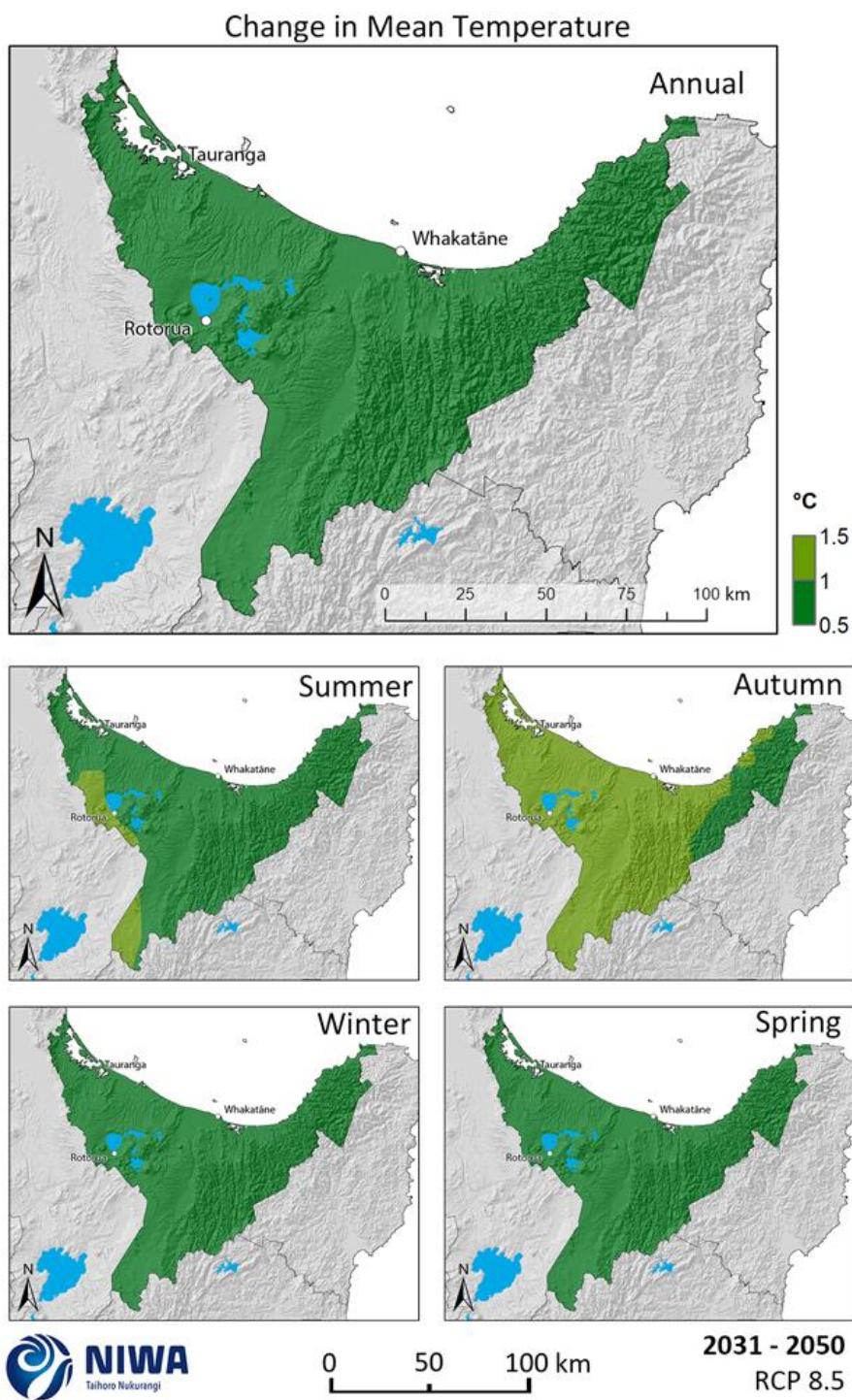


**Figure 3-3: Projected annual and seasonal mean temperature changes by 2040 for RCP8.5.** Relative to 1986-2005 average, based on the average of six global climate models. Results are based on dynamical downscaled projections using NIWA's Regional Climate Model. Resolution of projection is 5km x 5km.

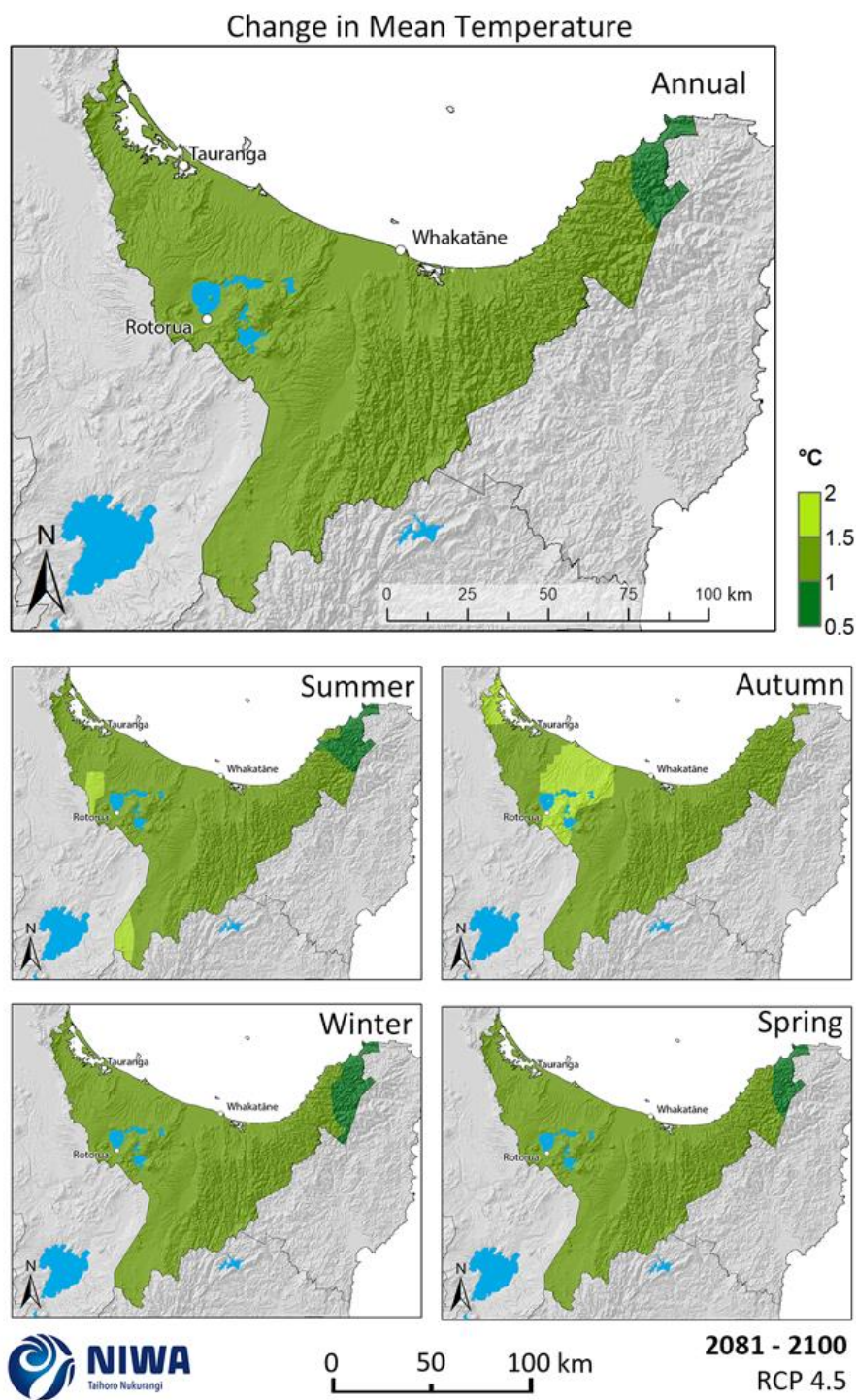


**Figure 3-4: Projected annual and seasonal mean temperature changes by 2090 for RCP4.5.** Relative to 1986-2005 average, based on the average of six global climate models. Results are based on dynamical downscaled projections using NIWA's Regional Climate Model. Resolution of projection is 5km x 5km.

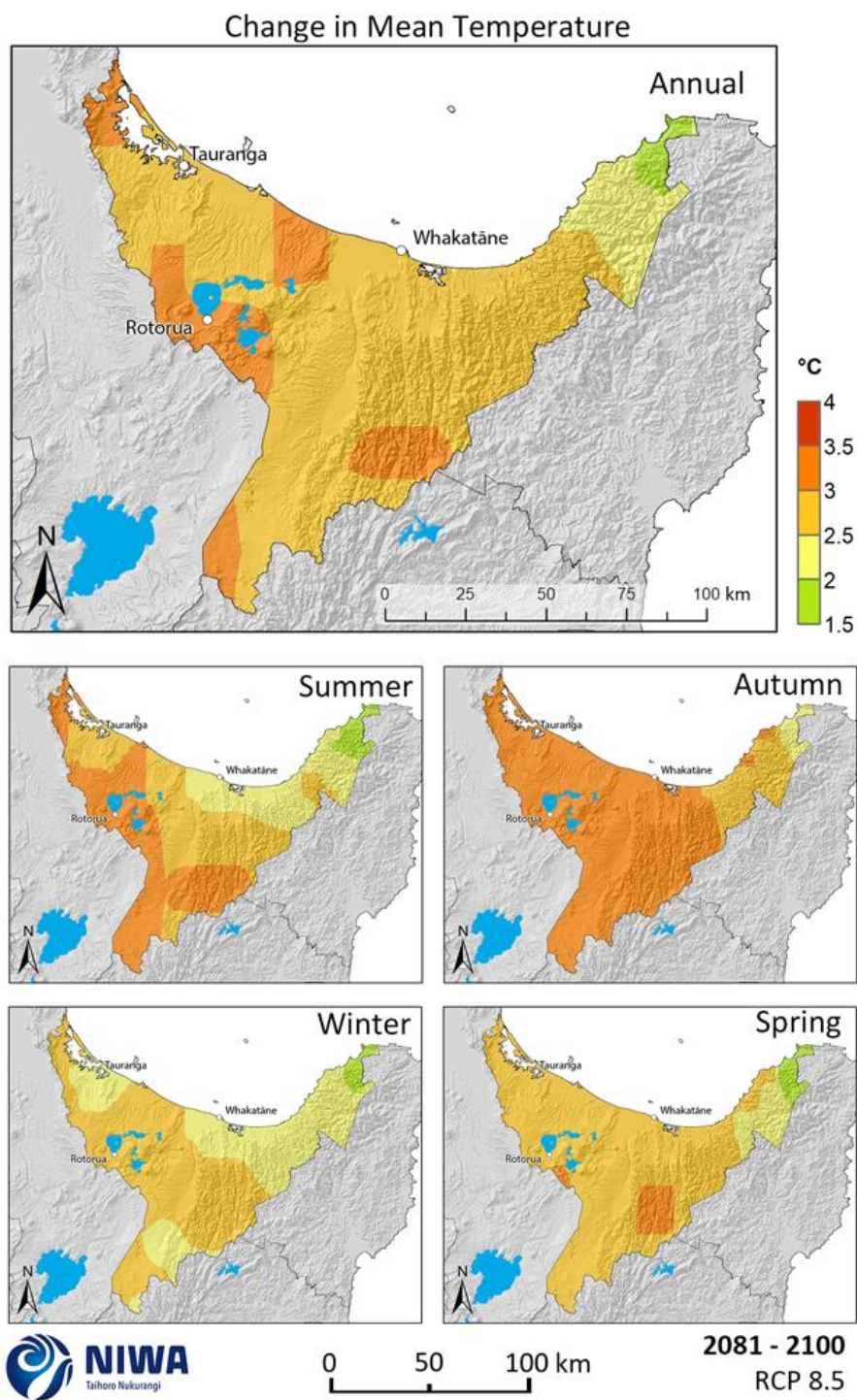


**Figure 3-5: Projected annual and seasonal mean temperature changes by 2090 for RCP8.5.** Relative to 1986-2005 average, based on the average of six global climate models. Results are based on dynamical downscaled projections using NIWA's Regional Climate Model. Resolution of projection is 5km x 5km.

## 3.2 Maximum temperature

Maximum temperatures are generally recorded in the afternoon, and therefore are known as daytime temperatures. Historic (average over 1986-2005) and future (average over 2031-2050 and 2081-2100) maps for mean maximum temperature are shown in this section. The historic maps show annual and seasonal mean maximum temperature in units of degrees Celsius (°C) and the future projection maps show the change in mean temperature compared with the present day, in units of °C. Note that the historic maps are on a different colour scale to the future projection maps.

For the historic period, the central and coastal Bay of Plenty has the warmest annual and seasonal mean maximum temperatures (Figure 3-6), particularly west of Whakatāne and around Kawerau. Mean annual maximum temperatures are 19-20°C, 24-25°C in summer and 14-15°C in winter. The areas furthest inland have the coolest mean maximum temperatures, with 15-16°C mean annual temperatures, 20-22°C in summer and 10-11°C in winter.

In the future, mean maximum temperature is projected to increase by 0.5-1.0°C for most parts of the region in all seasons (and annual) by 2040 under RCP4.5 (Figure 3-7). More warming occurs further inland in summer (1.0-1.5°C). Under RCP8.5 by 2040, most of the region experiences warming of 1.0-1.5°C during autumn and spring, as well as inland areas during summer (Figure 3-8). By 2090, most of the region is projected to warm by 1.0-1.5°C under RCP4.5 at the annual scale, with 1.5-2.0°C of warming for inland areas (Figure 3-9). Under RCP8.5 (Figure 3-10), warming is projected to be around 3.0-3.5°C for most of the region at the annual scale (with less warming for coastal areas of 2.5-3.0°C). At the seasonal scale, widespread warming of 3.0-3.5°C is projected for autumn and spring, as well as isolated inland areas experiencing 3.5-4.0°C of warming. The least warming is projected in winter (2.5-3.0°C for most of the region).

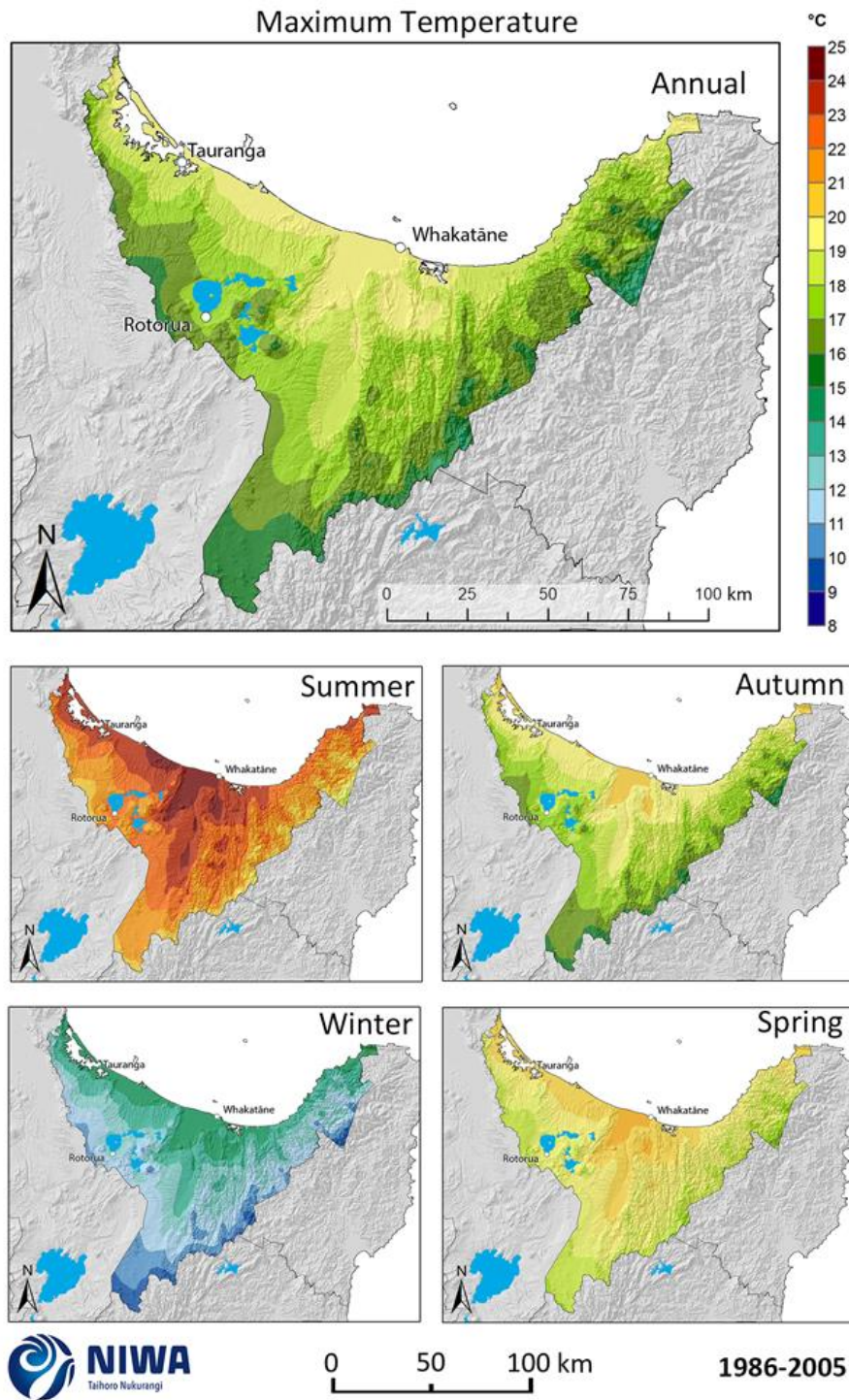


**Figure 3-6: Modelled annual and seasonal mean maximum temperature, average over 1986-2005.** Results are based on dynamical downscaled projections using NIWA's Regional Climate Model. Resolution of projection is 5km x 5km.

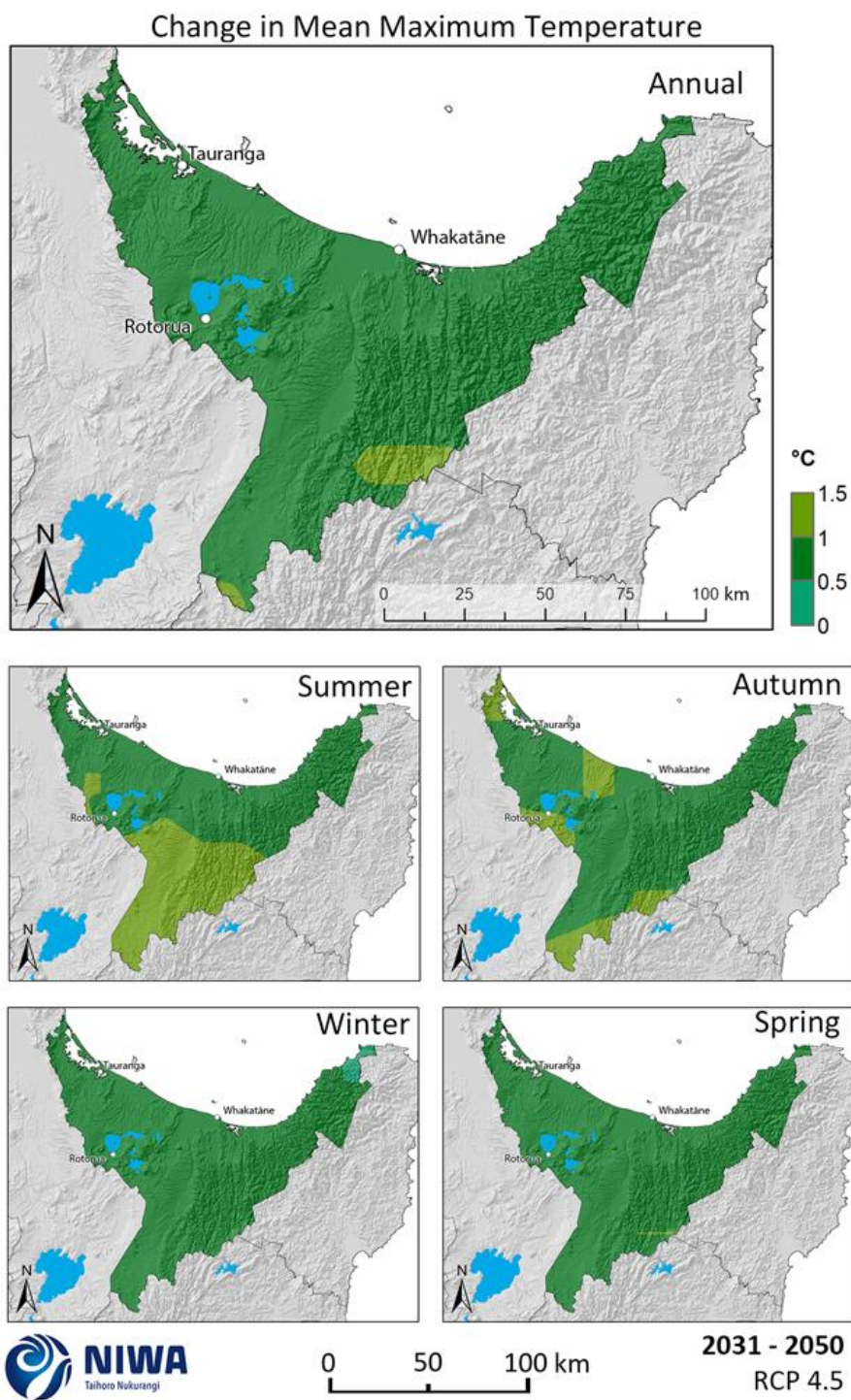


**Figure 3-7: Projected annual and seasonal mean maximum temperature changes by 2040 for RCP4.5.** Relative to 1986-2005 average, based on the average of six global climate models. Results are based on dynamical downscaled projections using NIWA's Regional Climate Model. Resolution of projection is 5km x 5km.



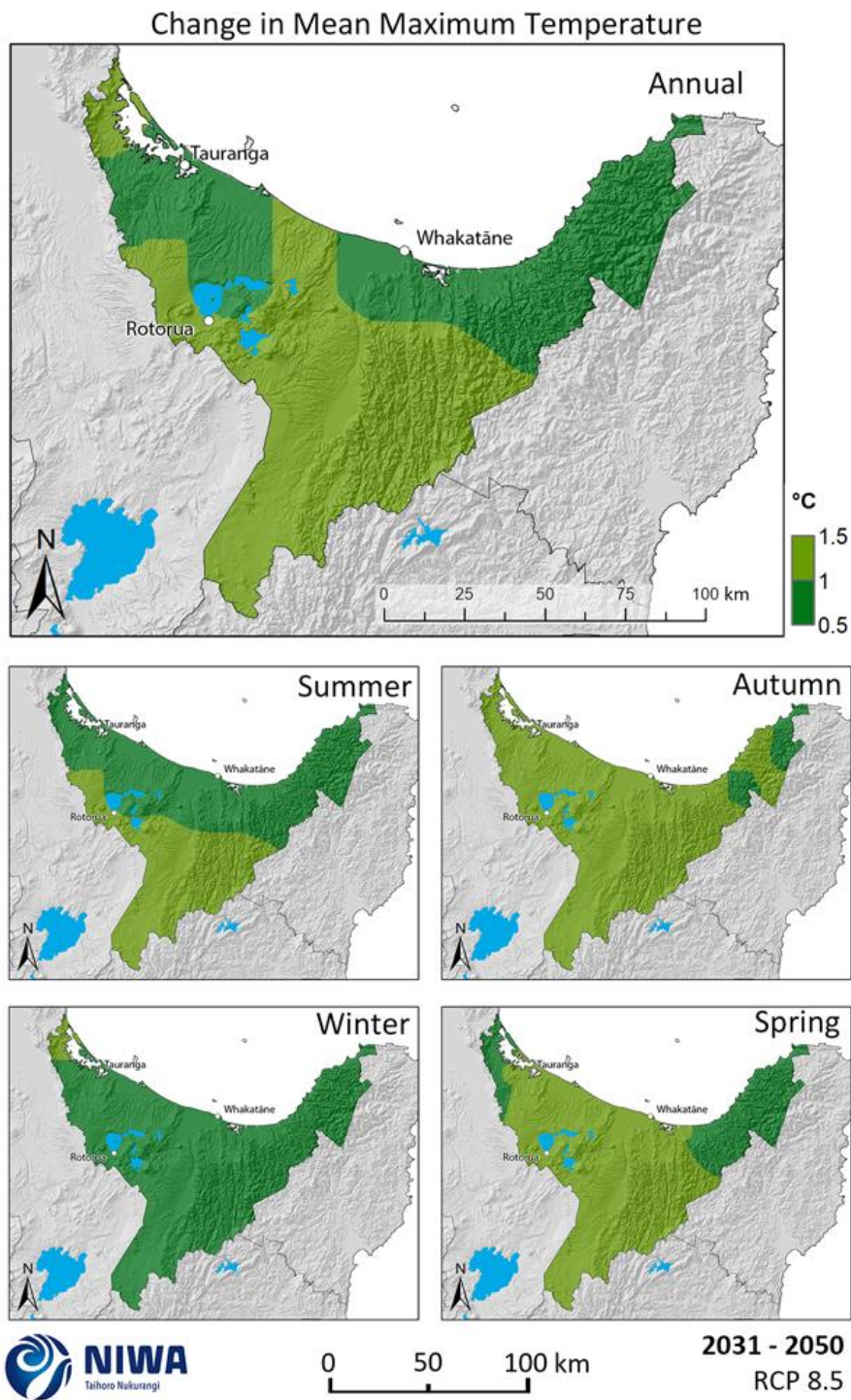


**Figure 3-8: Projected annual and seasonal mean maximum temperature changes by 2040 for RCP8.5.** Relative to 1986-2005 average, based on the average of six global climate models. Results are based on dynamical downscaled projections using NIWA's Regional Climate Model. Resolution of projection is 5km x 5km.

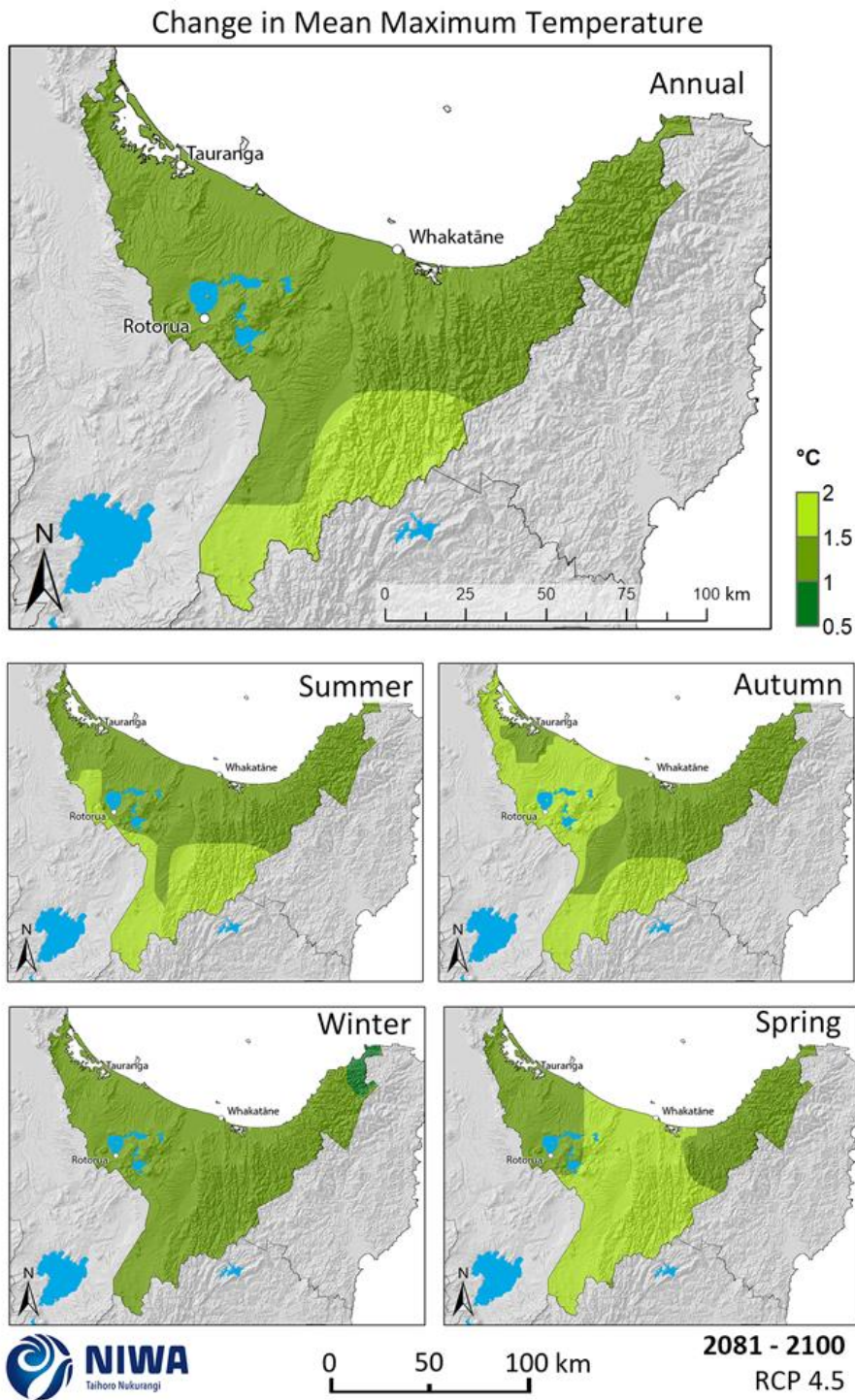


**Figure 3-9: Projected annual and seasonal mean maximum temperature changes by 2090 for RCP4.5.** Relative to 1986-2005 average, based on the average of six global climate models. Results are based on dynamical downscaled projections using NIWA's Regional Climate Model. Resolution of projection is 5km x 5km.

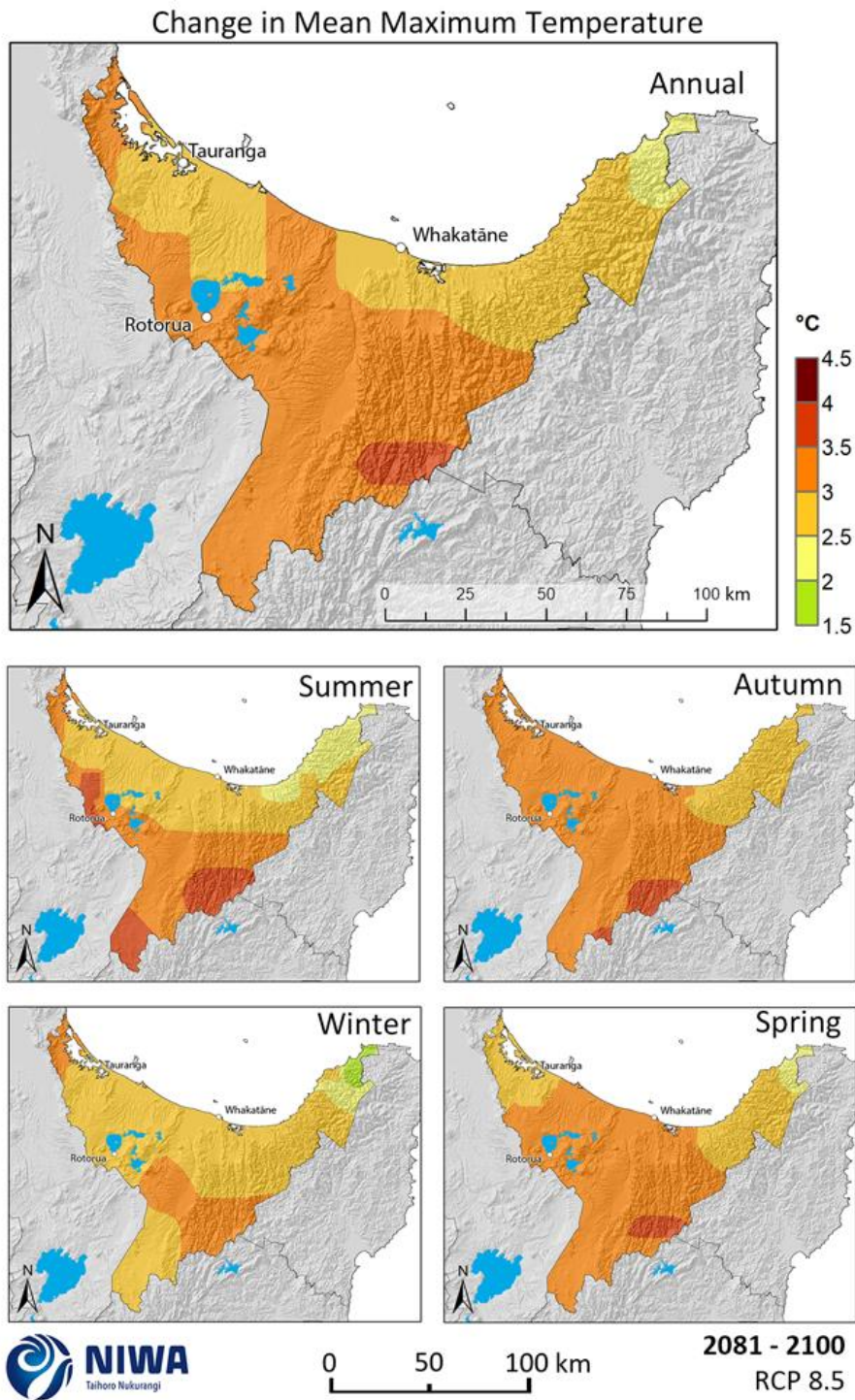


**Figure 3-10: Projected annual and seasonal mean maximum temperature changes by 2090 for RCP8.5.** Relative to 1986-2005 average, based on the average of six global climate models. Results are based on dynamical downscaled projections using NIWA's Regional Climate Model. Resolution of projection is 5km x 5km.

### 3.3 Minimum temperature

Minimum temperatures are generally recorded in the early hours of the morning, and therefore are known as night time temperatures. Historic (average over 1986-2005) and future (average over 2031-2050 and 2081-2100) maps for mean minimum temperature are shown in this section. The historic maps show annual and seasonal mean minimum temperature in units of degrees Celsius (°C) and the future projection maps show the change in mean minimum temperature compared with the historic period, in units of °C. Note that the historic maps are on a different colour scale to the future projection maps.

For the historic period, the coastal Bay of Plenty has the warmest annual and seasonal mean minimum temperatures (Figure 3-11), particularly in the west of the region. Mean annual minimum temperatures are 9-11°C, 13-14°C in summer and 5-6°C in winter. The areas furthest inland have the coolest mean minimum temperatures, with 5-6°C mean annual temperatures, 9-11°C in summer and 1-2°C in winter.

In the future, mean minimum temperature is projected to increase by 0.5-1.0°C for most parts of the region in all seasons (and annual) by 2040 under RCP4.5 (Figure 3-12). Under RCP8.5 by 2040, most of the region experiences warming of 1.0-1.5°C during autumn, but at the annual timescale warming is around 0.5-1.0°C (Figure 3-13). By 2090, most of the region is projected to warm by 1.0-1.5°C under RCP4.5 at the annual scale, as well as for summer, autumn and spring. For winter, 0.5-1.0°C of warming is widespread (Figure 3-14). Under RCP8.5 (Figure 3-15), warming is projected to be around 2.5-3.0°C for most of the region at the annual scale (with less warming for eastern areas of 1.5-2.5°C). At the seasonal scale, widespread warming of 3.0-3.5°C is projected for autumn and western areas in summer. The least warming is projected in winter (2.0-2.5°C for most of the region).

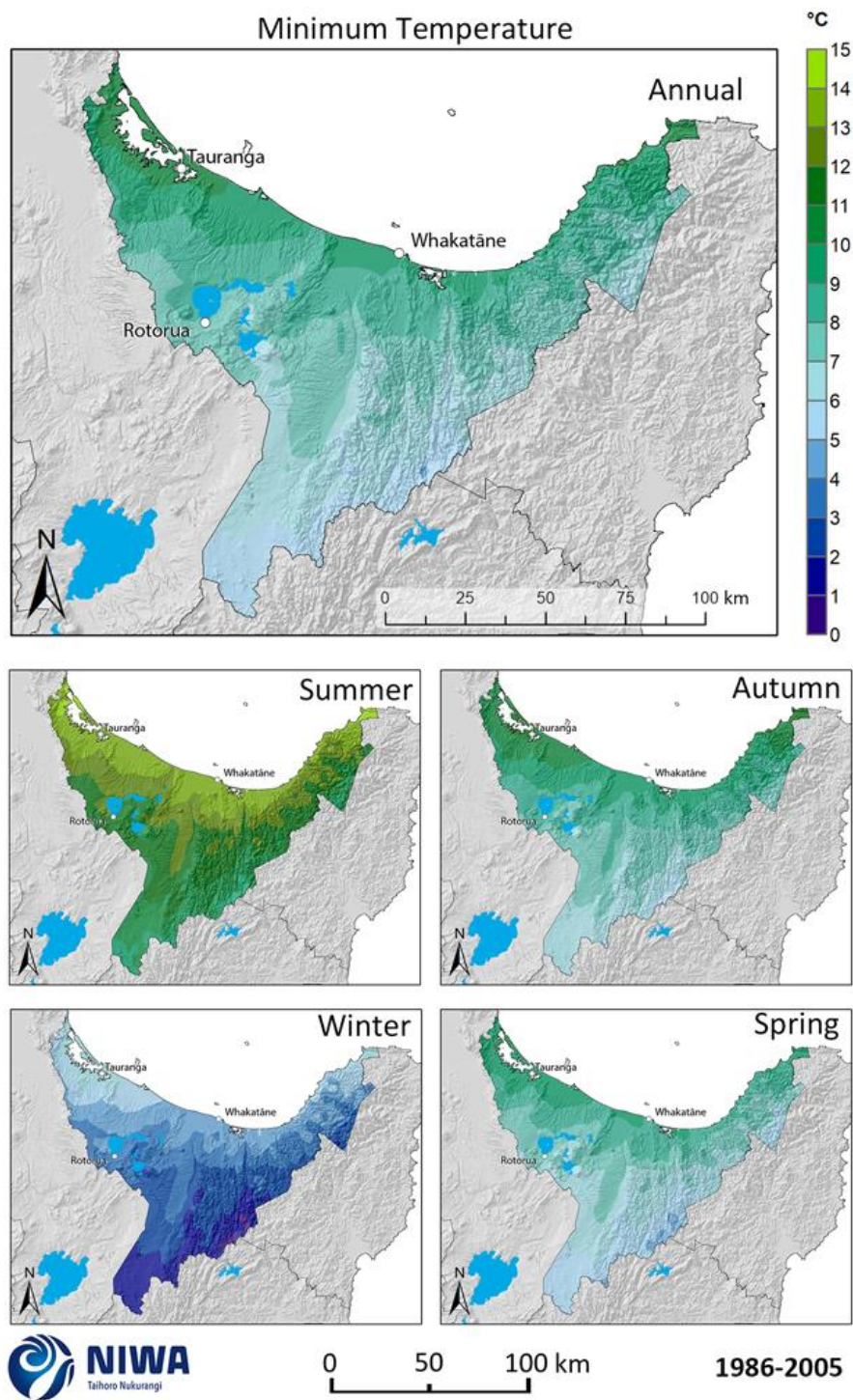


**Figure 3-11: Modelled annual and seasonal mean minimum temperature, average over 1986-2005.** Results are based on dynamical downscaled projections using NIWA's Regional Climate Model. Resolution of projection is 5km x 5km.

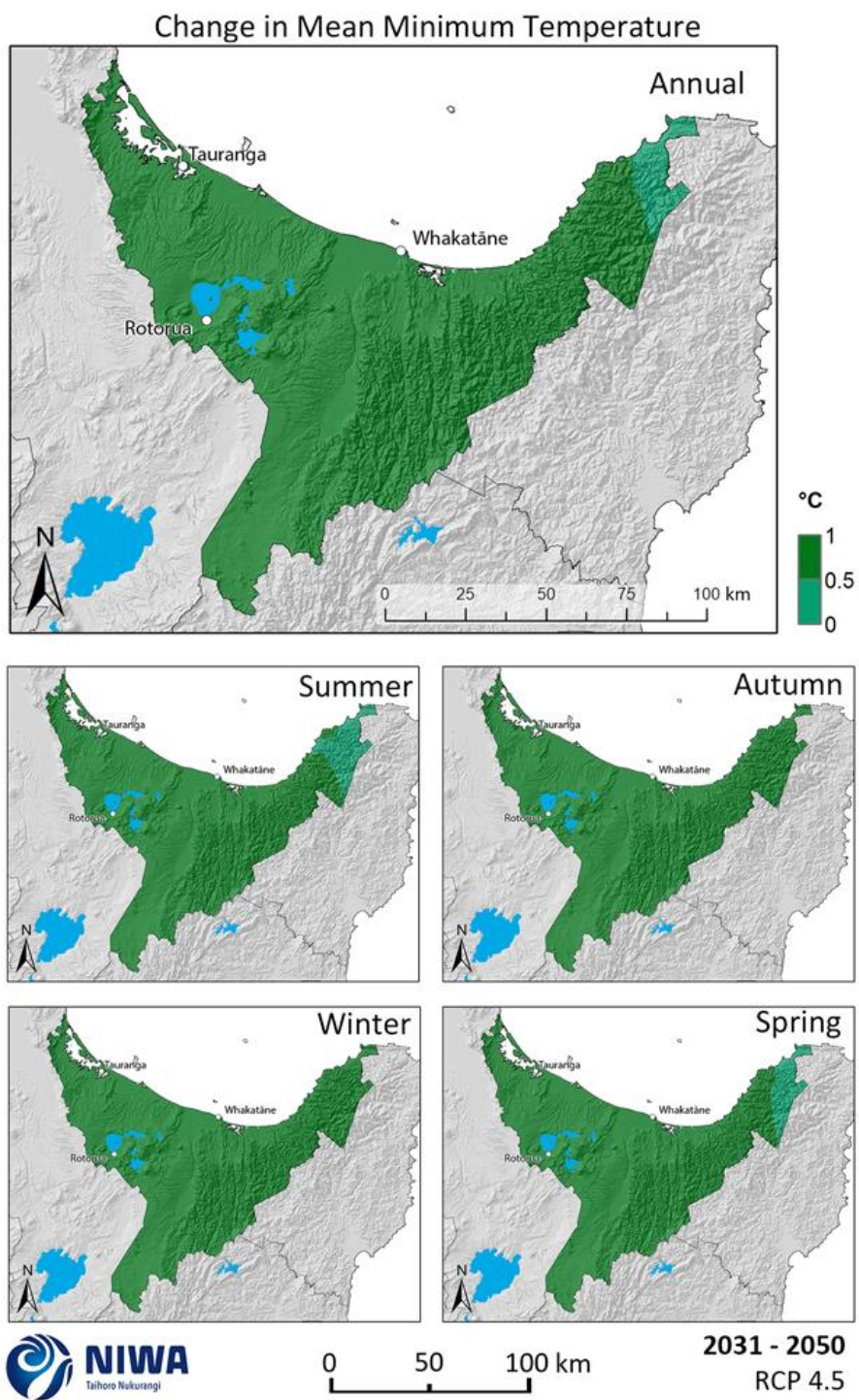


**Figure 3-12: Projected annual and seasonal mean minimum temperature changes by 2040 for RCP4.5.** Relative to 1986-2005 average, based on the average of six global climate models. Results are based on dynamical downscaled projections using NIWA's Regional Climate Model. Resolution of projection is 5km x 5km.

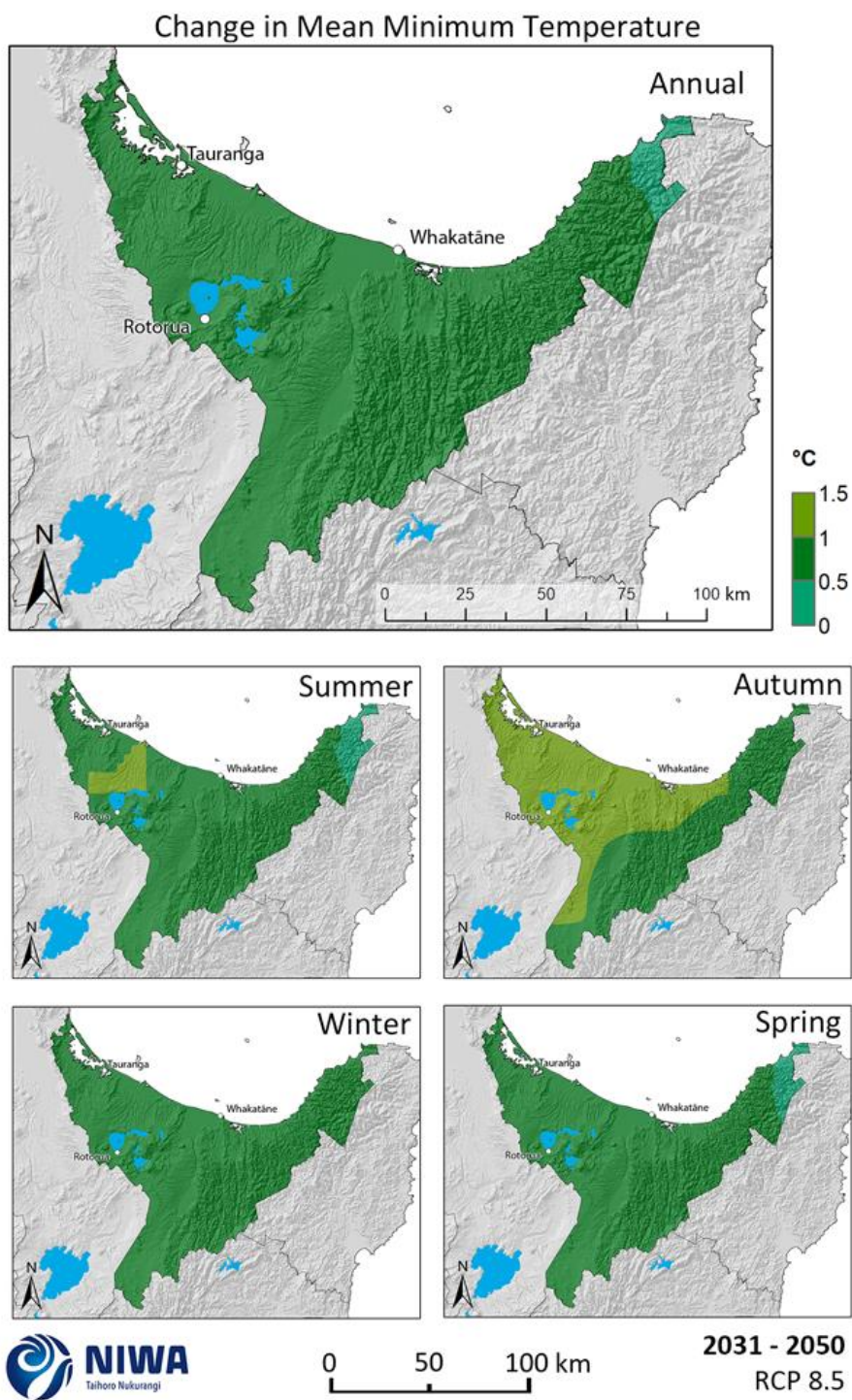


**Figure 3-13: Projected annual and seasonal mean minimum temperature changes by 2040 for RCP8.5.** Relative to 1986-2005 average, based on the average of six global climate models. Results are based on dynamical downscaled projections using NIWA's Regional Climate Model. Resolution of projection is 5km x 5km.

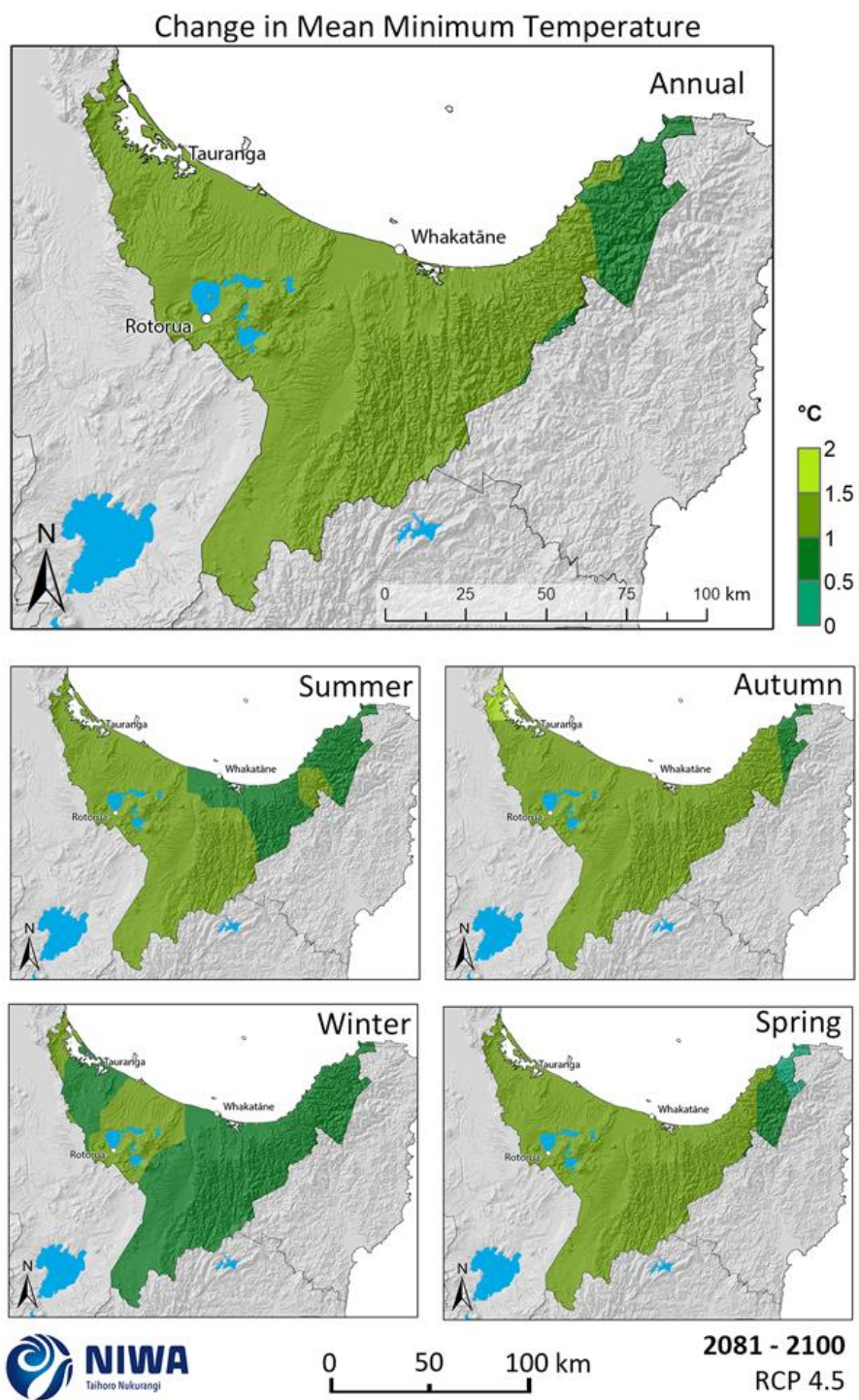


**Figure 3-14: Projected annual and seasonal mean minimum temperature changes by 2090 for RCP4.5.** Relative to 1986-2005 average, based on the average of six global climate models. Results are based on dynamical downscaled projections using NIWA's Regional Climate Model. Resolution of projection is 5km x 5km.



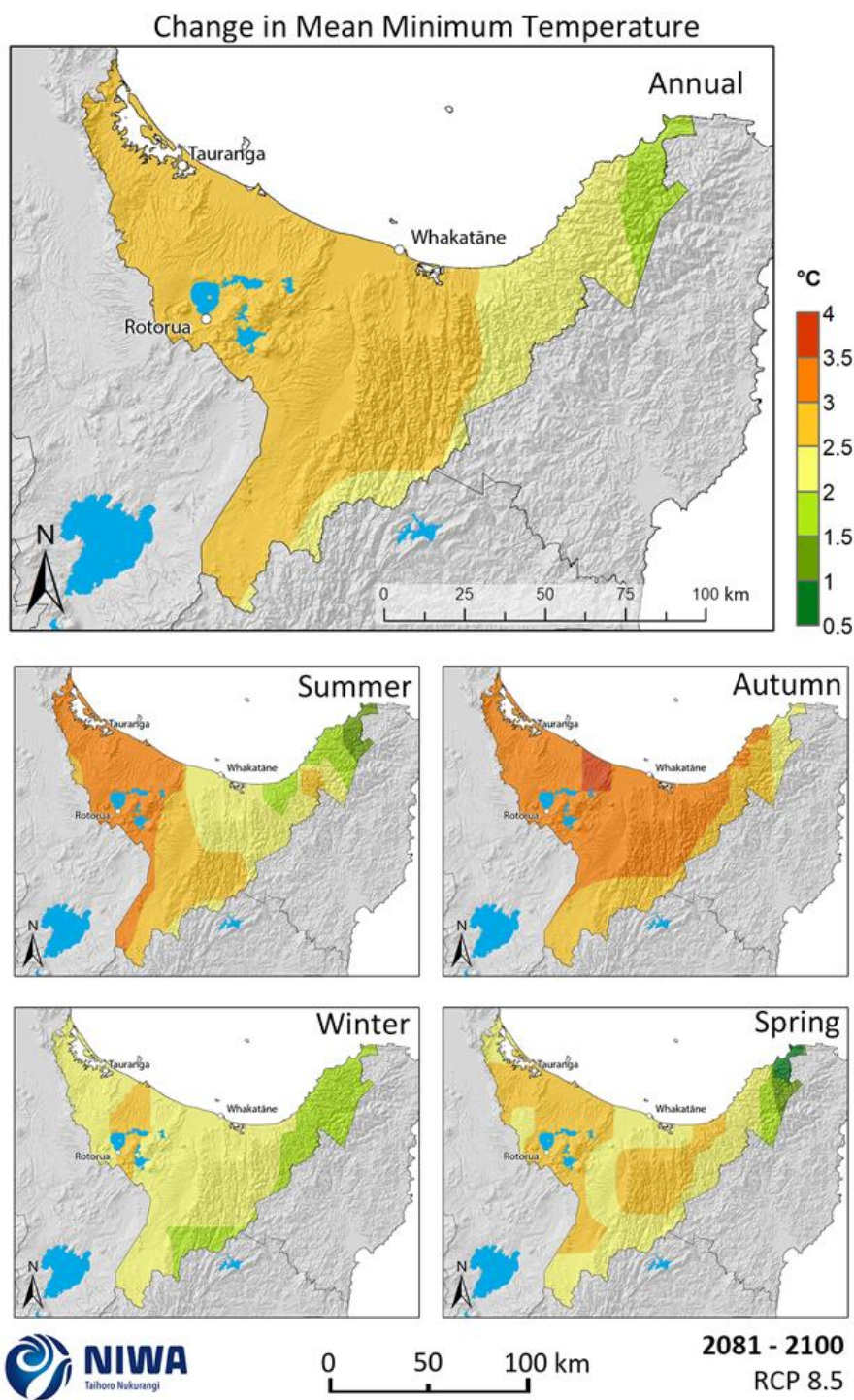


**Figure 3-15: Projected annual and seasonal mean minimum temperature changes by 2090 for RCP8.5.** Relative to 1986-2005 average, based on the average of six global climate models. Results are based on dynamical downscaled projections using NIWA's Regional Climate Model. Resolution of projection is 5km x 5km.

### 3.4 Diurnal temperature range

The diurnal temperature range is the average of the difference between the daily minimum and daily maximum temperatures over the seasons and years of the 20-year baseline (1986-2005) and future (2031-2050 and 2081-2100) periods. Historic (average over 1986-2005) and future (average over 2031-2050 and 2081-2100) maps for mean diurnal temperature range are shown in this section. The historic maps show annual and seasonal mean diurnal temperature range in units of degrees Celsius (°C) and the future projection maps show the change in mean diurnal temperature range compared with the historic period, in units of °C. Note that the historic maps are on a different colour scale to the future projection maps.

For the historic period, the central Bay of Plenty has the largest diurnal temperature range (Figure 3-16), particularly the area around Murupara. Mean annual diurnal temperature range is 11-12°C, 12-13°C in summer and 10-11°C in winter. Western areas have the lowest diurnal temperature range temperatures, with 8-9°C mean annual diurnal temperature range, 9-10°C in summer and 7-8°C in winter.

In the future, diurnal temperature range is projected to increase by 0-0.5°C for most parts of the region in all seasons (and annual) by 2040 under RCP4.5 and RCP8.5, with some small parts of the region projecting decreases of 0-0.5°C (Figure 3-17 and Figure 3-18). By 2090 under RCP4.5, much of the region is projected to experience increases in diurnal temperature range of 0-0.5°C, with some eastern high elevation region expecting increases of 0.5-1.0°C (Figure 3-19). Under RCP8.5 by 2090, the western and coastal parts of the region are expected to increase by 0-0.5°C and the eastern and southern hill country is expected to increase by 1.0-1.5°C (annual) (Figure 3-20). During autumn and summer, parts of the region are projected to decrease by 0-0.5°C. During summer, winter and spring, diurnal temperature range is projected to increase by 1.0-1.5°C in the hill country in the east and south.

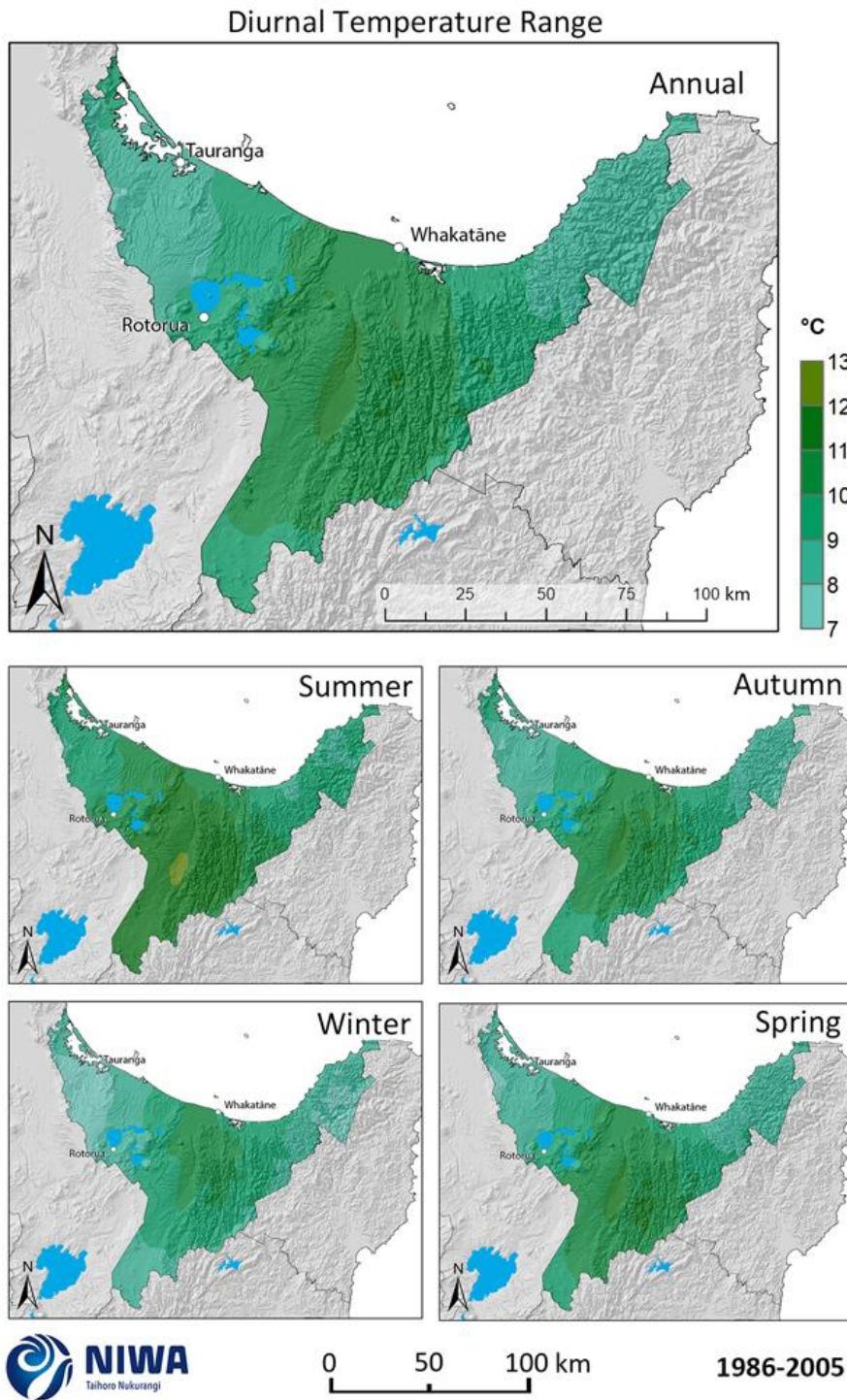


**Figure 3-16: Modelled annual and seasonal mean diurnal temperature range, average over 1986-2005.** Results are based on dynamical downscaled projections using NIWA's Regional Climate Model. Resolution of projection is 5km x 5km.

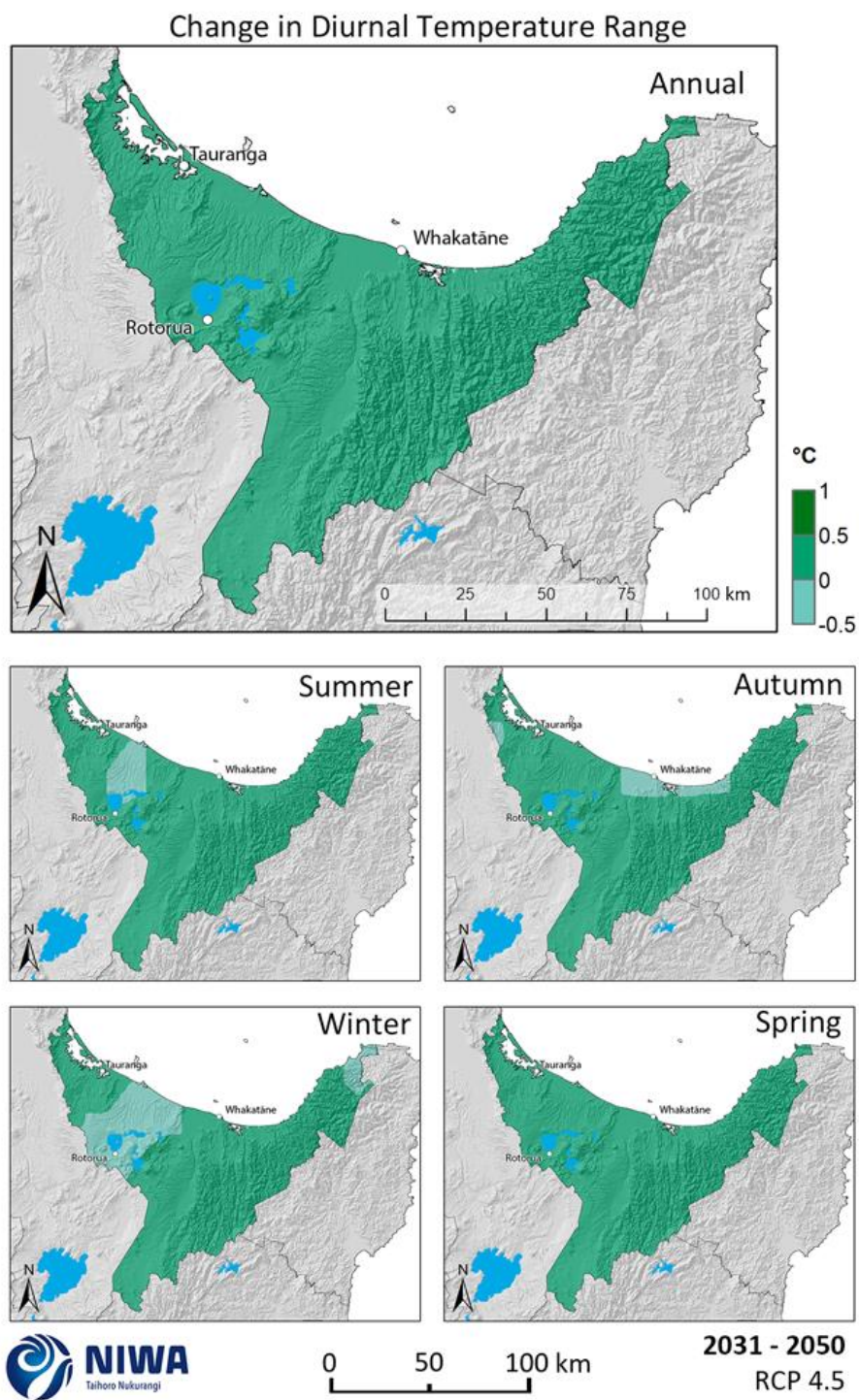


**Figure 3-17: Projected annual and seasonal diurnal temperature range changes by 2040 for RCP4.5.** Relative to 1986-2005 average, based on the average of six global climate models. Results are based on dynamical downscaled projections using NIWA's Regional Climate Model. Resolution of projection is 5km x 5km.

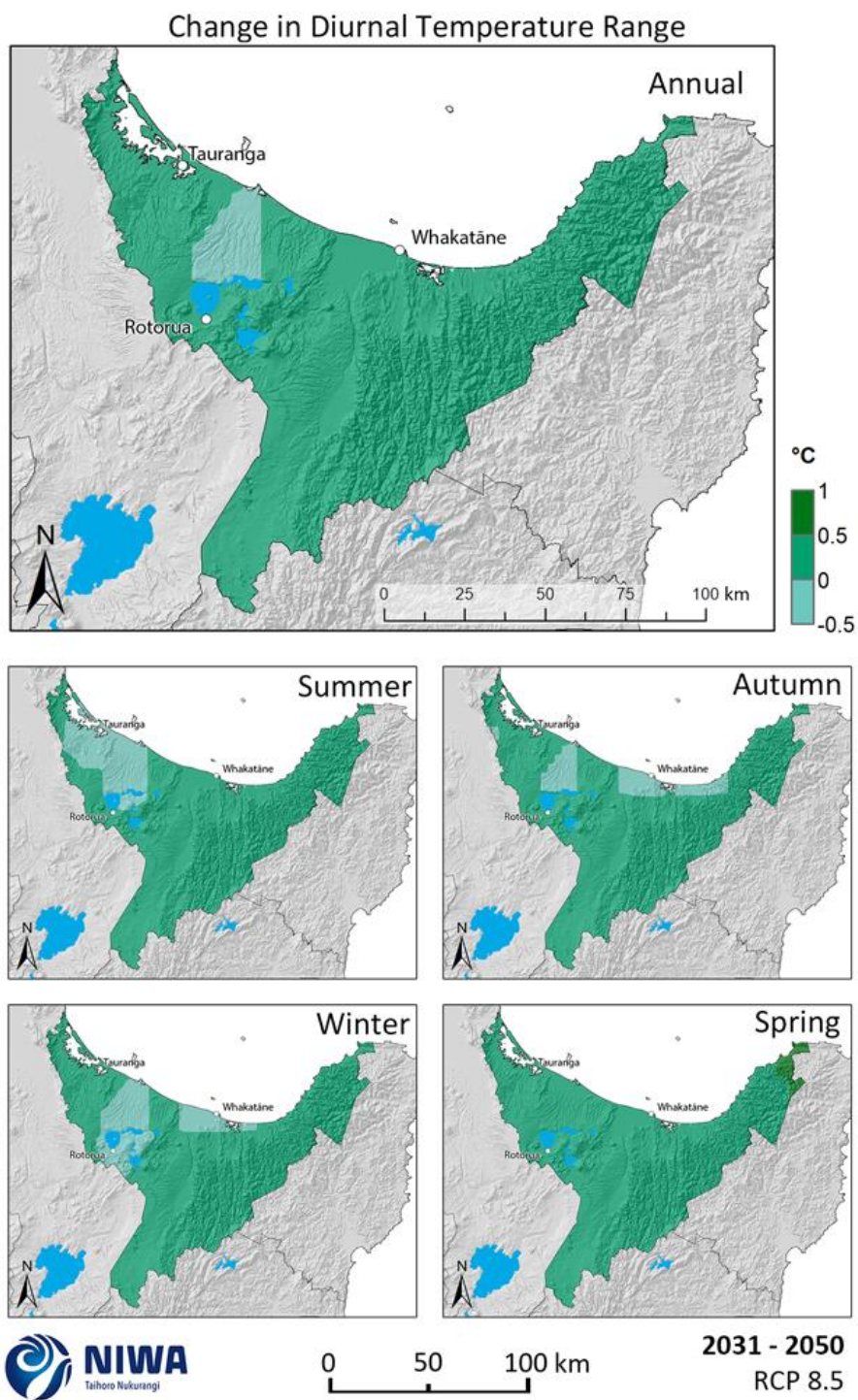


**Figure 3-18: Projected annual and seasonal diurnal temperature range changes by 2040 for RCP8.5.** Relative to 1986-2005 average, based on the average of six global climate models. Results are based on dynamical downscaled projections using NIWA's Regional Climate Model. Resolution of projection is 5km x 5km.

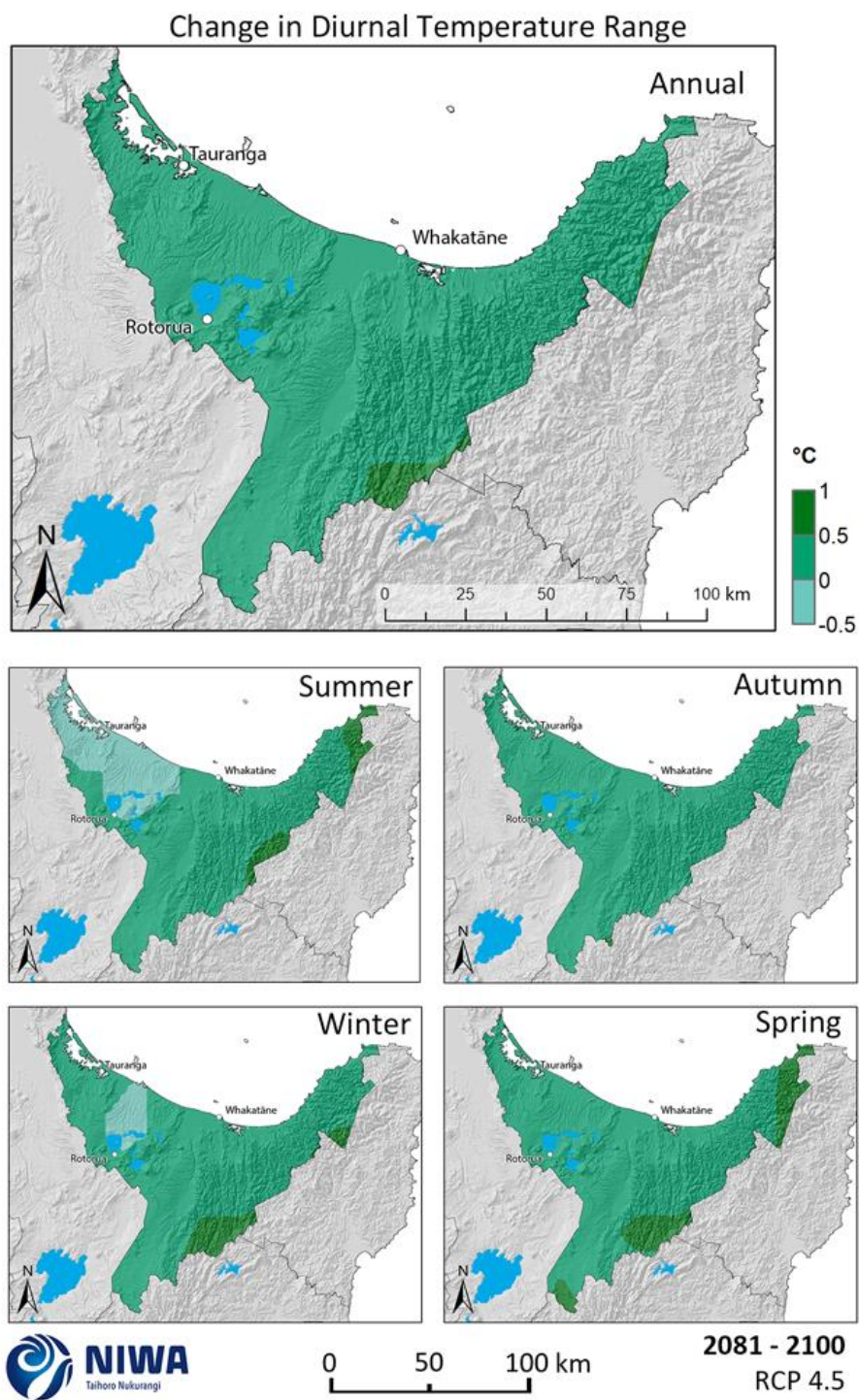


**Figure 3-19: Projected annual and seasonal diurnal temperature range changes by 2090 for RCP4.5.** Relative to 1986-2005 average, based on the average of six global climate models. Results are based on dynamical downscaled projections using NIWA's Regional Climate Model. Resolution of projection is 5km x 5km.

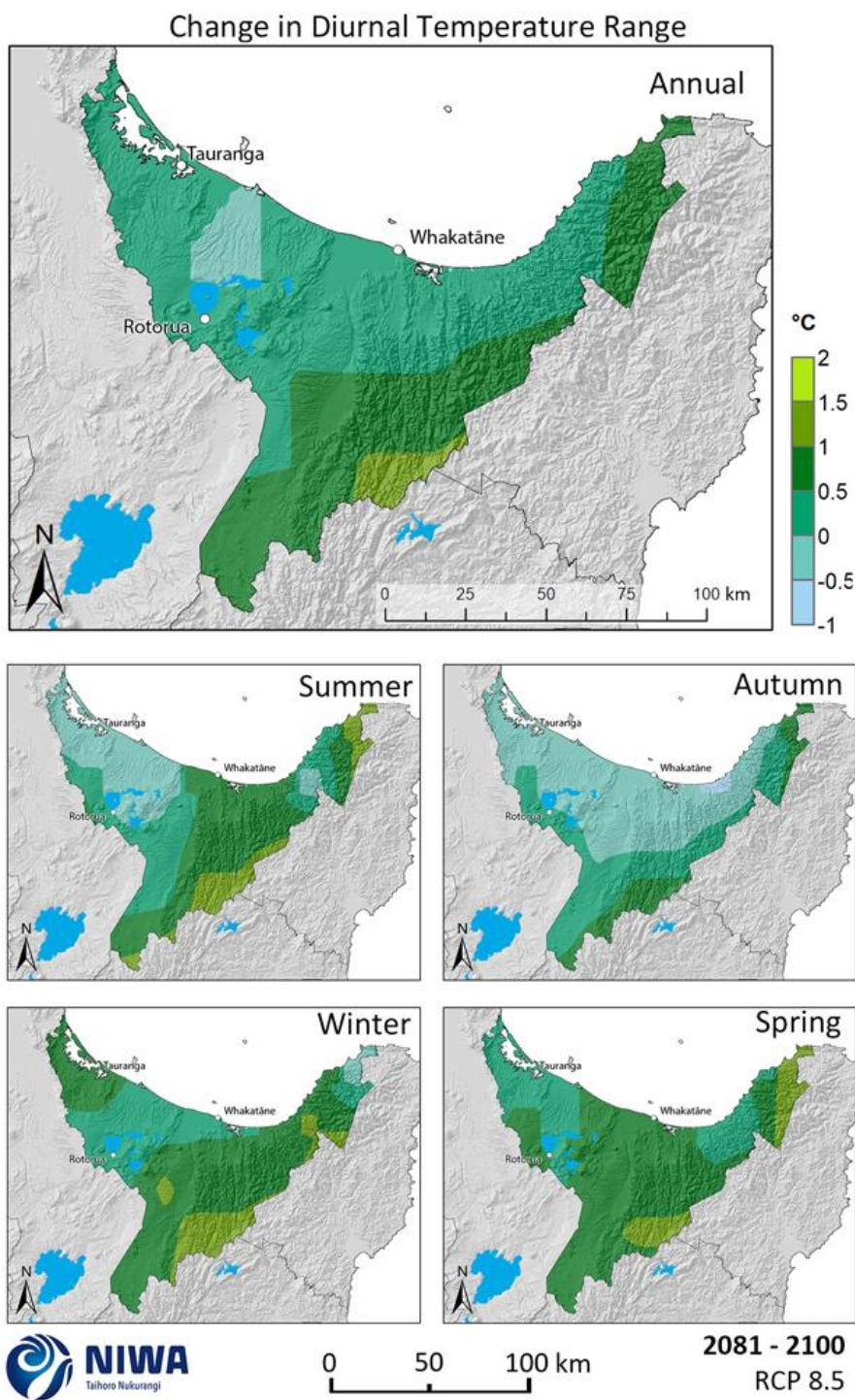


**Figure 3-20: Projected annual and seasonal diurnal temperature range changes by 2090 for RCP8.5.** Relative to 1986-2005 average, based on the average of six global climate models. Results are based on dynamical downscaled projections using NIWA's Regional Climate Model. Resolution of projection is 5km x 5km.

### 3.5 Hot days

In this report, a hot day is considered to be when the maximum temperature is above 25°C. Hot days are defined as such because temperatures over this threshold are considered 'hot' given New Zealand's temperate maritime climate. This threshold is consistent with Ministry for the Environment (2018). Historic (average over 1986-2005) and future (average over 2031-2050 and 2081-2100) maps for hot days are shown in this section. The historic maps show annual average numbers of hot days and the future projection maps show the change in the annual number of hot days compared with the historic period. Note that the historic maps are on a different colour scale to the future projection maps. Table 3-1 and Figure 3-23 shows the historic and future projected numbers of hot days for the model grid square closest to specific locations in the Bay of Plenty region.

For the historic period, the annual number of hot days is highest in the area around Kawerau (Figure 3-21), with >45 hot days per year. Areas around Maketu, Murupara, and coastward of Kawerau experience 40-45 hot days per year. The area around Tauranga experiences 25-30 hot days per year. The high elevations of the Raukumara Ranges experience 0-2 hot days per year in the historic period.

In the future, the number of hot days per year shows similar patterns under both RCP4.5 and RCP8.5 by 2040 (Figure 3-22). Hot days in the central part of the region between Maketu and Whakatāne and inland to Murupara have the largest projected changes and are projected to increase by 20-25 days per year. Other coastal areas and slightly higher elevations are projecting increases of 15-20 hot days per year. The inland borders of the region are projected to experience increases of 5-10 hot days per year, with fewer in the eastern hill country (1-5 more hot days per year). By 2090, the projected magnitude of changes in hot days are quite different between the two scenarios, although the spatial pattern is similar. Under RCP4.5, 30-40 more hot days per year are projected between Maketu and Whakatāne, and inland to Murupara, whereas under RCP8.5 70-80 more hot days per year are projected for this same area. Increases are smaller for other areas, but still substantial under RCP8.5 – most of the region outside of the highest elevations of the Raukumara Ranges is projected to experience at least 40 more hot days per year than for the historic period.



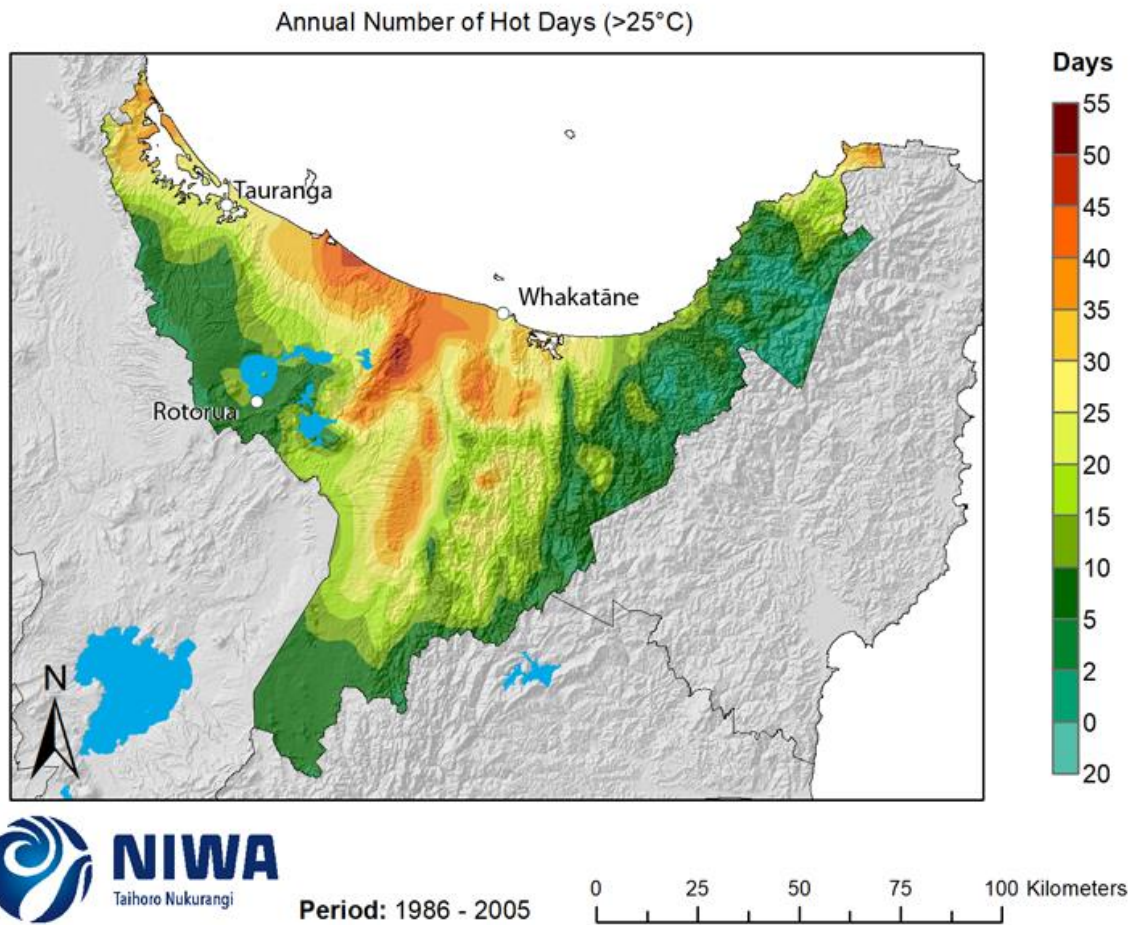


**Figure 3-21: Modelled annual number of hot days (days with maximum temperature >25°C), average over 1986-2005.** Results are based on dynamical downscaled projections using NIWA's Regional Climate Model. Resolution of projection is 5km x 5km.

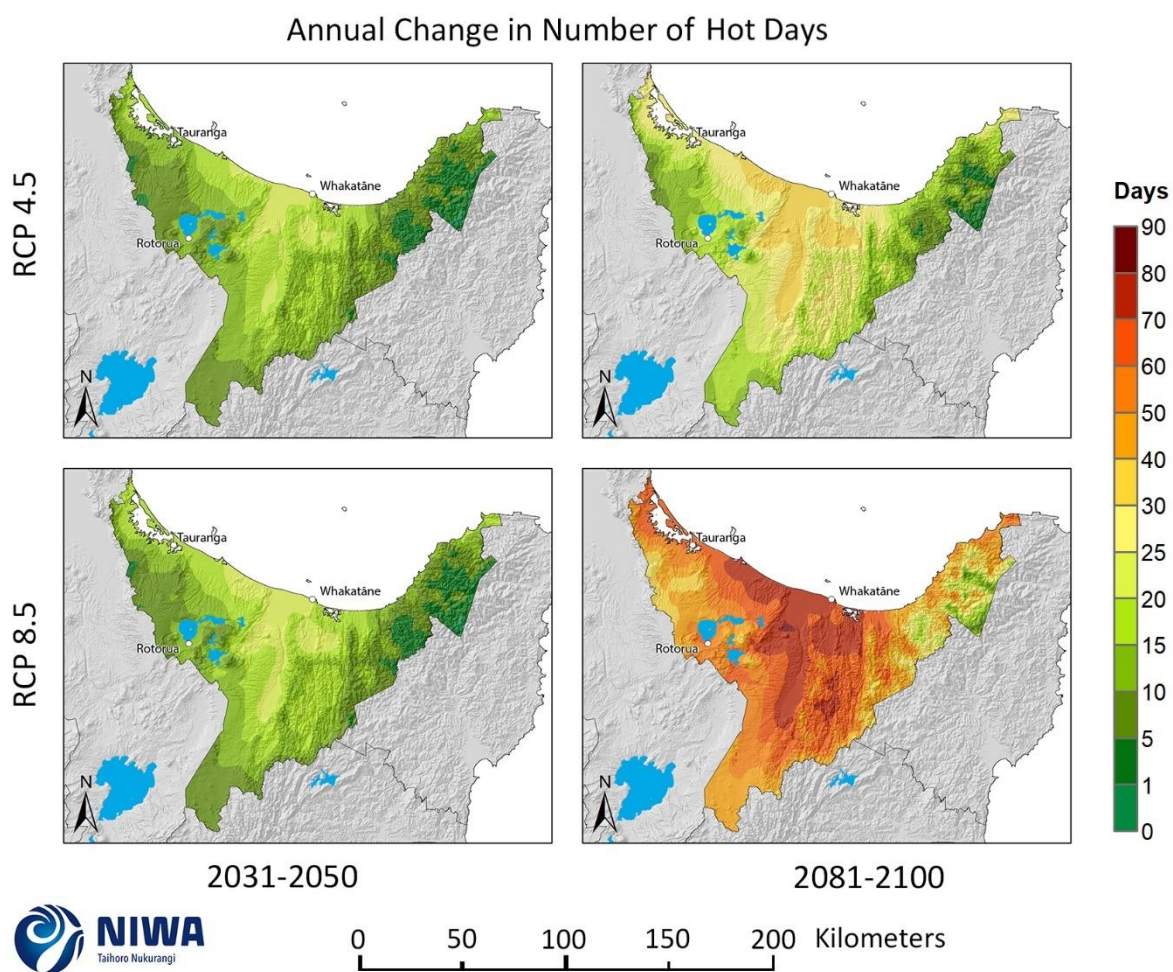


**Figure 3-22: Projected annual hot day (maximum temperature >25°C) changes for RCP4.5 and RCP8.5, by 2040 and 2090.** Relative to 1986-2005 average, based on the average of six global climate models. Results are based on dynamical downscaled projections using NIWA's Regional Climate Model. Resolution of projection is 5km x 5km.

**Table 3-1: Modelled annual average number of hot days (maximum temperature >25°C) for the historic period and two climate change scenarios (RCP4.5 and RCP8.5) at two future time periods.** Future projections are shown as the total future projected number of hot days outside the parentheses, and future change inside the parentheses. Time periods: historic: 1986-2005, mid-century: 2031-2050 "2040", end-century: 2081-2100 "2090"; based on the average of six global climate models.

Location	Historic	Future change		
Location	RCP	2040	2090	
Waihi Beach				
Tauranga				
Te Puke				
Rotorua				
Kawerau				
Whakatāne				
Ōpōtiki				
Katikati				

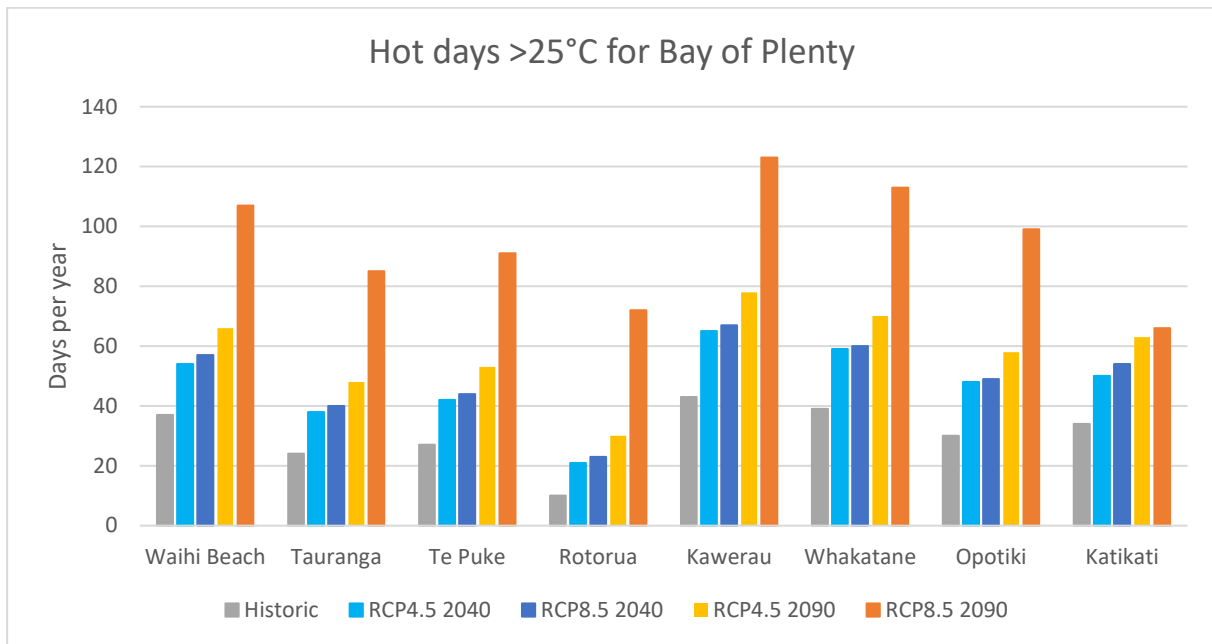


**Figure 3-23: Historic and future projected numbers of hot days for locations in the Bay of Plenty.**

### 3.6 Extreme hot days

In this report, an extreme hot day is considered to be when the maximum temperature is above 30°C. Historic (average over 1986-2005) and future (average over 2031-2050 and 2081-2100) maps for extreme hot days are shown in this section. The historic maps show annual average numbers of extreme hot days and the future projection maps show the change in the annual number of extreme hot days compared with the historic period. Note that the historic maps are on a different colour scale to the future projection maps.

For the historic period, there are only small occurrences of extreme hot days in the Bay of Plenty Region. The annual number of extreme hot days is highest in the coastal areas between Maketu and Whakatāne, and inland towards Kawerau (Figure 3-24), with 0.5-1 extreme hot days per year on average. The rest of the region has negligible extreme hot days in the historic period.

In the future, the number of extreme hot days per year shows similar patterns under both RCP4.5 and RCP8.5 by 2040 (Figure 3-25). Extreme hot days in the central part of the region between Maketu and Whakatāne and inland to Murupara have the largest projected changes of 1-2 more extreme hot days per year. Other coastal areas and slightly higher elevations are projecting increases of 15-20 hot days per year. Negligible change is apparent for other parts of the region at 2040. However, by 2090, more extreme hot days are expected to occur. Under RCP4.5, low elevation areas between Maketu and Whakatāne, and further inland, expect 2-4 more extreme hot days under RCP4.5 (negligible change elsewhere). Under RCP8.5, much of the central and coastal parts of the region are projected to experience at least 4 more extreme hot days per year, with some areas expecting 10-14 more hot days per year (around Waihi Beach, the coastal area from Maketu to Whakatāne, Kawerau, Murupara, and parts of Te Urewera National Park).

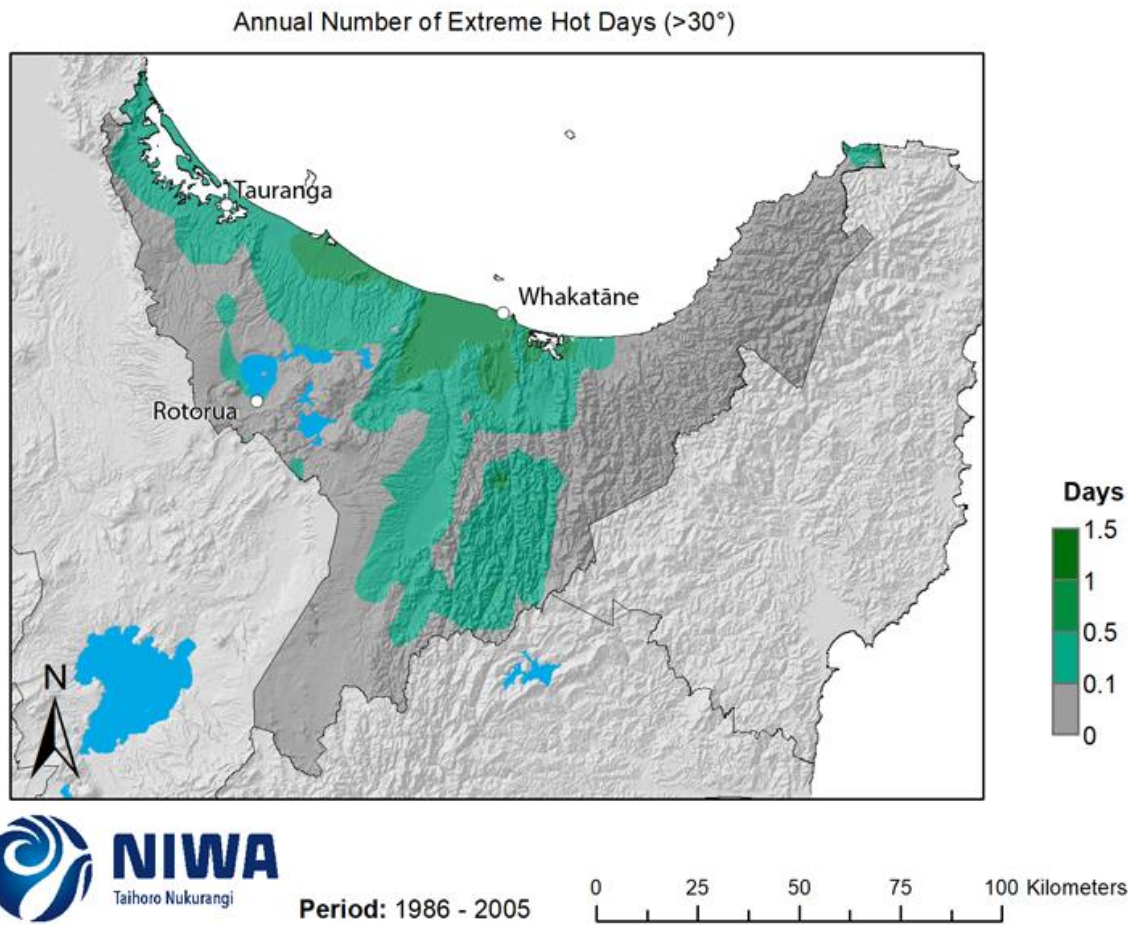


**Figure 3-24: Modelled annual number of extreme hot days (days with maximum temperature >30°C), average over 1986-2005.** Results are based on dynamical downscaled projections using NIWA's Regional Climate Model. Resolution of projection is 5km x 5km.

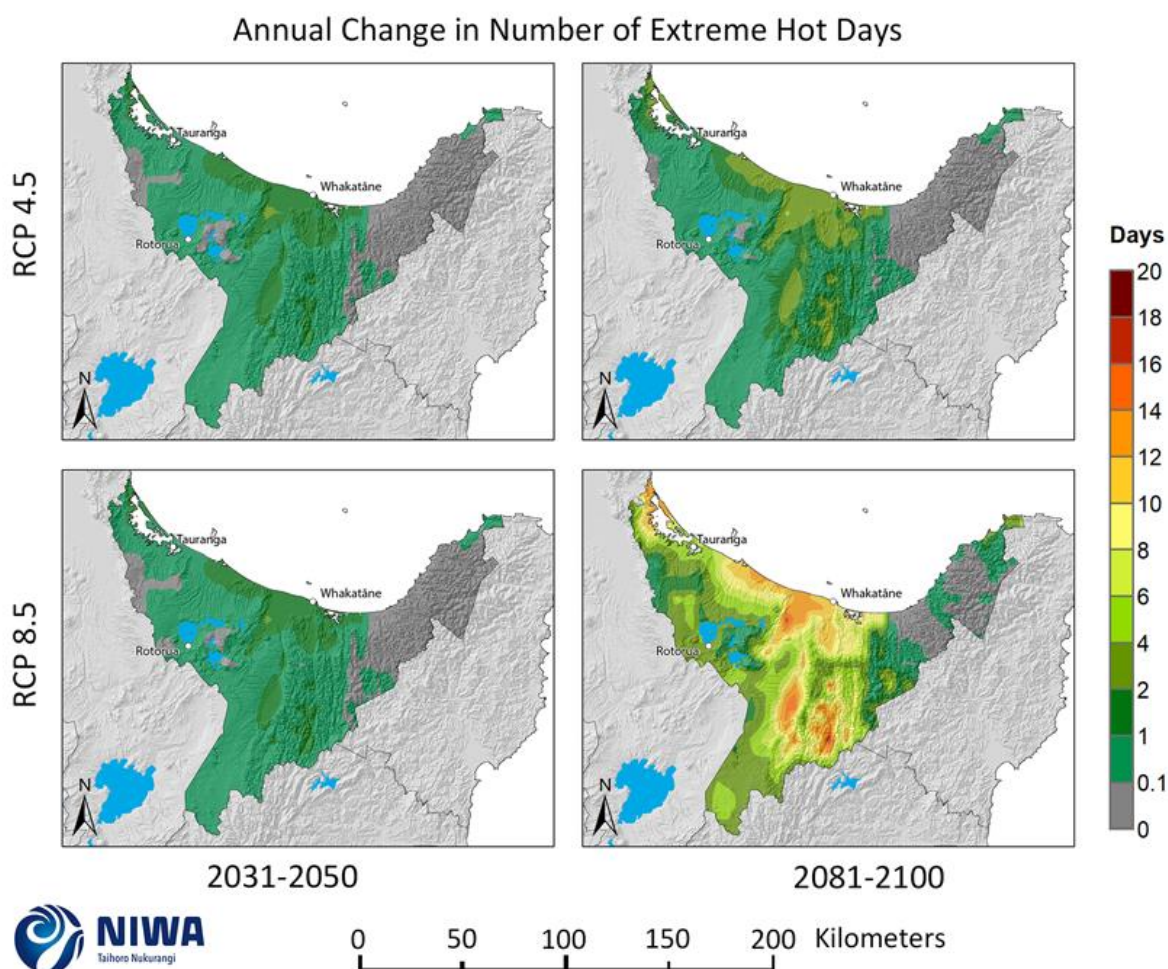


**Figure 3-25: Projected annual extreme hot day (maximum temperature >30°C) changes for RCP4.5 and RCP8.5, by 2040 and 2090.** Relative to 1986-2005 average, based on the average of six global climate models. Results are based on dynamical downscaled projections using NIWA's Regional Climate Model. Resolution of projection is 5km x 5km.

### 3.7 Heatwave days

The definition of a heatwave as considered here is a period of three or more consecutive days where the maximum daily temperature exceeds 25°C. This calculation is an aggregation of all days per year that are included in a heatwave (i.e., ≥ three consecutive days with maximum temperature > 25°C), no matter the length of the heatwave. The annual heatwave days are then averaged over the 20-year period of interest (e.g., 2031-2050) to get the average annual heatwave-day climatology (past) and future projections.

Historic (average over 1986-2005) and future (average over 2031-2050 and 2081-2100) maps for heatwave days are shown in this section. The historic maps show annual average numbers of heatwave days and the future projection maps show the change in the annual number of heatwave-days compared with the historic period. Note that the historic maps are on a different colour scale to the future projection maps.

For the historic period, the annual number of heatwave days is highest in the area around Kawerau (Figure 3-26), with 30-35 heatwave days per year. Areas around Maketu, Murupara, and coastward

of Kawerau experience 25-30 heatwave days per year. The Kaimai-Mamaku Ranges and Raukumara Ranges experience less than one heatwave day per year.

In the future, the number of heatwave days per year shows similar patterns under both RCP4.5 and RCP8.5 by 2040 (Figure 3-27). Heatwave days around Kawerau are projected to have the largest changes, with increases of 20-30 heatwave days per year by 2040. The central part of the region between Maketu and Whakatāne and inland to Murupara have projected increases of 15-20 heatwave days per year. The inland borders of the region are projected to experience increases of 2-5 heatwave days per year, with fewer in the eastern hill country (0.1-2 more heatwave days per year). By 2090, the projected magnitude of changes in hot days are quite different between the two scenarios, although the spatial pattern is similar. Under RCP4.5, 30-40 more heatwave days are projected for the areas around Kawerau and Murupara and 20-30 more heatwave days are projected for most of the central part of the region. Under RCP8.5, 70-80 more heatwave days per year are projected for the central part of the region (between Maketu and Whakatāne, inland to Kawerau and Murupara). A small area of 80-90 more heatwave days per year is projected for Kawerau. At least 30 more heatwave days per year is projected for the whole region aside from the Raukumara Ranges and the Kaimai-Mamaku Ranges.

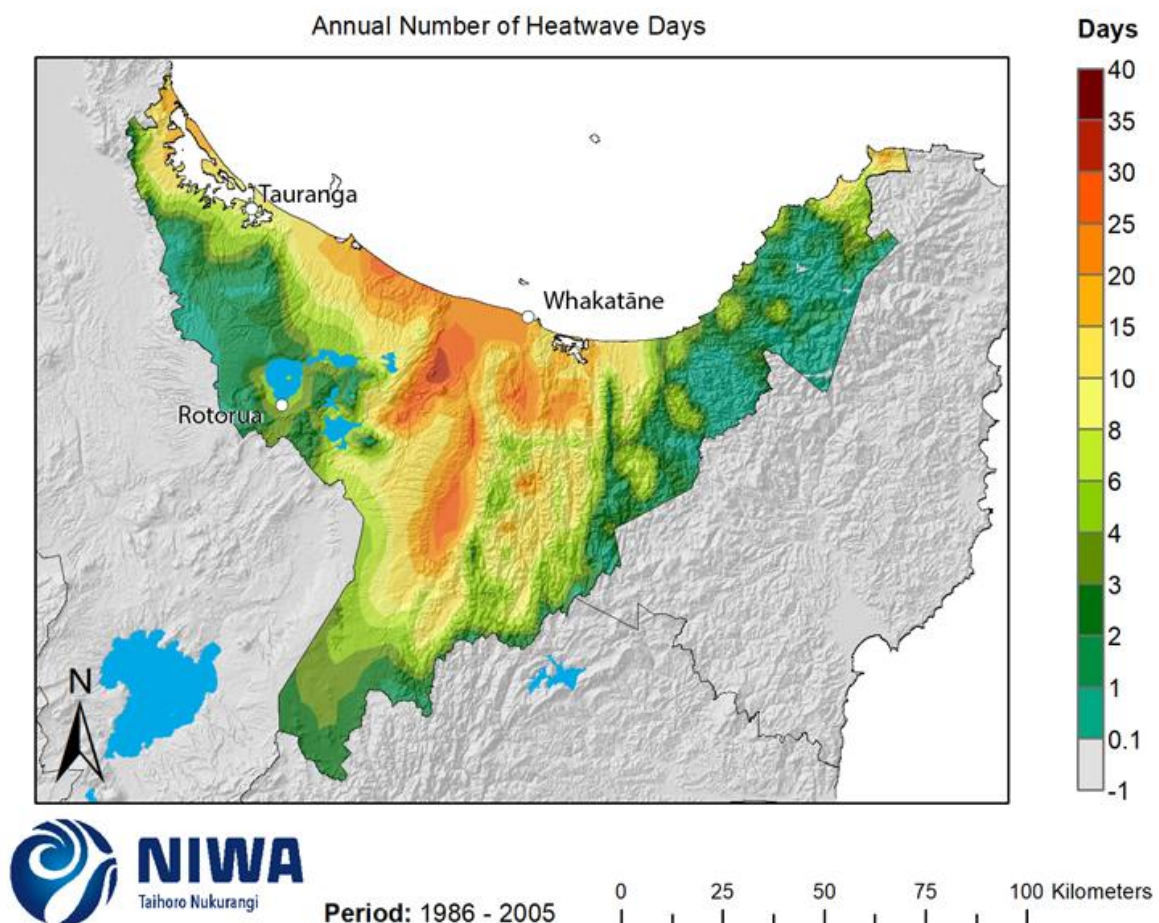


**Figure 3-26: Modelled annual number of heatwave days ( $\geq$  three consecutive days with maximum temperatures  $> 25^{\circ}\text{C}$ ), average over 1986-2005.** Results are based on dynamical downscaled projections using NIWA's Regional Climate Model. Resolution of projection is 5km x 5km.

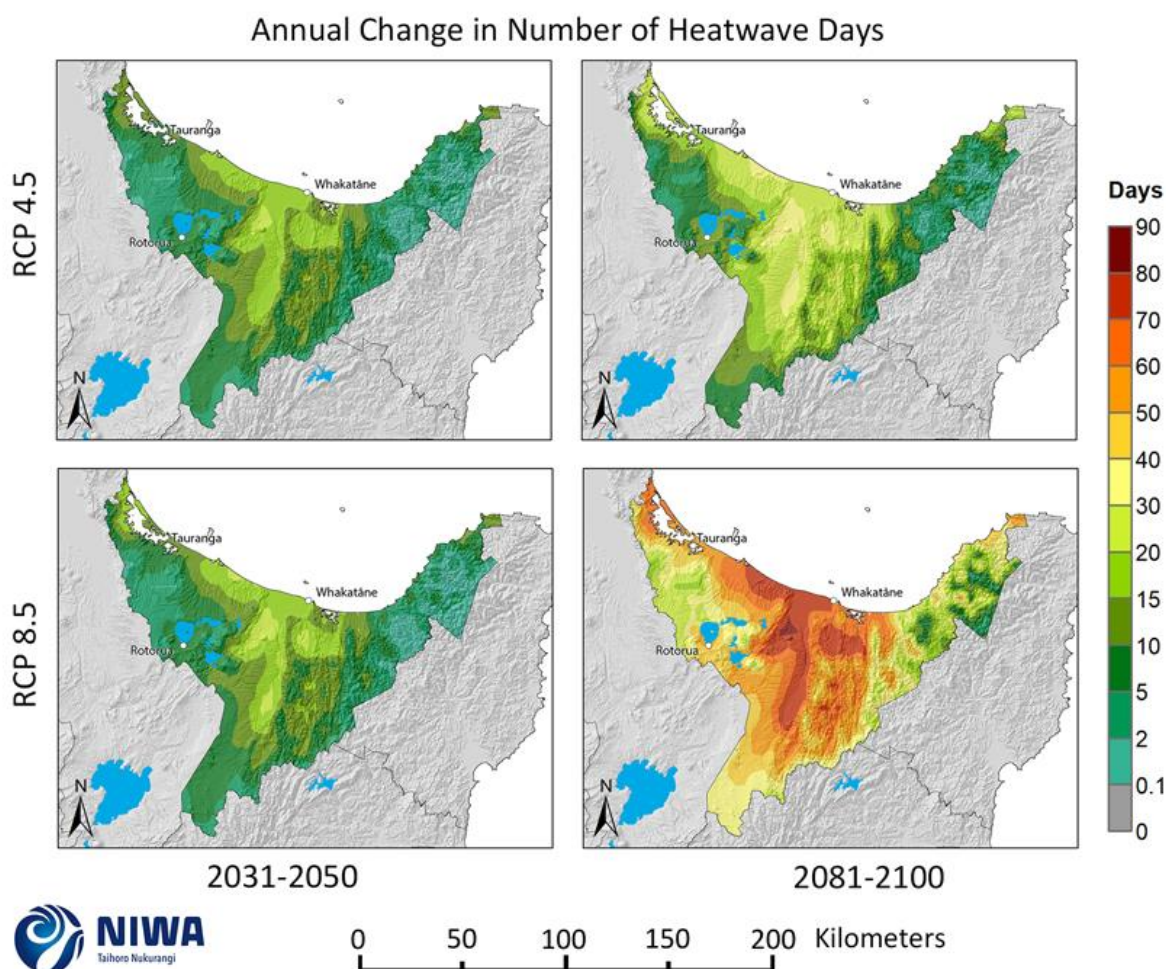


**Figure 3-27: Projected annual heatwave day ( $\geq$  three consecutive days with maximum temperatures  $> 25^{\circ}\text{C}$ ) changes for RCP4.5 and RCP8.5, by 2040 and 2090.** Relative to 1986-2005 average, based on the average of six global climate models. Results are based on dynamical downscaled projections using NIWA's Regional Climate Model. Resolution of projection is 5km x 5km.

### 3.8 Frost days

A frost day is defined in this report when the modelled daily minimum temperature falls below  $0^{\circ}\text{C}$ . This is purely a temperature-derived metric for assessing the potential for frosts over the 5 km x 5 km climate model grid. Frost conditions are influenced at the local scale (i.e. finer scale than 5 km x 5 km) by temperature, topography, wind, and humidity, so the results presented in this section can be considered as the large-scale *temperature* conditions conducive to frosts.

Historic (average over 1986-2005) and future (average over 2031-2050 and 2081-2100) maps for frost days are shown in this section. The historic maps show annual average numbers of frost days and the future projection maps show the change in the annual number of frost days compared with the historic period. Note that the historic maps are on a different colour scale to the future projection maps. Table 3-2 and Figure 3-30 show the present and future projected numbers of frost days for the model grid square closest to specific locations in the Bay of Plenty region.

For the historic period, the largest number of frost days per year occurs in the Urewera Ranges, with 60-70 frost days per year (Figure 3-28). Other inland parts of the region experience 30-40 frost days per year. In the far western and eastern parts of the region, the fewest frosts are experienced – less



than five frost days per year. Through much of the central low elevation part of the region, 5-15 frost days per year are experienced.

In the future, the number of frost days per year is projected to decline throughout the region, with larger reductions further inland (due to more frosts currently being experienced there) (Figure 3-29). By 2040, reductions of 6-10 frost days per year are possible for the furthest inland parts of the region under both RCP4.5 and RCP8.5, with the reductions getting smaller further north. By 2090, considerable reductions in frost days are projected for the furthest inland areas, around 15-25 fewer frost days for those areas under RCP8.5 and 10-15 fewer frost days under RCP4.5, with reductions getting smaller further north towards the coast.

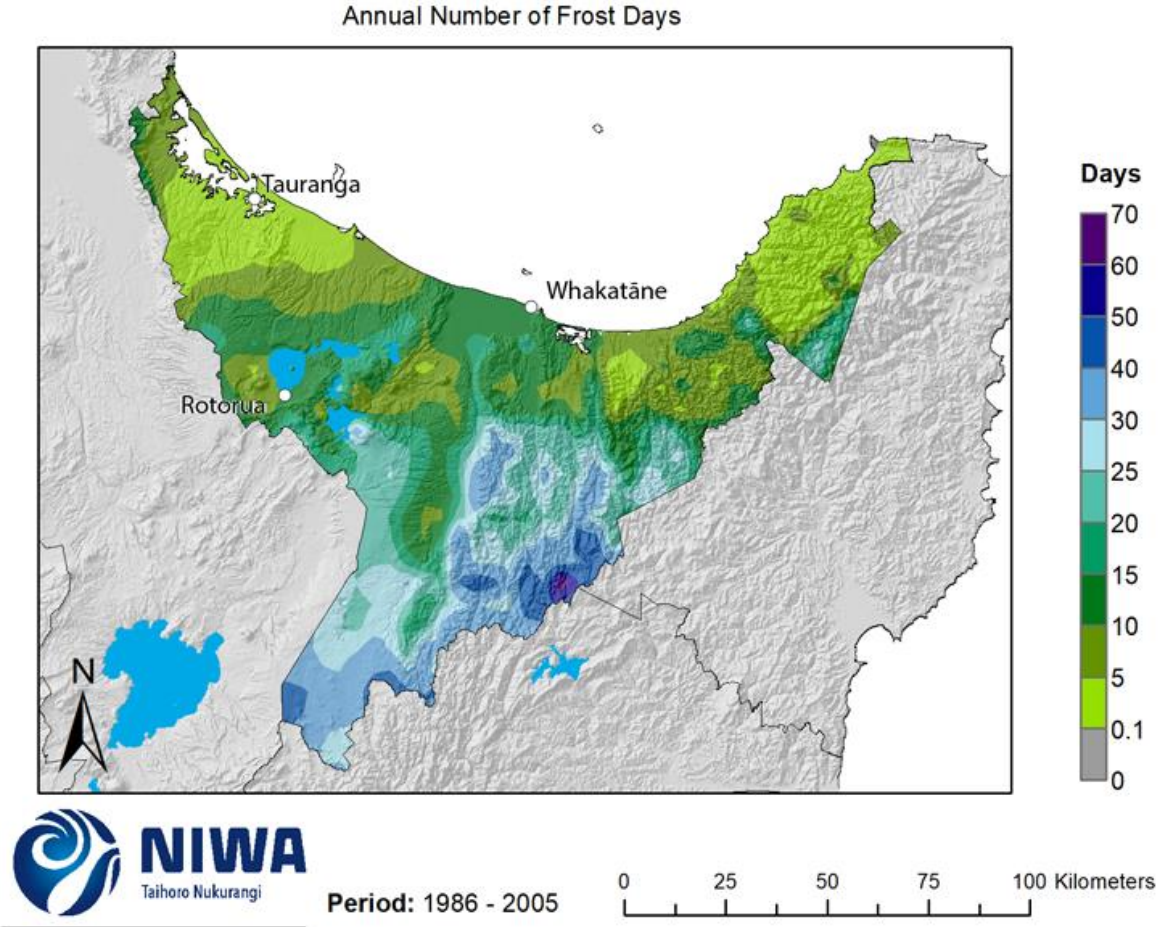


**Figure 3-28: Modelled annual number of frost days (daily minimum temperature <0°C), average over 1986-2005.** Results are based on dynamical downscaled projections using NIWA's Regional Climate Model. Resolution of projection is 5km x 5km.

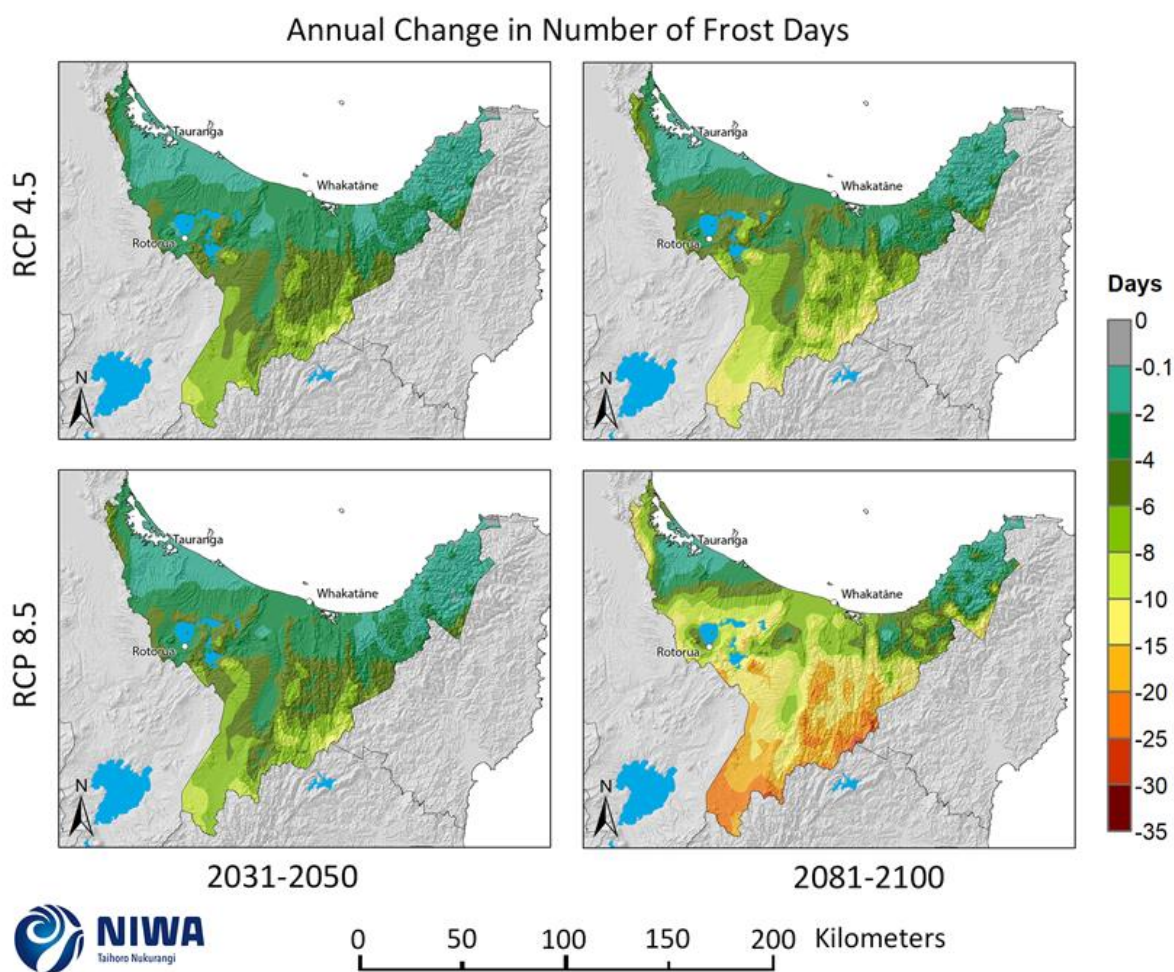


**Figure 3-29: Projected annual frost day (minimum temperature  $<0^{\circ}\text{C}$ ) changes for RCP4.5 and RCP8.5, by 2040 and 2090.** Relative to 1986-2005 average, based on the average of six global climate models. Results are based on dynamical downscaled projections using NIWA's Regional Climate Model. Resolution of projection is 5km x 5km.

**Table 3-2: Modelled annual average number of frost days (minimum temperature <0°C) for historic and two climate change scenarios (RCP4.5 and RCP8.5) at two future time periods.** Future projections are shown as the total future projected number of frost days outside the parentheses, and future change inside the parentheses. Time periods: historic: 1986-2005, mid-century: 2031-2050 "2040", end-century: 2081-2100 "2090"; based on the average of six global climate models.

Location	Historic	Future change		
Location	RCP	2040	2090	
Waihi Beach	7.8			
Tauranga	0.7			
Te Puke	1			
Rotorua	5.3			
Kawerau	5.7			
Whakatāne	10.7			
Ōpōtiki	9.2			
Katikati	7.9			
		Future change		
Location	RCP	2040	2090	
Waihi Beach	RCP4.5	5.7 (-2.1)	5 (-2.8)	
	RCP8.5	5.3 (-2.5)	2.3 (-5.5)	
Tauranga	RCP4.5	0.3 (-0.4)	0.3 (-0.4)	
	RCP8.5	0.3 (-0.4)	0 (-0.7)	
Te Puke	RCP4.5	0.5 (-0.5)	0.5 (-0.5)	
	RCP8.5	0.5 (-0.5)	0 (-1)	
Rotorua	RCP4.5	3.5 (-1.8)	2.7 (-2.6)	
	RCP8.5	3.2 (-2.1)	0.9 (-4.4)	
Kawerau	RCP4.5	4.2 (-1.5)	3.2 (-2.5)	
	RCP8.5	3.7 (-2)	1.3 (-4.4)	
Whakatāne	RCP4.5	8.5 (-2.2)	7.1 (-3.6)	
	RCP8.5	8 (-2.7)	4.2 (-6.5)	
Ōpōtiki	RCP4.5	7.3 (-1.9)	6.1 (-3.1)	
	RCP8.5	6.7 (-2.5)	3.6 (-5.6)	
Katikati	RCP4.5	5.8 (-2.1)	5 (-2.9)	
	RCP8.5	5.4 (-2.5)	2.3 (-5.6)	

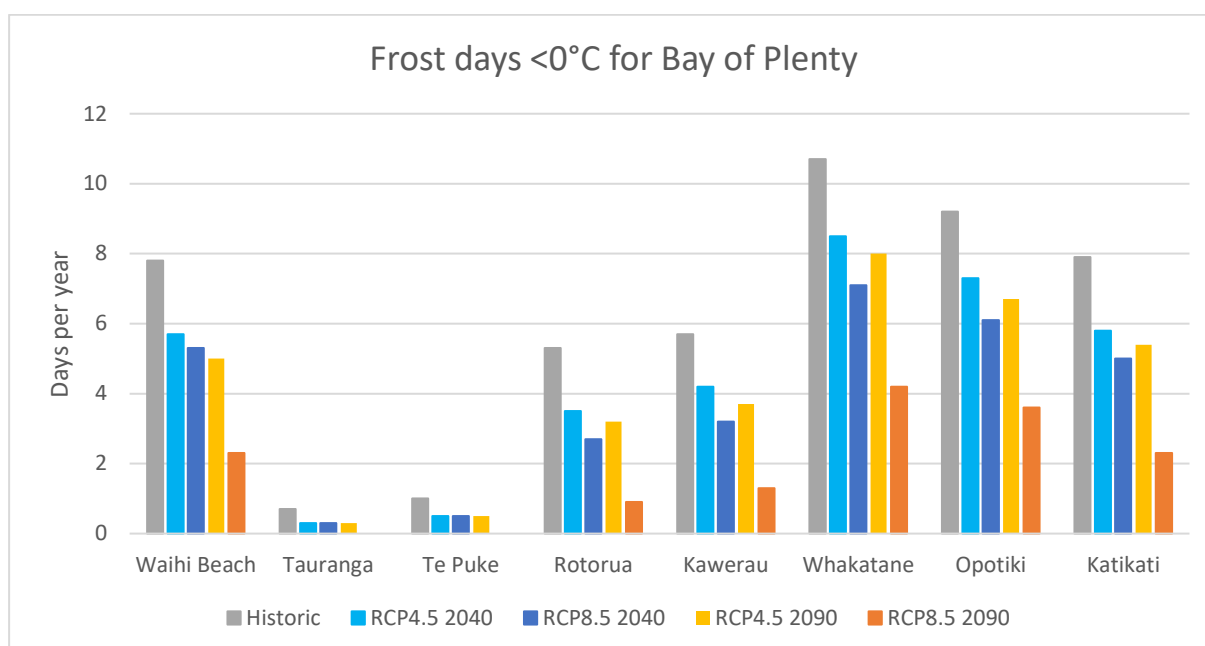


**Figure 3-30: Historic and future projected numbers of frost days for locations in the Bay of Plenty.**

### 3.9 Growing degree days

Growing degree-days (GDD) express the sum of daily temperatures above a selected base temperature (e.g. 10°C) that represent a threshold for plant growth. The average amount of GDD in a location may influence the choice of crops to grow, as different species have different temperature thresholds for survival. The daily GDD total is the amount the daily average temperature exceeds the threshold value (e.g. 10°C) per day. For example, a daily average temperature of 18°C would have a GDD base 10°C value of 8. Here, GDD are accumulated from July to June, and presented for historic (average over 1986-2005) and future change (average over 2031-2050 and 2081-2100).

Historic (average over 1986-2005) and future (average over 2031-2050 and 2081-2100) maps for GDD are shown in this section. The historic maps show annual average numbers of GDD and the future projection maps show the change in the annual number of GDD compared with the historic period. Note that the historic maps are on a different colour scale to the future projection maps.

For the historic period, the highest number of GDD is experienced in the far west and east of the region (1800-1900 GDD per year) (Figure 3-31). The area around Tauranga Harbour, Te Puke, and Maketu experiences 1700-1800 GDD per year. The number of GDD per year falls further inland and at higher elevations. The highest elevation areas experience only 600-700 GDD per year.

In the future, the number of GDD in the Bay of Plenty is projected to increase under both scenarios (Figure 3-32). By 2040 under RCP4.5, most of the region experiences increases of 200-250 GDD per year. The western Bay of Plenty between Waihi Beach and Matatā experiences increases of 250-300 GDD per year. Under RCP8.5, most of the region experiences increases of 250-300 GDD per year, with small areas around Katikati and Te Puke experiencing increases of 300-400 GDD per year. By 2090 under RCP4.5, most of the region experiences 300-400 GDD per year with the western Bay of Plenty experiencing 400-500 more GDD per year. Under RCP8.5, Waihi Beach, Katikati and Te Puke experience increases of 1000-1100 GDD per year, with much of the western half of the Bay of Plenty (including Rotorua and Murupara) experiencing 900-1000 more GDD per year. The eastern and southern parts of the region experience 700-900 more GDD per year under this scenario.

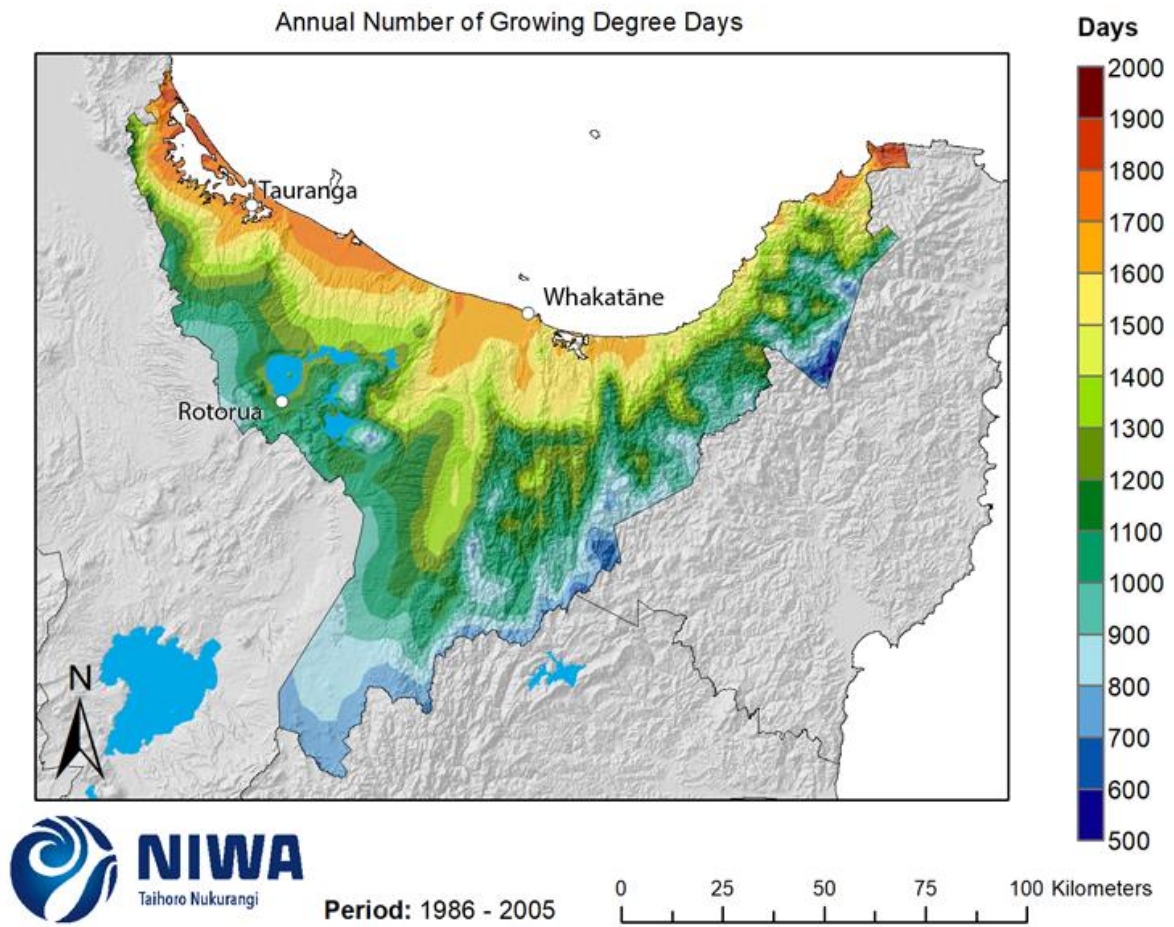


**Figure 3-31: Modelled annual number of growing degree days (base 10°C), average over 1986-2005.** Results are based on dynamical downscaled projections using NIWA's Regional Climate Model. Resolution of projection is 5km x 5km.

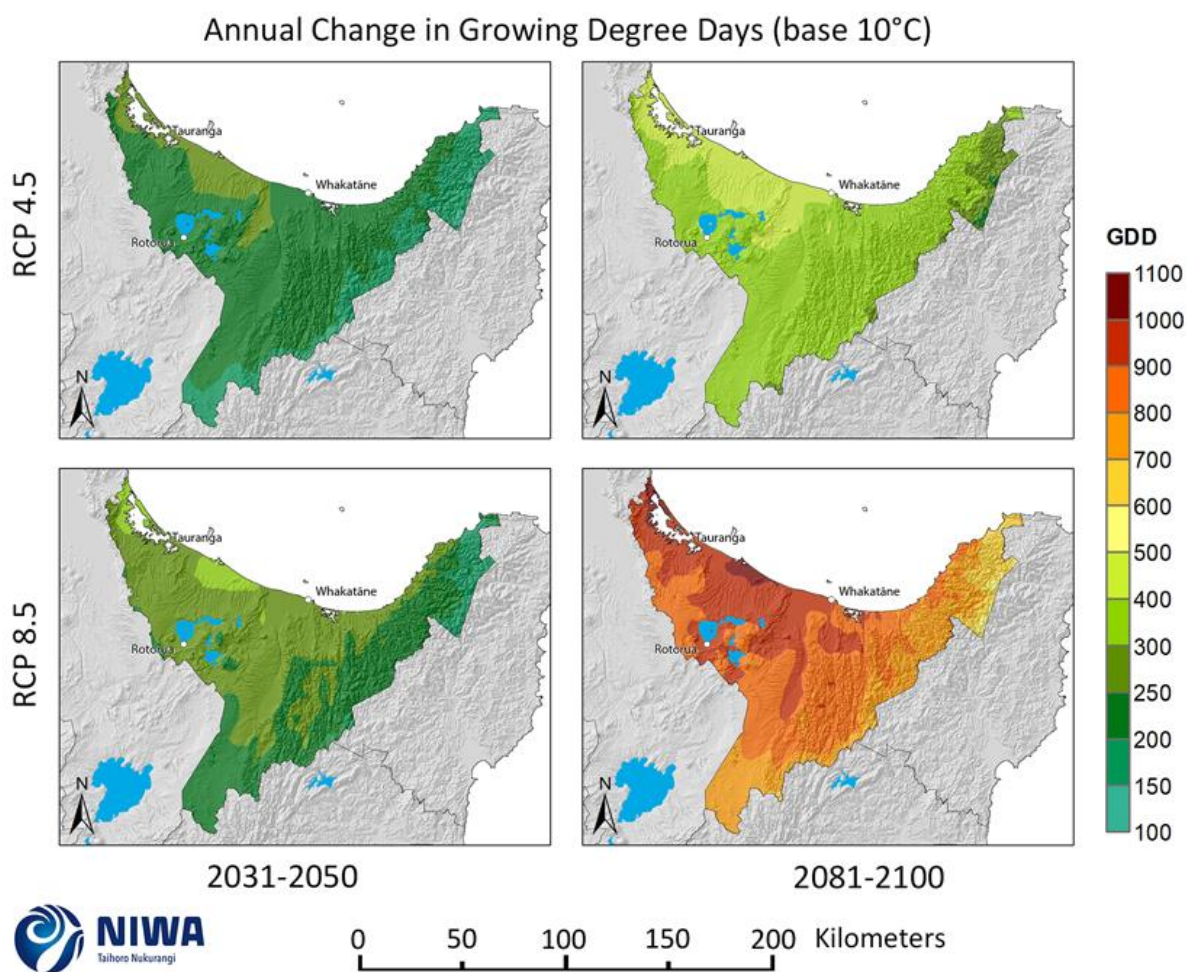


**Figure 3-32: Projected annual growing degree-day (base 10°C) changes for RCP4.5 and RCP8.5, by 2040 and 2090.** Relative to 1986-2005 average, based on the average of six global climate models. Results are based on dynamical downscaled projections using NIWA's Regional Climate Model. Resolution of projection is 5km x 5km.

## 4 Rainfall and Drought

### 4.1 Rainfall

This section contains maps showing historic total rainfall and the future projected change in total rainfall. Historic rainfall maps are in units of mm per year or season (average over 1986-2005) and future (average over 2031-2050 and 2081-2100) maps show the percentage change in rainfall compared with the historic total. Note that the historic maps are on a different colour scale to the future projection maps. Table 4-1 shows the historic and future projected rainfall for the model grid square closest to specific locations in the Bay of Plenty region.

For the historic period, the highest annual rainfall totals are recorded in the high elevations of the Raukumara Ranges (3000-3500 mm/year) (Figure 4-1). The lowest annual rainfall totals are recorded along the coast and inland of Rotorua (1000-1500 mm/year). Summer is the driest season and winter is the wettest, with seasonal patterns of high and low rainfall generally following annual patterns.

In the future, the seasonality of rainfall is projected to change in the Bay of Plenty. By 2040 under RCP4.5 (Figure 4-2), annual rainfall is not expected to change much ( $\pm 2\%$  for most of the region). Some coastal areas experience increases of up to 4% and some inland areas experience decreases of up to 4%. However, at the seasonal scale, changes are more significant. Summer rainfall is expected to decline everywhere, with the largest decreases being 8-15% for far western and eastern areas. On the other hand, winter rainfall is projected to increase by 10-15% for some coastal areas around Maketu and the far eastern end of the region, with increases of 6-10% around the Rotorua Lakes and hill country south of Whakatāne. Under RCP8.5 by 2040 (Figure 4-3), the annual pattern is similar to RCP4.5. However, spring rainfall is projected to decrease across the region in this scenario, by up to 8-10% for the far west of the region. Winter and autumn rainfall is projected to increase for most areas, by 8-10% for coastal areas during autumn.

By 2090 under RCP4.5 (Figure 4-4), annual rainfall decreases are more pronounced for inland and western coastal areas, with 2-4% reductions in rainfall for some locations. Small increases are expected for the coast. Winter rainfall is projected to increase for most areas, with 8-10% increases for the coast east of Whakatāne. Spring rainfall declines throughout the region, with the largest reductions of 8-10% in the western Bay of Plenty and the Huiarau Ranges in the south. By 2090 under RCP8.5 (Figure 4-5), annual rainfall is projected to decline by 2-6% across most of the region, with small increases of 0-2% for coastal areas. Summer and spring rainfall is projected to decrease, with some areas projecting 10-15% less rainfall in those seasons. Winter and autumn rainfall is expected to increase for some areas – for the west in autumn (by 10-15%) and for most of the region in winter (by 4-8%).

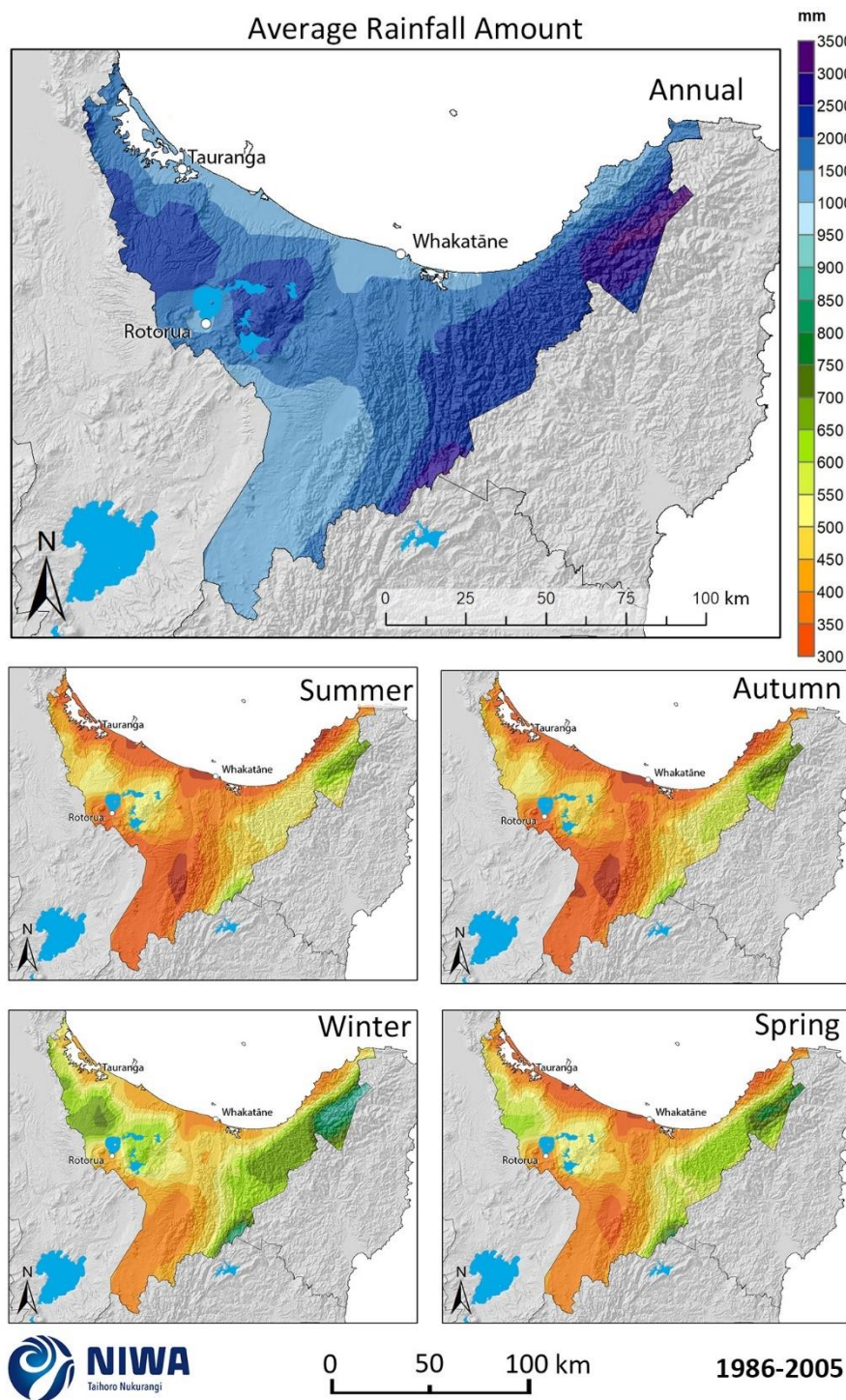


**Figure 4-1: Modelled annual and seasonal rainfall (mm), average over 1986-2005.** Results are based on dynamical downscaled projections using NIWA's Regional Climate Model. Resolution of projection is 5km x 5km.



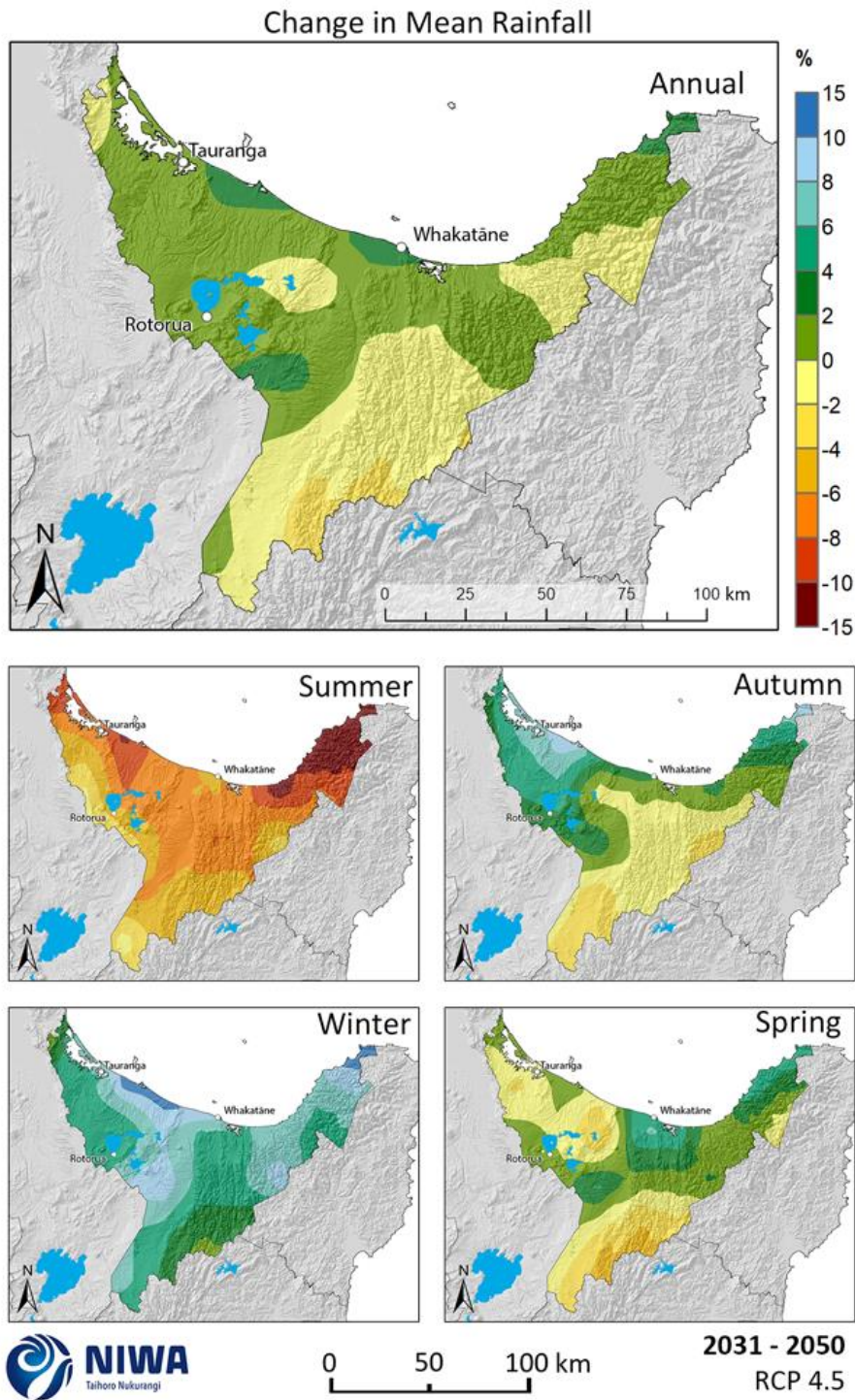


**Figure 4-2: Projected annual and seasonal mean rainfall changes by 2040 for RCP4.5.** Relative to 1986-2005 average, based on the average of six global climate models. Results are based on dynamical downscaled projections using NIWA's Regional Climate Model. Resolution of projection is 5km x 5km.

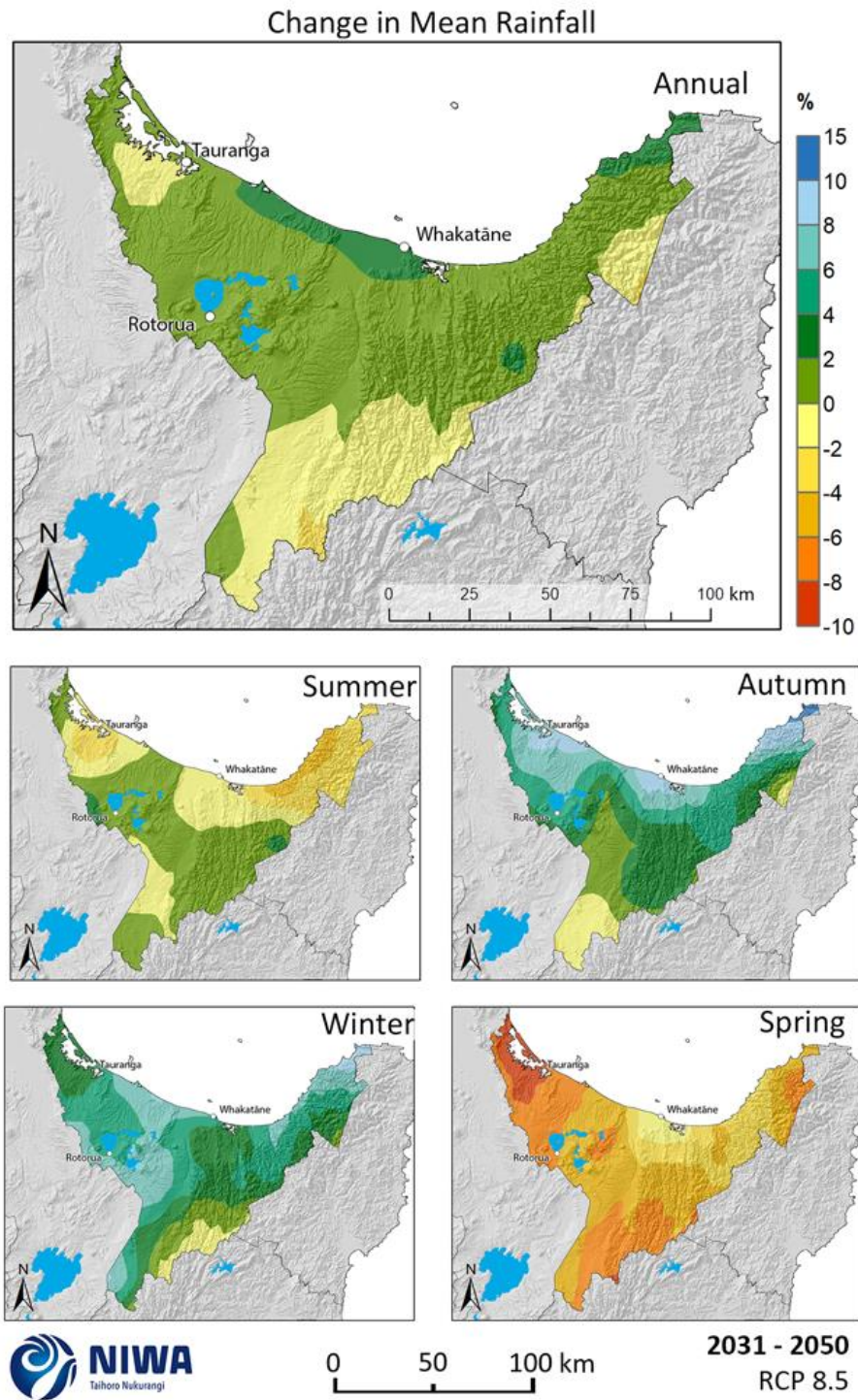


**Figure 4-3: Projected annual and seasonal mean rainfall changes by 2040 for RCP8.5.** Relative to 1986-2005 average, based on the average of six global climate models. Results are based on dynamical downscaled projections using NIWA's Regional Climate Model. Resolution of projection is 5km x 5km.

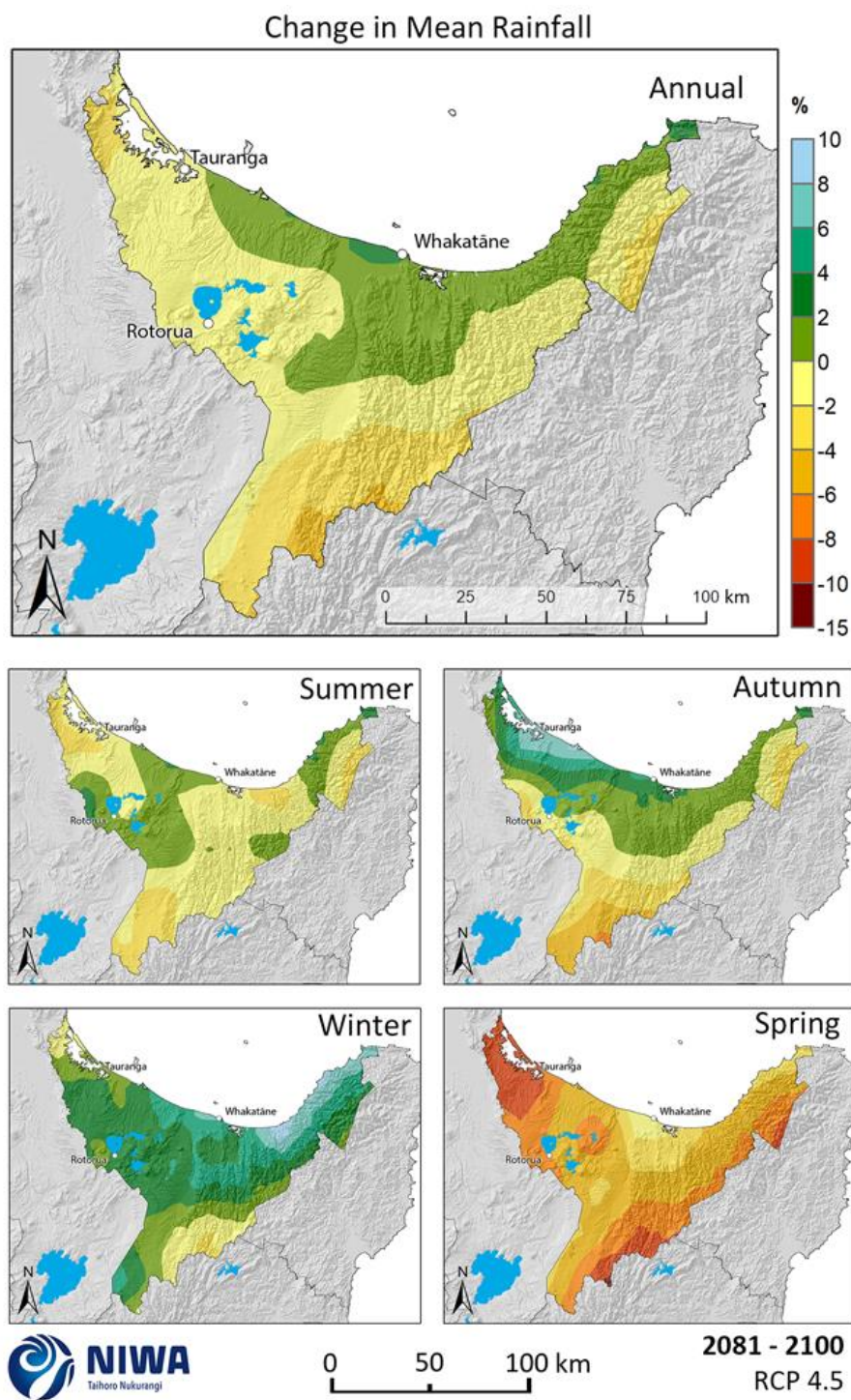


**Figure 4-4: Projected annual and seasonal mean rainfall changes by 2090 for RCP4.5.** Relative to 1986-2005 average, based on the average of six global climate models. Results are based on dynamical downscaled projections using NIWA's Regional Climate Model. Resolution of projection is 5km x 5km.

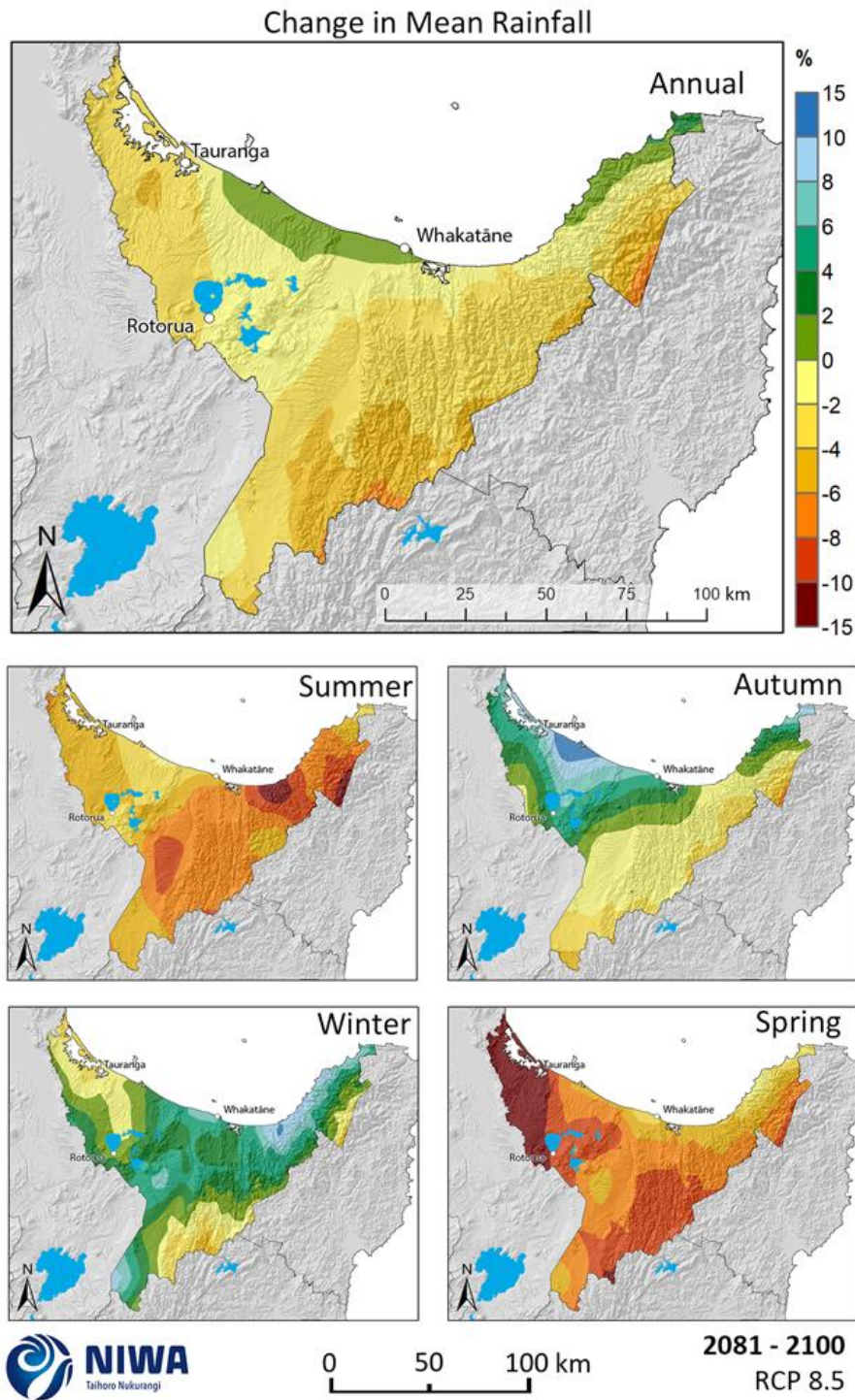


**Figure 4-5: Projected annual and seasonal mean rainfall changes by 2090 for RCP8.5.** Relative to 1986-2005 average, based on the average of six global climate models. Results are based on dynamical downscaled projections using NIWA's Regional Climate Model. Resolution of projection is 5km x 5km.

**Table 4-1: Modelled annual average rainfall for historic and two climate change scenarios (RCP4.5 and RCP8.5) at two future time periods.** Time periods: historic: 1986-2005, mid-century: 2031-2050 "2040", end-century: 2081-2100 "2090"; based on the average of six global climate models. Note that historic rainfall is in millimetres and future rainfall change is in per cent.

Location	Historic (mm)
Waihi Beach	1718
Tauranga	1407
Te Puke	1479
Rotorua	1529
Kawerau	2021
Whakatāne	1355
Ōpōtiki	1393
Katikati	1851

Location	Future change (%)		
	RCP	2040	2090
Waihi Beach	RCP4.5	0.4	-1.6
	RCP8.5	0.1	-2.9
Tauranga	RCP4.5	1.3	-0.7
	RCP8.5	0.0	-3.2
Te Puke	RCP4.5	2.5	0.5
	RCP8.5	1.6	0.0
Rotorua	RCP4.5	1.0	-1.2
	RCP8.5	1.2	-2.5
Kawerau	RCP4.5	-0.6	-0.7
	RCP8.5	0.4	-1.8
Whakatāne	RCP4.5	2.3	1.8
	RCP8.5	2.8	0.3
Ōpōtiki	RCP4.5	0.4	0.6
	RCP8.5	1.2	-1.9
Katikati	RCP4.5	0.2	-2.1
	RCP8.5	0.1	-3.2

## 4.2 Wet days

In this report, 'wet days' are days when greater than 1 mm of rainfall is recorded. Historic (average over 1986-2005) and future (average over 2031-2050 and 2081-2100) maps for wet days are shown in this section. The historic maps show annual and seasonal average numbers of wet days and the future projection maps show the change in the number of wet days compared with the historic period. Note that the historic maps are on a different colour scale to the future projection maps.

For the historic period, the most wet days are observed in the high elevations of the Urewera Ranges (200-220 days per year) and the lowest number of wet days are observed in the coastal areas (100-120 days per year) (Figure 4-6). In general, for the seasonal scale, the largest number of wet days across the region is in spring and the smallest number is in autumn. The area around Whakatāne

experiences 20-25 wet days during summer and autumn, compared with the high elevations of the eastern ranges experiencing 50-60 wet days in winter and spring.

By 2040 under RCP4.5 (Figure 4-7), the annual number of wet days is projected to decrease by 4-8 days on the eastern boundary of the region including Te Urewera. 2-4 fewer wet days is projected for the inland western Bay of Plenty, including Rotorua, as well as the foothills of the Urewera Ranges and Raukumara Ranges. Under RCP8.5 by 2040 (Figure 4-8), the pattern is slightly amplified with larger reductions in wet days along the eastern border of the region (6-8 fewer wet days per year). The largest reductions are projected for spring (2-4 fewer wet days for most of the region).

By 2090 under RCP4.5 (Figure 4-9), the pattern of reduction in wet days is amplified. 10-15 fewer wet days per year are projected for the eastern boundary of the region, along the Huiarau, Urewera and Raukumara Ranges. Most of the region experiences 6-10 fewer wet days per year, and the coastal areas experience 2-6 fewer wet days per year. The largest seasonal decreases are in spring and autumn. Under RCP8.5 (Figure 4-10), this pattern is continued. Decreases of 15-25 wet days per year are projected for the Huiarau, Urewera and Raukumara Ranges, and 10-15 fewer wet days per year are projected for Rotorua, the Kaimai-Mamaku Ranges and central areas. Coastal areas may expect decreases of 4-6 wet days per year. The largest seasonal reductions are for spring (6-8 fewer wet days for inland areas) and winter experiences some increases (0-2 more wet days for central and coastal parts).

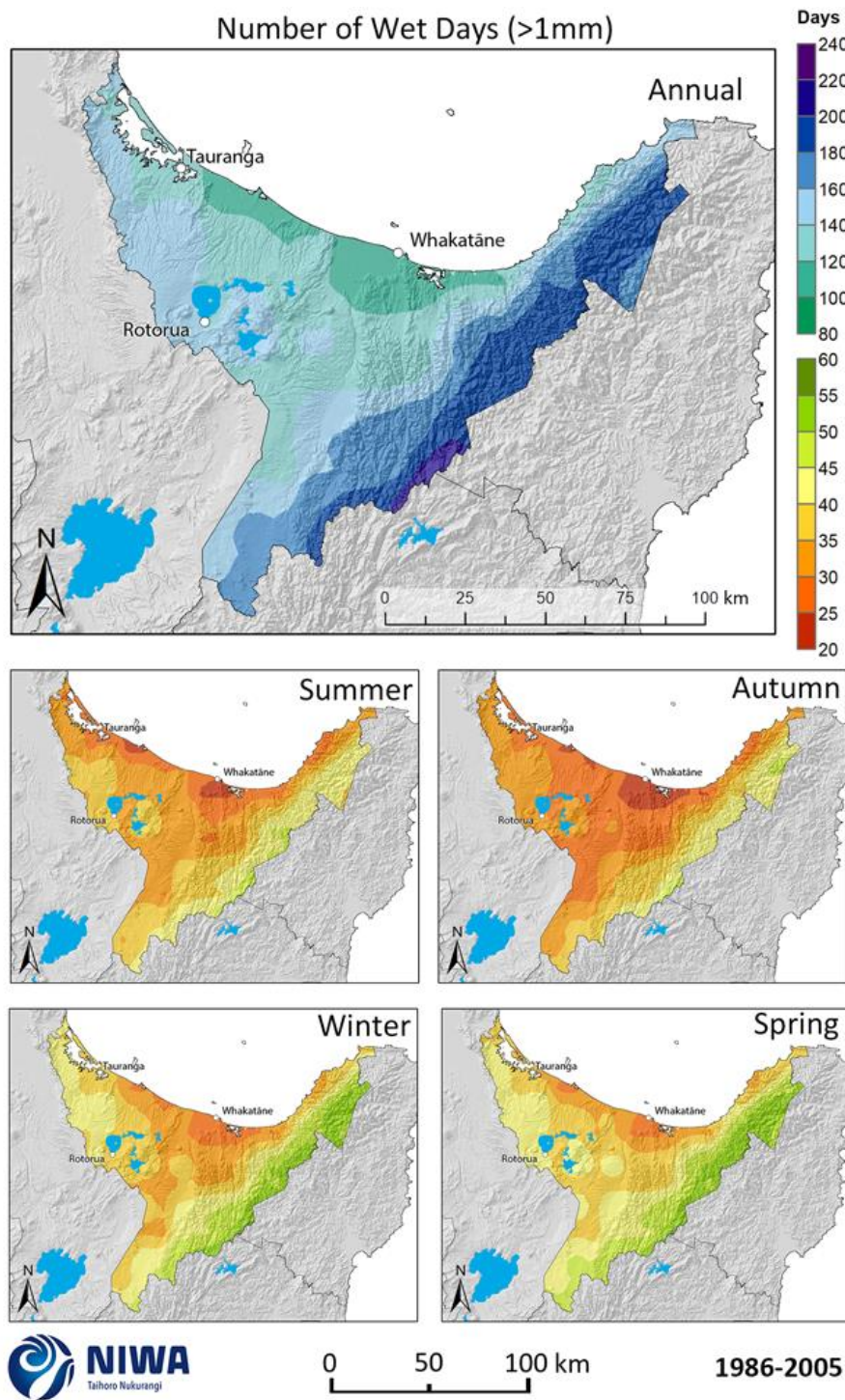


**Figure 4-6: Modelled annual and seasonal number of wet days (daily rainfall >1mm), average over 1986-2005.** Results are based on dynamical downscaled projections using NIWA's Regional Climate Model. Resolution of projection is 5km x 5km.

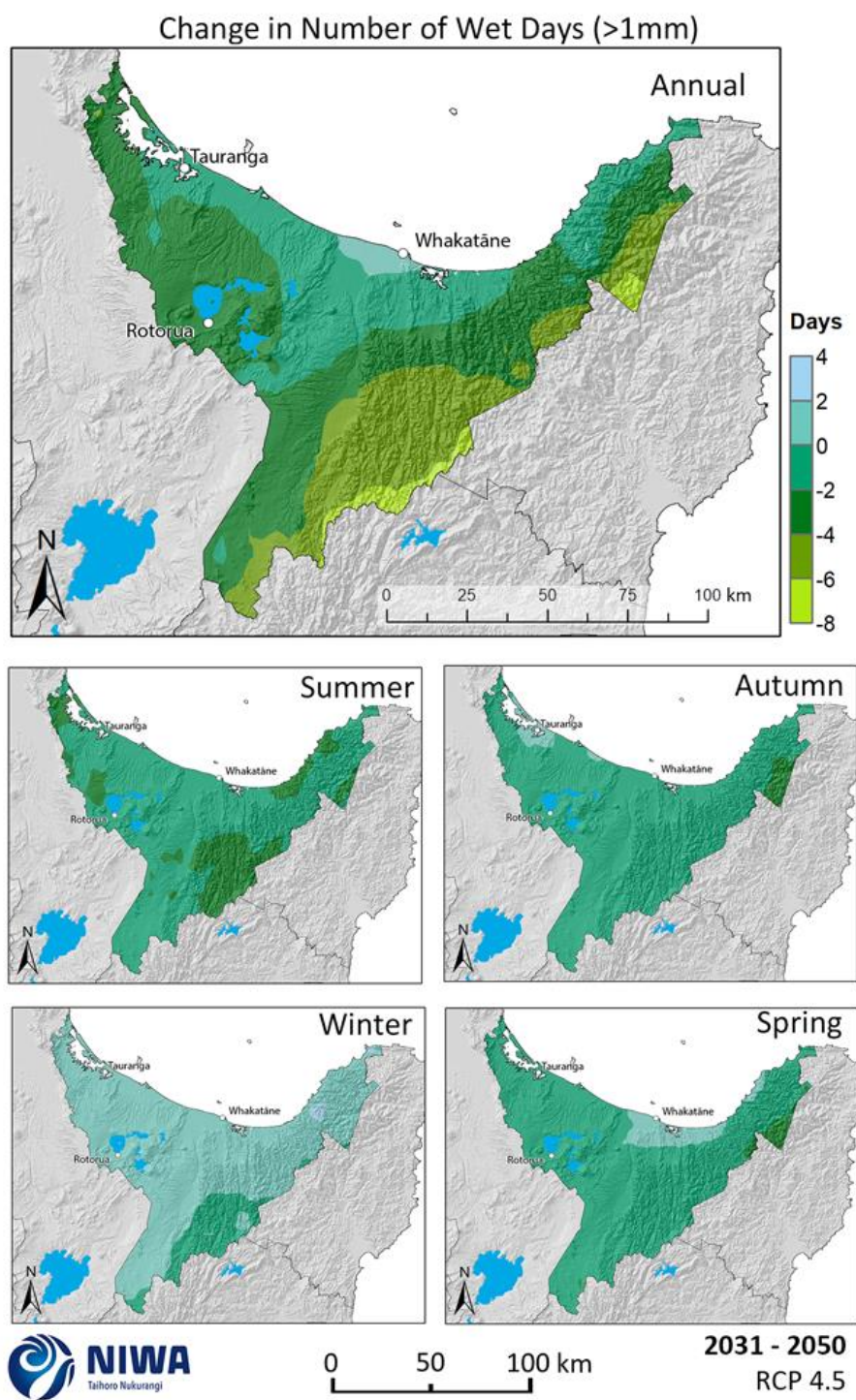


**Figure 4-7: Projected annual and seasonal wet day (>1mm rain) changes by 2040 for RCP4.5.** Relative to 1986-2005 average, based on the average of six global climate models. Results are based on dynamical downscaled projections using NIWA's Regional Climate Model. Resolution of projection is 5km x 5km.



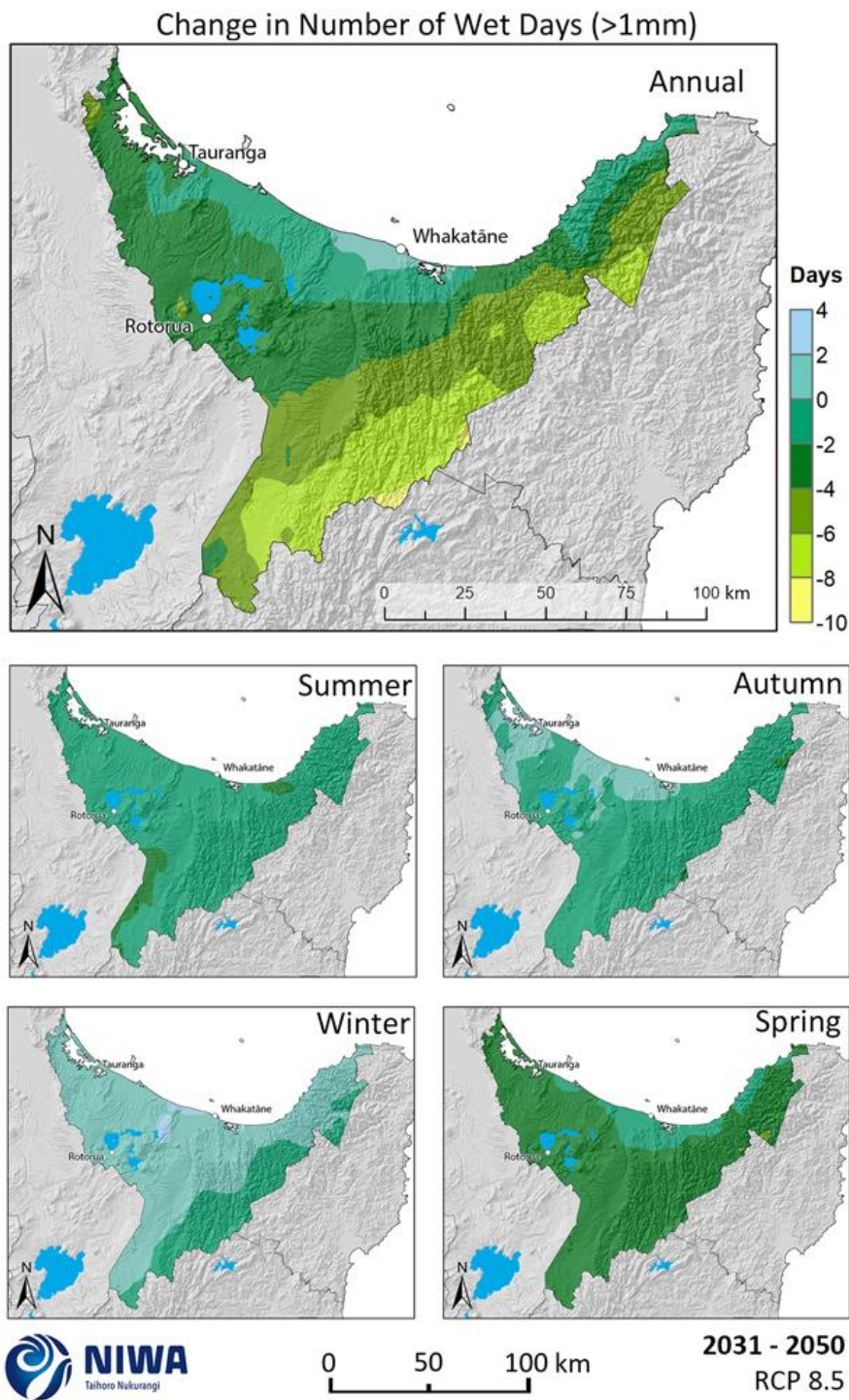


**Figure 4-8: Projected annual and seasonal wet day (>1mm rain) changes by 2040 for RCP8.5.** Relative to 1986-2005 average, based on the average of six global climate models. Results are based on dynamical downscaled projections using NIWA's Regional Climate Model. Resolution of projection is 5km x 5km.

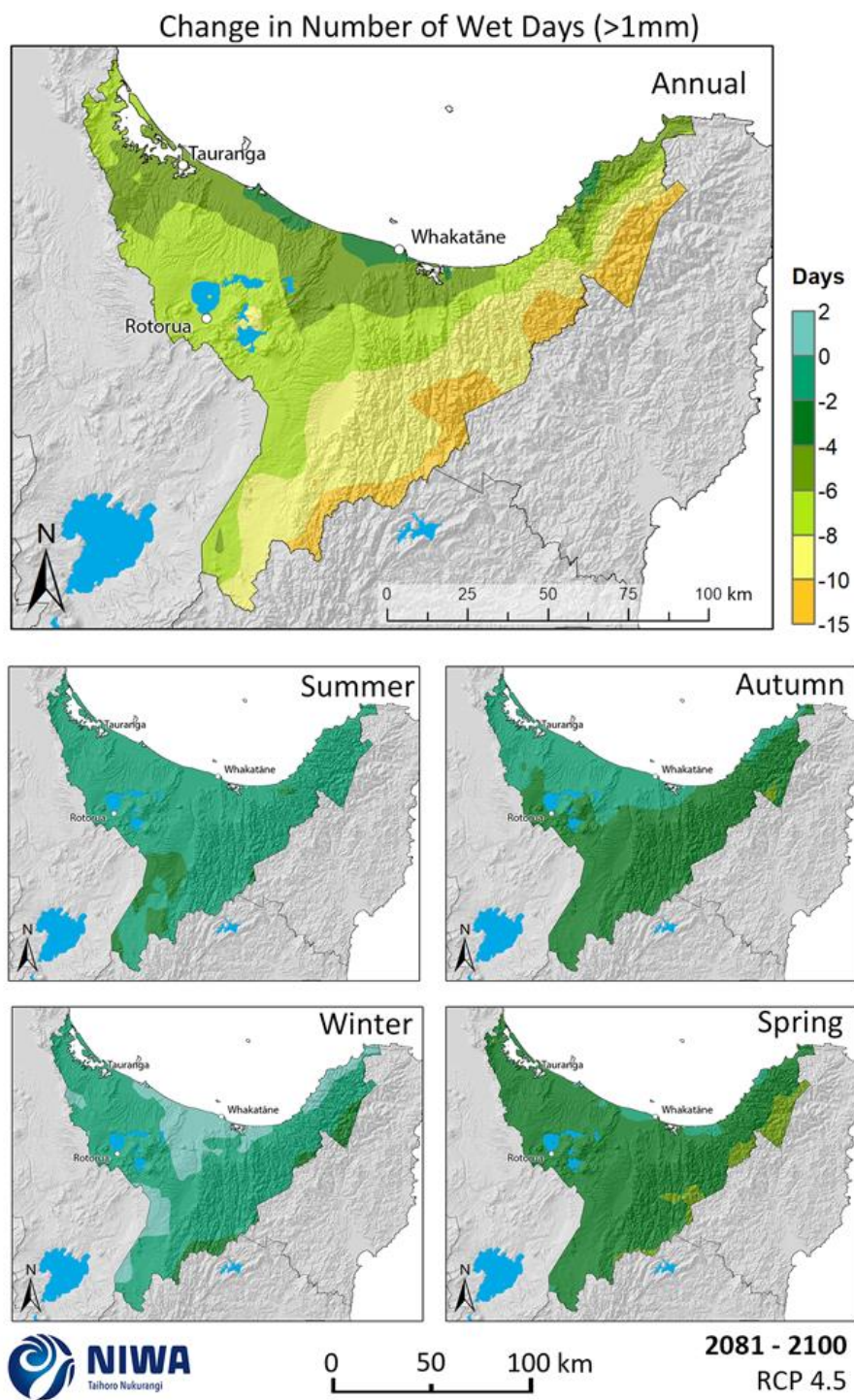


**Figure 4-9: Projected annual and seasonal wet day (>1mm rain) changes by 2090 for RCP4.5.** Relative to 1986-2005 average, based on the average of six global climate models. Results are based on dynamical downscaled projections using NIWA's Regional Climate Model. Resolution of projection is 5km x 5km.

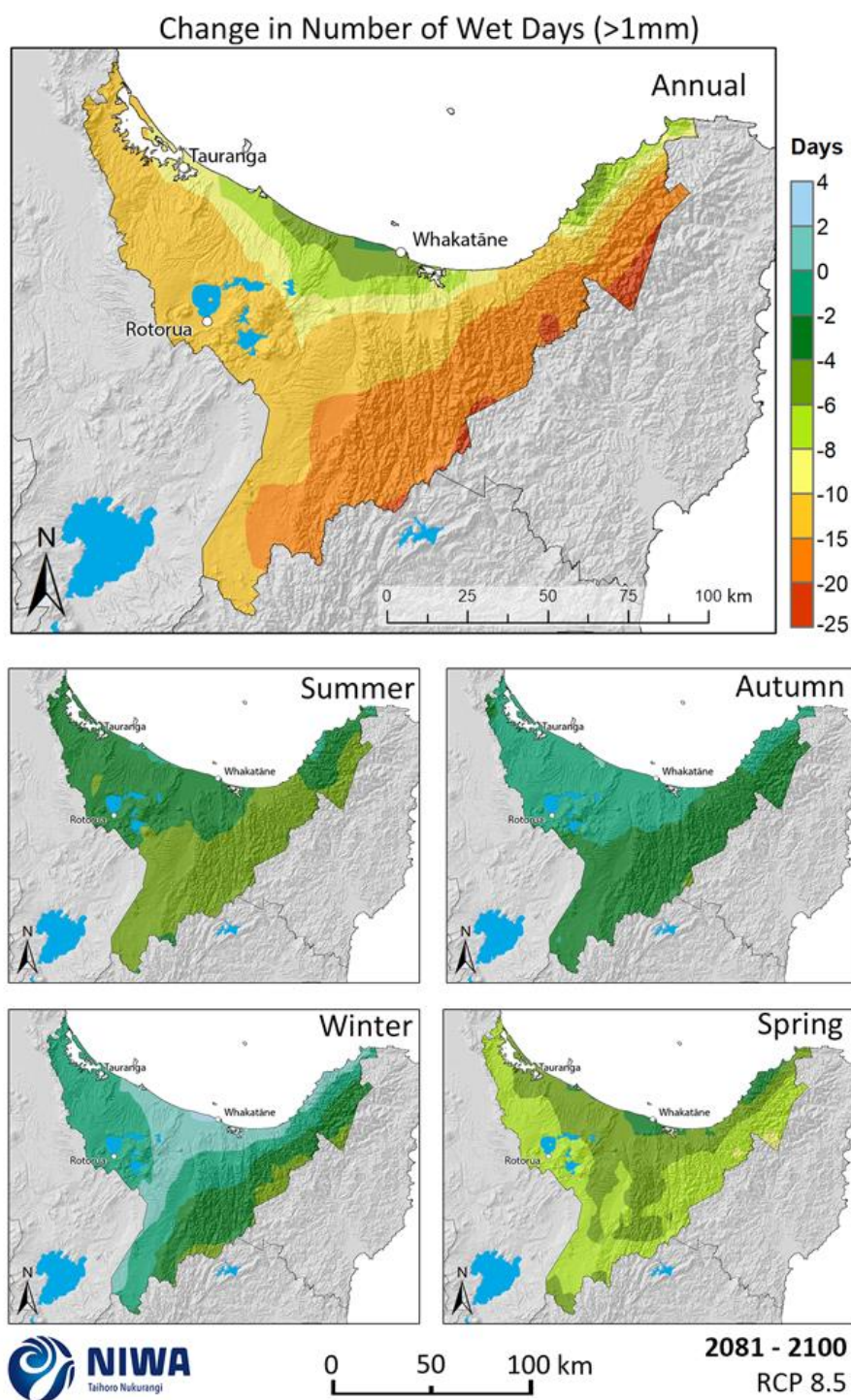


**Figure 4-10: Projected annual and seasonal wet day (>1mm rain) changes by 2090 for RCP8.5.** Relative to 1986-2005 average, based on the average of six global climate models. Results are based on dynamical downscaled projections using NIWA's Regional Climate Model. Resolution of projection is 5km x 5km.

### 4.3 Heavy rain days

A heavy rain day considered here is a daily rainfall total above 25 mm. Historic (average over 1986-2005) and future (average over 2031-2050 and 2081-2100) maps for heavy rain days are shown in this section. The historic maps show annual and seasonal average numbers of heavy rain days and the future projection maps show the change in the number of heavy rain days compared with the historic period. Note that the historic maps are on a different colour scale to the future projection maps.

For the historic period, the area with the highest number of heavy rain days is the highest elevations of the Urewera Ranges (35-40 heavy rain days per year) (Figure 4-11). The area inland of Murupara has the lowest number of heavy rain days per year (7-8 days per year). Winter has the most heavy rain days and summer has the least heavy rain days.

In the future, the number of heavy rain days in the Bay of Plenty is not projected to change much (change of  $\pm 0-1$  day per year and season for RCP4.5 and RCP8.5 by 2040). By 2090, the number of heavy rain days is projected to decrease in the Raukumara Ranges by 1-3 days per year under RCP4.5, and reductions of 1-2 days per year are projected for Katikati and Waihi Beach. Under RCP8.5, reductions of 1-2 days per year are more widespread but patchy in an east-west swathe across the region, with 2-3 fewer heavy rain days projected for the Raukumara Ranges.

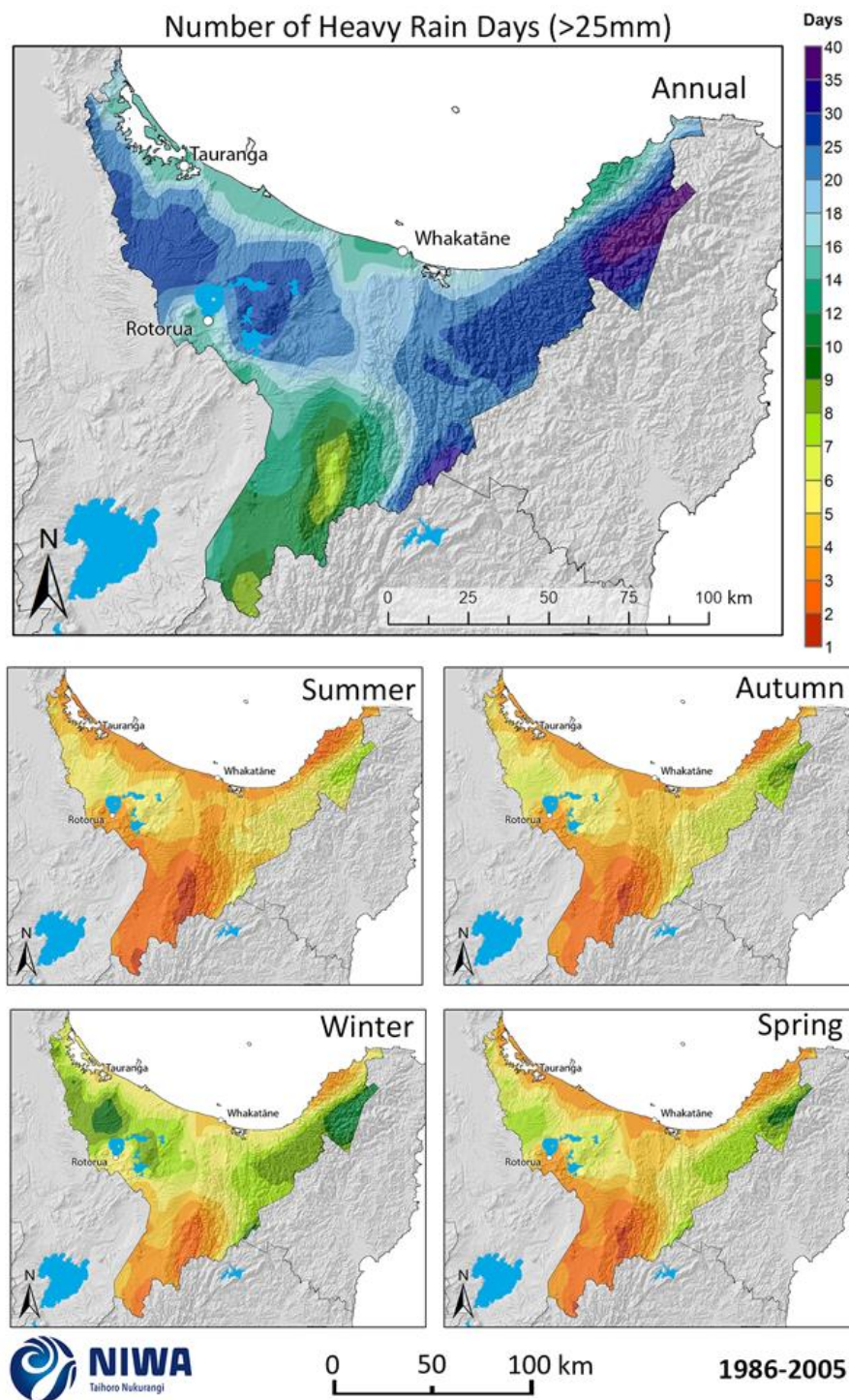


**Figure 4-11: Modelled annual and seasonal number of heavy rain days (daily rainfall >25mm), average over 1986-2005.** Results are based on dynamical downscaled projections using NIWA's Regional Climate Model. Resolution of projection is 5km x 5km.

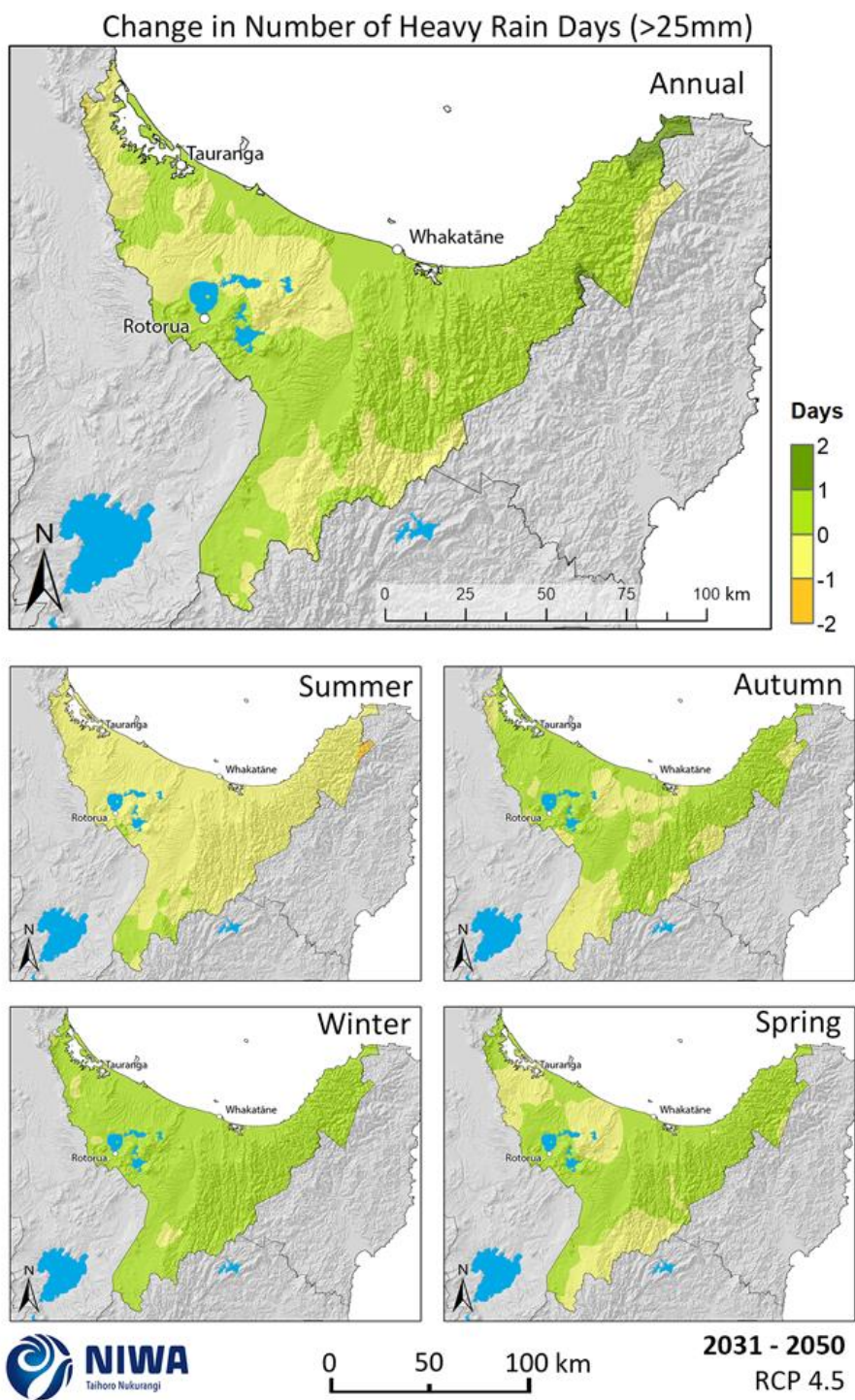


**Figure 4-12: Projected annual and seasonal number of heavy rain day (>25mm) changes by 2040 for RCP4.5.** Relative to 1986-2005 average, based on the average of six global climate models. Results are based on dynamical downscaled projections using NIWA's Regional Climate Model. Resolution of projection is 5km x 5km.

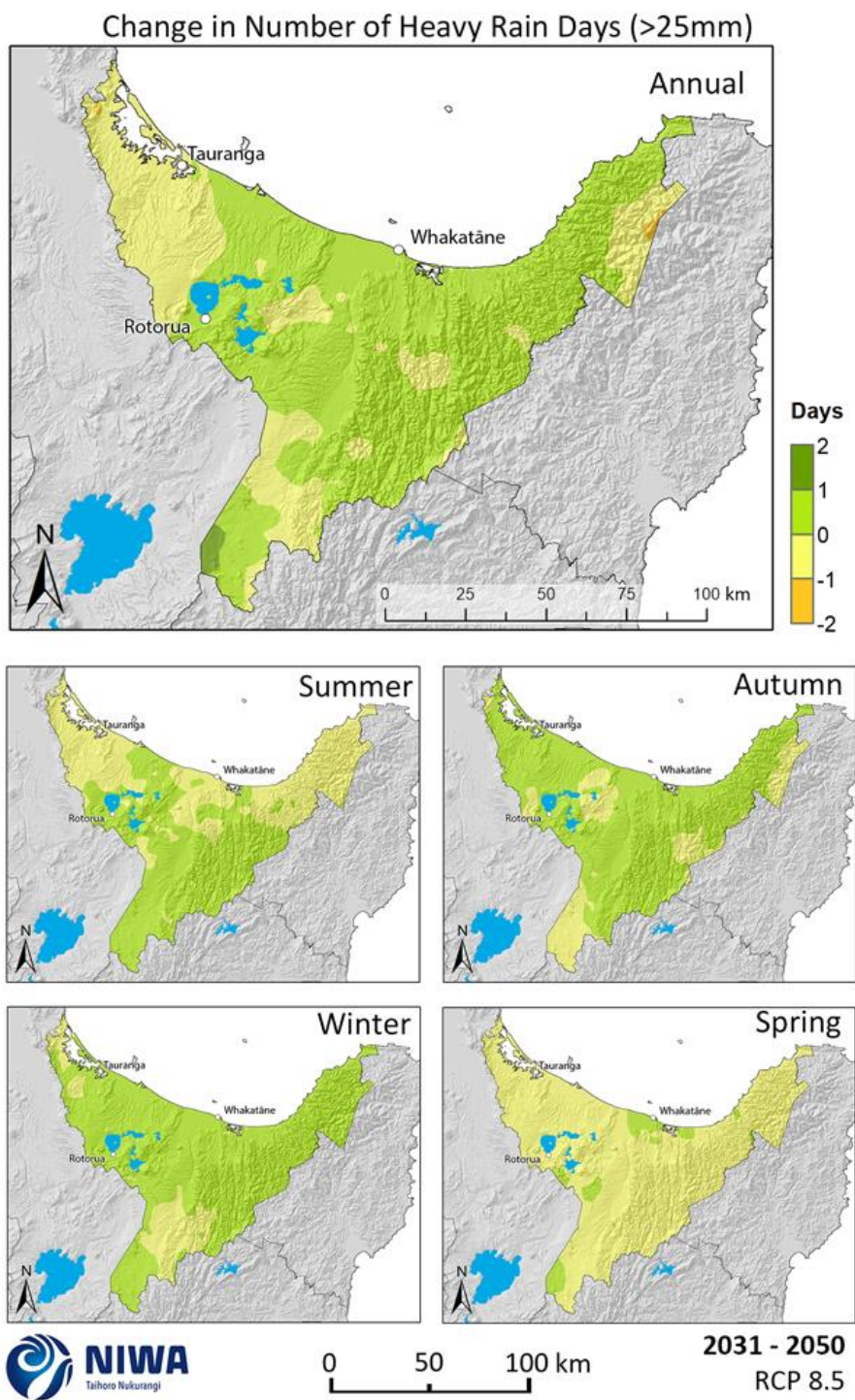


**Figure 4-13: Projected annual and seasonal number of heavy rain day (>25mm) changes by 2040 for RCP8.5.** Relative to 1986-2005 average, based on the average of six global climate models. Results are based on dynamical downscaled projections using NIWA's Regional Climate Model. Resolution of projection is 5km x 5km.

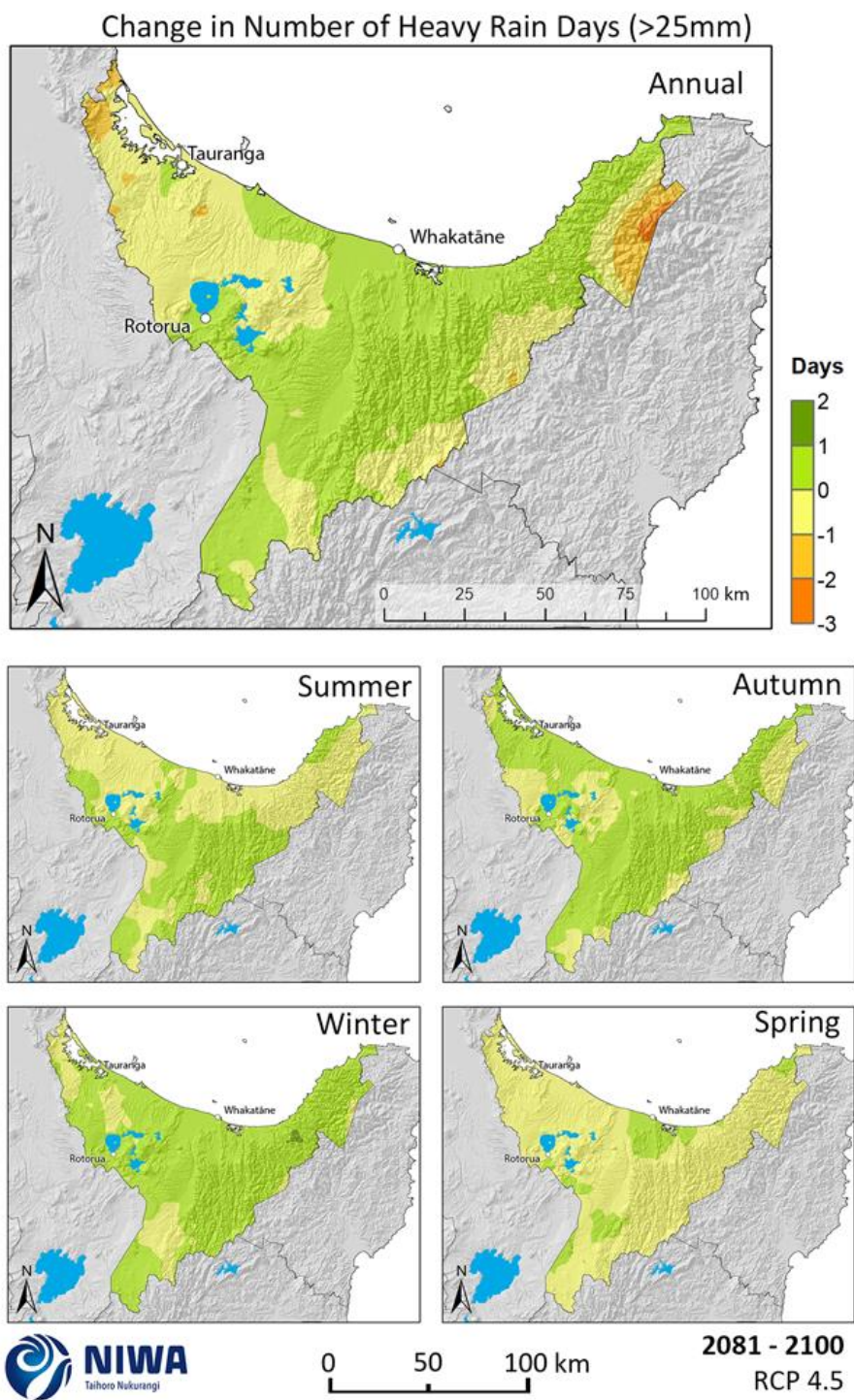


**Figure 4-14: Projected annual and seasonal number of heavy rain day (>25mm) changes by 2090 for RCP4.5.** Relative to 1986-2005 average, based on the average of six global climate models. Results are based on dynamical downscaled projections using NIWA's Regional Climate Model. Resolution of projection is 5km x 5km.



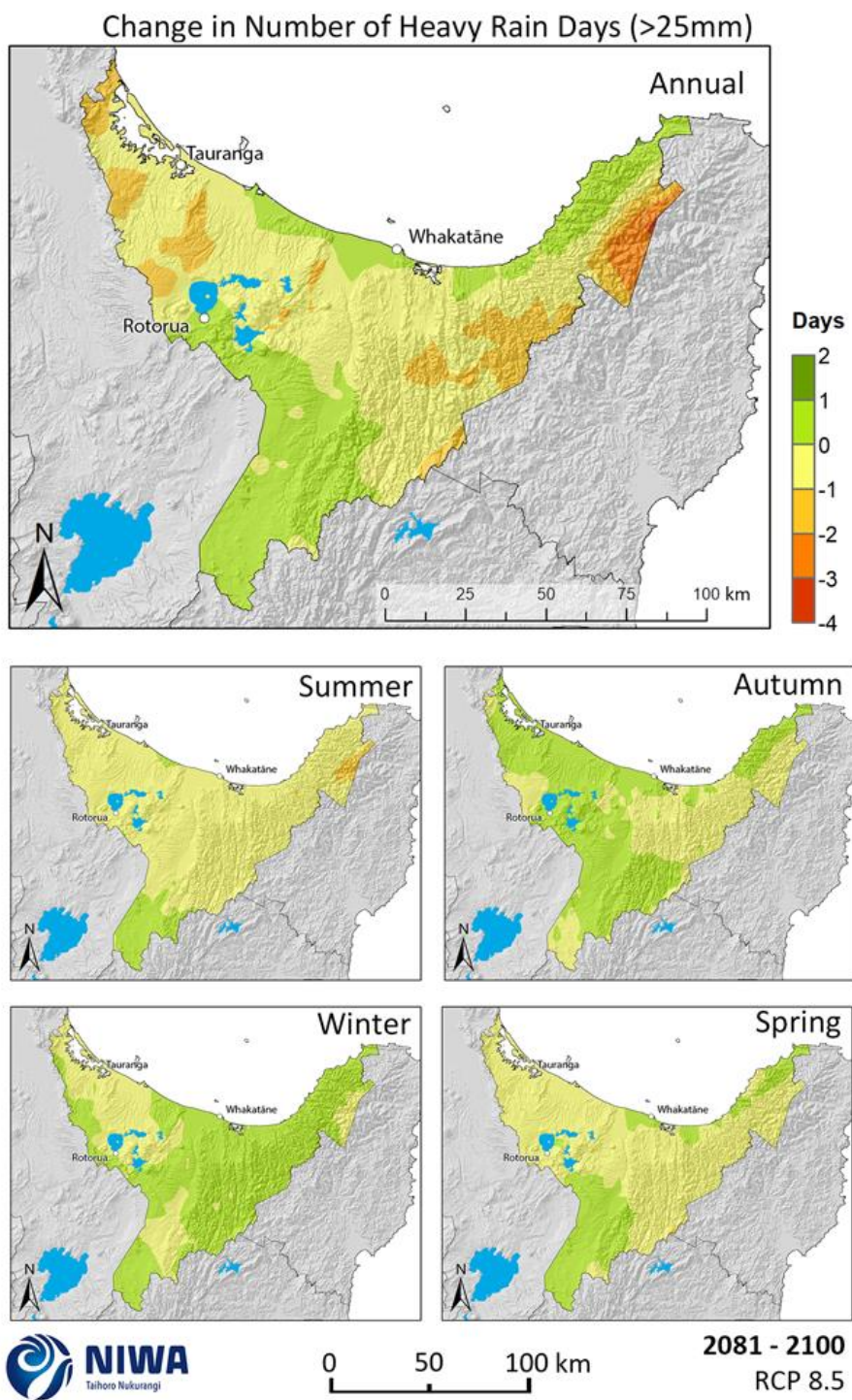


**Figure 4-15: Projected annual and seasonal number of heavy rain day (>25mm) changes by 2090 for RCP8.5.** Relative to 1986-2005 average, based on the average of six global climate models. Results are based on dynamical downscaled projections using NIWA's Regional Climate Model. Resolution of projection is 5km x 5km.

**Table 4-2: Modelled annual average number of heavy rain days (>25 mm) for historic and two climate change scenarios (RCP4.5 and RCP8.5) at two future time periods.** Time periods: historic: 1986-2005, mid-century: 2031-2050 "2040", end-century: 2081-2100 "2090"; based on the average of six global climate models. Note that historic rainfall is in millimetres and future rainfall change is in per cent.

Location	Historic (days)	Future change (days)		
Location	RCP	2040	2090	
Waihi Beach	18			
Tauranga	15			
Te Puke	16			
Rotorua	16			
Kawerau	25			
Whakatāne	16			
Ōpōtiki	16			
Katikati	20			
		Future change (days)		
Location	RCP	2040	2090	
Waihi Beach	RCP4.5	18 (0)	16.8 (-1.2)	
	RCP8.5	17.4 (-0.6)	16.8 (-1.2)	
Tauranga	RCP4.5	15.3 (+0.3)	15 (0)	
	RCP8.5	14.7 (-0.3)	14.1 (-0.9)	
Te Puke	RCP4.5	16.1 (+0.1)	15.8 (-0.2)	
	RCP8.5	16.3 (+0.3)	15.6 (-0.4)	
Rotorua	RCP4.5	16.3 (+0.3)	16.1 (+0.1)	
	RCP8.5	16.2 (+0.2)	16 (0)	
Kawerau	RCP4.5	24.3 (-0.7)	24.5 (-0.5)	
	RCP8.5	24.7 (-0.3)	24 (-1)	
Whakatāne	RCP4.5	16.7 (+0.7)	16.7 (+0.7)	
	RCP8.5	16.6 (+0.6)	16.2 (+0.2)	
Ōpōtiki	RCP4.5	16.5 (+0.5)	16.6 (+0.6)	
	RCP8.5	16.4 (+0.4)	16.3 (+0.3)	
Katikati	RCP4.5	20.1 (+0.1)	19 (-1)	
	RCP8.5	19.8 (-0.2)	19.2 (-0.8)	

#### 4.4 99<sup>th</sup> percentile of daily rainfall

The 99<sup>th</sup> percentile of daily rainfall refers to the amount of rainfall exceeded by the top 1% of wet days (days over 1 mm of rainfall). This equates to approximately the amount of rainfall that is exceeded roughly once per year in the Bay of Plenty, as many parts of the region experience about 100-120 days of rain (>1 mm) per year. Note that the 99<sup>th</sup> percentile is a relatively low threshold for engineering purposes (Ministry for the Environment, 2008). Projections for larger, rarer extreme rainfall events are presented in Section 4.7.

For the historic period, the highest annual average 99<sup>th</sup> percentile daily rainfall total is recorded inland from Matatā (100-110 mm) (Figure 4-16). The lowest total is inland from Murupara (30-40 mm). Generally, the broad swath west to east, inland from the coast, has higher totals than the coast and further inland.

In the future (Figure 4-17), the magnitude of the annual 99<sup>th</sup> percentile daily rainfall is expected to increase in some parts of the region and decrease in other parts. By 2040, some patchy decreases are expected for central and eastern areas (0-2% decrease in magnitude) under both RCP4.5 and RCP8.5. Most areas project increases in the magnitude of the 99<sup>th</sup> percentile daily rainfall, with 2-8% increases for most areas under RCP8.5. By 2090, all areas project increases, with widespread increases of 10-15% under RCP8.5 for central, eastern and western coastal areas.

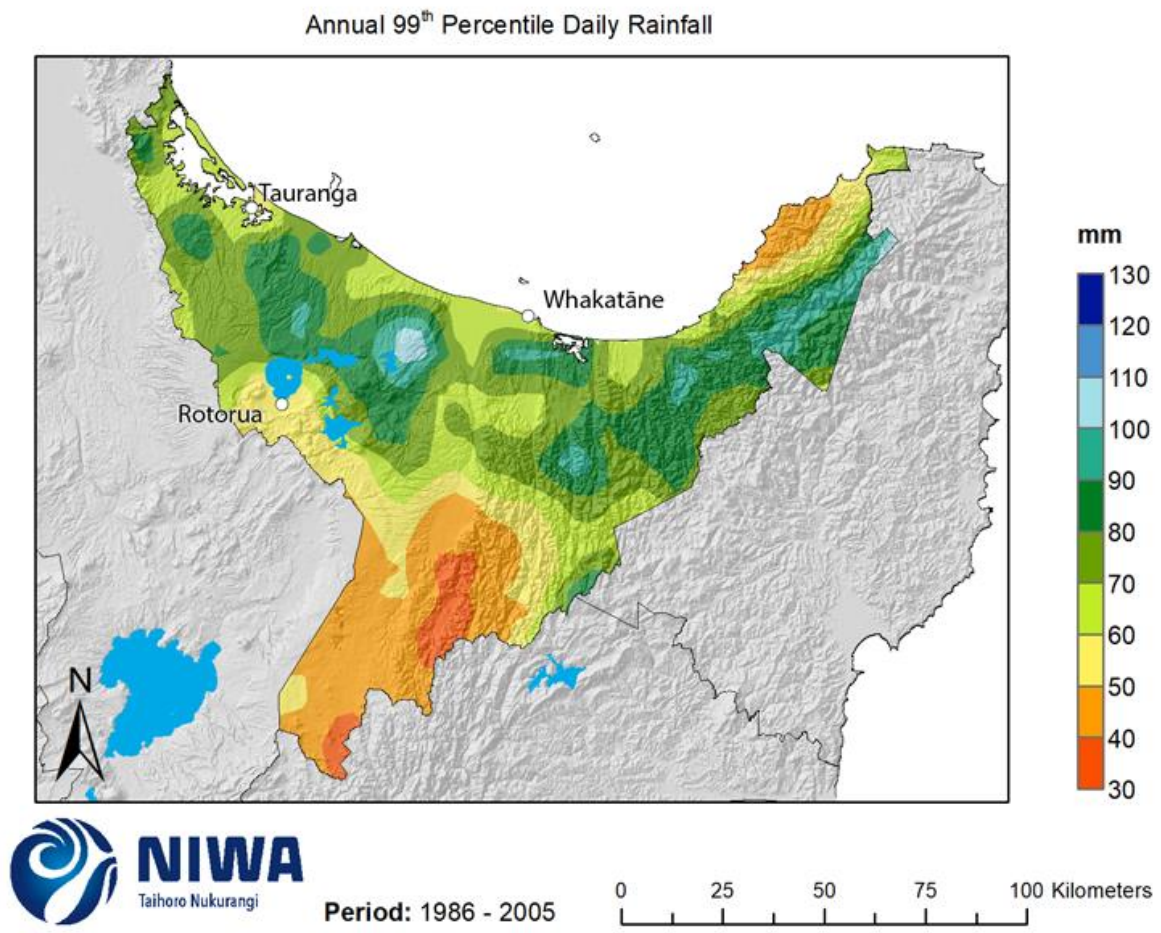


**Figure 4-16: Modelled annual 99<sup>th</sup> percentile daily rainfall average over 1986-2005.** Results are based on dynamical downscaled projections using NIWA's Regional Climate Model. Resolution of projection is 5km x 5km.

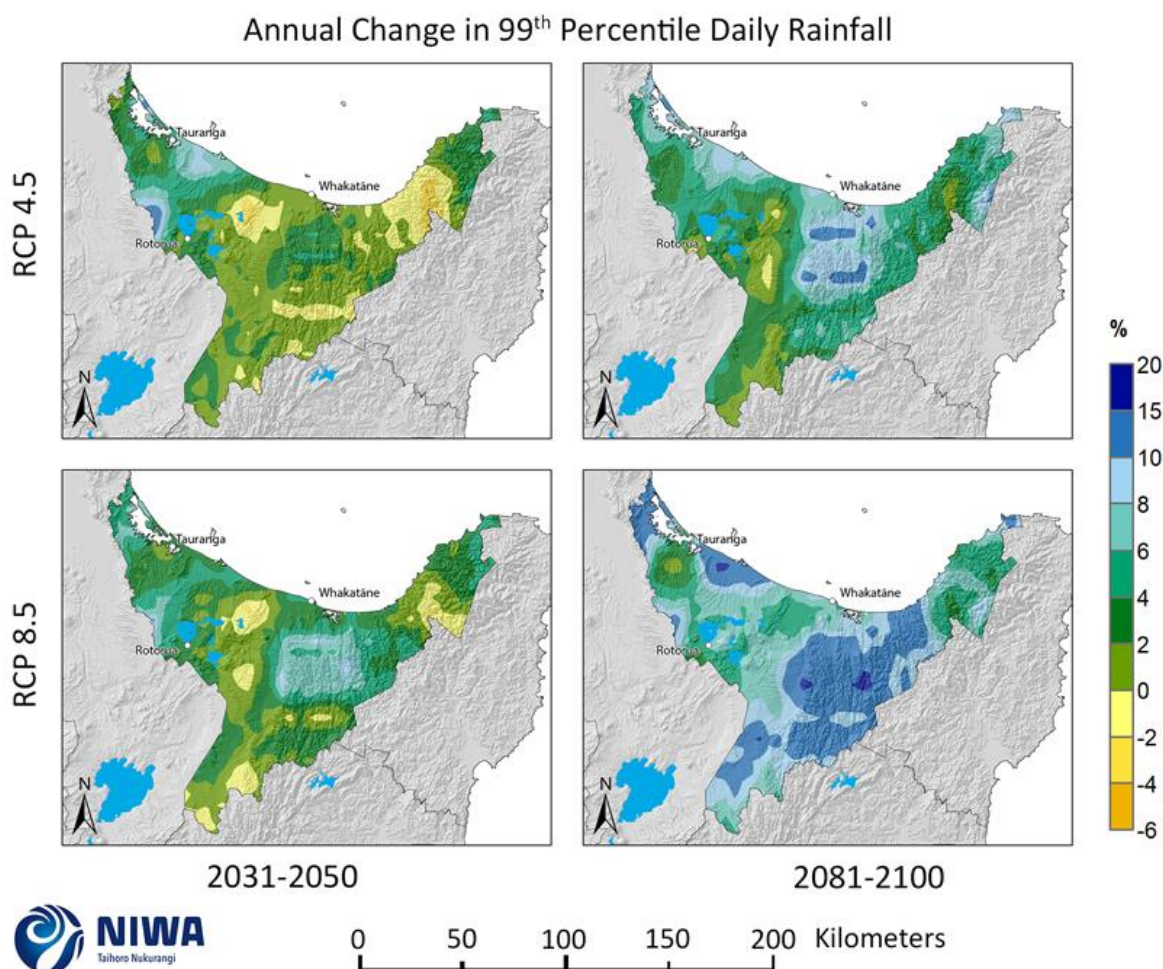


**Figure 4-17: Projected annual 99<sup>th</sup> percentile daily rainfall changes for RCP4.5 and RCP8.5, by 2040 and 2090.** Relative to 1986-2005 average, based on the average of six global climate models. Results are based on dynamical downscaled projections using NIWA's Regional Climate Model. Resolution of projection is 5km x 5km.

#### 4.5 Maximum 1-day rainfall

The annual maximum 1-day rainfall (otherwise known as Rx1day) is calculated as the wettest day of each year, which is then averaged over the 20-year period (e.g., 1986-2005 for the historic period and 2031-2050 and 2081-2100 for the future projections). Historic Rx1day maps are in units of mm per year (average over 1986-2005) and future (average over 2031-2050 and 2081-2100) maps show the change in rainfall compared with the historic total (units of mm). Note that the historic maps are on a different colour scale to the future projection maps. Rx1day totals are more extreme than 99<sup>th</sup> percentile daily rainfall totals (Section 4.4), because Rx1day takes the single maximum daily rainfall total each year, compared with the 99<sup>th</sup> percentile of daily rainfall which is an average of the amount of rainfall exceeded by the top 1% of wet days.

For the historic period, the Rx1day is highest in the high elevations of the Raukumara Ranges (140-160 mm) (Figure 4-18) and lowest in the furthest inland parts of the region, as well as Rotorua (60-80 mm). Most of the rest of the region has Rx1day totals of between 80 and 120 mm.

In the future (Figure 4-19), the maximum 1-day rainfall is generally projected to increase. However, by 2040 under RCP4.5, the maximum 1-day rainfall is projected to decline by 0-10 mm for the

eastern half of the region. Under RCP8.5 by 2040, increases of 5-15 mm are projected for most of the region, with the largest increases in the Raukumara Ranges. By 2090, under RCP4.5 increases of 0-15 mm are projected for most of the region (with 30-35 mm increases projected for the Raukumara Ranges), and under RCP8.5 10-25 mm increases are projected almost everywhere (with 35-45 mm increases projected for the Raukumara Ranges).

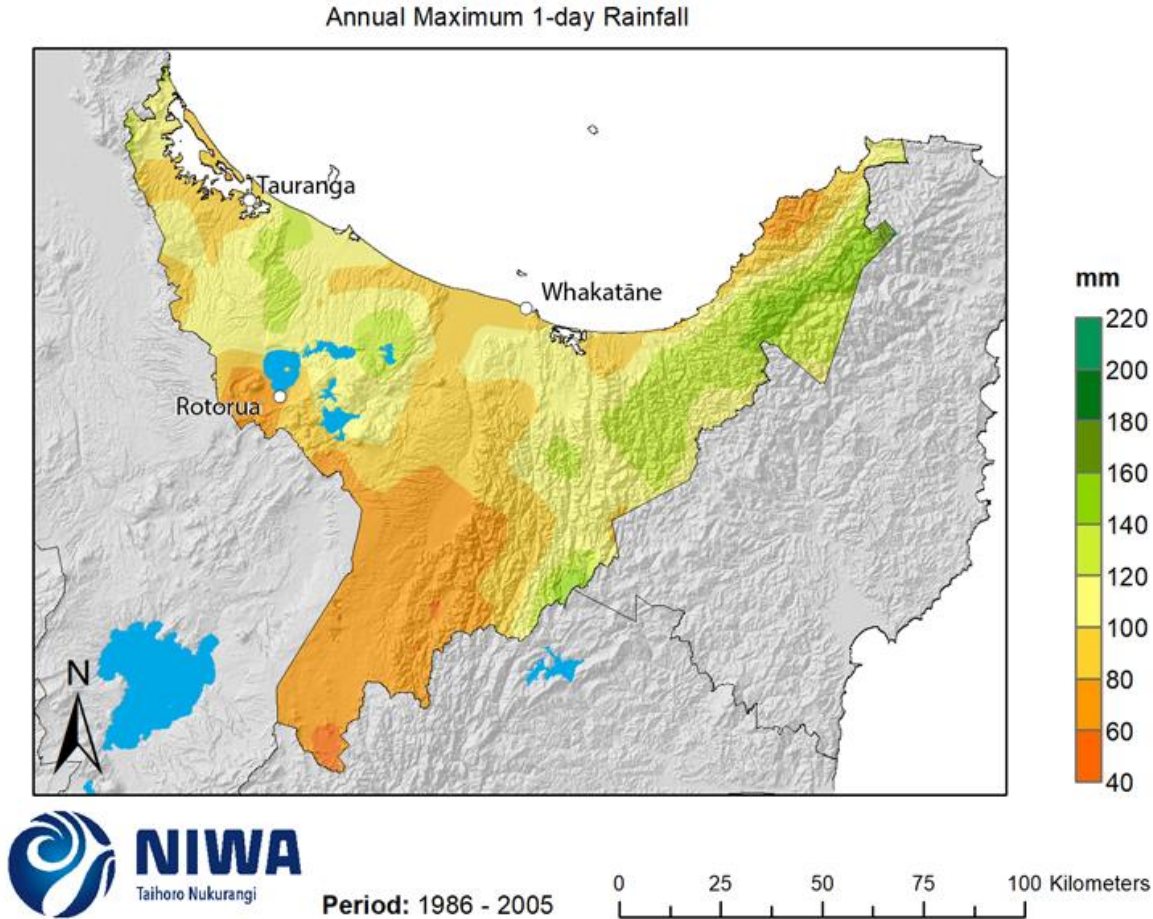


**Figure 4-18: Modelled annual maximum daily rainfall (Rx1day), average over 1986-2005.** Results are based on dynamical downscaled projections using NIWA's Regional Climate Model. Resolution of projection is 5km x 5km.

### Annual Change in Mean Maximum 1-Day Rainfall

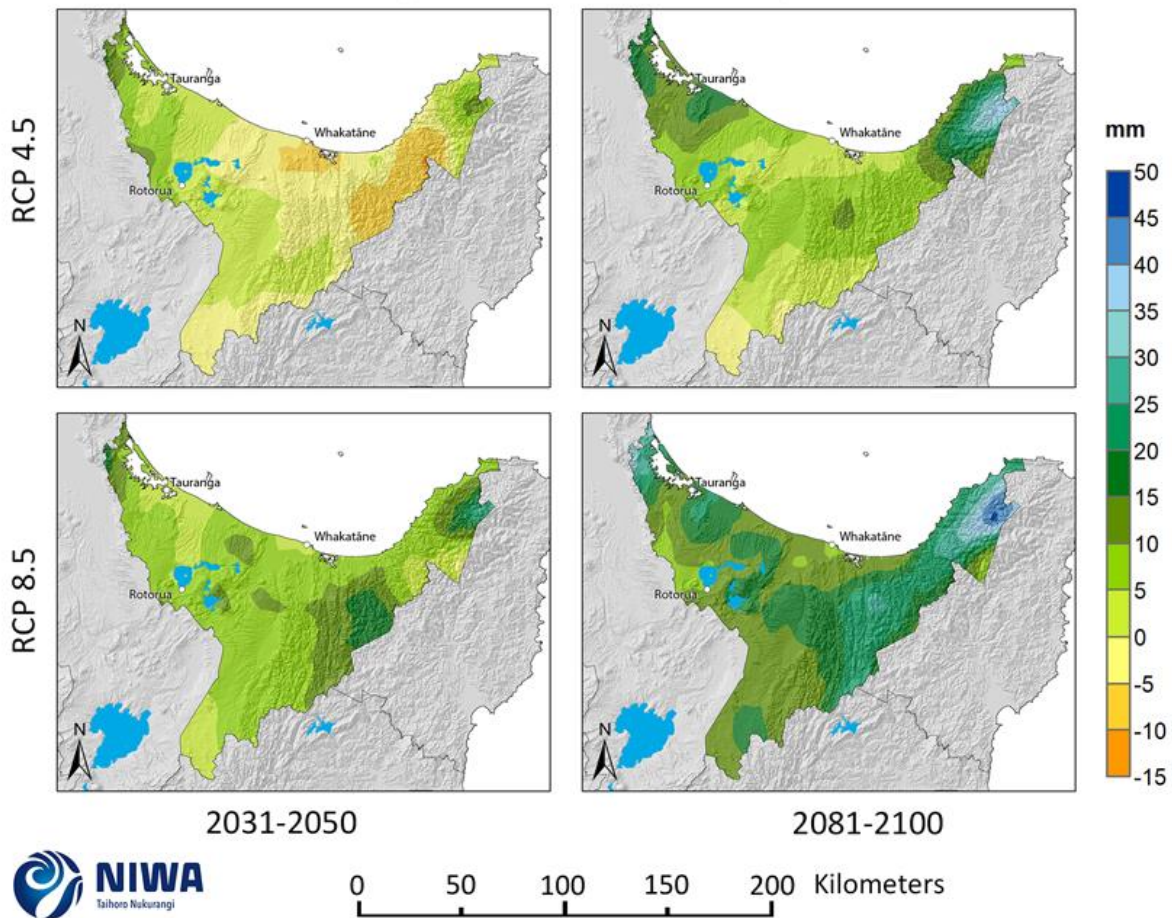


**Figure 4-19: Projected annual mean maximum 1-day rainfall (Rx1day) changes for RCP4.5 and RCP8.5, by 2040 and 2090.** Relative to 1986-2005 average, based on the average of six global climate models. Results are based on dynamical downscaled projections using NIWA's Regional Climate Model. Resolution of projection is 5km x 5km.

#### 4.6 Maximum 5-day rainfall

The annual maximum 5-day rainfall (otherwise known as Rx5day) is calculated as the wettest 5-day period of each year, which is then averaged over the 20-year period (e.g., 1986-2005 for the historic period and 2031-2050 and 2081-2100 for the future projections). Historic Rx5day maps are in units of mm per year (average over 1986-2005) and future (average over 2031-2050 and 2081-2100) maps show the change in 5-day rainfall compared with the historic total (units of mm). Note that the historic maps are on a different colour scale to the future projection maps.

For the historic period, the highest Rx5day total is in the highest elevations of the Raukumara Ranges (260-300 mm) (Figure 4-20). The lowest Rx5day total is the part of the region inland from Murupara (100-120 mm).

In the future (Figure 4-21), Rx5day is generally projected to increase, with larger increases by 2090. Overall, increases of 0-10 mm are common for most areas, with larger increases for the Urewera and Raukumara Ranges, particularly by 2090 (20-30 mm increases). However, there are isolated areas projecting decreases of 0-5 mm (western areas around Rotorua and eastern areas near Ōpōtiki).

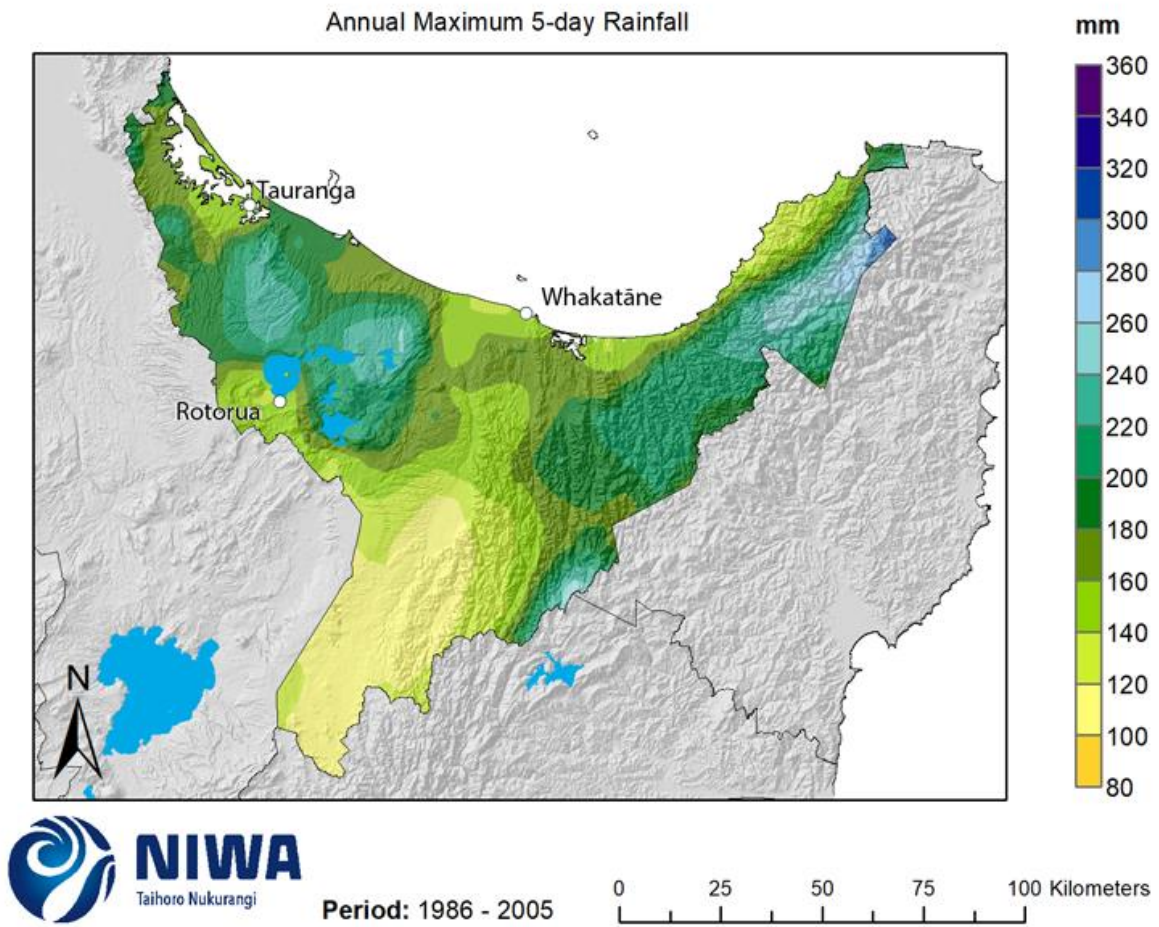


**Figure 4-20: Modelled annual maximum 5-day rainfall (Rx5day), average over 1986-2005.** Results are based on dynamical downscaled projections using NIWA's Regional Climate Model. Resolution of projection is 5km x 5km.

### Annual Change in Mean Maximum 5-Day Rainfall

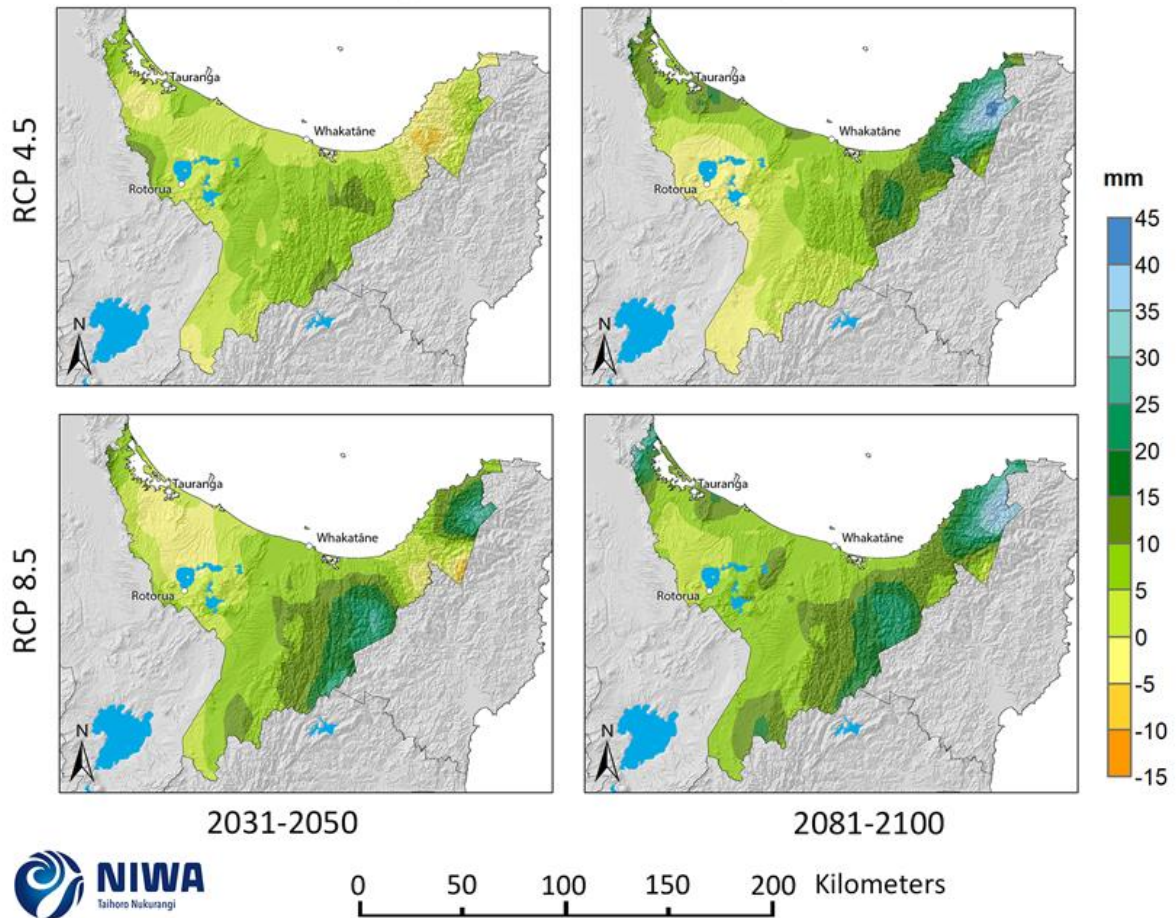


**Figure 4-21: Projected annual mean maximum 5-day rainfall (Rx5day) changes for RCP4.5 and RCP8.5, by 2040 and 2090.** Relative to 1986-2005 average, based on the average of six global climate models. Results are based on dynamical downscaled projections using NIWA's Regional Climate Model. Resolution of projection is 5km x 5km.



## 4.7 Extreme, rare rainfall events (HIRDS v4)

### Key messages

- Extreme, rare rainfall events are likely to increase in intensity in New Zealand because a warmer atmosphere can hold more moisture.
- Augmentation factors (percentage increases per degree of warming) are provided which allow calculation of increases in rainfall depths for events of different durations.
- Short duration, rare rainfall events have the largest relative increases which approach 14% increase per degree of warming, while the longest duration events increase by 5-6% per degree of warming.
- Extreme rainfall projections for any New Zealand location can be viewed at [www.hirds.niwa.co.nz](http://www.hirds.niwa.co.nz)
- Increases in extreme rainfall accumulations may cause more flooding, but this is yet to be thoroughly researched in New Zealand.

Extreme, rare rainfall events may cause significant damage to land, buildings, and infrastructure. This section analyses how these rainfall events may change in the future for New Zealand.

Extreme rainfall events (and floods) are often considered in the context of return periods (e.g. 1-in-100-year rainfall events). A return period, also known as a recurrence interval, is an estimate of the likelihood of an event. It is a statistical measure typically based on historic data and probability distributions which calculate how often an event of a certain magnitude may occur. Return periods are often used in risk analysis and infrastructure design.

The theoretical return period is the inverse of the probability that the event will be exceeded in any one year. For example, a 1-in-10-year rainfall event has a  $1/10 = 0.1$  or 10% chance of being exceeded in any one year and a 1-in-100-year rainfall event has a  $1/100 = 0.01$  or 1% chance of being exceeded in any one year. However, this does not mean that a 1-in-100-year rainfall event will happen regularly every 100 years, or only once in 100 years. The events with larger return periods (i.e. 1-in-100-year events) have larger rainfall amounts for the same duration as events with smaller return periods (i.e. 1-in-2-year events) because larger events occur less frequently (on average).

A warmer atmosphere can hold more moisture, so there is potential for heavier extreme rainfall with global increases in temperatures under climate change (Fischer and Knutti, 2016, Trenberth, 1999). The frequency of heavy rainfall events is 'very likely' to increase over most mid-latitude land areas (this includes New Zealand; IPCC, 2013). Given the mountainous nature of New Zealand, spatial patterns of changes in rainfall extremes are expected to depend on changes in atmospheric circulation and storm tracks.

NIWA's High Intensity Rainfall Design System (HIRDS) allows rainfall event recurrence intervals to be calculated for any location in New Zealand. HIRDS calculates historic recurrence intervals as well as future potential recurrence intervals based on climate change scenarios. The 2018 HIRDS version 4

(Carey-Smith et al., 2018) updated the scenarios to those presented in this report (i.e. the IPCC's Fifth Assessment Report scenarios). The future rainfall increases calculated by the HIRDS v4 tool are based on a percent change per degree of warming. The short duration, rare events have the largest relative increases of around 14%, while the longest duration events increase by about 5 to 6%. HIRDS v4 can be freely accessed at [www.hirds.niwa.co.nz](http://www.hirds.niwa.co.nz), and more background information to the HIRDS methodology can be found at <https://www.niwa.co.nz/information-services/hirds/help>. HIRDS rainfall projections for locations in the Bay of Plenty are presented in Table 4-4.

The return periods for these historic 1:50 and 1:100-year, 24 hour duration rainfall events are projected to change significantly in the future. For example, what is currently a 1:100-year event at Whakarewarewa (215 mm) may become a 1:33-year event by 2090, i.e. it may be three times more likely to happen in any given year (i.e. it may have a 3.3% AEP instead of a 1% AEP).

**Table 4-3: Historic rainfall depths for a 1:50 year return period, 24 hour duration event (millimetres) and projected changes to the return period of this size event under two climate change scenarios at two future time periods. Data source: HIRDS v4 ([www.hirds.niwa.co.nz](http://www.hirds.niwa.co.nz))**

Location	Historic 1:50 year, 24h duration amount (mm)	RCP4.5 ARI		RCP8.5 ARI	
		2040	2090	2040	2090
Whakarewarewa	191	1:36	1:30	1:35	1:19
Waihi Beach	262	1:36	1:30	1:35	1:19
Te Puke	246	1:36	1:30	1:35	1:19
Tauranga	220	1:36	1:30	1:35	1:19
Whakatāne	201	1:36	1:30	1:35	1:19
Ōpōtiki	187	1:36	1:29	1:35	1:18

**Table 4-4: Historic rainfall depths for a 1:100 year return period, 24 hour duration event (millimetres) and projected changes to the return period of this size event under two climate change scenarios at two future time periods. Data source: HIRDS v4 ([www.hirds.niwa.co.nz](http://www.hirds.niwa.co.nz))**

Location	Historic 1:100 year, 24h duration amount (mm)	RCP4.5 ARI		RCP8.5 ARI	
		2040	2090	2040	2090
Whakarewarewa	215	1:71	1:59	1:67	1:33
Waihi Beach	294	1:70	1:56	1:66	1:33
Te Puke	277	1:71	1:57	1:67	1:34
Tauranga	248	1:70	1:56	1:67	1:34
Whakatāne	226	1:70	1:56	1:67	1:33
Ōpōtiki	210	1:70	1:56	1:66	1:33

## 4.8 Dry days

A dry day considered here is when < 1 mm of rainfall is recorded. Historic (average over 1986-2005) and future (average over 2031-2050 and 2081-2100) maps for dry days are shown in this section. The historic maps show annual and seasonal average numbers of dry days and the future projection maps show the change in the number of dry days compared with the historic period. Note that the historic maps are on a different colour scale to the future projection maps.

For the historic period, the largest annual number of dry days is experienced near Ōhope (220-240 days per year) (Figure 4-22). The area around Whakatāne and Kawerau also has high numbers of dry days (200-220 days per year). Most of the central and western part of the region experiences 180-200 dry days per year, and the eastern high elevation hill country experiences 120-160 dry days per year, on average. Autumn is the season with the largest number of dry days (50-60 dry days for most of the region) and spring has the fewest dry days (35-40 dry days for most of the region).

By 2040 under RCP4.5 (Figure 4-23), the number of dry days per year decreases near the coast (2-6 fewer dry days per year) and increases further inland (up to 4-6 more dry days for the Huiarau, Urewera and Raukumara Ranges). The largest increases are projected for summer and spring, with coastal reductions projected for winter and autumn. This pattern is amplified under RCP8.5 (Figure 4-24), with 4-6 more dry days per year for most of the region inland from the coast, and 0-4 fewer dry days per year for the coastal areas. By 2090 under RCP4.5 (Figure 4-25), 8-10 more dry days are projected for a large part of the central and eastern hill country, with 10-15 more dry days projected for the high elevations of the ranges. Smaller increases of 0-4 dry days per year are projected for coastal areas. Under RCP8.5 (Figure 4-26), 15-20 more dry days per year are projected for inland areas (with 20-25 more dry days for the highest elevations of the ranges). The smallest increases are projected around Whakatāne, of 0-4 days per year. The largest increases are projected for spring, and the smallest increases are projected for winter.

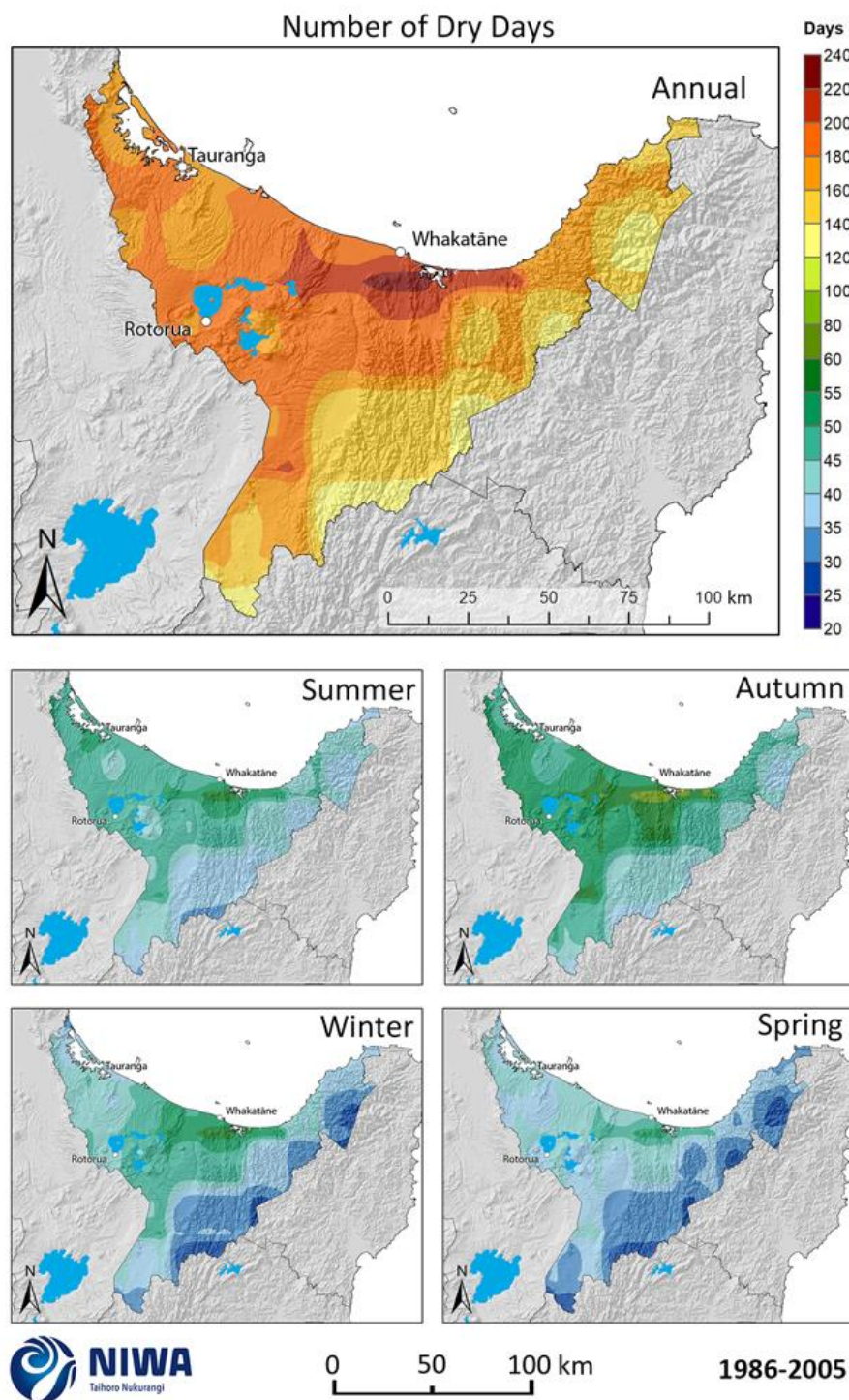


**Figure 4-22: Modelled annual and seasonal number of dry days (daily rainfall <1mm), average over 1986-2005.** Results are based on dynamical downscaled projections using NIWA's Regional Climate Model. Resolution of projection is 5km x 5km.

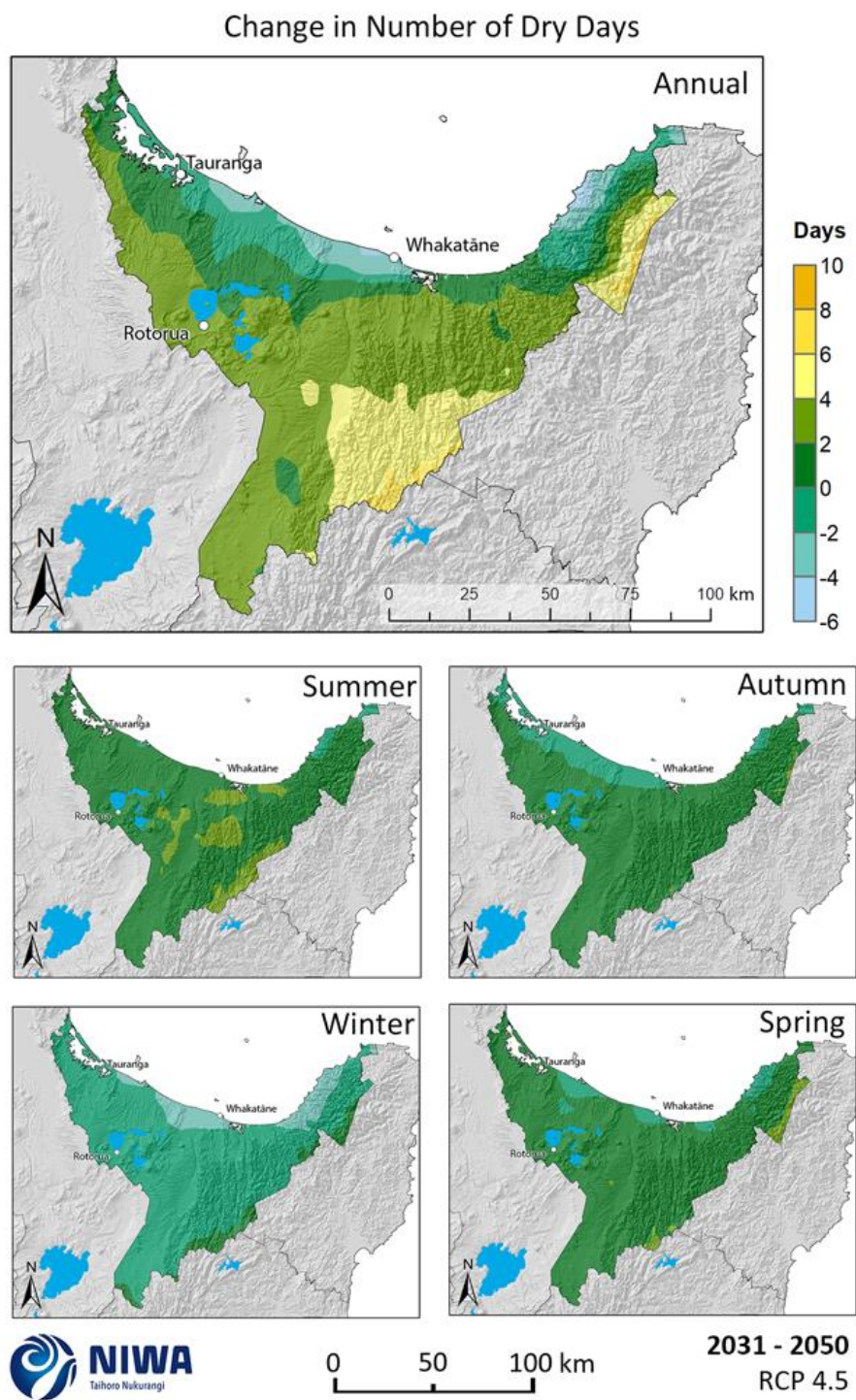


**Figure 4-23: Projected annual and seasonal number of dry day (<1mm rainfall) changes by 2040 for RCP4.5.** Relative to 1986-2005 average, based on the average of six global climate models. Results are based on dynamical downscaled projections using NIWA's Regional Climate Model. Resolution of projection is 5km x 5km.

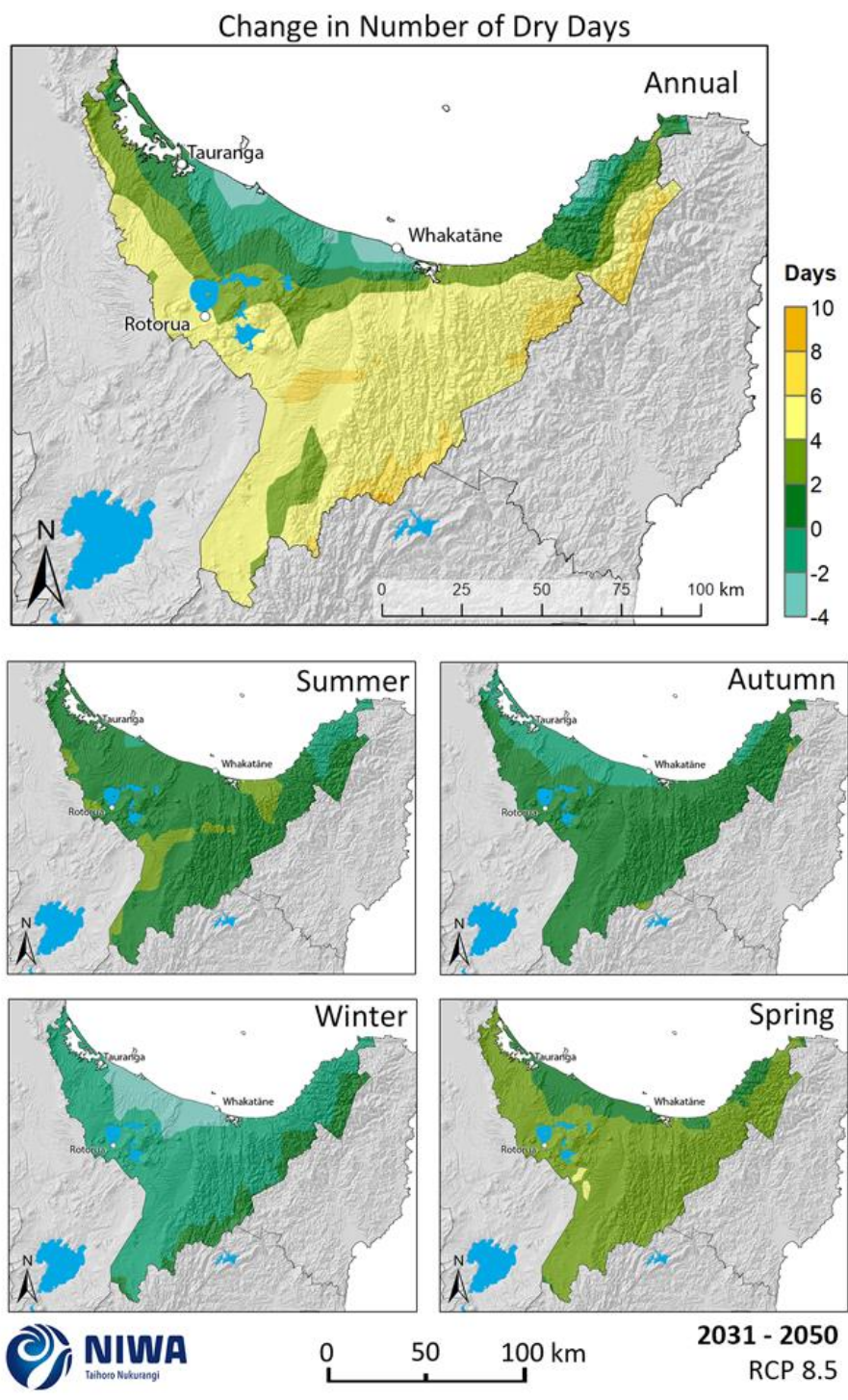


**Figure 4-24: Projected annual and seasonal number of dry day (<1mm rainfall) changes by 2040 for RCP8.5.** Relative to 1986-2005 average, based on the average of six global climate models. Results are based on dynamical downscaled projections using NIWA's Regional Climate Model. Resolution of projection is 5km x 5km.

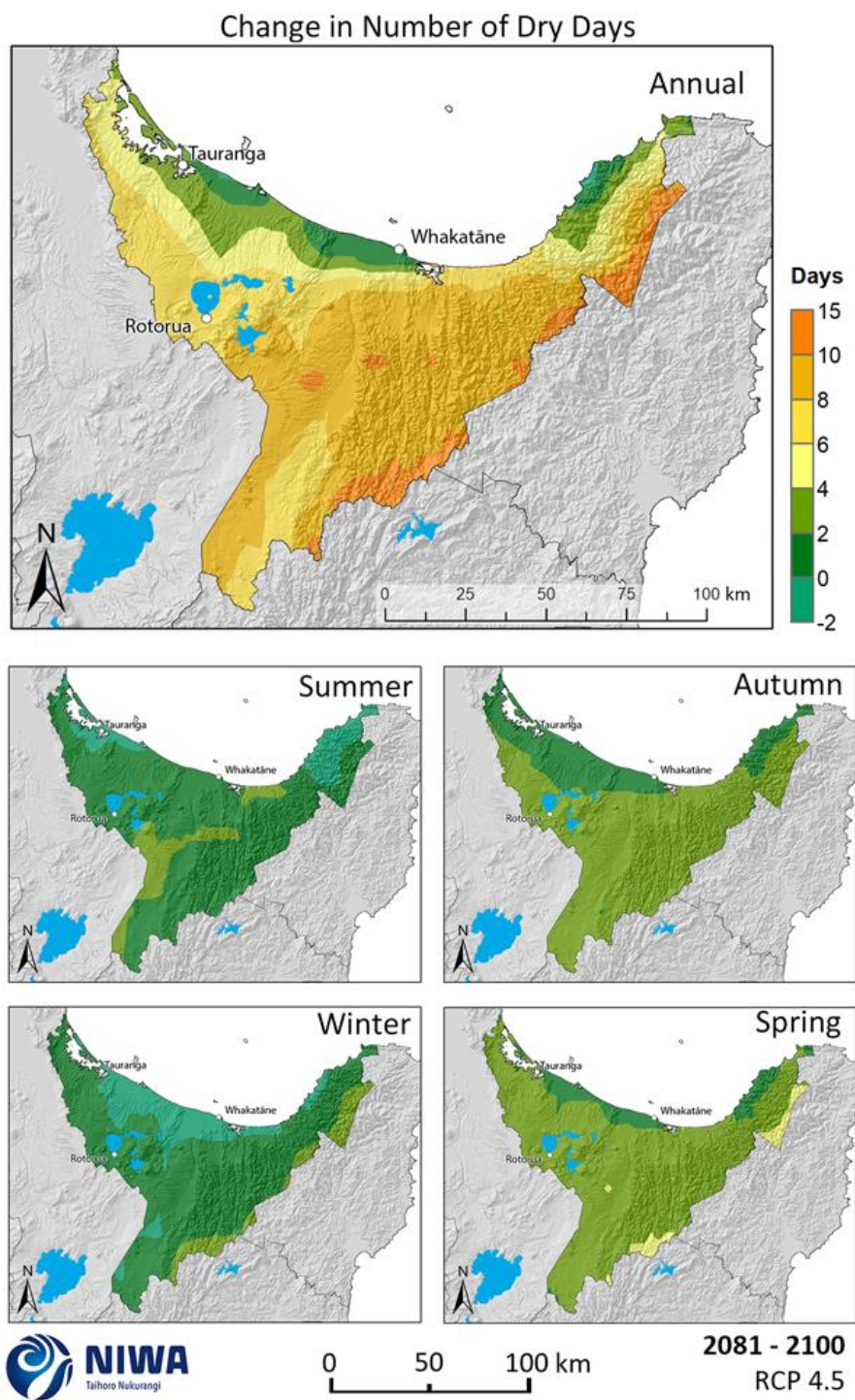


**Figure 4-25: Projected annual and seasonal number of dry day (<1mm rainfall) changes by 2090 for RCP4.5.** Relative to 1986-2005 average, based on the average of six global climate models. Results are based on dynamical downscaled projections using NIWA's Regional Climate Model. Resolution of projection is 5km x 5km.

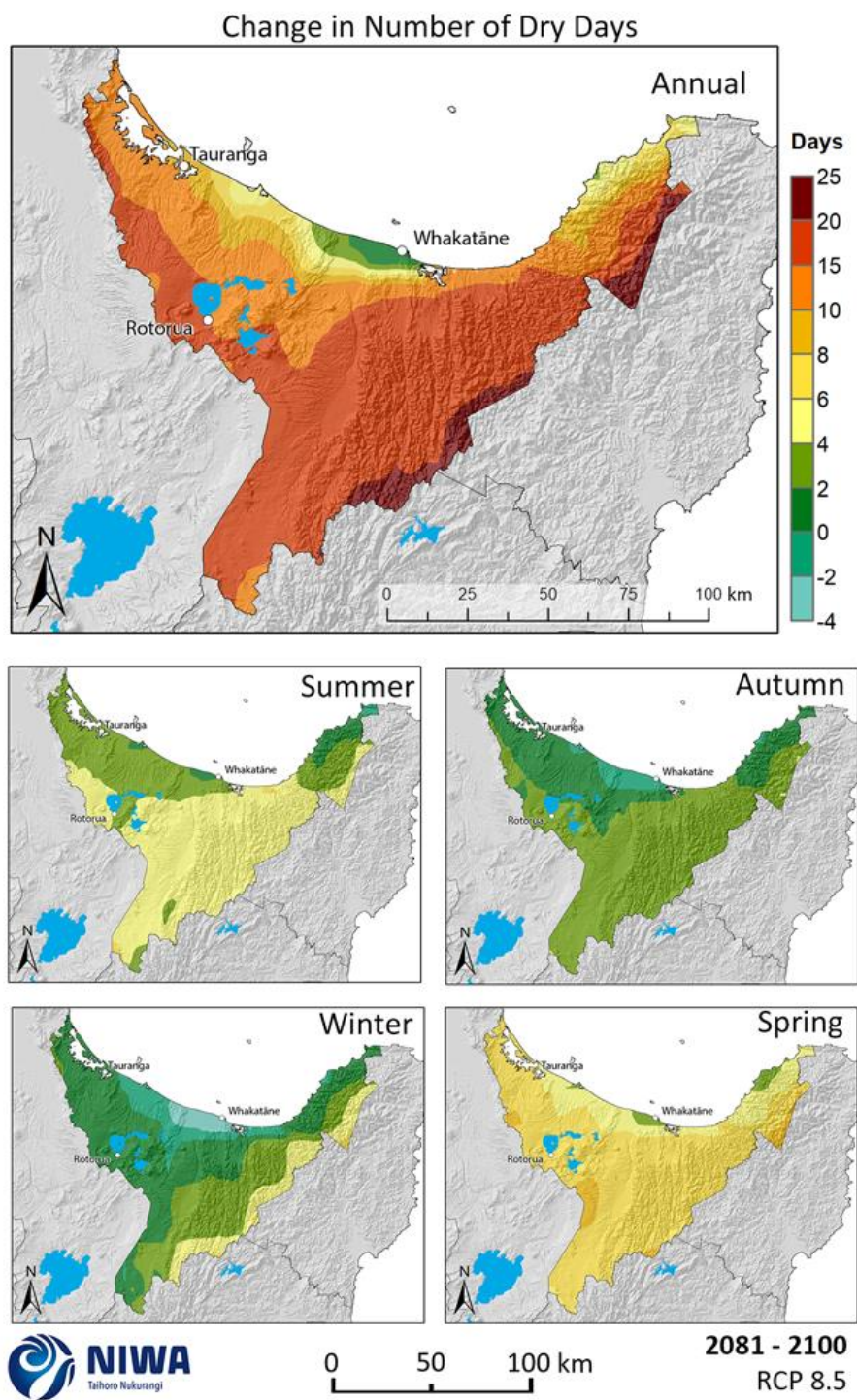


**Figure 4-26: Projected annual and seasonal number of dry day (<1mm rainfall) changes by 2090 for RCP8.5.** Relative to 1986-2005 average, based on the average of six global climate models. Results are based on dynamical downscaled projections using NIWA's Regional Climate Model. Resolution of projection is 5km x 5km.



## 4.9 Potential Evapotranspiration Deficit

The measure of meteorological drought<sup>2</sup> that is used in this section is ‘potential evapotranspiration deficit’ (PED). Evapotranspiration is the process where water held in the soil is gradually released to the atmosphere through a combination of direct evaporation and transpiration from plants. As the growing season advances, the amount of water lost from the soil through evapotranspiration typically exceeds rainfall, giving rise to an increase in soil moisture deficit. As soil moisture decreases, pasture production becomes moisture-constrained and evapotranspiration can no longer meet atmospheric demand.

The difference between this demand (evapotranspiration deficit) and the actual evapotranspiration is defined as the ‘potential evapotranspiration deficit’ (PED). In practice, PED represents the total amount of water required by irrigation, or that needs to be replenished by rainfall, to maintain plant growth at levels unconstrained by water shortage. As such, PED estimates provide a robust measure of drought intensity and duration. Days when water demand is not met, and pasture growth is reduced, are often referred to as days of potential evapotranspiration deficit.

PED is calculated as the difference between potential evapotranspiration (PET) and rainfall, for days of soil moisture under half of available water capacity (AWC), where an AWC of 150mm for silty-loamy soils is consistent with estimates in previous studies (e.g. Mullan et al., 2005). PED, in units of mm, can be thought of as the amount of missing rainfall needed in order to keep pastures growing at optimum levels. Higher PED totals indicate drier soils. An increase in PED of 30 mm or more corresponds to an extra week of reduced grass growth. Accumulations of PED greater than 300 mm indicate very dry conditions.

Historic (average over 1986-2005) and future (average over 2031-2050 and 2081-2100) maps for PED are shown in this section. The historic maps show annual accumulated PED in units of mm and the future projection maps show the change in the annual accumulated PED compared with the historic period, in units of mm. Note that the historic maps are on a different colour scale to the future projection maps.

For the historic period, the highest PED accumulation is experienced near Te Puke (280-300 mm per year, on average) (Figure 4-27). Coastal areas between Tauranga and Whakatāne generally experience >200 mm of PED per year. PED declines at higher elevations, with most of the high country experiencing only 20-60 mm of PED per year.

In the future, the amount of accumulated PED is projected to increase across the Bay of Plenty region (Figure 4-28), therefore drought potential is projected to increase. The increase in PED is amplified with time and RCP. By 2040 under both RCPs, most of the region outside of the high elevations of the Urewera and Raukumara Ranges is projected to experience an increase in PED of 60-80 mm per year. Some coastal areas experience an additional 100-120 mm of PED per year. By 2090 under RCP4.5, the coastal area around Tauranga and Te Puke experiences an additional 120-140 mm of PED per year, and much of the rest of the region experiences an additional 80-100 mm of PED per year. Under RCP8.5, PED is projected to increase by 100-140 mm per year for most of the region outside of the high elevations of the ranges. In the coastal area around Tauranga and Te Puke, an additional 160-180 mm of PED per year is projected.

---

<sup>2</sup> Meteorological drought happens when dry weather patterns dominate an area and resulting rainfall is low. Hydrological drought occurs when low water supply becomes evident, especially in streams, reservoirs, and groundwater levels, usually after an extended period of meteorological drought.

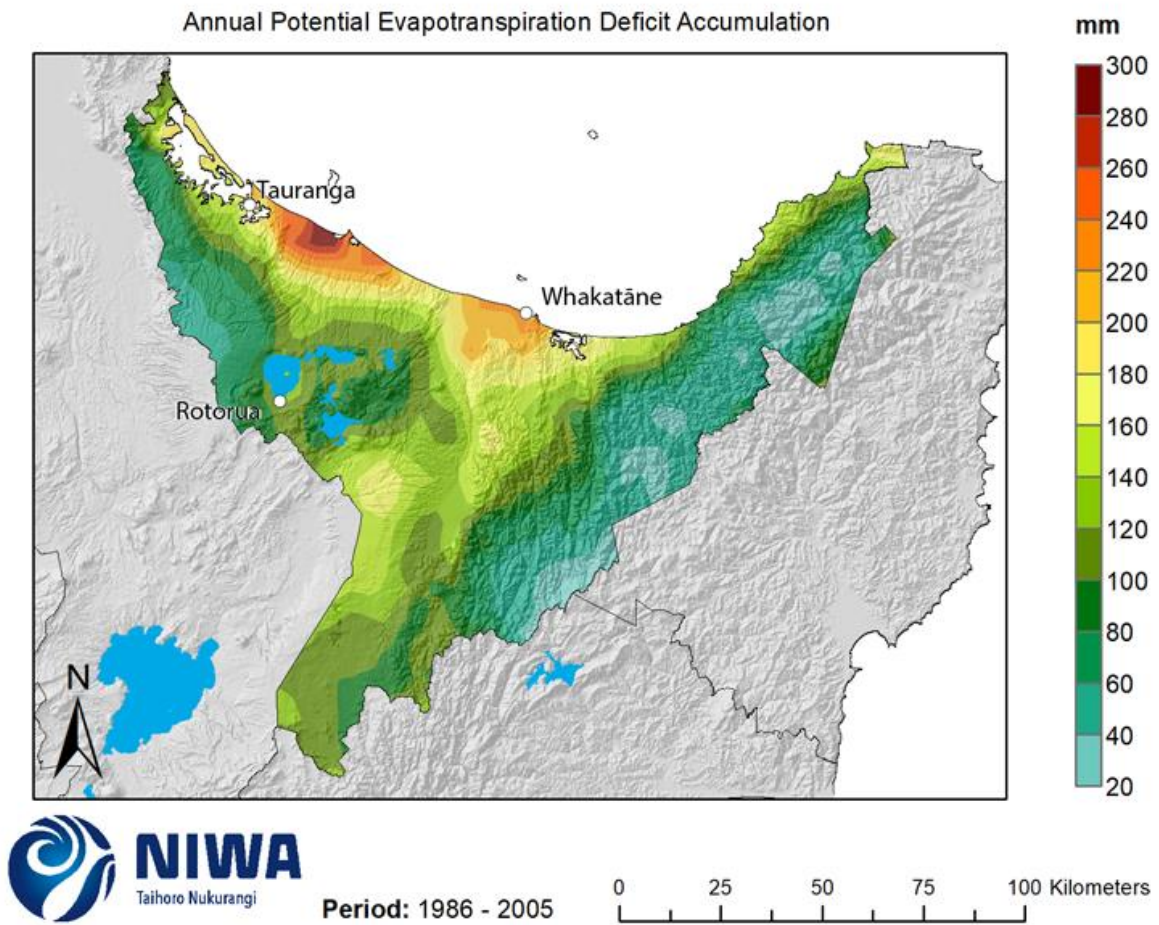


**Figure 4-27: Modelled annual potential evapotranspiration deficit accumulation (mm), average over 1986-2005.** Results are based on dynamical downscaled projections using NIWA's Regional Climate Model. Resolution of projection is 5km x 5km.

## Annual Change in Potential Evapotranspiration Deficit Accumulation

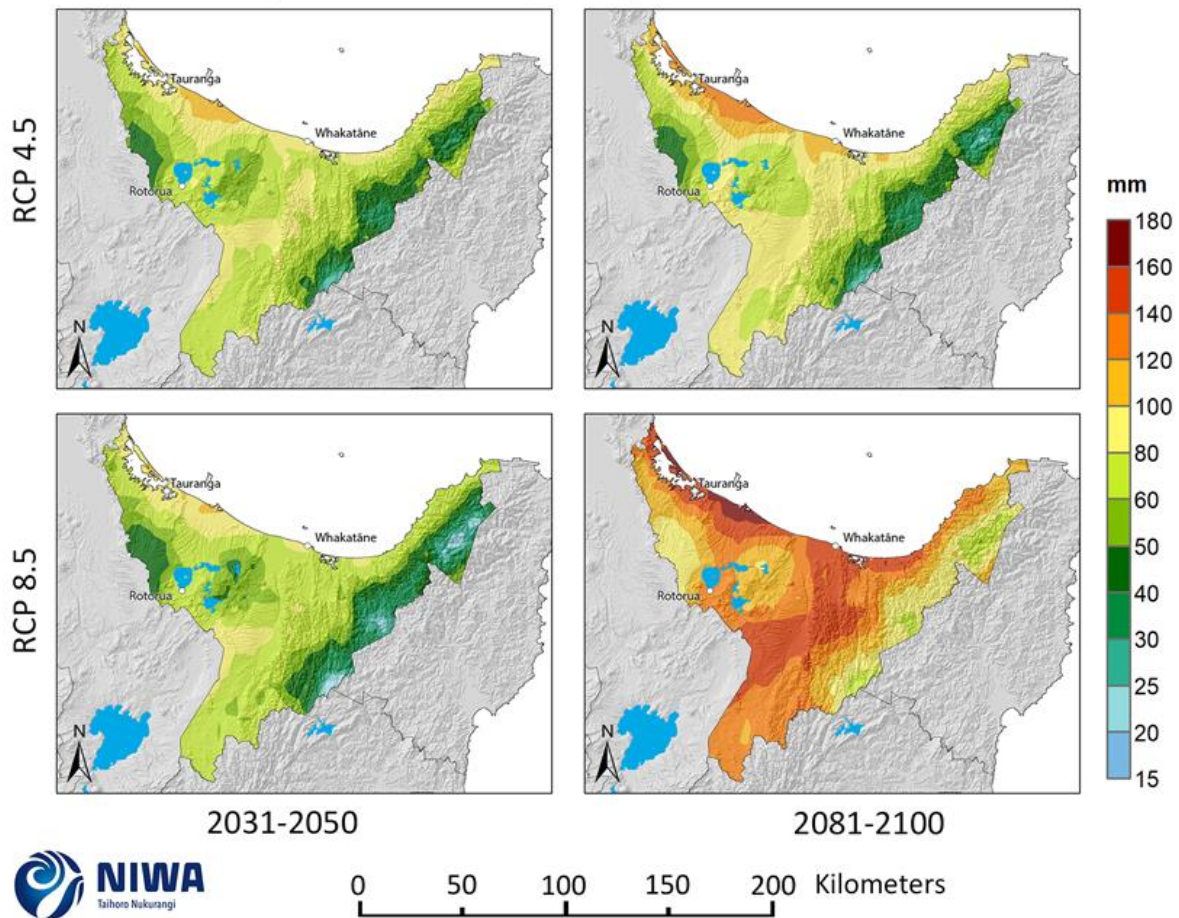


**Figure 4-28: Projected annual potential evapotranspiration deficit (PED) accumulation changes for RCP4.5 and RCP8.5, by 2040 and 2090.** Relative to 1986-2005 average, based on the average of six global climate models. Results are based on dynamical downscaled projections using NIWA's Regional Climate Model. Resolution of projection is 5km x 5km.

### 4.10 Soil moisture deficit

Soil moisture deficit (SMD) is calculated based on incoming daily rainfall (mm), outgoing daily potential evapotranspiration (PET), and a fixed available water capacity of 150 mm (the amount of water in the soil 'reservoir' that plants can use). In the calculation, evapotranspiration continues at its potential rate until about half of the water available to plants is used up (75 mm out of the total 150 mm available). Subsequently, the rate of evapotranspiration decreases, in the absence of rain, as further water extraction takes place. Evapotranspiration is assumed to cease if all the available water is used up (i.e. all 150 mm).

A day of SMD is considered in this report to be when soil moisture is below 75 mm of available soil water capacity. The timing of changes in the days of soil moisture deficit projections indicates how droughts may change in timing throughout the year. Soil moisture deficit and PED are similar measures of dryness, but in this report SMD is measured in days and PED is measured in mm of accumulation, so PED is a more sensitive measure of drought intensity than SMD.

Historic (average over 1986-2005) and future (average over 2031-2050 and 2081-2100) maps for days of SMD are shown in this section. The historic maps show the annual and seasonal number of

days of SMD and the future projection maps show the change in the number of days of SMD compared with the historic period. Note that the historic maps are on a different colour scale to the future projection maps.

For the historic period, the highest number of SMD days is experienced around Maketu and Whakatāne (220-240 days of SMD per year) (Figure 4-29). The coastal strip generally has the highest number of SMD days in all seasons. Most of the central and inland part of the region experiences 140-160 SMD days per year. The number of SMD days decreases with increasing elevation, so the highest elevations of the Raukumara Ranges have 60-80 SMD days per year. Summer is the season with the highest number of SMD days (60-80 SMD days for most low elevation areas), and winter has the least SMD days (0-5 SMD days for all areas inland of the coastal strip).

In the future, the days of SMD per year generally reduce near the coast and increase inland. By 2040 under RCP4.5 (Figure 4-30), days of SMD per year reduce by 4-8 days around Te Puke and increase by 8-15 days per year for most inland parts of the region. The largest increases are projected for summer (6-10 days) and the largest coastal decreases are projected for winter (0-4 days near Te Puke). The pattern is broadly similar under RCP8.5 (Figure 4-31), with coastal SMD days reducing by 2-8 days per year near Whakatāne and increases of 8-15 days per year inland. By 2090 under RCP4.5 (Figure 4-32), the increases of days of SMD are more pronounced inland, with 15-25 more SMD days per year projected for many parts of the region. For the coastal area between Tauranga and Whakatāne however, only small increases of 0-6 SMD days per year are projected under this scenario. Under RCP8.5 (Figure 4-33), at least 20 more SMD days per year are projected for almost the entire region, with some areas in the ranges and around Katikati experiencing increases of 30-35 SMD days per year. The coastal area between Tauranga and Whakatāne experiences increases of 10-15 SMD days per year. The largest increases are projected for spring (10-15 more SMD days for most areas) and the smallest increases for winter (0-4 more SMD days for most areas).

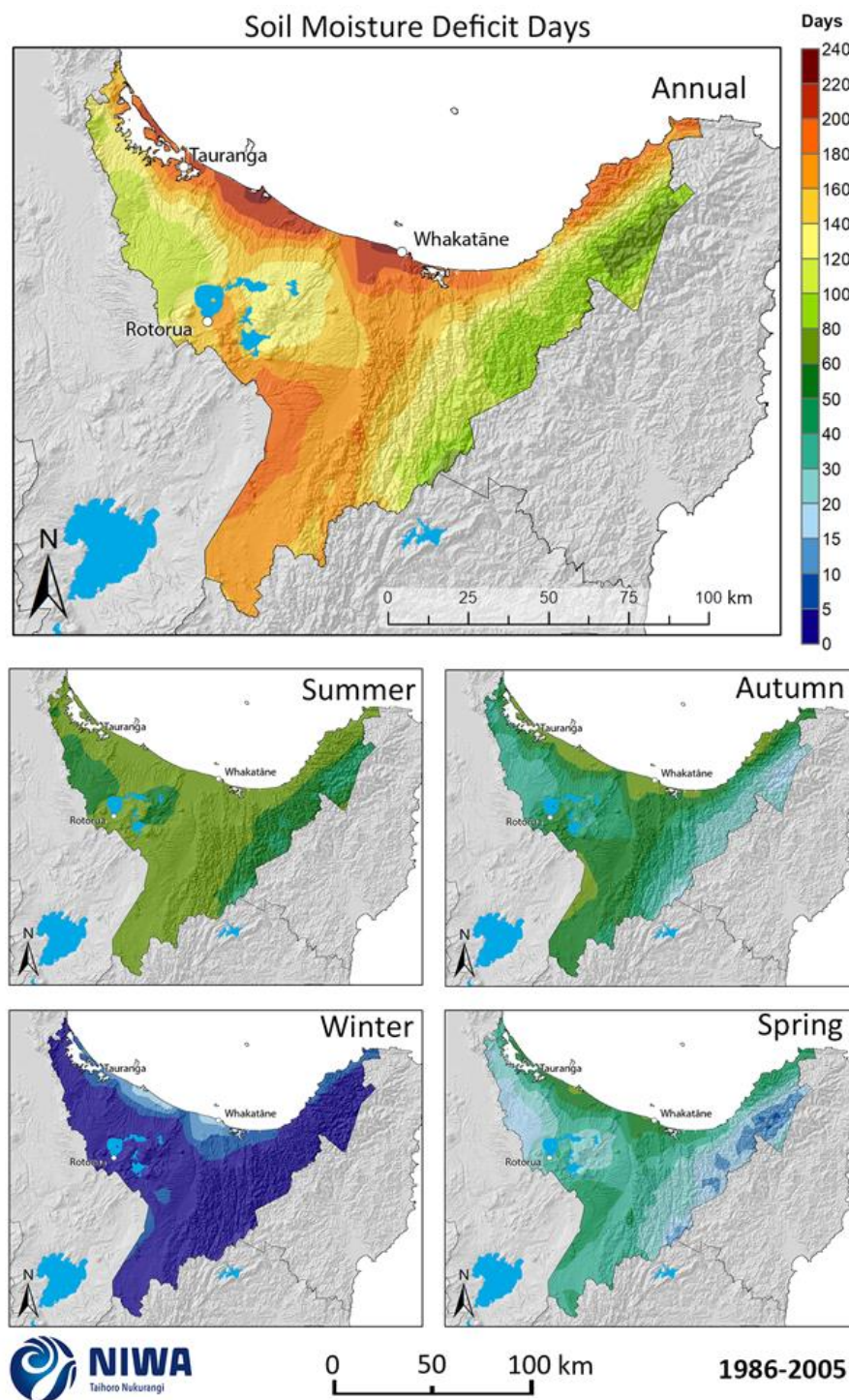


**Figure 4-29: Modelled annual and seasonal number of days of soil moisture deficit, average over 1986-2005.** Results are based on dynamical downscaled projections using NIWA's Regional Climate Model. Resolution of projection is 5km x 5km.

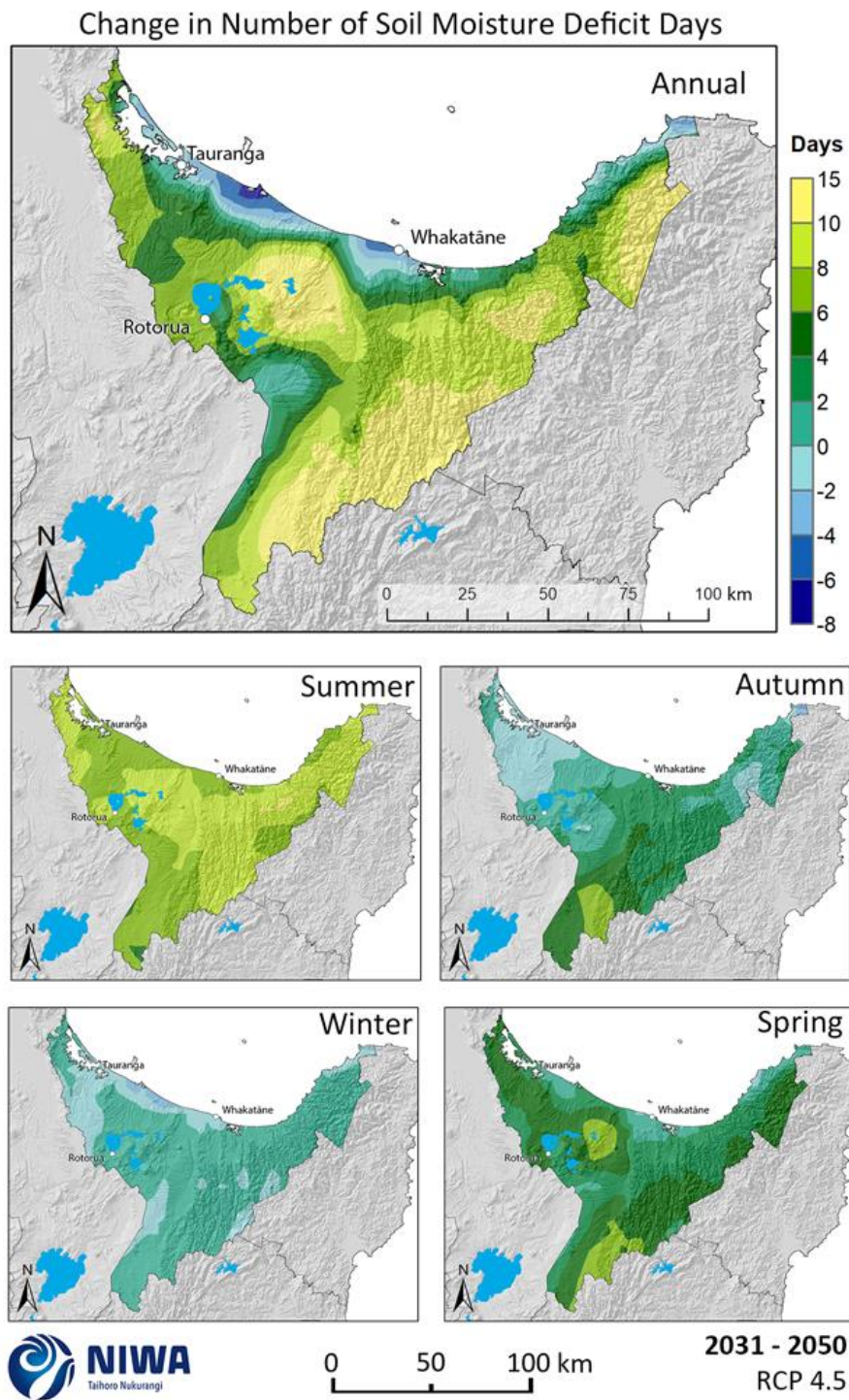


**Figure 4-30: Projected change in the number of annual and seasonal soil moisture deficit days by 2040 for RCP4.5.** Relative to 1986-2005 average, based on the average of six global climate models. Results are based on dynamical downscaled projections using NIWA's Regional Climate Model. Resolution of projection is 5km x 5km.

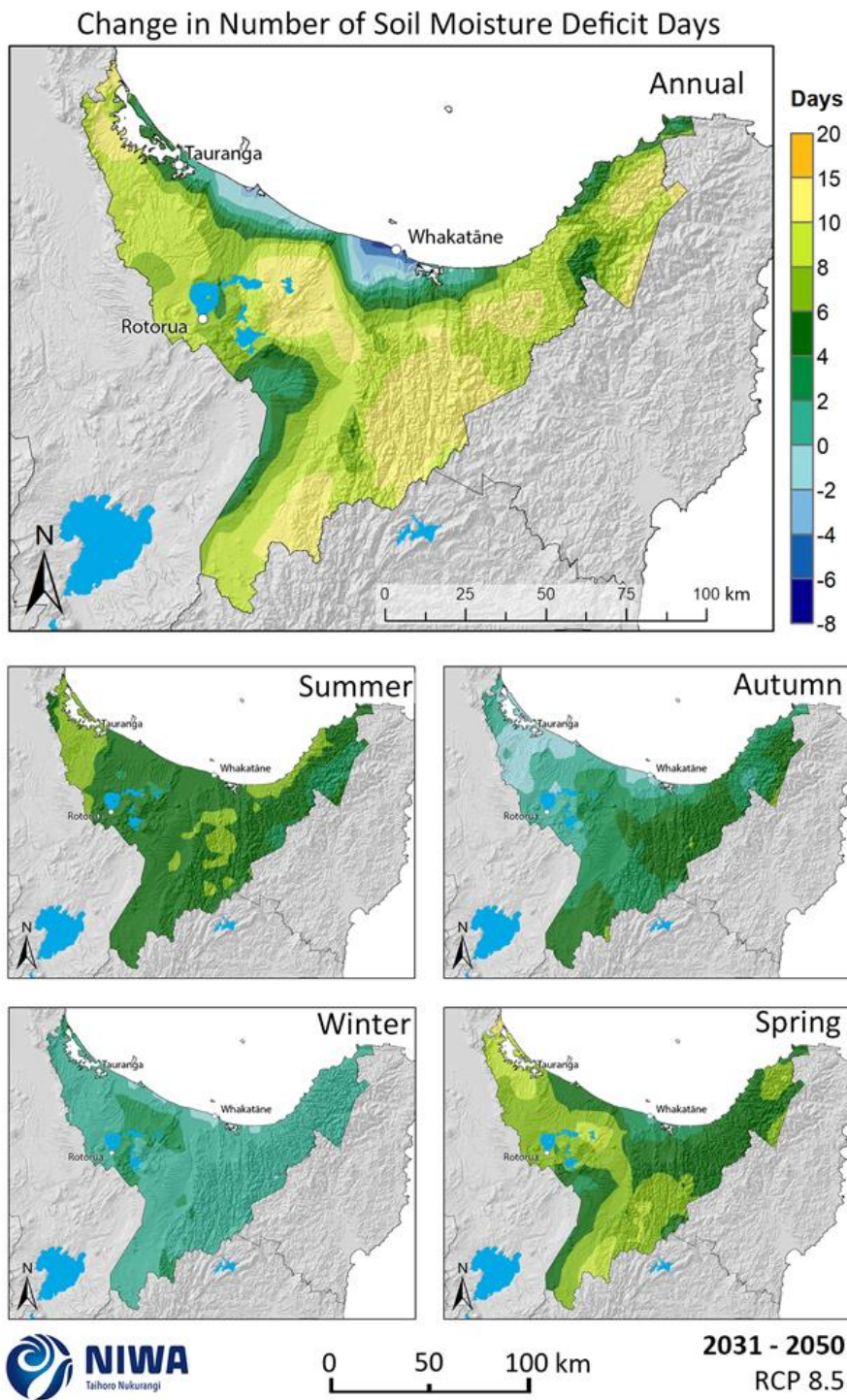


**Figure 4-31: Projected change in the number of annual and seasonal soil moisture deficit days by 2040 for RCP8.5.** Relative to 1986-2005 average, based on the average of six global climate models. Results are based on dynamical downscaled projections using NIWA's Regional Climate Model. Resolution of projection is 5km x 5km.

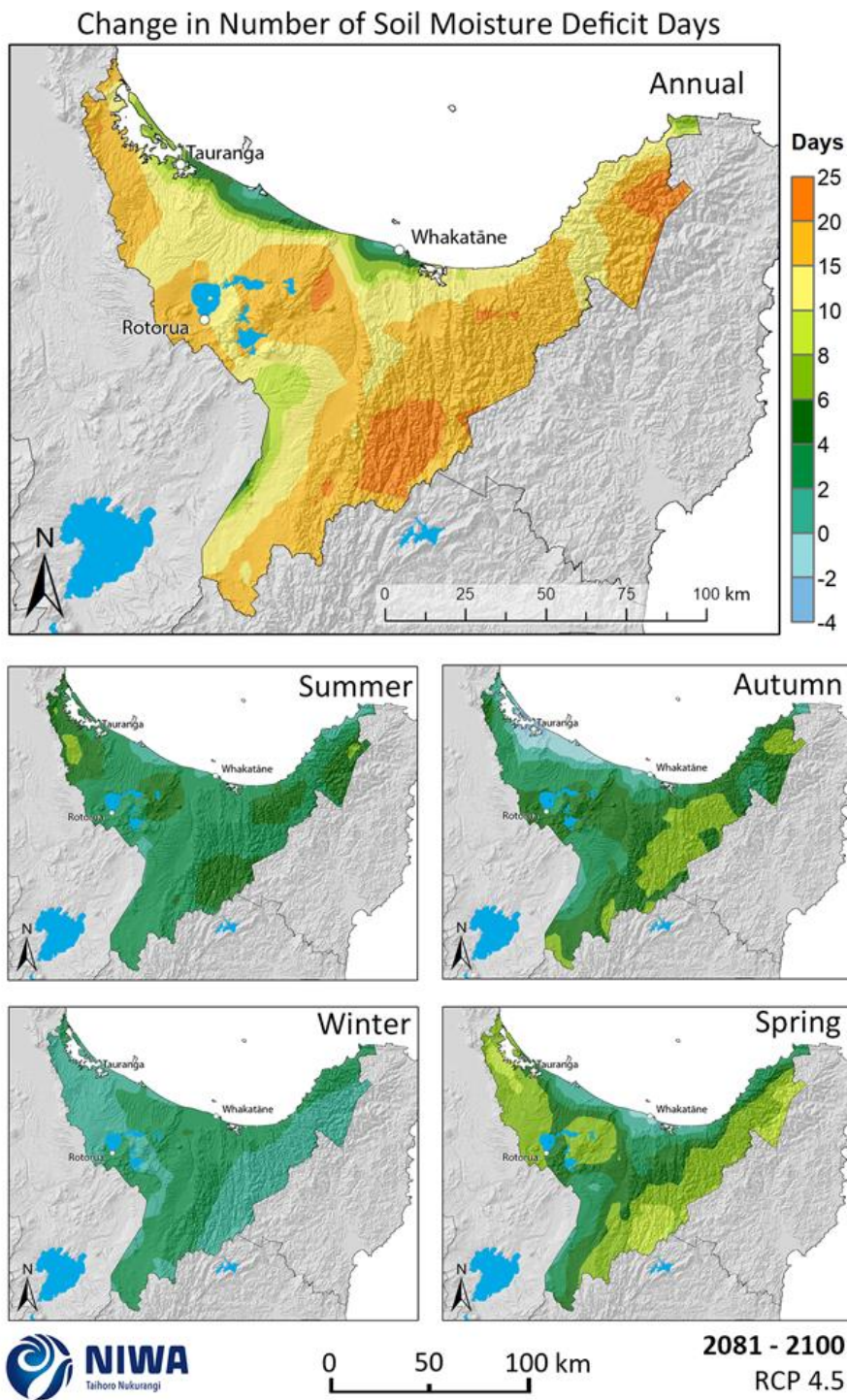


**Figure 4-32: Projected change in the number of annual and seasonal soil moisture deficit days by 2090 for RCP4.5.** Relative to 1986-2005 average, based on the average of six global climate models. Results are based on dynamical downscaled projections using NIWA's Regional Climate Model. Resolution of projection is 5km x 5km.



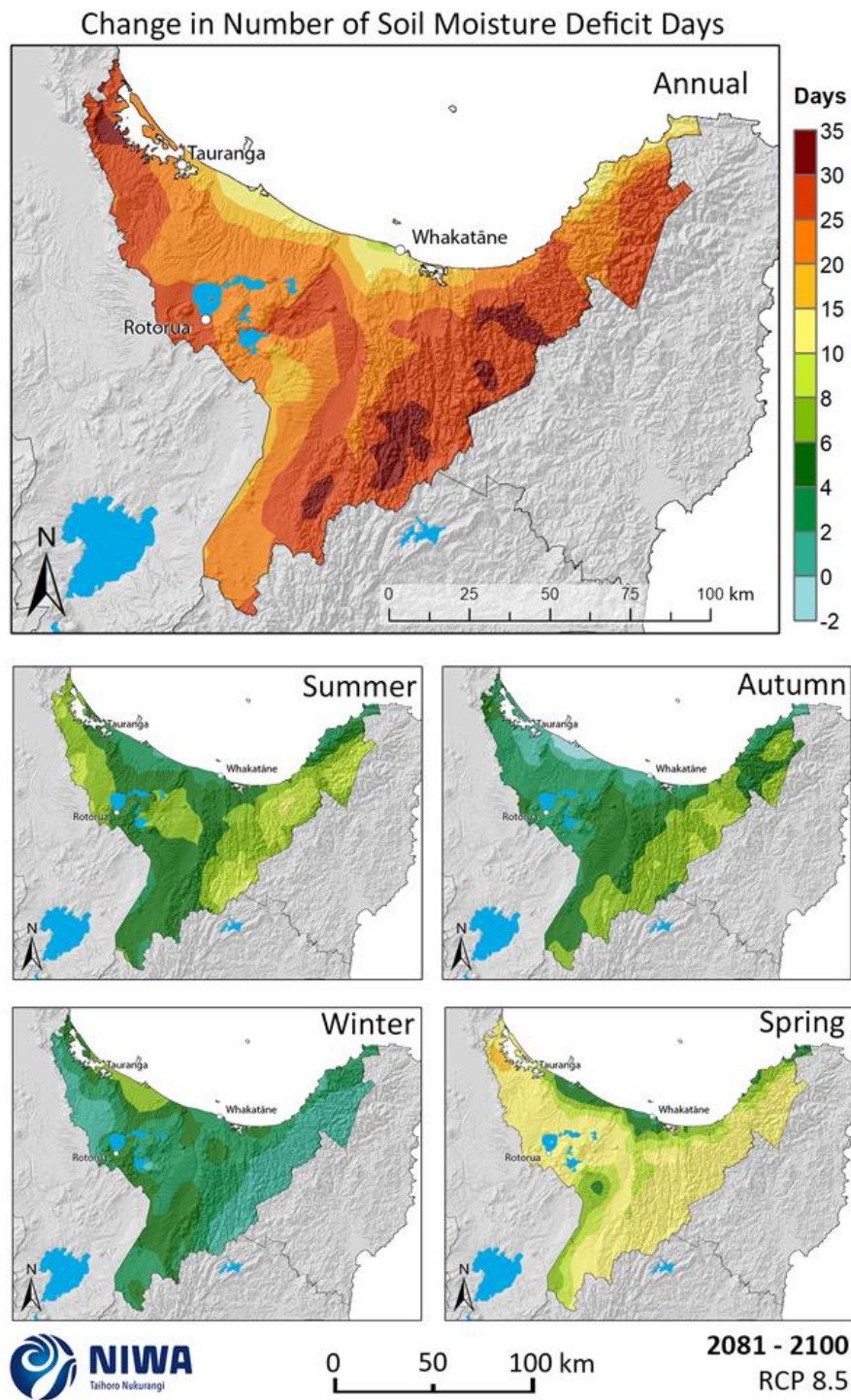


**Figure 4-33: Projected change in the number of annual and seasonal soil moisture deficit days by 2090 for RCP8.5.** Relative to 1986-2005 average, based on the average of six global climate models. Results are based on dynamical downscaled projections using NIWA's Regional Climate Model. Resolution of projection is 5km x 5km.

## 5 Wind and other variables

Modelled wind, surface solar radiation and relative humidity data have not had bias correction processes applied as has been carried out for temperature and rainfall. For this reason, only the future *relative changes* in these variables have been reported here using the modelled climate data. By doing this, the effect of biases in absolute values of these variables are minimised.

### 5.1 Mean wind speed

Future change (average over 2031-2050 and 2081-2100) maps for annual and seasonal mean wind speed are shown in this section.

In the future, annual mean wind speed is projected to slightly decrease in the Bay of Plenty. However, there is a mixed direction of change for different seasons. By 2040 under RCP4.5 (Figure 5-1), a 1-2% reduction in mean annual wind speed is projected for most of the region. At the seasonal level, larger reductions are projected for summer (2-4%) and small increases are projected for spring (0-1%). Under RCP8.5 (Figure 5-2), the pattern is similar at the annual scale but larger reductions in summer (3-6% reductions for most of the region, particularly the west) and larger increases in spring (1-3% increases for the central part of the region). By 2090 under RCP4.5 (Figure 5-3), negligible change is projected at the annual scale and at seasonal scales except for summer, where reductions in mean wind speed of 1-3% are expected across the region. Under RCP8.5 (Figure 5-4), reductions in annual mean wind speed of 2-4% are expected across the northern half of the region. For summer mean wind speed, reductions of 6-10% are projected for the northern half of the region, and reductions of 4-6% elsewhere. Autumn is expected to have reductions in mean wind speed of 4-6% for most of the region. Winter is projecting increases of 4-6% around Rotorua Lakes, and smaller increases elsewhere, and spring is expecting negligible change for most areas but 1-2% increase in mean wind speed around Rotorua Lakes and further south.

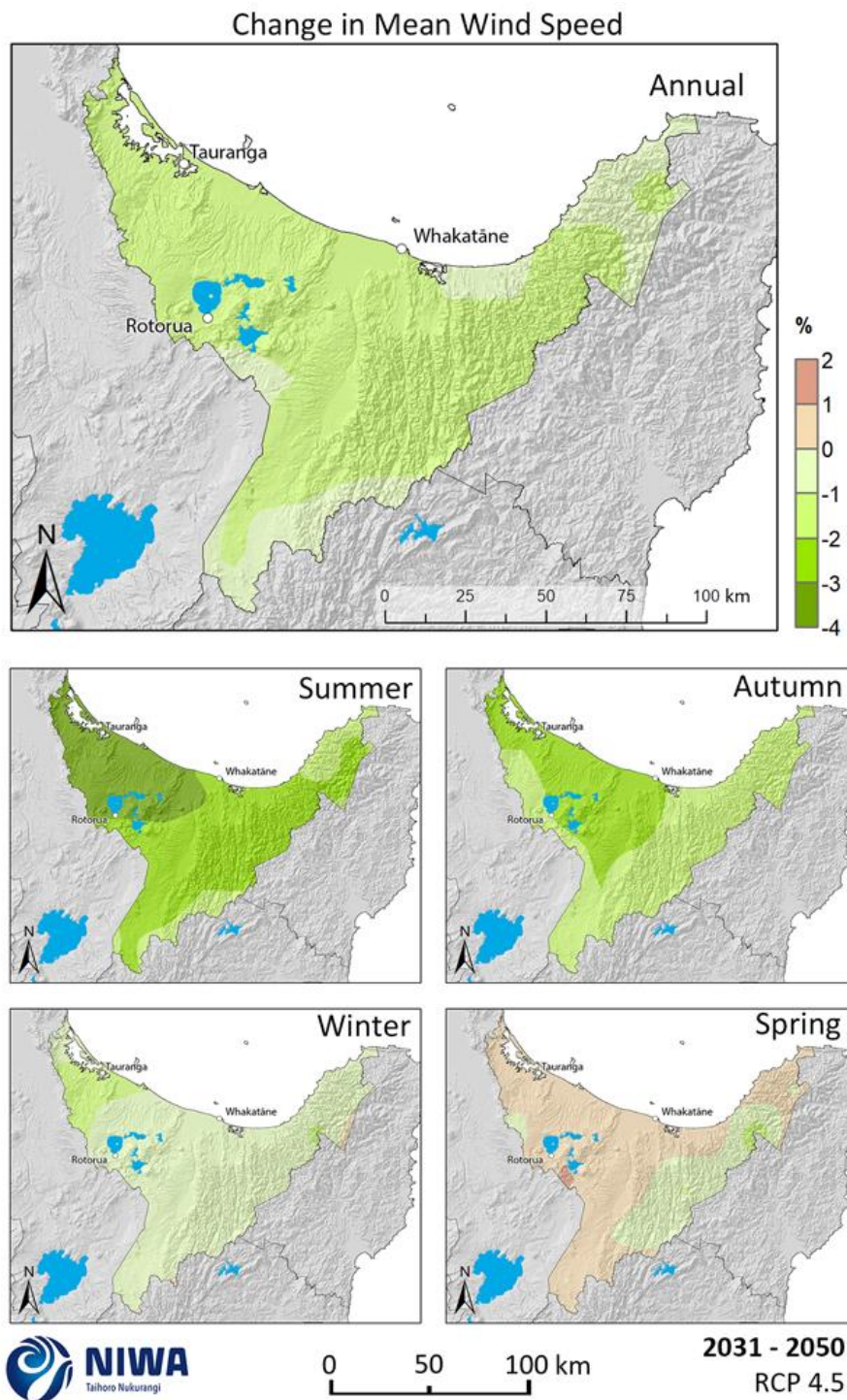


**Figure 5-1: Projected annual and seasonal mean wind speed changes by 2040 for RCP4.5.** Relative to 1986-2005 average, based on the average of six global climate models. Results are based on dynamical downscaled projections using NIWA's Regional Climate Model. Resolution of projection is 5km x 5km.

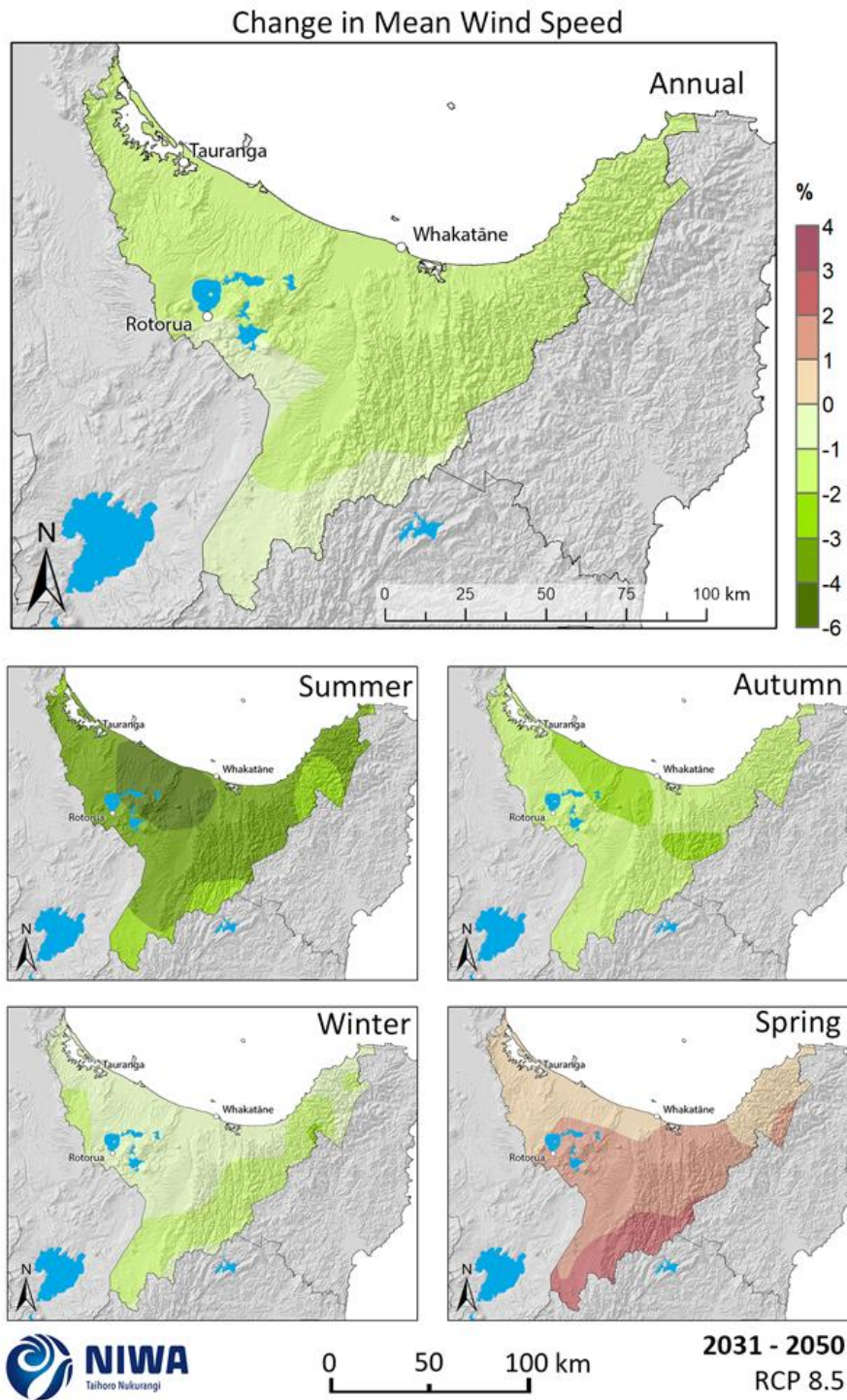


**Figure 5-2: Projected annual and seasonal mean wind speed changes by 2040 for RCP8.5.** Relative to 1986-2005 average, based on the average of six global climate models. Results are based on dynamical downscaled projections using NIWA's Regional Climate Model. Resolution of projection is 5km x 5km.

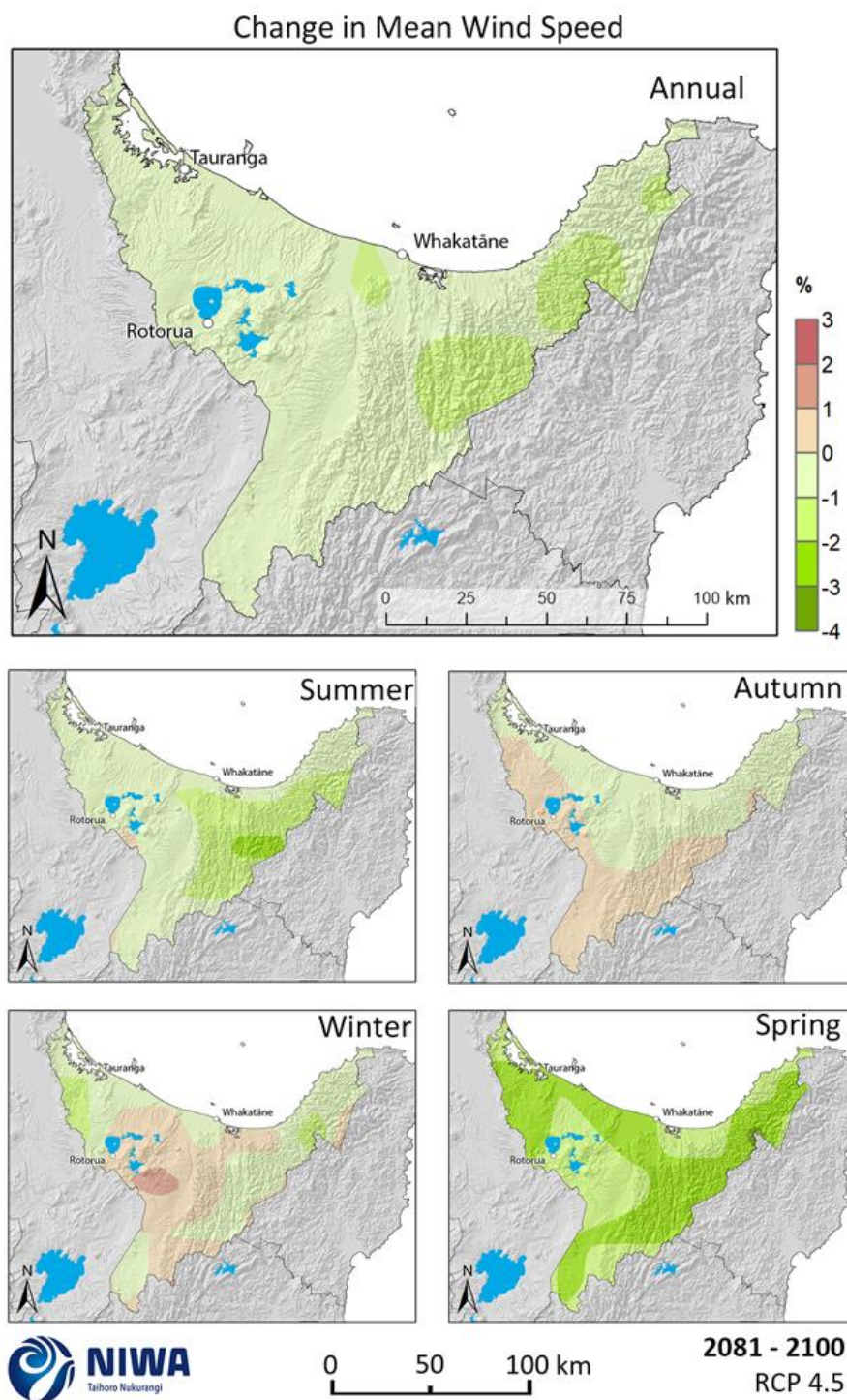


**Figure 5-3: Projected annual and seasonal mean wind speed changes by 2090 for RCP4.5.** Relative to 1986-2005 average, based on the average of six global climate models. Results are based on dynamical downscaled projections using NIWA's Regional Climate Model. Resolution of projection is 5km x 5km.

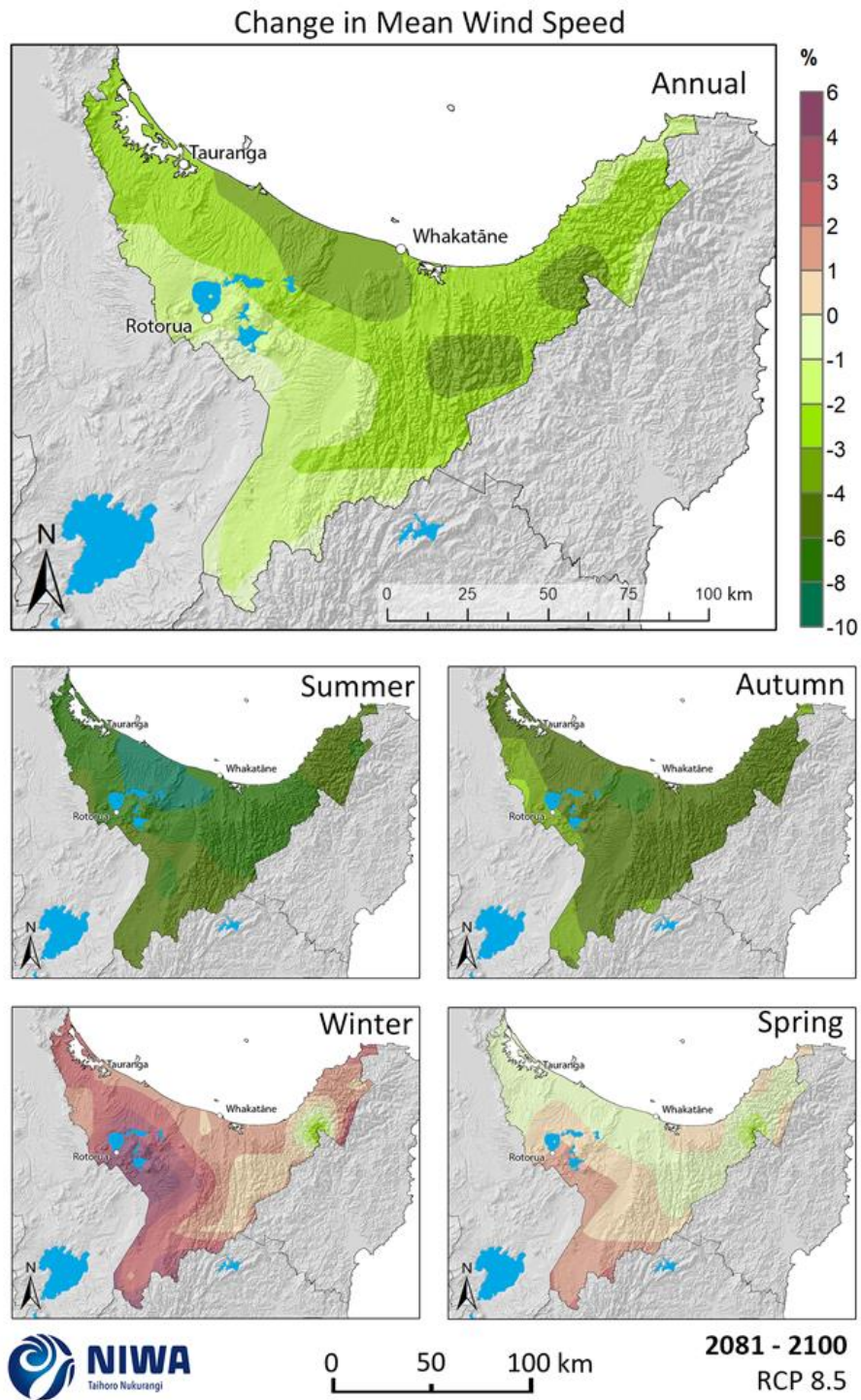


**Figure 5-4: Projected annual and seasonal mean wind speed changes by 2090 for RCP8.5.** Relative to 1986-2005 average, based on the average of six global climate models. Results are based on dynamical downscaled projections using NIWA's Regional Climate Model. Resolution of projection is 5km x 5km.

## 5.2 Windy days

A 'windy day' is considered to have a daily mean wind speed of 10 m/s or more. Future change (average over 2031-2050 and 2081-2100) maps for the annual number windy days are shown in this section.

In the future (Figure 5-5), the number of windy days is projected to decrease over most of the region, albeit by a very small amount in general (0-1 fewer windy days per year). The largest decreases are for the eastern part of the region (1-3 fewer windy days per year). Some small increases (0-1 days per year) are projected around the Rotorua Lakes area.

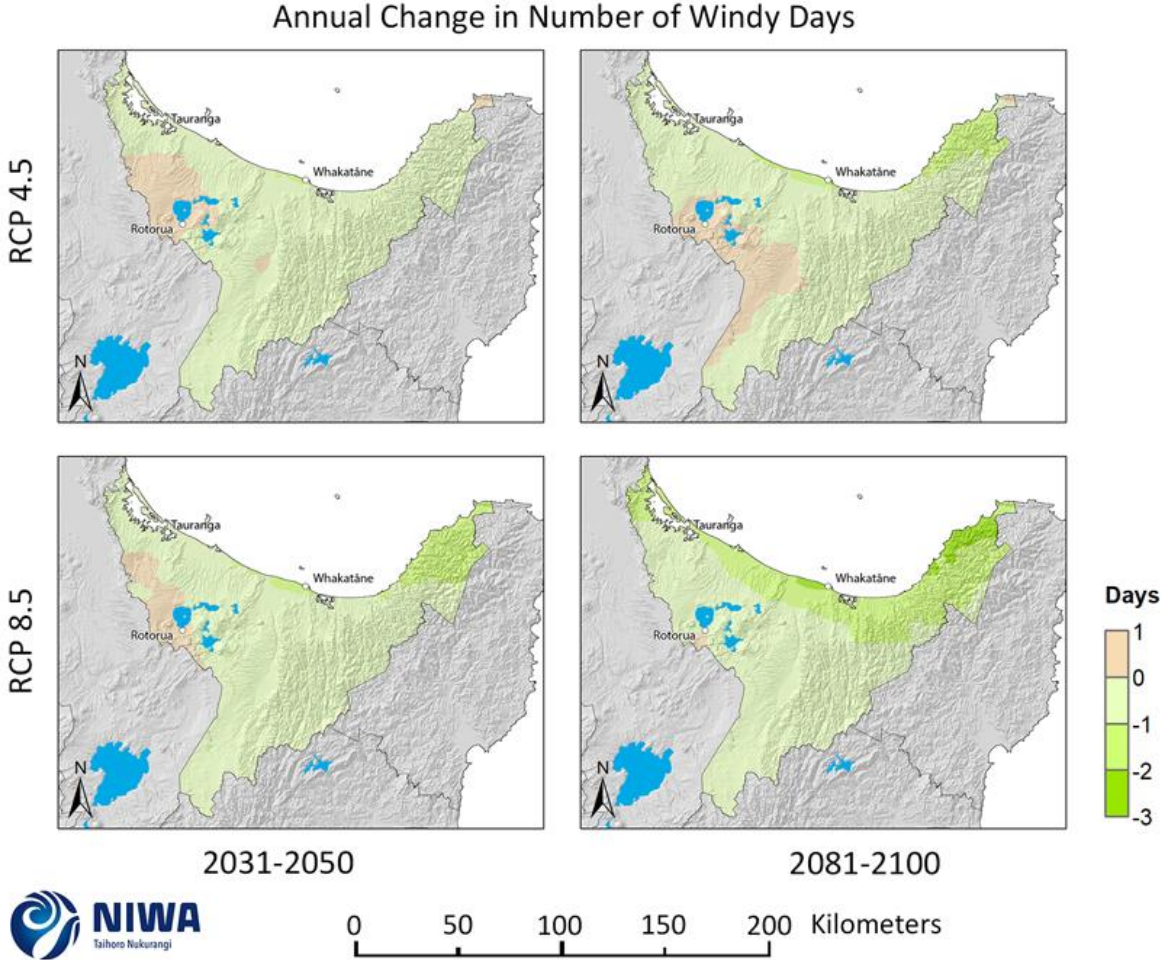


**Figure 5-5: Projected change in the annual number of windy days (>10 m/s) by 2040 and 2090, for RCP4.5 and RCP8.5.** Relative to 1986-2005 average, based on the average of six global climate models. Results are based on dynamical downscaled projections using NIWA's Regional Climate Model. Resolution of projection is 5km x 5km.

### 5.3 99<sup>th</sup> percentile of mean wind speed

Extreme wind is considered here as the 99<sup>th</sup> percentile of daily mean wind speeds. This equates to the wind speed that is exceeded by the top 1% of daily mean winds recorded, i.e. the wind speed exceeded by about the top three windiest days each year. Future change (average over 2031-2050 and 2081-2100) maps for the 99<sup>th</sup> percentile of daily mean wind speed are shown in this section, and the units are per cent.

In the future (Figure 5-6), the 99<sup>th</sup> percentile of daily wind speed is projected to decline in all parts of the region, under both RCP4.5 and RCP8.5, at 2040 and 2090. The magnitude of change is generally amplified by time and RCP. The largest reductions in the 99<sup>th</sup> percentile of daily wind speed is by 2090 under RCP8.5, where reductions of 3-6% are projected for much of the eastern half of the region, as well as west of Tauranga.

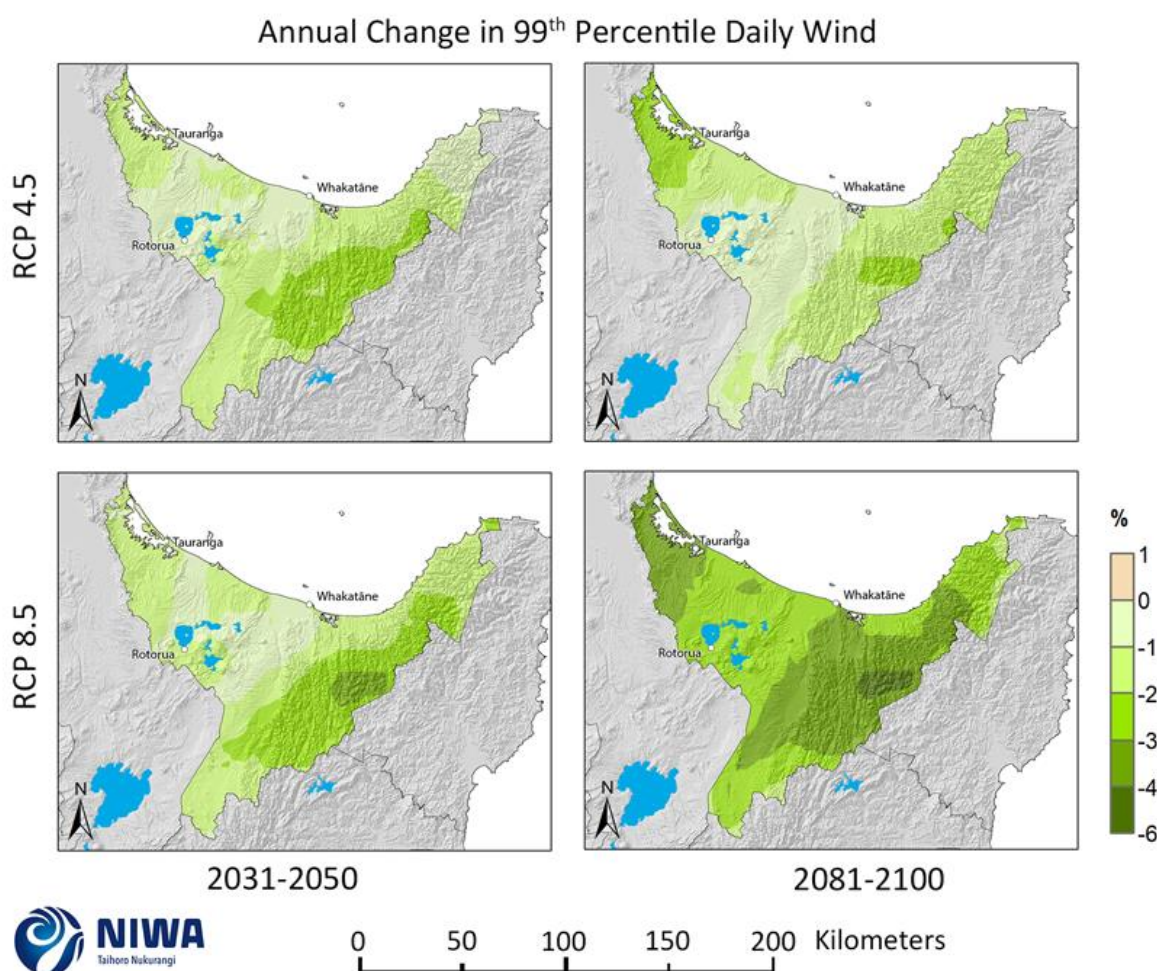


**Figure 5-6: Projected annual 99<sup>th</sup> percentile daily mean wind speed changes for RCP4.5 and RCP8.5, by 2040 and 2090.** Relative to 1986-2005 average, based on the average of six global climate models. Results are based on dynamical downscaled projections using NIWA's Regional Climate Model. Resolution of projection is 5km x 5km.

## 5.4 Surface solar radiation

This section contains maps showing the future projected change in surface solar radiation (solar radiation received at the land surface). Surface solar radiation is affected by cloud cover, so can be thought of as a proxy for changes in sunshine. Future change (average over 2031-2050 and 2081-2100) maps of annual and seasonal surface solar radiation are shown in this section, and the units are watts per square metre.

In the future, by 2040 under RCP4.5 (Figure 5-7), surface solar radiation is projected to decline for most of the lowland Bay of Plenty region, by 1-4 W/m<sup>2</sup> at the annual scale. Small increases of 1-2 W/m<sup>2</sup> are projected for the high elevation ranges. The largest decreases are projected for winter and largest increases in the ranges are projected for summer. Under RCP8.5 (Figure 5-8), reductions are more widespread in all seasons except for spring, which shows increases of 4-6 W/m<sup>2</sup> for the Huiarau Ranges. By 2090 under RCP4.5 (Figure 5-9), increases are more pronounced at the annual scale over the Huiarau, Urewera and Raukumara Ranges (1-4 W/m<sup>2</sup>), with small reductions for the coastal area from Tauranga to Whakatāne. Spring and autumn surface solar radiation increases in the eastern half of the region are also more widespread (1-6 W/m<sup>2</sup>). Under RCP8.5 (Figure 5-10), increases at the



annual scale are projected for the eastern ranges (2-6 W/m<sup>2</sup>) and small increases for the western part of the region (0-2 W/m<sup>2</sup>). Increases of up to 10-12 W/m<sup>2</sup> are projected for spring along the eastern ranges, with increases of at least 4 W/m<sup>2</sup> for inland areas.

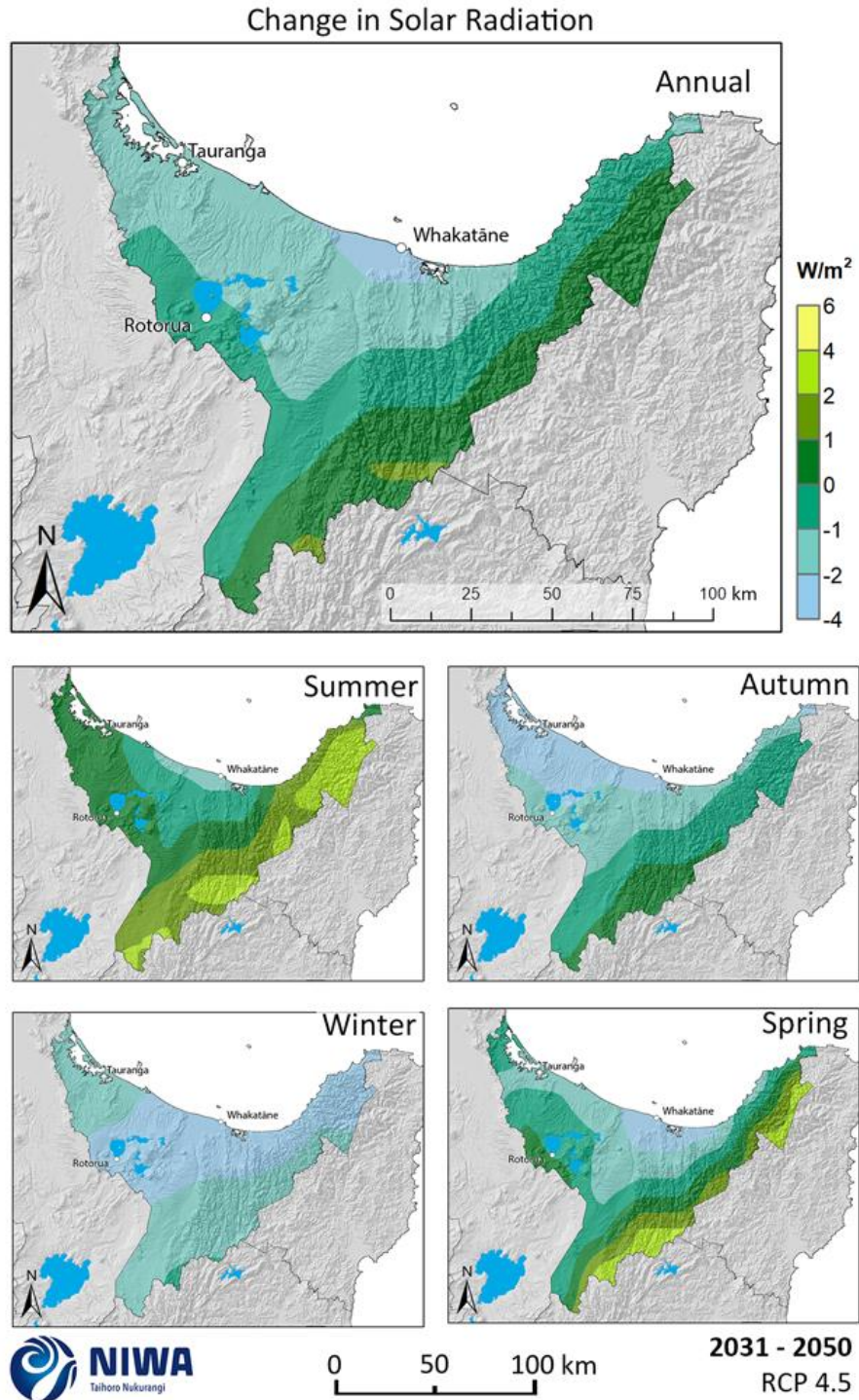


**Figure 5-7: Projected annual and seasonal mean surface solar radiation changes by 2040 for RCP4.5.** Relative to 1986-2005 average, based on the average of six global climate models. Results are based on dynamical downscaled projections using NIWA's Regional Climate Model. Resolution of projection is 5km x 5km.

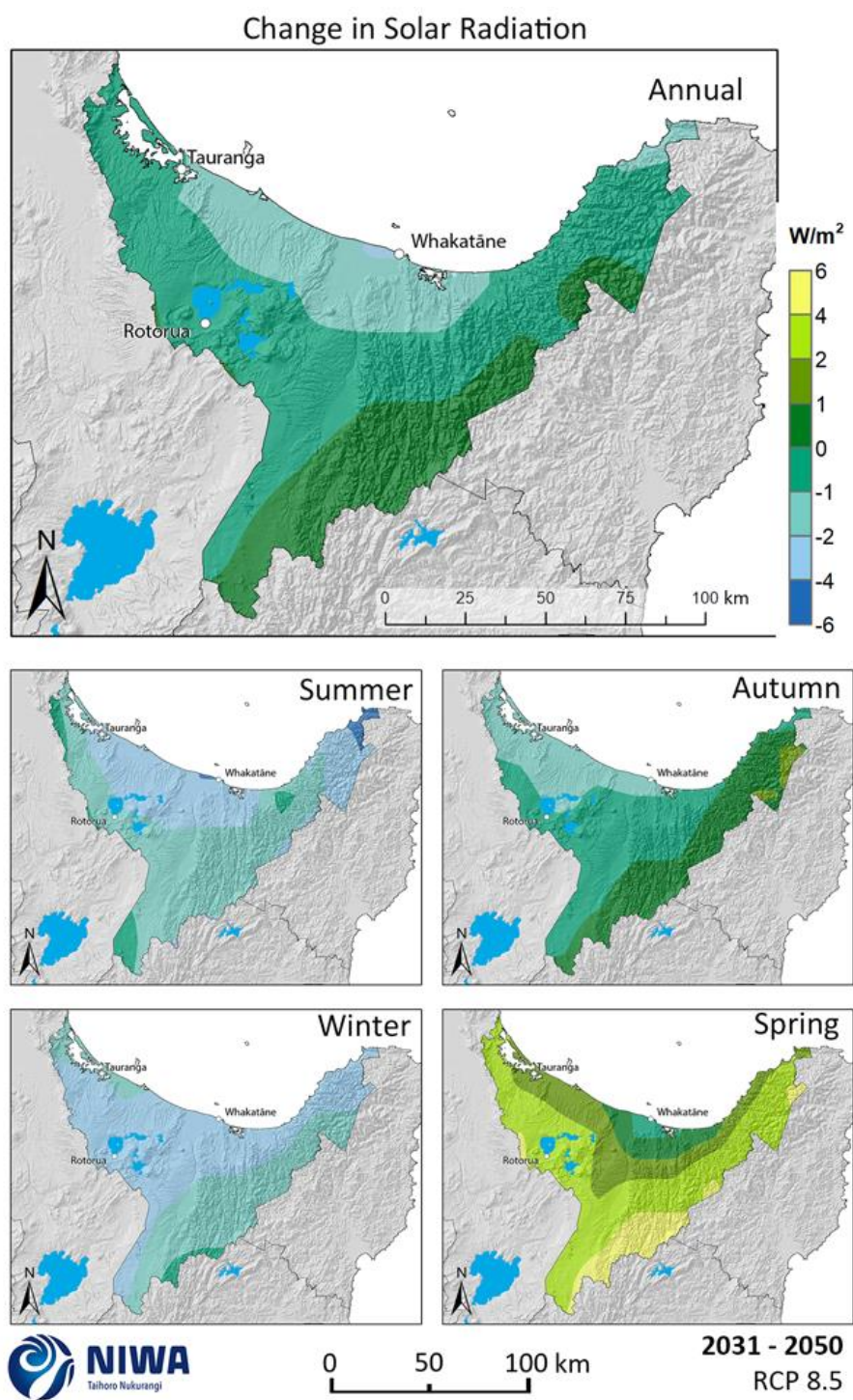


**Figure 5-8: Projected annual and seasonal mean surface solar radiation changes by 2040 for RCP8.5.** Relative to 1986-2005 average, based on the average of six global climate models. Results are based on dynamical downscaled projections using NIWA's Regional Climate Model. Resolution of projection is 5km x 5km.

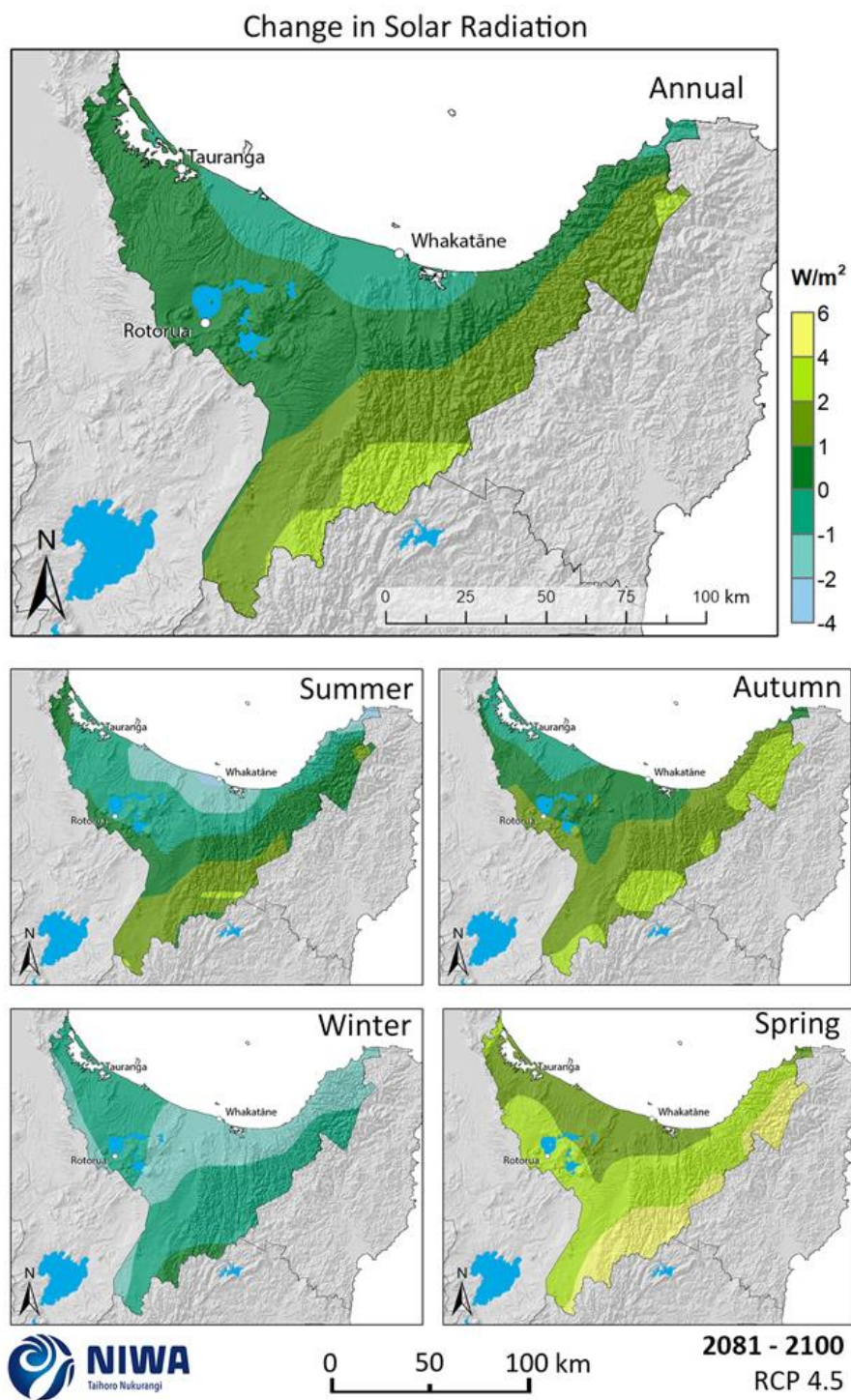


**Figure 5-9: Projected annual and seasonal mean surface solar radiation changes by 2090 for RCP4.5.** Relative to 1986-2005 average, based on the average of six global climate models. Results are based on dynamical downscaled projections using NIWA's Regional Climate Model. Resolution of projection is 5km x 5km.

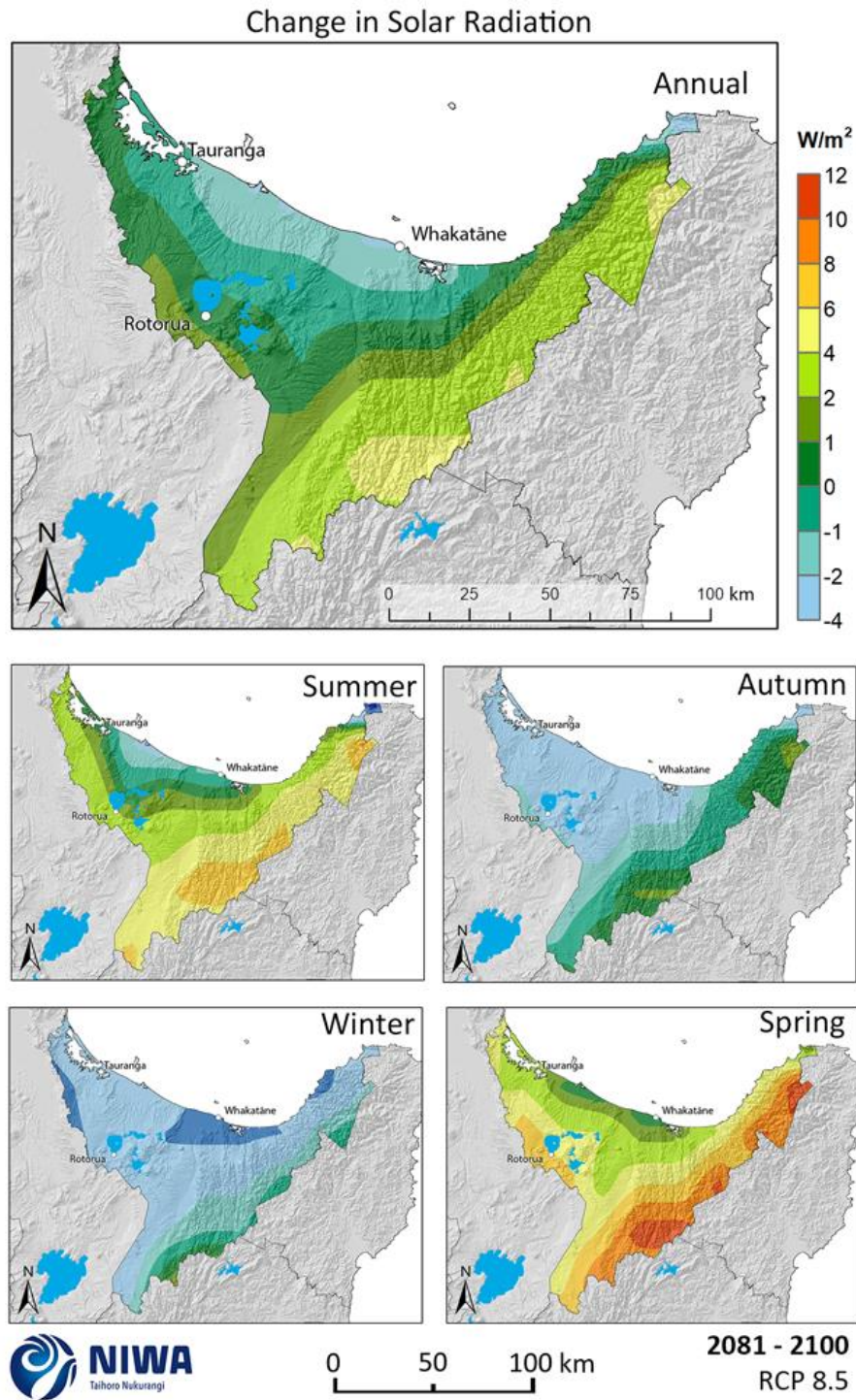


**Figure 5-10: Projected annual and seasonal mean surface solar radiation changes by 2090 for RCP8.5.** Relative to 1986-2005 average, based on the average of six global climate models. Results are based on dynamical downscaled projections using NIWA's Regional Climate Model. Resolution of projection is 5km x 5km.

## 5.5 Relative humidity

Future change (average over 2031-2050 and 2081-2100) maps of annual and seasonal relative humidity are shown in this section.

In the future, relative humidity is generally expected to decline in the Bay of Plenty. By 2040 under RCP4.5 (Figure 5-11), reductions of 0-1% are expected at annual and seasonal scales. Under RCP8.5 (Figure 5-12), this is more pronounced, particularly for spring where reductions of 1.5-2% are projected for inland areas. This is similar for RCP4.5 by 2090 (Figure 5-13), with spring reductions for inland areas between 1.5-2%. Under RCP8.5 by 2090 (Figure 5-14) the pattern is more extreme, with spring reductions of 3.5-4% for inland areas. At the annual scale, reductions of 2-3% are projected for inland areas, with small increases of 0-0.5% near the coast. Increases of 0.5-1.5% near the coast are projected for summer and autumn.

**A note about relative humidity compared to specific humidity:** Projected decreases in relative humidity are a consequence of the higher temperatures. The absolute water content of the air, as measured by specific humidity, increases with time, but the temperature effect is larger; the rate of decrease in relative humidity over New Zealand is mostly 1–2 per cent per degree increase in mean temperature, consistent with estimates from a recent international study (Byrne & O’Gorman, in press). This is also in line with evidence in the recent observations (Simmons et al., 2010) in reanalysis and station data over low and mid latitudes.

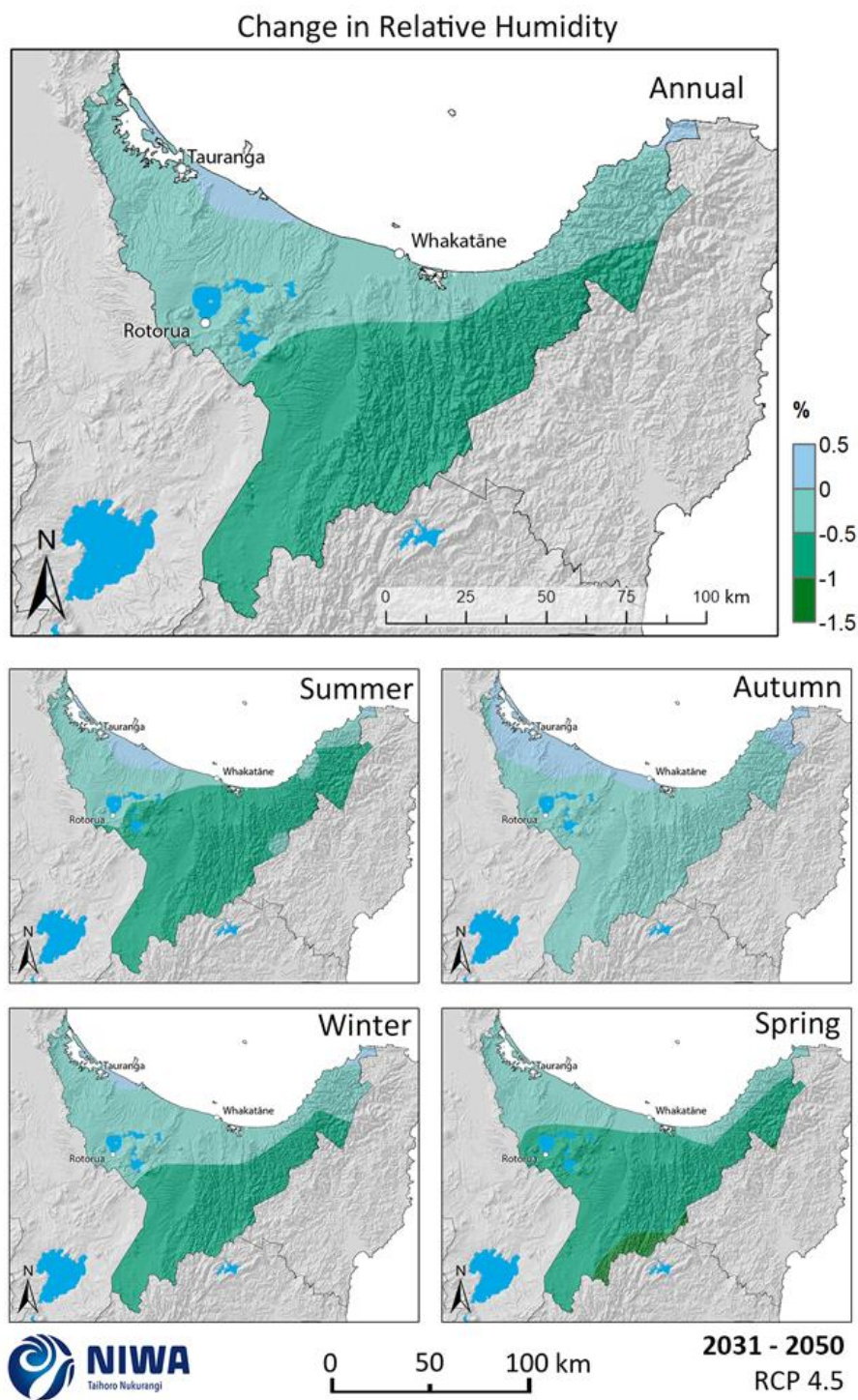


**Figure 5-11: Projected annual and seasonal mean relative humidity changes by 2040 for RCP4.5.** Relative to 1986-2005 average, based on the average of six global climate models. Results are based on dynamical downscaled projections using NIWA's Regional Climate Model. Resolution of projection is 5km x 5km.

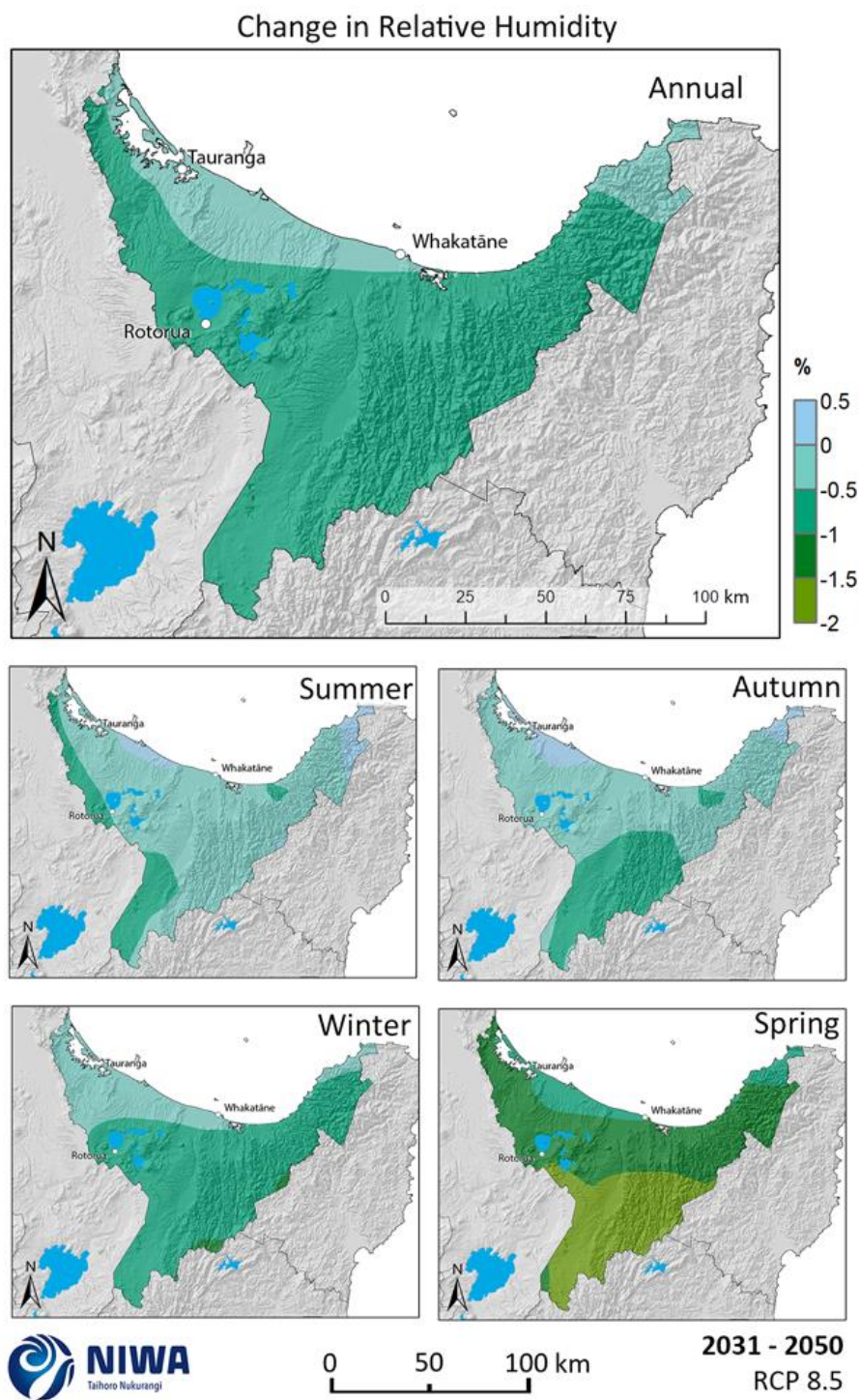


**Figure 5-12: Projected annual and seasonal mean relative humidity changes by 2040 for RCP8.5.** Relative to 1986-2005 average, based on the average of six global climate models. Results are based on dynamical downscaled projections using NIWA's Regional Climate Model. Resolution of projection is 5km x 5km.

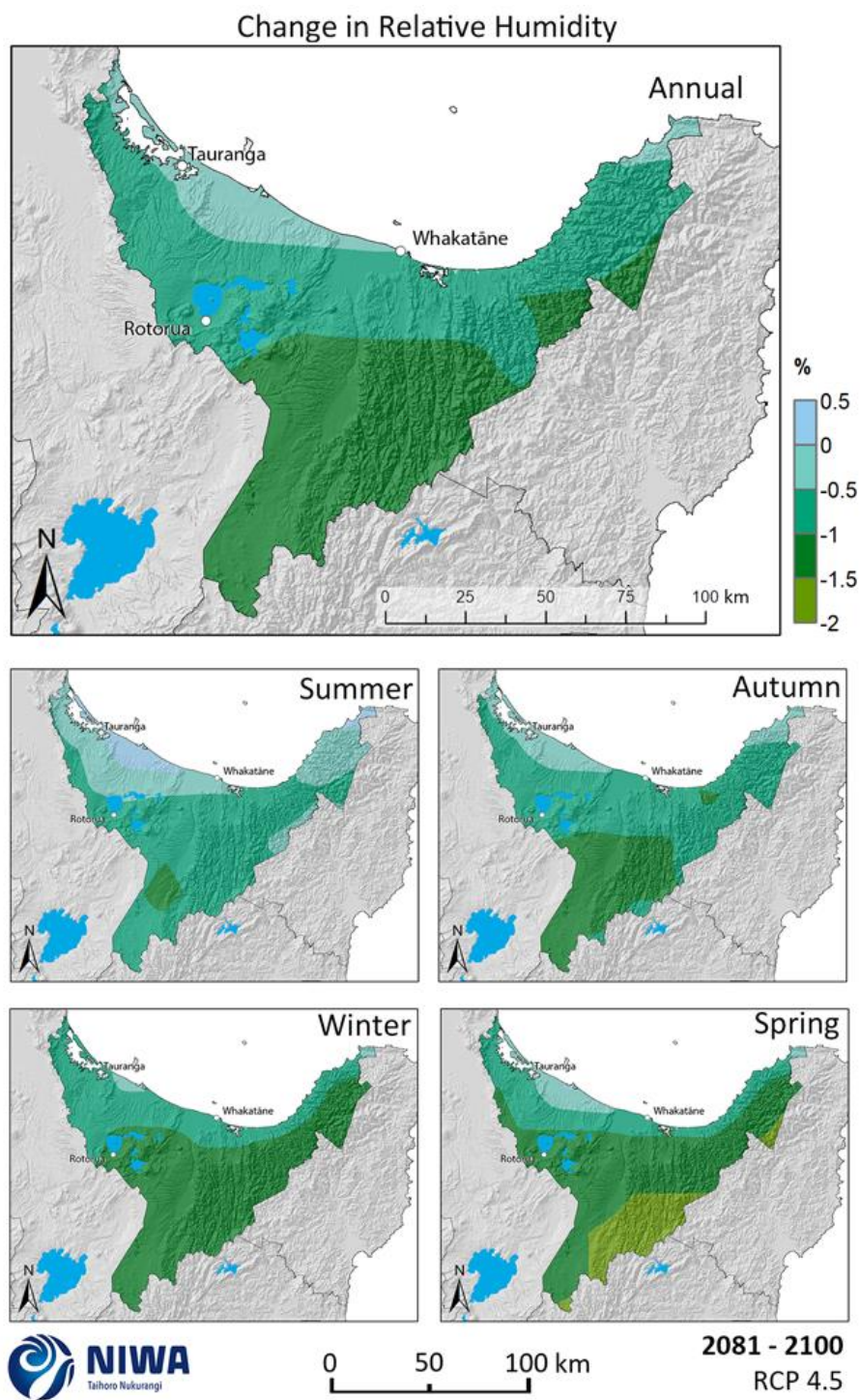


**Figure 5-13: Projected annual and seasonal mean relative humidity changes by 2090 for RCP4.5.** Relative to 1986-2005 average, based on the average of six global climate models. Results are based on dynamical downscaled projections using NIWA's Regional Climate Model. Resolution of projection is 5km x 5km.



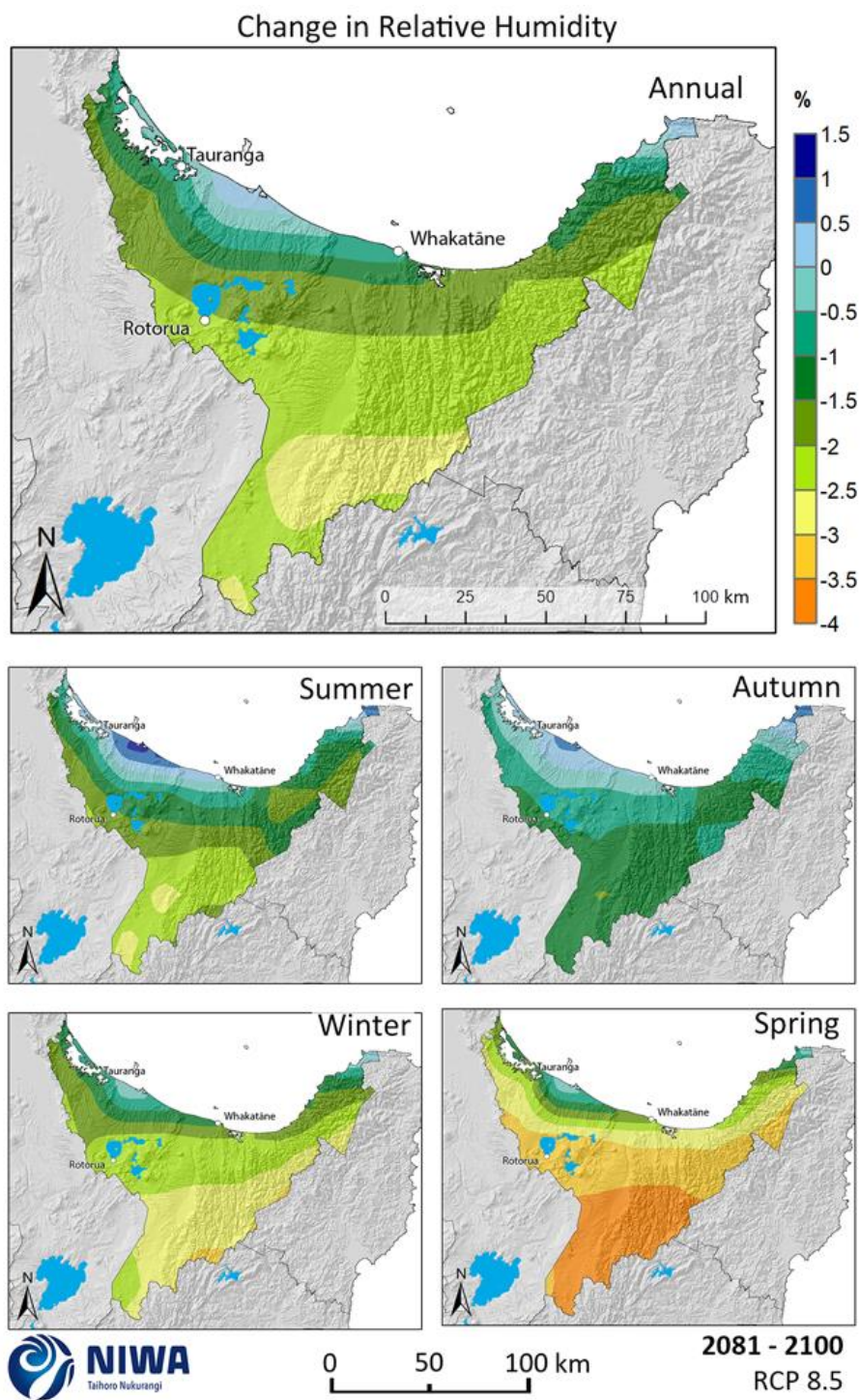


**Figure 5-14: Projected annual and seasonal mean relative humidity changes by 2090 for RCP8.5.** Relative to 1986-2005 average, based on the average of six global climate models. Results are based on dynamical downscaled projections using NIWA's Regional Climate Model. Resolution of projection is 5km x 5km.

## 6 Projections for storms affecting the Bay of Plenty

### Key messages

- The six global climate models from the IPCC Fifth Assessment used by NIWA have been analysed in terms of “wet spells” affecting Bay of Plenty. A “wet spell” begins with a daily rainfall exceeding 25 mm and ends when the daily rainfall drops below 1 mm.
- Storms associated with the first day of a wet spell have been tracked back in time for up to a week or more to identify the storm origin. The projected changes in frequency and intensity of such rain-bearing systems are diagnosed for RCPs 4.5 and 8.5.
- In summer, the models suggest that storms producing wet spells in the Bay of Plenty are likely to be more frequent and more intense. The associated wet spells are projected to last longer and produce larger rainfall accumulations over the lifetime of the event. These changes may be caused by warmer sea temperatures allowing ex-tropical low-pressure systems to maintain their intensity as they approach New Zealand from the north.
- In winter (and to some extent other seasons), the models suggest fewer storms to the north and northwest of the North Island. The associated wet spells exceeding the 25 mm threshold are nonetheless more frequent, presumably due to the warmer atmosphere holding more moisture. The wet spells are also shorter-lived but more intense.

Extreme weather events can cause significant damage and disruption to crops, livestock, forests and infrastructure. For example, ex-tropical cyclone Bernie caused widespread damage in the Bay of Plenty and other regions of the North Island in April 1982 (Revell and Ward (1982); NIWA’s NZ Historic Weather Events Catalogue, [https://hwe.niwa.co.nz/event/April\\_1982\\_North\\_Island\\_Ex-tropical\\_Cyclone\\_Bernie](https://hwe.niwa.co.nz/event/April_1982_North_Island_Ex-tropical_Cyclone_Bernie)), as had ex-tropical cyclone Gisele (the “Wahine” storm) 14 years earlier in April 1968 (Revell and Gorman, 2003). The most recent projections of future New Zealand climate (Ministry for the Environment, 2018) show maps of future rainfall amounts, and a short commentary on tropical and extra-tropical cyclones, but give little information on how changes in high rainfall are related to individual weather events.

In this section, especially commissioned by Bay of Plenty Regional Council, a study is made of how storms affecting the Bay of Plenty region are projected to change in future climates. A particular focus is on those low-pressure systems exiting the tropics which subsequently produce heavy rainfall over the Bay of Plenty. In this study, ‘heavy rainfall’ is taken to mean a daily rainfall accumulation of 25 mm or more.

### 6.1 Model simulations

Ministry for the Environment (2018) summarises the regional climate model (RCM) simulations carried out by NIWA to generate scenarios of future New Zealand climate change. Six CMIP5 models (from the IPCC Fifth Assessment) are used, as listed in Table 3 of Ministry for the Environment (2018), and simulations were carried out from 1971 to 2005 for the so-called ‘historical’ period, and from 2006 onwards to either 2100 or 2120 for the ‘future’ period, under four emission pathways known as RCPs 2.6, 4.5, 6.0 and 8.5 (more details about the climate modelling methodology is presented in Appendix A). Behind each of the RCM simulations, there is actually a global climate model (GCM) simulation done first.

This study relies solely on the GCM simulations, since the RCM domain is too small to allow us to track incoming cyclone centres as they approach New Zealand. The data analysed here corresponds to archived daily data for six models, for the historical period and future periods out to 2100 under the RCP4.5 and RCP8.5 scenarios. Following the approach of Ministry for the Environment (2018) and the rest of this report, any climate changes are described by comparing the 1986-2005 20-year climatology with a future 20-year climatology, either 2031-2050 or 2081-2100. Ex-tropical storms are relatively rare in the New Zealand region: on average, at least one ex-tropical cyclone passes within 550 km of Auckland each year (Lorrey et al., 2014). Because of the small sample size for ex-tropical storms, consideration was given to comparing 30-year periods instead of 20-year periods, but this had minimal effect on the statistics.

To set the scene, Figure 6-1 provides an example for one day, 6<sup>th</sup> January 1986, according to the HadGEM2-ES model simulation (note that this event did not happen in reality, since the model has its own sequence of weather events). The mean-sea-level pressure pattern for that day is mapped in the left-hand panel and shows what appears to be an ex-tropical cyclone centred just south of New Caledonia, and on its way to New Zealand. It is encouraging to see such a feature in the GCM, although the model’s relatively low spatial resolution (1.25° latitude by 1.875° longitude grid spacing) means that the intense wind and pressure gradients that characterise tropical cyclones in the real world are not well-resolved by the climate model. The consequence is that tropical low-pressure systems in the model world are typically substantially weaker than in reality. For this reason, we will subsequently refer to such features as appear in Figure 6-1 as an ‘ex-tropical low-pressure system’ rather than an ‘ex-tropical cyclone’.

The rainfall map associated with the same day (right panel of Figure 6-1) shows two active rainfall regions bearing down on New Zealand: that associated with the low-pressure system to the north-northwest of New Zealand, and a second band associated with an active frontal system stretching from just east of the Australian coast to south of New Zealand. Two days later, on 8<sup>th</sup> January 1986 (not shown), the frontal band is weakening as it approaches southern New Zealand and slips away to the south, whereas the northern low-pressure system has dragged its associated rain band down over the northern half of the North Island and delivered 32.7mm of rain to a box located over the Bay of Plenty region. These are the types of rainfall events that this study aims to identify.

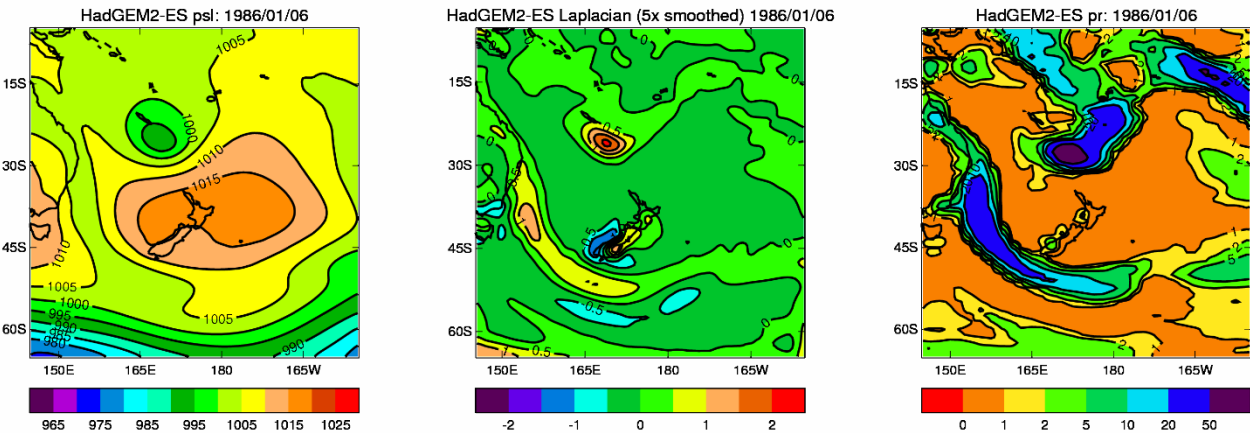


**Figure 6-1: Example maps of weather and circulation for 6<sup>th</sup> January 1986, according to the NIWA global climate model simulation driven by sea surface temperatures taken from the UK MetOffice Hadley model (HadGEM2-ES).** The three panels show: mean sea-level pressure (in hPa, left panel), with darker green and blue colours indicating lower pressure; scaled Laplacian of the pressure field (centre panel), with orange and

red shading indicating more intense circulation centres; and daily rainfall accumulation (in mm, right panel), where darker blue shading denotes daily rainfall accumulation above 20mm.

## 6.2 Identifying storm tracks

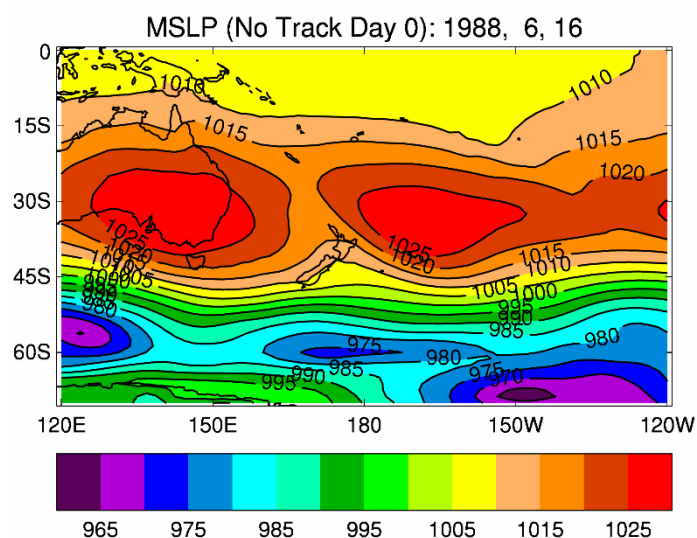
The purpose of this study is to assess how weather systems bringing heavy rainfall to the Bay of Plenty region might change in a future climate. The starting point is the daily rainfall accumulations from the model simulations, which were averaged over a box covering most of the Bay of Plenty region, (37.0-38.5°S, 175.5-178.0°E). All days with the area-average rainfall exceeding 25 mm were interpreted as ‘end dates’ of a storm track. Sometimes consecutive days of heavy rainfall were found, but only the first day of such an event was used as a target date or “Day 0” of a rainfall event, also referred to as a “Wet Spell”.

A tracking algorithm (described further below) was developed to first identify a low-pressure centre or vorticity centre associated with the heavy rainfall at “Day 0”, and then track back day by day as far as possible (up to nine days prior to “Day 0”), in order to identify the source and path of the weather system responsible for the heavy rainfall. The aim was to develop a large sample of tracks and calculate statistics from them; for example, changes in frequency or intensity of the weather systems, and changes in rainfall amount.

The storm tracking was a two-step process. In the first step, all low-pressure centres or vorticity centres on the daily weather map in the New Zealand region were identified. This involved calculating the Laplacian (or double-derivative) of the pressure field; a low-pressure centre is associated with a maximum in the Laplacian field, and the Laplacian maximum was a much sharper feature, and therefore easier to identify, than the pressure minimum. This technique has commonly applied in other tracking software (Wang et al., 2006, Eichler et al., 2013). The Laplacian maximum of the pressure field for 6<sup>th</sup> January 1986 is displayed in the middle panel of Figure 6-1.

The second step was to link the low-pressure centres together in time, working backwards from “Day 0” of the start of the heavy rainfall event. The emphasis was on finding the centre closest to the low centre of the previous day, and stopping when no further centre within a pre-specified distance could be located.

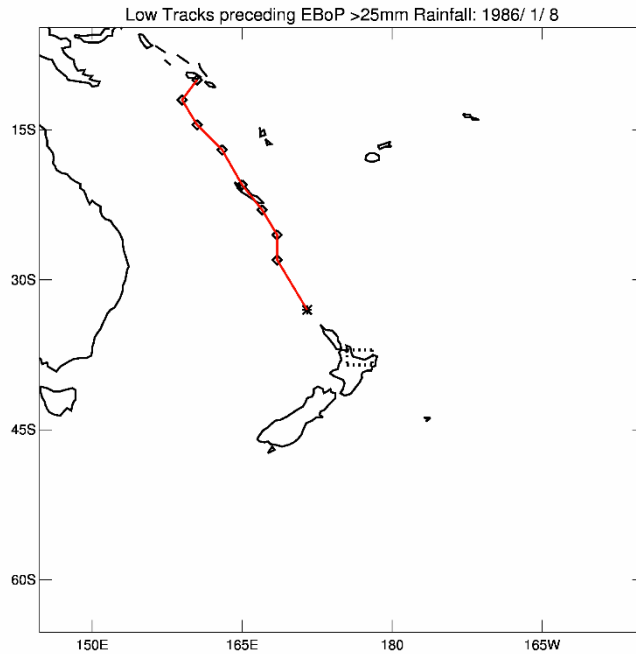
The centre identification and tracking algorithms involved a number of parameters, and considerable time was spent in setting these to optimise the results relative to a visual inspection of the daily weather maps. Nonetheless, for some days associated with heavy rainfall in the Bay of Plenty there were no storm centres anywhere near the North Island. Figure 6-2 is an example of such a day, where the Bay of Plenty rainfall is produced in the model from a front being compressed between two high pressure systems. This active trough has become detached from the low near 60°S, which can no longer be considered the real ‘source’ of the rainfall. Fortunately, for a heavy rainfall threshold of 25 mm, the failure rate in identifying storm centres was relatively low (about 5%).



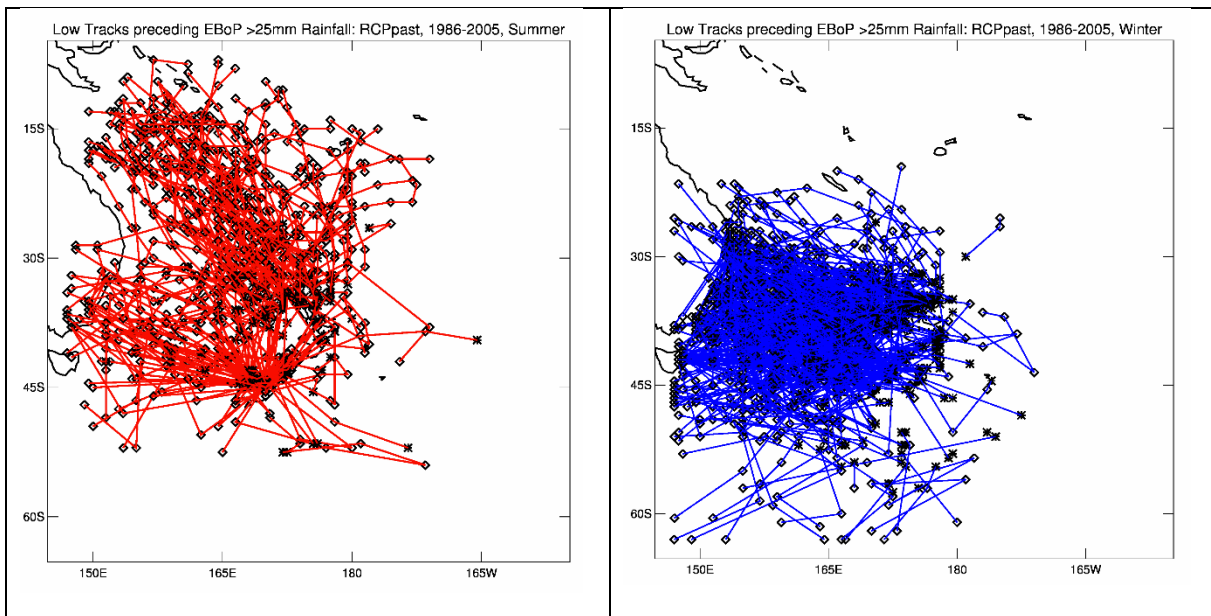
**Figure 6-2: Mean sea-level pressure map on 16<sup>th</sup> June 1988 of the HadGEM2-ES simulation.** On this day there was 25.2mm of rainfall over the Bay of Plenty, but the tracking algorithm was unable to identify a low centre or vorticity centre associated with the rainfall.

Figure 6-3 displays the track of the first storm occurring in the 1986-2005 period for the HadGEM2-ES model. It is the same ex-tropical low-pressure system as highlighted in Figure 6-1. While some low-pressure systems were difficult to track back from “Day 0”, the ex-tropical systems were usually straightforward: the low centres were deep and well-defined, well separated from any other circulation centres and did not move very far from one day to the next.

The tracking algorithm was applied to all the model daily pressure data files from the six GCMs, for the three periods of interest (1986-2005, 2031-2050 and 2081-2100) and three RCPs (RCPpast, RCP4.5 and RCP8.5). Figure 6-4 displays all cyclone tracks from all six GCMs over the historical 1986-2005 period that produced rainfall exceeding 25mm in Bay of Plenty. The tracks are shown separately for the summer and winter seasons. Similar tracks were produced for other periods and RCPs. Note that there is a clear pattern of storms affecting Bay of Plenty being further south in the winter season. Even more storms originating from the Southern Ocean would be involved were the rainfall threshold to be reduced from 25 mm to 20 mm.



**Figure 6-3: Track of low-pressure weather system producing heavy rainfall in Bay of Plenty on 8<sup>th</sup> January 1986, according to the HadGEM2-ES GCM simulation.** The end-point of the track marks the position of the circulation centre on the first day of heavy rainfall (i.e., on the 8<sup>th</sup>) and is denoted by the star, with diamonds denoting the centre locations on previous days back to 31<sup>st</sup> December 1985. The dotted box over the Bay of Plenty region marks the area over which the model rainfall is averaged.



**Figure 6-4: All cyclone tracks producing more than 25mm of daily rainfall over the Bay of Plenty region, for all six GCM simulations and all years 1986-2005.** The track maps apply to the summer months (January, February and December, left panel), and the winter months (June, July and August, right panel). Diamonds and stars as in Figure 6-3.

### 6.3 Characteristics of storm track changes

An archive of all storm tracks resulting in a “Wet Spell” for the Bay of Plenty region was generated. The Wet Spell was identified by a starting day (“Day 0”) of at least 25 mm accumulated daily rainfall, and the Spell was continued until the daily rainfall dropped below 1 mm. Other wet days of 25 mm or more could occur subsequently within the same Wet Spell, but the storm tracking was only carried out with respect to “Day 0”. Tracks were extended back in time for up to 10 days if it was possible to track the low centre back this far.

Results were obtained for all six global climate models (GCMs) used by NIWA in Ministry for the Environment (2018), and for five scenarios/period combinations: RCPpast (1986-2005), RCP4.5 and RCP8.5 at mid-century 2031-2050, and RCP4.5 and RCP8.5 at end-of-century 2081-2100. Table 6-1 shows the total number of identified events by GCM and scenario/time period. In the historical period, there are approximately 12 Wet Spells per year (i.e. 240 spells per model over each 20-year period). There is some suggestion from Table 6-1 of an increase of one more wet spell per year by the end of the century. About 5% of these Wet Spells were unable to be identified with a storm centre: these situations were associated either with an active front over the North Island between two high centres, or with north-easterly airflow into the Bay of Plenty region. There is approximately a 30 percent low bias in the number of modelled Wet Spells compared with observed Wet Spells calculated using NIWA’s Virtual Climate Station Network (Tait et al., 2006).

**Table 6-1: Total number of identified Wet Spells (25mm or more on “Day 0”) over a 20-year period, per model and scenario/period.**

Scenario, Period	HadGEM	CAM5	NorESM	GFDL	GISS	BCC
RCPpast, 1995	227	227	245	250	239	232
RCP4.5, 2040	231	226	255	233	286	254
RCP8.5, 2040	240	217	268	240	256	258
RCP4.5, 2090	229	225	293	264	266	252
RCP8.5, 2090	236	230	302	230	282	274

In order to obtain a reasonable sample size, the storm track characteristics were aggregated over 5° latitude-longitude ‘squares’. The number of storms passing through a given square were totalled, and averages calculated for the central pressure and vorticity (as represented by the local Laplacian of the pressure field).

Figure 6-5 shows the summer and winter changes between the historical period (1986-2005) and end-of-century under the mid-range emission scenario RCP4.5. Changes for other times and scenarios show a similar pattern. At least five storm centres had to be present in each 5° square; otherwise the square is left blank. A simple t-test has been applied to assess the statistical significance of the changes, and white asterisks in the Figure 6-5 panels denote where significant changes in track statistics occurs. It is not possible to carry out this test for the frequency of occurrence due to the small sample size.

The left-hand column of Figure 6-5 shows the changes in the summer season storms affecting Bay of Plenty. The results are noisy due to the small sample size, but **the overall pattern suggests an increase in the number of summer storms near New Zealand, especially to the west and**

**northwest, associated with mostly lower pressures and higher vorticity<sup>3</sup>: i.e., stronger storms.** On the other side of the Tasman offshore of New South Wales, there are fewer and weaker storms for those that go on to affect Bay of Plenty rainfall.

In winter (right-hand column of Figure 6-5), the pattern is rather different. There is a clear pattern of fewer storms north of 35°S and more storms south of 35°S, but a mixed signal in terms of storm strength. The patterns for the intermediate seasons of autumn and spring are mixed and show less consistency. However, in the grid-square immediately **over the Bay of Plenty region, there is a noticeable increase in frequency of low centres in the winter season**, particularly for RCP4.5. The higher frequency of storms to the south of New Zealand suggest more storms may originate from this area in winter.

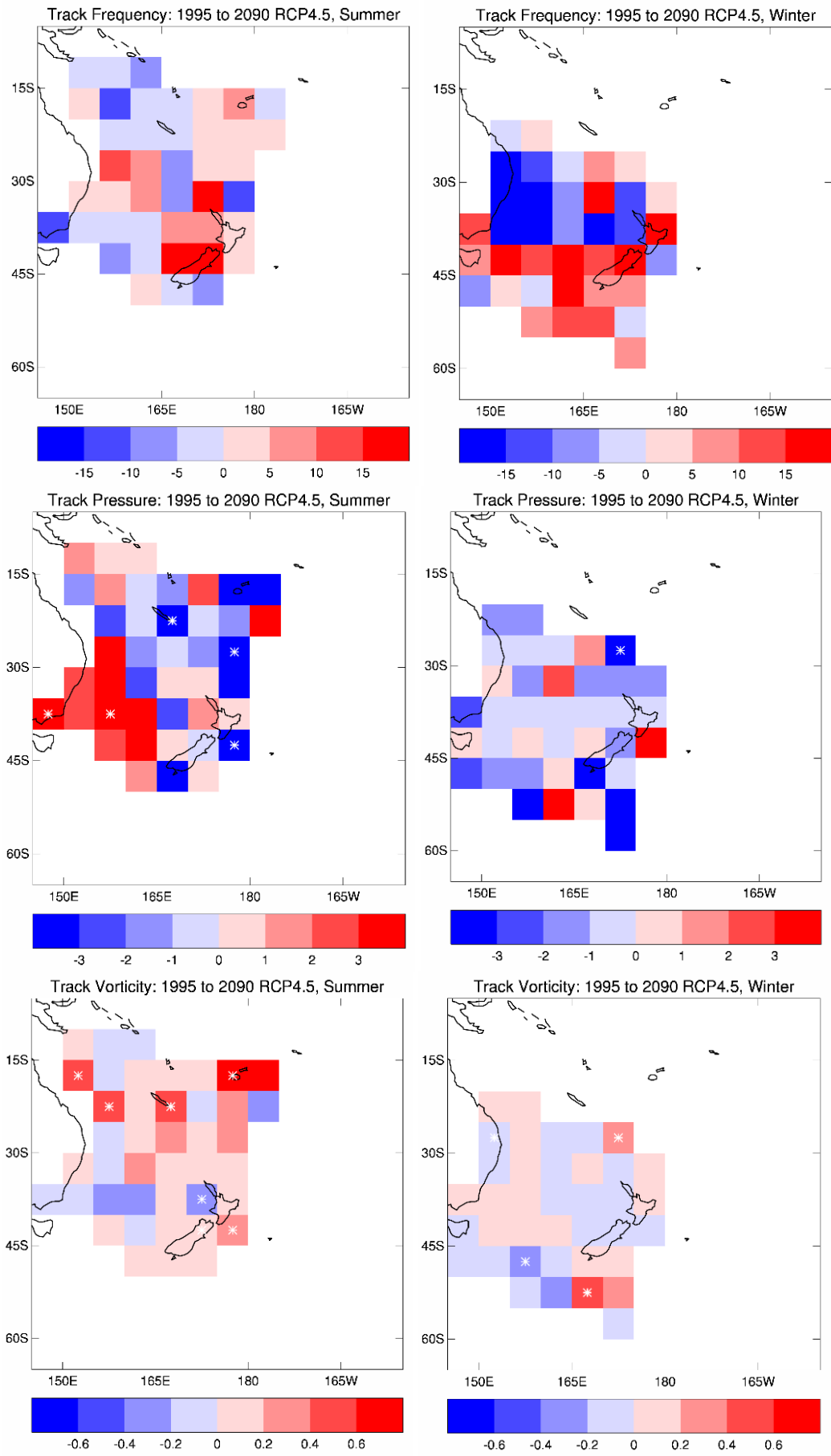
The general finding of a southward shift in storms tracks (but still referencing those storms producing heavy rain in Bay of Plenty) is in line with many other findings in the literature of a poleward movement of extra-tropical storm tracks in both historical observations (Bender et al., 2012), and in future projections (Yin, 2005, Chang et al., 2012). Our result for winter track frequency is also consistent with Dowdy et al. (2013), who analysed two GCMs from the IPCC Fourth Assessment and found a reduction in the number of Australian ‘east coast lows’ – active weather systems forming off the coast of New South Wales and southern Queensland, primarily in the winter season.

**Figure 6-5: (Next page) Change in track statistics between 1986-2005 (RCPpast) and 2081-2100 (RCP4.5) per 5°x5° square, for summer months (left) and winter months (right): number of lows over 20 years and 6 models (top row), average mean sea-level pressure (centre row), average vorticity (bottom row).** Increases are shown in red, decreases in blue. Stronger storms have lower pressures (blue) and higher vorticity (red). Asterisks indicate changes are statistically significant at the 5% level. The units are as follows: frequency is the change totalled over the 20-year period shown and over all six model simulations; pressure is in hPa; vorticity is in  $10^{-10}$  hPa/m<sup>2</sup>.

---

<sup>3</sup> Vorticity is a term used in fluid mechanics to describe the degree of spinning motion of a fluid about some point. It is considered to be a better metric for the intensity of a rotating mid-latitude storm than the central pressure, since this latter decreases towards higher latitudes whereas vorticity can be conserved following the storm’s motion under certain circumstances





### 6.3.1 Ex-tropical storms

The most severe storms to affect the northern half of the North Island are those originating as tropical cyclones and transitioning into extra-tropical systems as they move south into the cooler waters of the Tasman Sea. A special focus was therefore given to storms producing heavy rainfall in the Bay of Plenty that could be identified as originating in the tropics. Note again that we are careful not to label these as true “tropical cyclones” because of the low resolution of the GCMs. We will refer to them as “ex-tropical low-pressure systems” or “ex-tropical storms”.

The storm track database was polled to identify all storms, irrespective of season, which originated in the tropics. Specifically, it was required that the identified track had at least two days at 20°S or northwards (strictly any storm north of the Tropic of Capricorn at 23.5°S is a ‘tropical’ system).

Figure 6-6 shows a map of all such ex-tropical storms under the model historical climate (1986-2005) and end-of-century 2081-2100 under RCP4.5. The tracks of all six GCMs are combined in these maps, and the tracks are colour-coded according to the season of their occurrence. Most of the ex-tropical storms occur in the summer (tracks shown in red) or autumn (yellow) seasons.

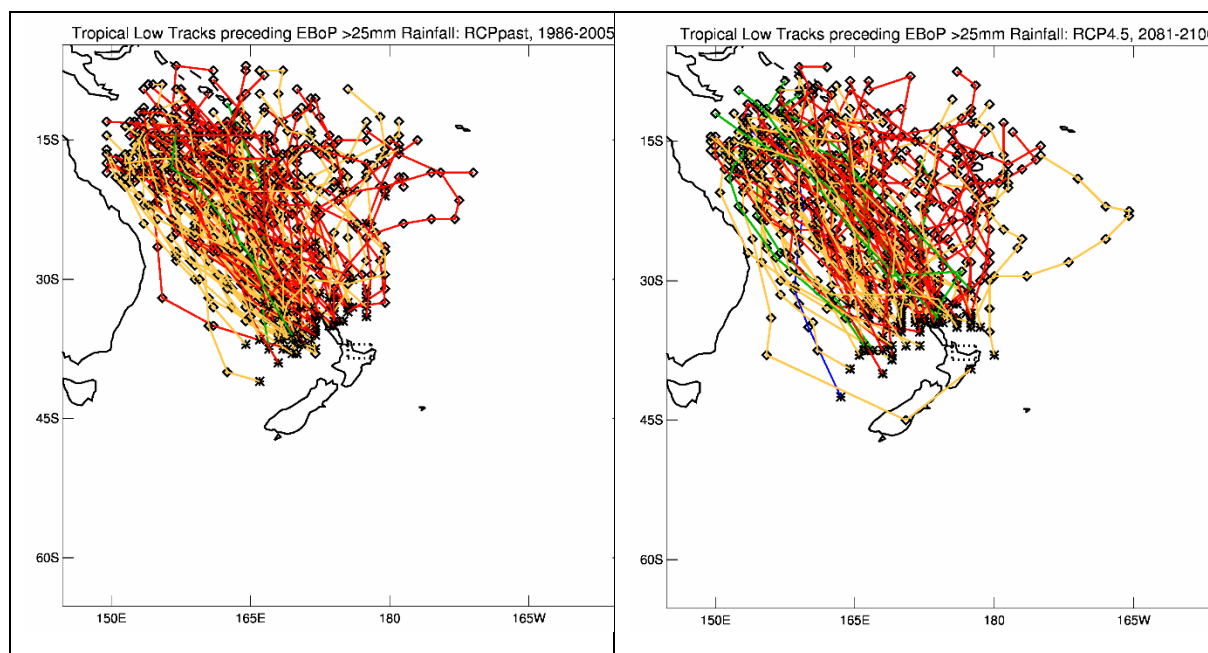


**Figure 6-6:** All tracks of ex-tropical storms producing more than 25mm of daily rainfall over the Bay of Plenty region, for all six GCM simulations, for the historical 1986-2005 period (left) and 2081-2100 period under RCP4.5 (right). The tracks are colour-coded by season: summer (red), autumn (yellow), winter (blue) and spring (green). Diamonds and stars as in Figure 6-3.

Table 6-2 shows the ex-tropical storm count (summed over all six GCMs) according to calendar month. There are several interesting points to note in this table.

- The *total number* of ex-tropical storms in the GCMs averages at slightly less than one per ‘tropical-cyclone season’ (120 storms would correspond to one per year for each of 20 years and six GCMs). This is close to the observed number of ex-tropical cyclones which are recognised as affecting New Zealand (and we would expect almost every such ex-tropical cyclone to bring heavy rainfall to the Bay of Plenty). This gives us good confidence in the

realism of the global climate models at representing such circulation systems in the southwest Pacific region.

- The seasonality of ex-tropical storms in the models matches well with the observed distribution; that is, the ‘season’ is very much concentrated on the period November to April, with occasional storms outside this core period.
- There is some evidence from the table of future storms extending outside the core November-April season. Note that at the end of the century in the RCP4.5 simulation of the CAM5 model, there is one ex-tropical storm occurring in winter (June of 2086).

**Table 6-2: Numbers of ex-tropical storms summed over all six GCMs, by month and scenario/period, producing heavy rainfall in the Bay of Plenty region.**

Scenario, Period	Jan	Feb	Mar	Apr	May	Jun	Jul	Aug	Sep	Oct	Nov	Dec	Annual
RCPpast, 1995	13	26	24	20	5	0	0	0	0	0	3	12	103
RCP4.5, 2040	13	15	21	11	3	0	0	0	2	4	6	10	85
RCP8.5, 2040	30	20	23	12	5	0	0	0	0	1	4	18	113
RCP4.5, 2090	20	14	22	13	4	1	0	0	0	3	4	10	91
RCP8.5, 2090	21	25	16	6	6	0	0	0	0	1	4	16	91

Once again, the storm tracks have been aggregated over 5° squares, and the changes in frequency, central pressure and vorticity calculated. Results are shown in Figure 6-7 for the changes between 1986-2005 and 2081-2100 under RCP4.5, for the ex-tropical storm season. The pattern of changes is generally more pronounced than that for the standard summer/winter seasons shown above. Over the ex-tropical storm season, there are generally fewer storms exiting the tropics and passing down the western side of New Zealand (note they are not tracked past “Day 0” of the >25 mm Bay of Plenty rainfall). During their time within the tropics, storm intensity changes are unclear, but a very consistent pattern emerges as the storms travel further south towards New Zealand: to the west of New Zealand the storms intensify (lower central pressure and higher vorticity), whereas to the north of the North Island the storms weaken (higher central pressure and lower vorticity).

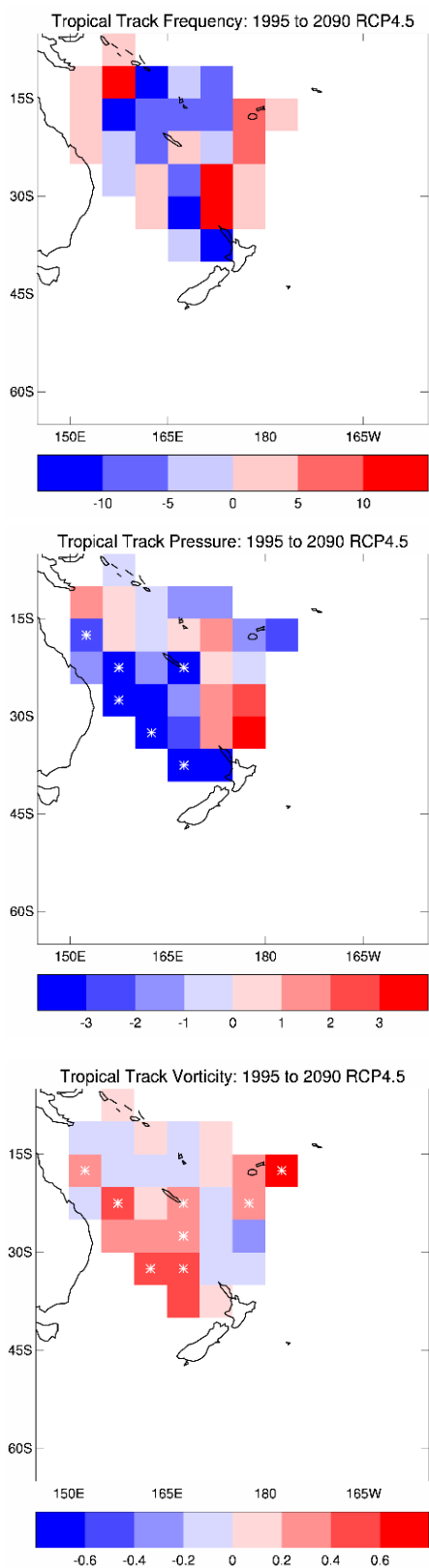


**Figure 6-7: Change in track statistics for ex-tropical storms, between 1986-2005 (RCPpast) and 2081-2100 (RCP4.5) per 5°x5° square: number of lows over 20 years and 6 models (top), average mean sea-level pressure (centre), average vorticity (bottom). Increases are shown in red, decreases in blue. Asterisks indicate changes are statistically significant at the 5% level. Units as in Figure 6-5.**

Similar trends are seen at 2081-2100 under RCP8.5, and at mid-century similar but weaker trends are also seen (not shown). There are some interesting aspects to the diagnosed changes in intensity of these ex-tropical storms.

- Bell et al. (2019) described a detailed analysis of southern hemisphere tropical cyclones in 12 CMIP5 models. A special algorithm was applied for detecting and tracking tropical cyclones in coarse resolution climate models. The overall results showed a substantial decrease (by about 1-3 tropical cyclones per decade) in track density over most parts of the southern hemisphere by the end of the century. Our study is consistent with such a decrease in such tropical systems, and our diagnosis identified fewer such ex-tropical systems exiting the tropics and affecting Bay of Plenty by the end of the century.
- Conversely, while the number of ex-tropical storms decrease, there is a consistent picture of their intensity increasing, and this intensification occurs south of 20°S in the north Tasman. We speculate on two possible mechanisms for this intensification relative to the historical climate. One of the widely-accepted conditions for tropical cyclone formation and maintenance is a warm sea-surface temperature (SST) above 26°C. Figure 6-8 shows SST increases by the end-of-century under RCP8.5 of 3°C or more in the Tasman Sea, with the position of the 26°C isotherm marked for the historic climate (1986-2005) and the future (2081-2100 RCP8.5). The 26°C isotherm moves at least 5 degrees further south in the Tasman, and even more on the Queensland coast, suggesting that tropical cyclones could travel further south before they lose the latent heating necessary to maintain their structure.
- What is also observed with ex-tropical systems in the real-world is that sometimes they re-intensify south of about 30°S as they interact with an approaching extra-tropical low-pressure system. Under the RCP8.5 scenario, the whole Tasman Sea has warmed significantly by the end of the century, but the maximum warming is centred around 35-40°S. South of this line, the north-south temperature gradient intensifies, and this might be expected to intensify any extra-tropical lows in this region. Thus, it is possible that the extra-tropical lows could be stronger as well.

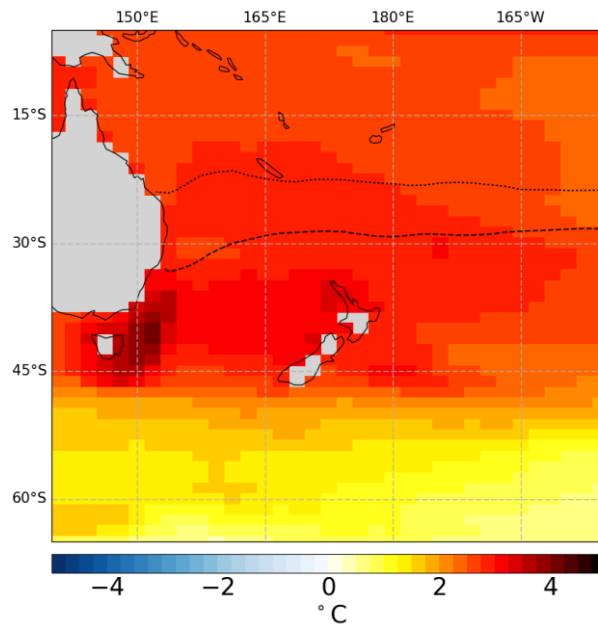


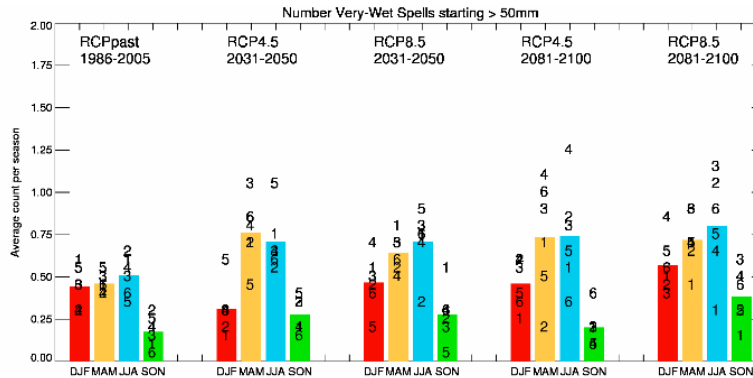
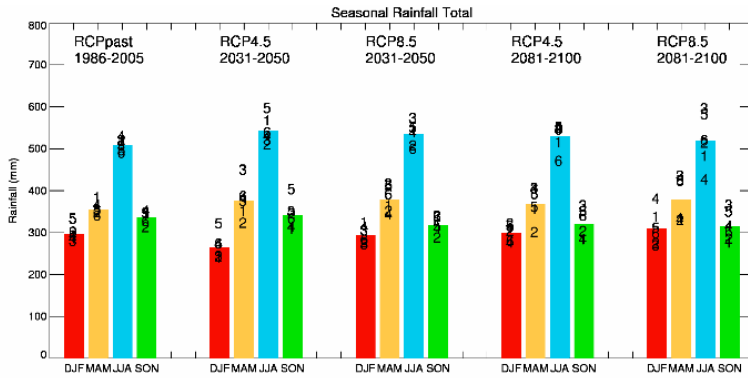
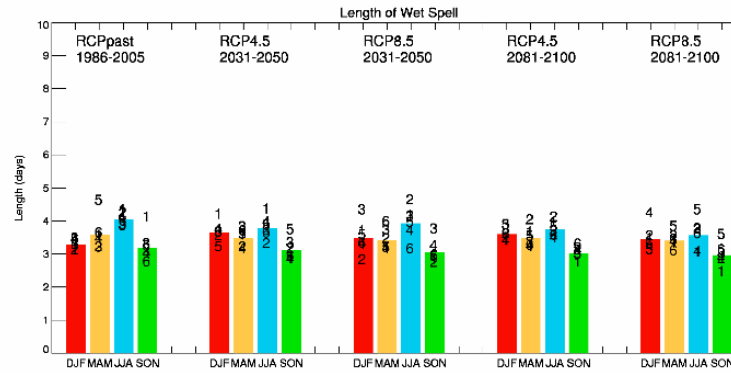
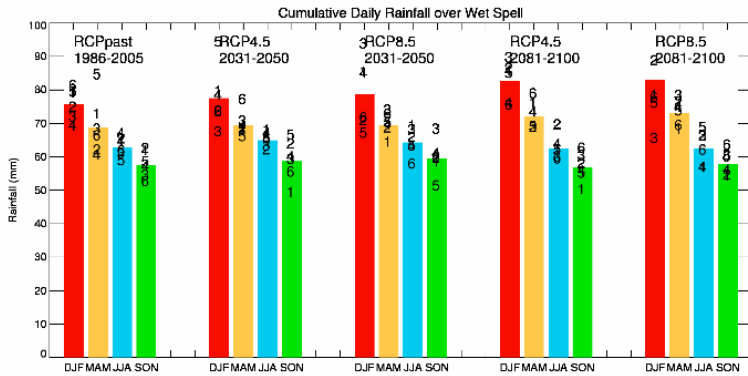
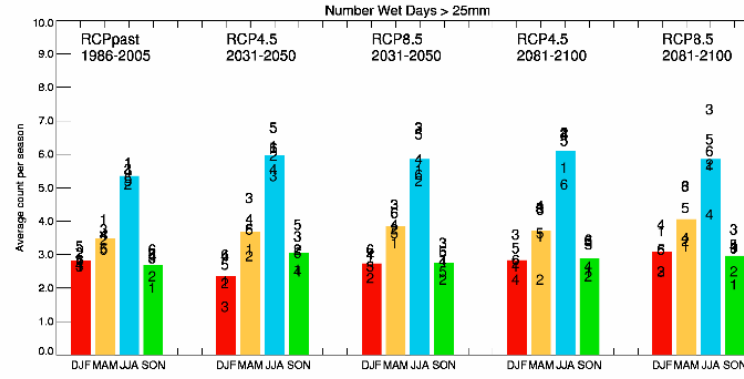
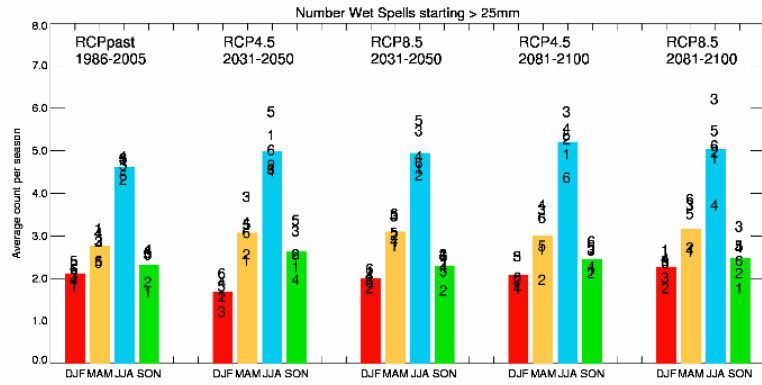
**Figure 6-8:** Ensemble-average change in sea-surface temperature (in °C) for the summer season between the historical 1986-2005 period and 2081-2100 under RCP8.5. The dotted line indicates the position of the 26°C isotherm for 1986-2005 and the dashed line its position for 2081-2100 under RCP8.5.

#### 6.4 Changes in Wet Spell Rainfalls

The previous analysis considered the behaviour of storms associated with wet spells in the Bay of Plenty. In this section, we focus just on the wet spells themselves. A “Wet Spell” begins when the area-average daily rainfall over the Bay of Plenty exceeds 25 mm, and continues until the daily rainfall drops below 1 mm. The statistics of such events in the climate models are presented in Figure 6-9. The number of wet spells per season varies from about two in summer to about five in winter (top left panel, Figure 6-9). Given that winter is the wettest season overall (bottom left panel), it is not surprising to find more wet spells in winter.

However, the average cumulative rainfall over a wet spell is highest in summer (centre left panel), and lowest in spring. The average length of wet spells varies a little with the season as well, with the winter wet spells being longest (centre right panel). It is clear, then, that the rainfall intensity (rain per rain-day) is highest in the warmest season. In the cool season (winter), there are more events, but they are not as intense, on average. In all panels, the histogram bars represent the ensemble-average statistics, with the individual models indicated by number 1 through 6. As with all rainfall characteristics, there is considerable variation from model to model.

**Figure 6-9:** (Next page) Bay of Plenty rainfall statistics, by season, for RCPpast 1986-2005, RCP 4.5 and RCP8.5 at mid-century (2031-2050), and RCP4.5 and RCP8.5 at end-of-century (2081-2100). Panels show (from top left): number of wet spells, number of wet days, cumulative rainfall over the wet spells, length of wet spell, seasonal rainfall, number of extremely-wet spells. Further explanation is given in the text. Seasons are colour-coded: summer (red), autumn (orange), winter (blue) and spring (green). The histogram bars show the ensemble-average, with individual models indicated by numbers 1 through 6 (in order HadGEM, CAM5, NorESM, GFDL, GISS, and BCC).



Two additional panels in Figure 6-9 merit discussion. The top right panel shows the average number of wet-days per season, and closely follows the pattern of wet spells. The wet-day graph (note the different vertical scale) includes any additional days >25 mm within a wet spell sequence after the first day recorded in the top-left wet-spell graph. Finally, the bottom right panel shows the number of ‘very wet’ spells where the rainfall on the first day exceeds 50 mm instead of 25 mm. These are relatively uncommon, and the winter season no longer dominates to the same extent as with the 25mm wet spells.

Figure 6-10 demonstrates that the GCM simulations of wet spells matches up well with observed wet spells as diagnosed from NIWA’s Virtual Climate Station Network (VCSN, Tait et al. (2006)). The top panel of Figure 6-10 displays the frequency of >25mm wet spells by season, and the bottom panel the average cumulative rainfall over the wet spells. The left-hand set of histograms in each panel reproduce the Figure 6-9 histograms (top left and middle left) for the 1986-2005 RCPpast period. The right-hand set of histograms shows the corresponding result from the VCSN for the same >25 mm threshold (averaged over all VCSN points within the Bay of Plenty region). There is a similarity between model and observed for the both the magnitude and seasonal variation of these two statistics defining wet spells.

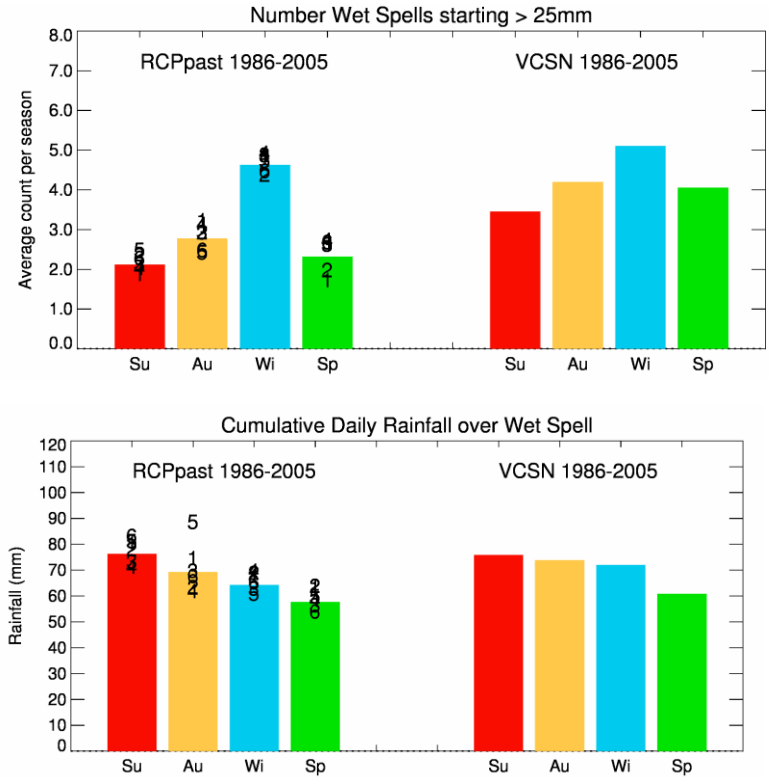


**Figure 6-10: Comparison of seasonal GCM wet-spell statistics with those from NIWA’s VCSN data set (interpolated observations): number of wet spells (top) and cumulative rainfall over the wet spells (bottom).** Seasons are colour-coded as in Figure 6-9. The RCPpast histograms on the left of each panel correspond to those of Figure 6-9.

Progressive changes in the rainfall statistics through time can be seen from the Figure 6-9 graphs. Figure 6-11 brings these changes together, showing the percentage changes between the historical 1986-2005 period and future scenarios. Results are given for changes to the end of the century under two emission scenarios, RCP4.5 and RCP8.5. The number of >25 mm wet spells increases by the end of the century for all seasons except for summer under RCP4.5. Only in the high RCP8.5 scenario do



the number of summer wet spells show much of an increase, and only then at the end of the century (2090), not by 2040 (not shown). The lack of an increase in summer wet spells could be a consequence of fewer ex-tropical storms in this season as the century progresses compensating for the rainfall per event (the cumulative rainfall).

What does change noticeably in summer is the length of the wet spell and the cumulative rainfall over the events. This results in the rainfall intensity (cumulative rainfall divided by length) not changing very much in summer. Nonetheless, adverse impacts would be expected from longer wet spells with more total rainfall. Conversely for the other three seasons, the cumulative rainfall hardly changes but instead the wet spell length decreases, and the rainfall intensity shows a compensating increase.

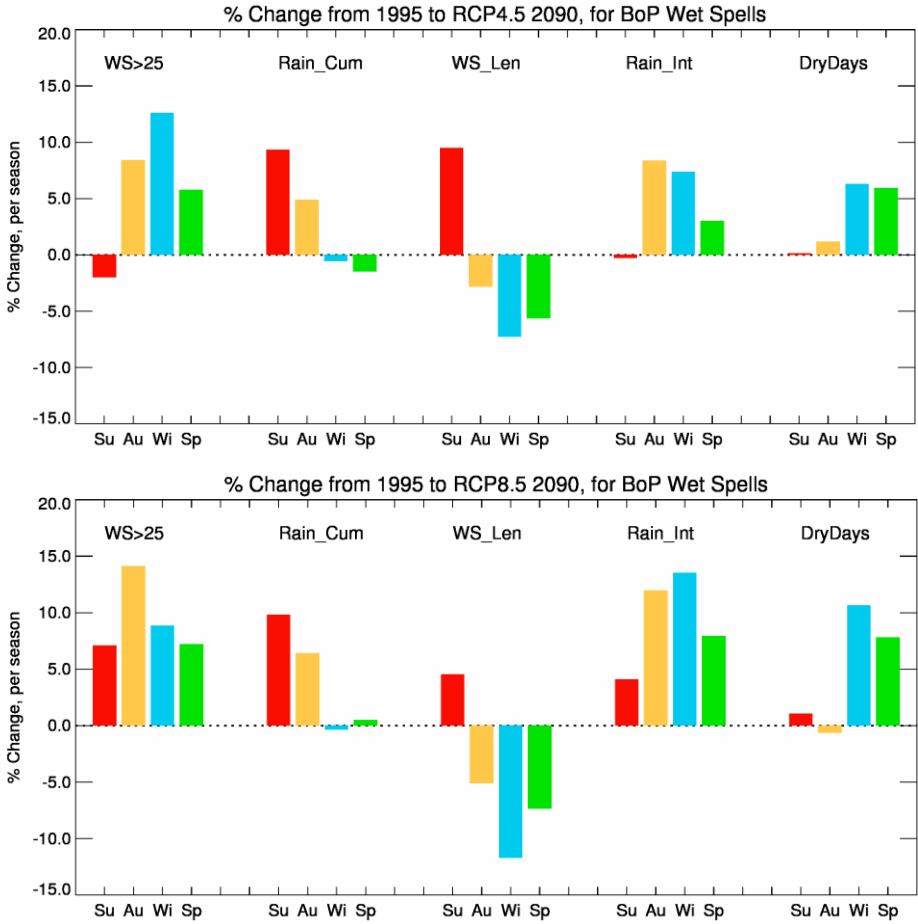


**Figure 6-11: Ensemble-average summary of Bay of Plenty rainfall statistics, by season, for the percentage change between RCPpast 1986-2005 and RCP 4.5 2081-2100 (top), or between RCPpast and RCP8.5 2081-2100 (bottom).** Seasons are colour-coded as in Figure 6-9. Statistics shown are for: number of >25mm wet spells (WS>25), cumulative rainfall over the wet spell (Rain\_Cum), wet spell length (WS\_Len), rainfall intensity (Rain\_Int; cumulative rainfall divided by length), and number of dry days (DryDays).

### 6.5 Conclusions

This analysis assesses how weather systems bringing heavy rainfall to the Bay of Plenty may change under a future warmer climate. The focus is on “Wet Spells” where a threshold of 25 mm is exceeded on the first day. Such wet spells are more common in winter, but produce the greatest rainfall accumulation over the wet spell in the summer season. In summer, the projections indicate that the

length and accumulated rainfall from wet spells increase, but there is less confidence about changes in the total number of summer events. Conversely, in the other three seasons, the projections suggest an increase in the frequency of wet spells: they don't last as long, but their intensity is greater.

Increasing summer rainfall accumulations match up with the more intense ex-tropical storms to the west of the North Island later in the century, while at the same time there are fewer such storms exiting the tropics and moving towards New Zealand. The poleward movement of extra-tropical storms, commented on by many researchers, is quite evident in this analysis in the winter season. However, this southward movement does not prevent these storms from affecting the Bay of Plenty, and indeed increases the number of wet spells (above the 25 mm threshold) in winter.

**There is good evidence that storms originating from the sub-tropics in the summer that impact on the Bay of Plenty have more intense circulation that is likely to lead to stronger winds, greater storm surge and higher rainfall accumulations. Evidence for such changes in other seasons is less clear. However, there is also good evidence that heavy rainfall intensity associated with storms increases in all seasons with global warming, particularly in winter, likely associated with the increased moisture carrying capacity of a warmer atmosphere.**

## 7 Climate change impacts for the Bay of Plenty Region

The remainder of this report presents information on potential climate change impacts for the Bay of Plenty Region. Included in the following sections, following discussions with Bay of Plenty Regional Council staff, is information about climate change impacts on sea-level rise, biosecurity and pests, drought and pasture growth, horticulture, forestry, and health.

## 8 Impacts of sea-level rise

### 8.1 Ministry for the Environment coastal hazards and climate change guidance

Updated coastal hazards and climate change guidance has been published by Ministry for the Environment (2017). This section provides a summary of recent sea-level rise (SLR) trends and future projections for New Zealand. NZ projections have been applied to the Bay of Plenty context in Section 8.2.1.

Rising sea level in past decades has already affected human activities and infrastructure in coastal areas, with a higher base mean sea level contributing to increased vulnerability to storms and tsunamis. Key impacts of rising sea level are:

- gradual inundation of low-lying marsh and adjoining dry land on spring high tides
- escalation in the frequency of nuisance and damaging coastal flooding events
- exacerbated erosion of sand/gravel shorelines and unconsolidated cliffs (unless sediment supply increases)
- increased incursion of saltwater in lowland rivers and nearby groundwater aquifers, raising water tables in tidally-influenced groundwater systems.

These impacts will have increasing implications for development in coastal areas, along with environmental, societal and cultural effects. Local government road and 'three waters' infrastructure will also be increasingly affected, such as wastewater treatment plants and potable water supplies, besides capacity and performance issues with stormwater and overland drainage systems. Public transportation infrastructure and roads will also be affected, both by nuisance shallow flooding of saltwater (e.g. vehicle corrosion) and more disruptive flooding and damage from elevated storm-tides and wave overtopping.

There are three types of SLR in relation to observations and projections:

- absolute (or eustatic) rise in ocean levels, measured relative to the centre of the Earth, and usually expressed as a global mean (which is used in most sea-level projections e.g. IPCC).
- offsets (or departures) from the global mean absolute SLR for a regional sea, e.g. the sea around New Zealand. Significant variation can occur in response to warming and wind patterns between different regional seas around the Earth.
- local (or relative) SLR, which is the net rise from absolute, regional-sea offsets and local vertical land movement, measured relative to the local landmass. Local or regional adaptation to SLR needs to focus on this local rise.

The first two types of sea-level change are measured directly by satellites, using radar altimeters, or by coalescing several tide-gauge records after adjusting for local vertical land movement and ongoing changes in the Earth’s crust following ice loading during the last Ice Age<sup>4</sup>.

Local SLR is measured by tide gauges. One advantage of knowing the local SLR from these gauge measurements is that this directly tracks the SLR that has to be adapted to locally, or over the wider region represented by the gauge. If, for instance, the local landmass is subsiding, then the local (relative) SLR will be larger than the absolute rise in the adjacent ocean level acting alone (Figure 8-1).



**Figure 8-1: Difference in mean sea level (MSL) shoreline between absolute and local (relative) SLR where land subsidence occurs.**

### Changes in rate of rise

After a period of relative local stability over the past 2000–3000 years, with small rates of sea-level change of up to  $\pm 0.2$  mm/year (Kopp et al., 2016), global sea level began to rise in the late 1800s. The steady rise in global mean sea level (MSL) since then is shown in Figure 8-2, based on updates of the data from Church and White (2011).

<sup>4</sup> Scientific term is glacial isostatic adjustment (GIA)

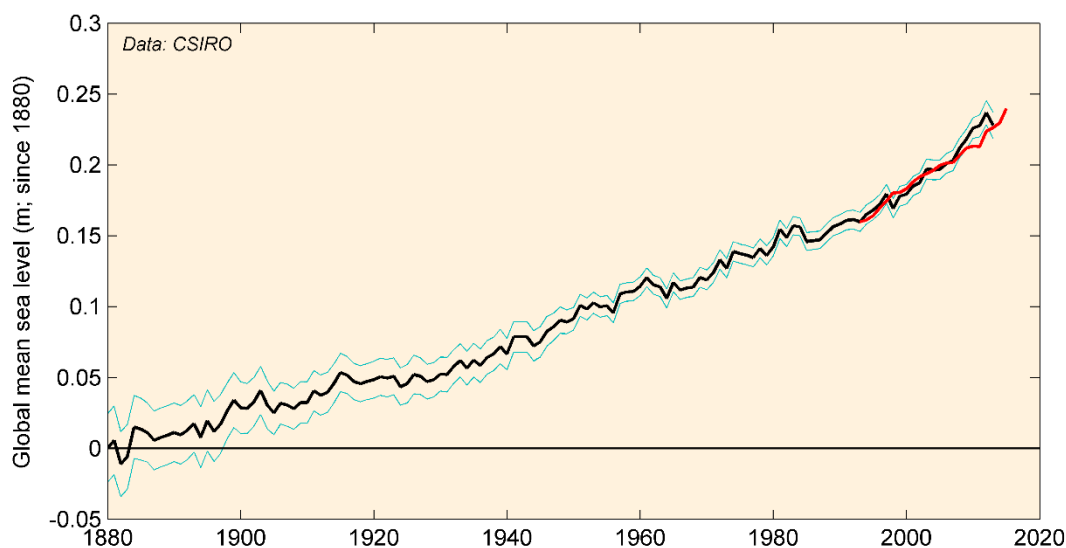


**Figure 8-2: Cumulative changes in global mean sea level (MSL) since 1880, based on a reconstruction of long-term tide gauge measurements to end of 2013 (black) and recent satellite measurements to end 2015 (red).** Lighter lines are the upper and lower bounds of the likely range ( $\pm 1$  standard deviation) of the MSL from available tide gauges, which is a function of the number of measurements collected and the precision of the methods. Tide gauge data from Church and White (2011), updated to 2013; satellite data from CSIRO (2016).

From a synthesis of scientific publications, the Intergovernmental Panel on Climate Change determined that it is very likely that the mean rate of globally averaged SLR was  $1.7 \pm 0.2$  mm/year between 1901 and 2010, producing a total rise in global sea level over that period of 0.19 metres ( $\pm 0.02$  metres). A slightly higher annual rise of  $2.0 \pm 0.3$  mm/year occurred in the 40-year period from 1971 to 2010 (Church et al., 2013b).

### Contributors to global sea-level rise

As the temperature of the Earth's atmosphere changes so does sea level, although with a lagged response. Rising atmospheric temperature and sea-level change are linked by two main processes:

- **Volume increase:** As ocean water warms, its volume expands slightly – an effect that is cumulative over the entire depth of the oceans. This is converted mainly into a height increase as the oceans are largely constrained by continental coastlines (despite inundation of low-lying land areas).
- **Mass increase:** Changes in the land-based volumes of ice and water on land (namely glaciers and ice sheets, and to a lesser extent the net change in freshwater budgets) have led to an increase in the mass of water in the ocean, especially as ice stores diminish with increasing surface and ocean temperatures.

Recent studies have demonstrated that the anthropogenic contribution to the observed global SLR in the 20th century has been around 45–50%. The anthropogenic contribution since 1970 has risen to 69% [ $\pm 31\%$ ] of the observed increase in global mean sea level (Slangen et al., 2016).

For the satellite era (from 1993 onwards, Figure 8-3), the recent trend in global-average MSL to July 2017, based on the CSIRO analysis of satellite altimeter data<sup>5</sup>, is  $3.4 \pm 0.1$  mm/year. This rate of increase, averaged over the past 24 years, is nearly double the global-average rate over the historic rate over the entire 20th century of 1.7-1.8 mm/year (Church et al., 2013b, Church and White, 2011). Natural climate variability from inter-annual to decadal climate cycles, especially the 20–30-year Interdecadal Pacific Oscillation (IPO) (which changed phase around 1999, partway into the satellite era), has contributed to part of the increased rate of rise. However, it is clear that anthropogenic climate change is also contributing an increasing proportion of this more recent increase in global SLR (Slangen et al., 2016).

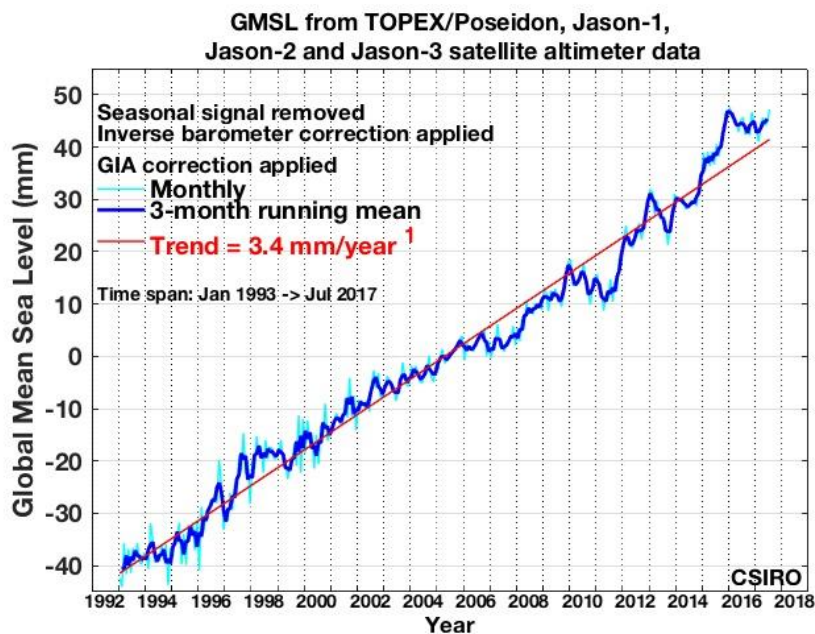


**Figure 8-3: Time series and trend in global average sea level over the satellite era from January 1993 to July 2017.** Adjustments for glacial isostatic adjustment (GIA), following crustal response to the last Ice Age, and inverted barometer (annual air pressure differences) have been made. Retrieved from CSIRO web site: [http://www.cmar.csiro.au/sealevel/sl\\_hist\\_last\\_decades.html](http://www.cmar.csiro.au/sealevel/sl_hist_last_decades.html)

### Sea-level rise for New Zealand waters

Changes in annual local MSL at the four main ports in New Zealand from 1900 to 2015 are shown in Figure 8-4. MSL is plotted relative to the average for each time series over the same 1986–2005 baseline period used for IPCC AR5 projections. The initial period of IPCC global-mean projections of SLR for RCP8.5 and RCP2.6 scenarios are also shown for a general comparison.

Considerable variability occurs from year to year, influenced by seasonal changes, the two- to four-year El Niño-Southern Oscillation and the IPO over 20-30-year cycles. The notable rapid rise in SLR in 1999 across all port sites is a result of a regime shift to the negative phase of the IPO.

Climate variability masks the underlying rise caused by climate change. This requires long records to extract robust trends, and also may require one or two decades more of monitoring to confirm which

<sup>5</sup> [www.cmar.csiro.au/sealevel/sl\\_hist\\_last\\_decades.html](http://www.cmar.csiro.au/sealevel/sl_hist_last_decades.html) - Rate includes adjustments for both inverse barometer and glacial isostatic adjustment.

SLR scenario is being followed (because there is little difference at present between scenarios - Figure 8-4).

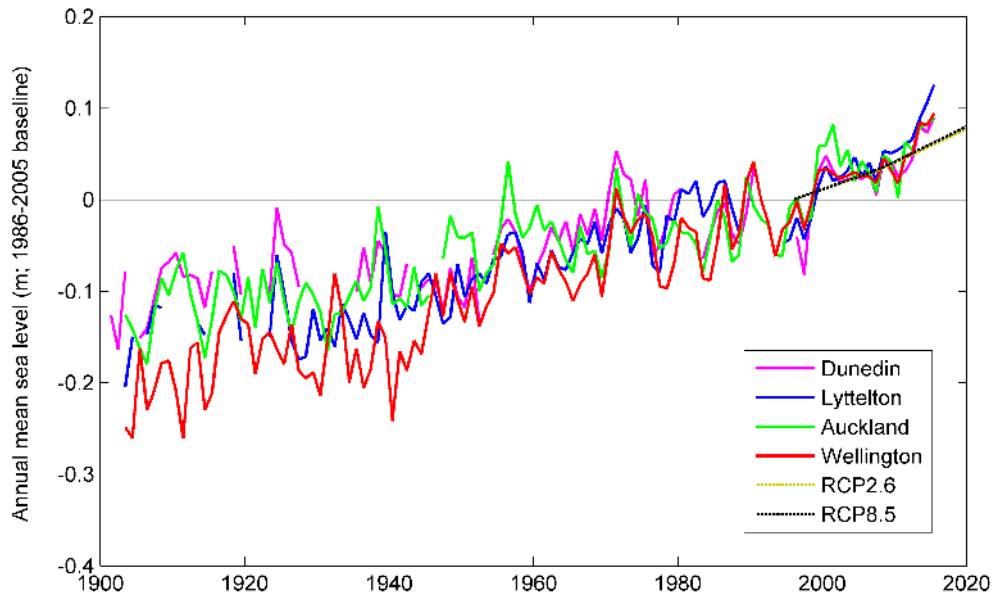


**Figure 8-4: Change in annual local MSL for the four main ports from 1900–2015, and initial global-mean SLR projections for RCP2.6 and RCP8.5 to 2020 (dashed lines).** Relative to the average MSL over the baseline period 1986–2005 (used for IPCC AR5 projections of SLR, with mid-point at 1996). (Source data: Hannah and Bell (2012), updated to 2015; Church et al. (2013a)).

Trends from these long-term port records, along with inferred trends from six other gauge sites used to establish local survey datums last century, were derived by Hannah and Bell (2012) for records up to and including 2008. The average trend for the local or relative SLR at the four main ports up to 2008 was  $1.7 \pm 0.1$  mm/yr, ranging from a local rate of 1.3 mm/yr at Dunedin to 2.0 mm/yr in Wellington.

Adding on the average glacial isostatic adjustment (GIA) for New Zealand, due to post-Ice Age rebound of the Earth’s crust of around 0.3 mm/yr (Hannah and Bell, 2012) yields an absolute SLR of around 2.0 mm/yr for New Zealand ocean waters. This is at the upper end of observations of global mean SLR of  $1.7 \pm 0.2$  mm/yr from 1900 to 2010 from the IPCC AR5 (Church et al, 2013).

Local sea-level or RSLR trends over the past 60-100 years with standard deviations were analysed at 10 gauge sites by Hannah and Bell (2012), with an average rise of 1.7 mm/year from early last century up to 2008. The trends were updated to 2015 (except for Whangarei), as shown in Figure 8-5, with the national average rate now closer to 1.8 mm/year.

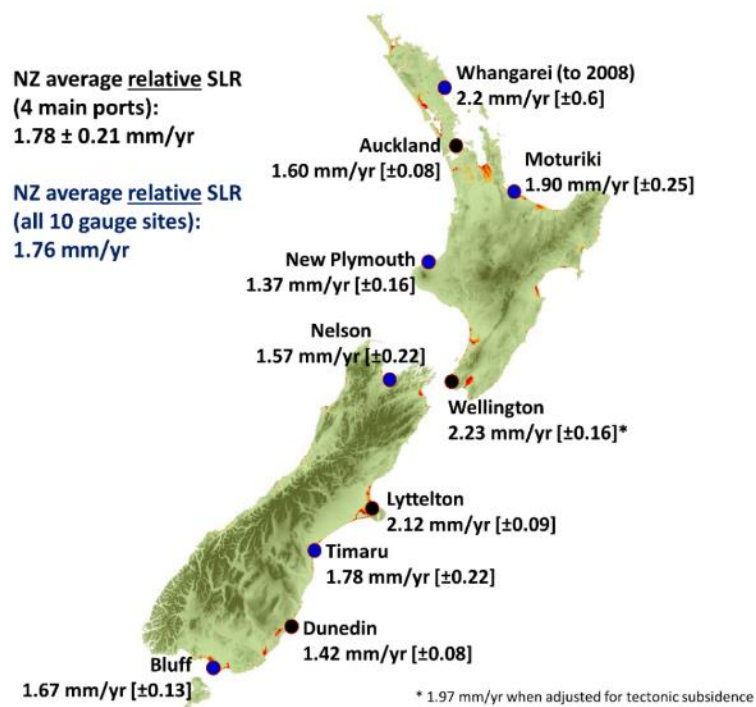


**Figure 8-5: Historic long-term RSLR rates for the 20<sup>th</sup> century up to and including 2015 (excluding Whangarei), determined from longer sea-level gauge records at the four main ports.** Note: Standard deviations of the trend are listed in the brackets. Sources: analysis up to end of 2008 from Hannah and Bell (2012) updated with seven years of MSL data to end of 2015 (J Hannah, pers. comm., 2016); sea-level data from various port companies is acknowledged.

Adaptation to SLR requires knowledge on why and how local SLR around New Zealand is affected by ongoing vertical land movement. Of most concern is the presence of any significant ongoing subsidence of the landmass, which will exacerbate the absolute ocean SLR (Figure 8-1).

Future projections of SLR at some locations or regions in New Zealand will need to factor in estimates of ongoing vertical land movement. Measurements of vertical (and horizontal) land movement have been undertaken by continuous GPS (cGPS) stations around New Zealand over the past decade or more. Vertical land movement was analysed by Beavan and Litchfield (2012), who determined that much of the Bay of Plenty area around Matatā was uplifting. However, this was assumed to be due to swarms of earthquakes in the area during the measurement period (pre-2012), and was not expected to continue long-term (Figure 8-6). Any significant long-term vertical land movement (beyond  $\pm 0.5$  mm/yr, the accuracy of the rate at which trends can be extracted from 10-year records) should be factored into local SLR projections, especially if the land is subsiding, because this will exacerbate the local net rise in sea level that will need to be adapted to (Figure 8-1).

Future major earthquake displacements for a particular locality are deeply uncertain (both when and by how much). Unlike the ongoing SLR, they could be either subsidence or uplift, other than those areas with a clear geological history of only uplift or subsidence (Beavan and Litchfield, 2012).



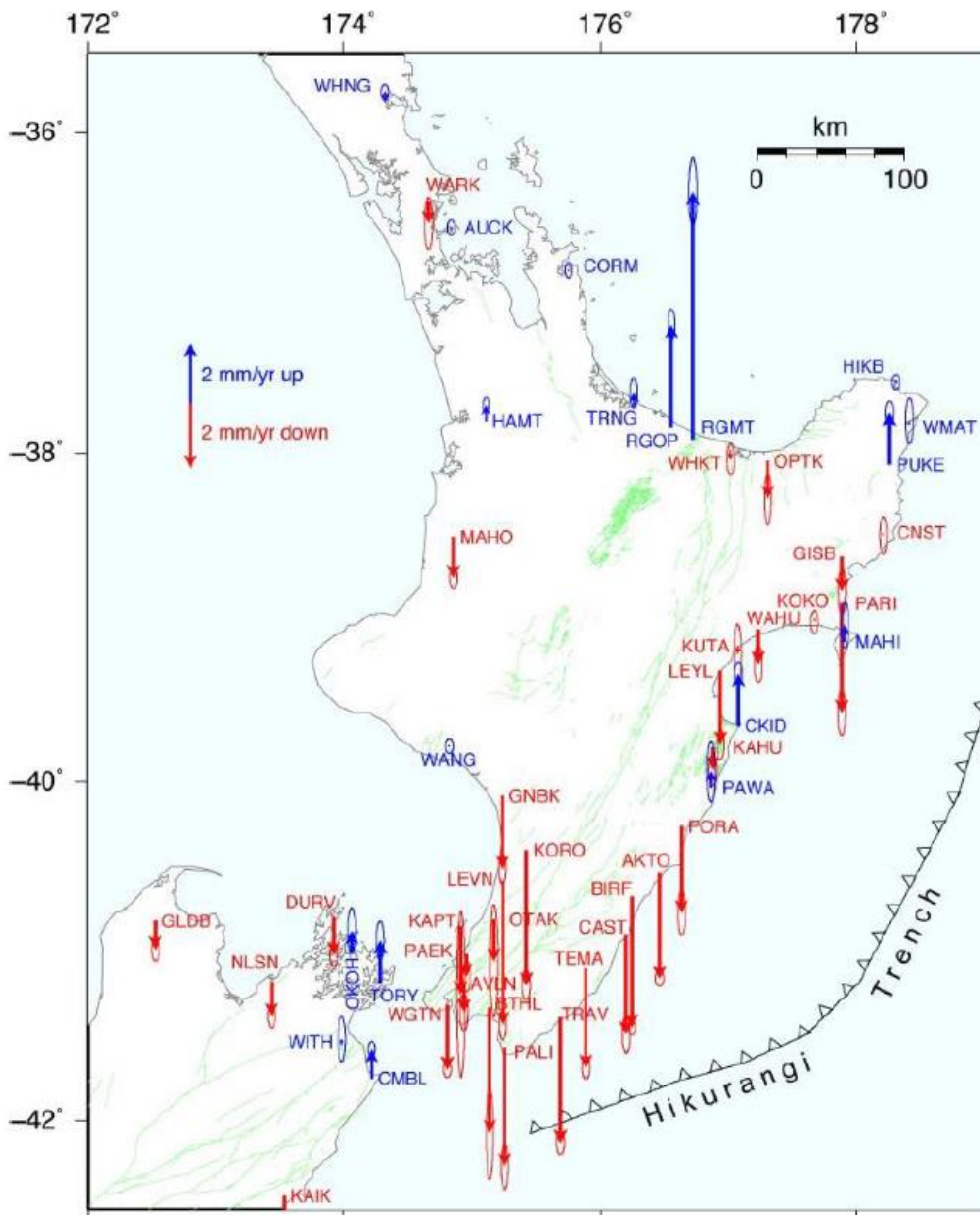


**Figure 8-6: Average vertical land movements (mm/yr) for near-coastal continuous GPS sites across central New Zealand regions.** Source: Beavan and Litchfield (2012).

### Projections for sea-level rise

The primary climate driver for SLR is global and regional surface temperature, which is strongly influenced by greenhouse gas emissions. With the greenhouse gases currently in the atmosphere and the heat stored in the ocean, the world is already committed to further temperature increases, and an ongoing lagged response to SLR, because of the inertia in warming the deep oceans and the melting of the vast polar ice sheets. Cumulative global emissions to date have already committed the Earth to an eventual 1.6–1.7 m of global SLR relative to the present level (Strauss et al., 2015, Clark et al., 2016), even if no further net global emissions occur. However, depending on how continuing emissions track during the rest of this century (particularly the next few decades), realising this present commitment to SLR could take one to two centuries.

The IPCC AR5 (Church et al., 2013a) projections out to 2100 are provided in Figure 8-7. These projections cover the likely range of variability for the lowest and highest RCP2.6 and RCP8.5 scenarios out to 2100, and all four RCPs for the averaging period 2081-2100. The zero baseline for these projections is the averaging period for MSL from 1986–2005 (same as for Figure 8-4).

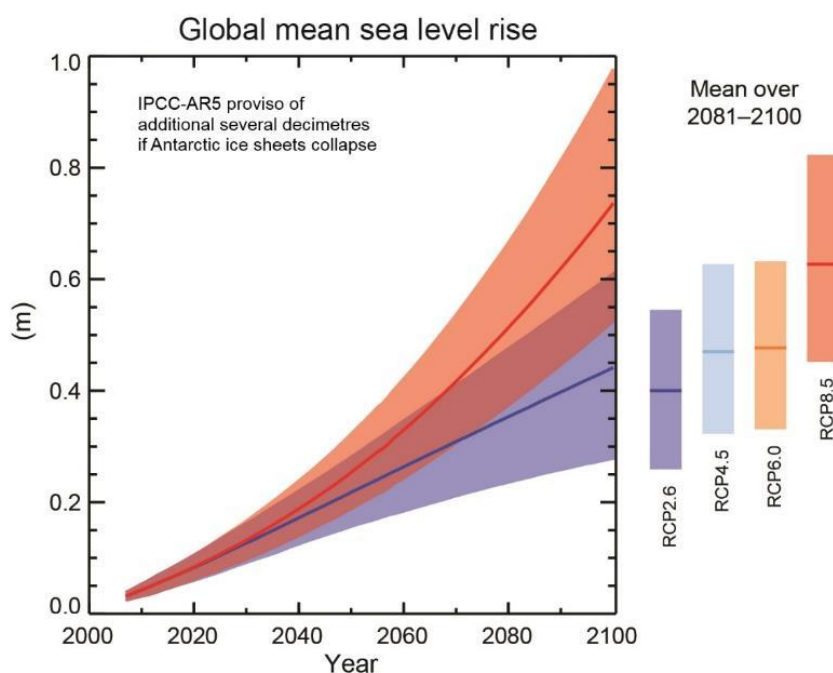


**Figure 8-7: IPCC AR5 projections of global-average MSL rise (metres, relative to a base MSL of 1986-2005) covering the range of scenarios from RCP2.6 to RCP8.5.** The heavy line shows the median estimate for that RCP, while the shaded area covers the “likely range” projections for the RCP, with a 33% chance SLR could be outside that range. The bars on the right show the median and “likely range” for all four RCPs averaged over the last two decades of this century (2081–2100), hence are lower than projections ending at 2100 in the main plot. (From IPCC (2013)).

Key statements on SLR in the IPCC AR5 (using the calibrated language for uncertainty and confidence in italics), include (Church et al., 2013a):

- Global mean SLR will continue during the 21st century, *very likely* at a faster rate than observed from 1971 to 2010.
- By 2100, global-average SLR will *likely* (i.e. 66% chance) be in the range 0.28–0.61 m [RCP2.6], 0.36–0.71 m [RCP4.5], 0.38–0.73 m [RCP6.0] and 0.52–0.98 m [RCP8.5].
- Onset of the collapse of the marine components of the Antarctic ice sheets could cause global MSL to rise substantially above the *likely* range (Figure 8-7) during this century. While the contribution cannot be precisely quantified, there is *medium confidence* that it would not exceed several tenths of a metre<sup>6</sup> of SLR by 2100.
- It is *virtually certain* that global mean SLR will continue for many centuries beyond 2100, with the amount of rise dependent on future emissions.

<sup>6</sup> Or decimetres (one-tenth of a metre).

- The threshold for the loss of the Greenland ice sheet over a millennium or more, and an associated SLR of up to 7 metres, is greater than about 1°C (*low confidence*) but less than about 4°C (*medium confidence*) of global warming with respect to pre-industrial temperatures.
- Abrupt and irreversible ice loss from the Antarctic ice sheet is possible, but current evidence and understanding is insufficient to make a quantitative assessment.

### Use of global projections to generate New Zealand SLR scenarios

A set of all four RCP projections for New Zealand is shown in Figure 8-8, based on the median projections from IPCC (Church et al., 2013b). An additional scenario is presented here, which is the 83rd percentile of RCP8.5 (i.e., upper end of the “likely range”). This more extreme scenario is presented to cover the possibility of polar ice sheet instabilities not factored into the IPCC projections (Stephens et al., 2017). Small offsets have been added to the global average SLR projections to account for a slightly higher (5-10%) increase in SLR in seas around New Zealand compared to the global average projections (Ackerley et al., 2013). The base set of global SLR projections is extended to 2130, to align with the planning timeframe of at least 100 years stipulated in the New Zealand Coastal Policy Statement 2010 (Stephens, 2017).

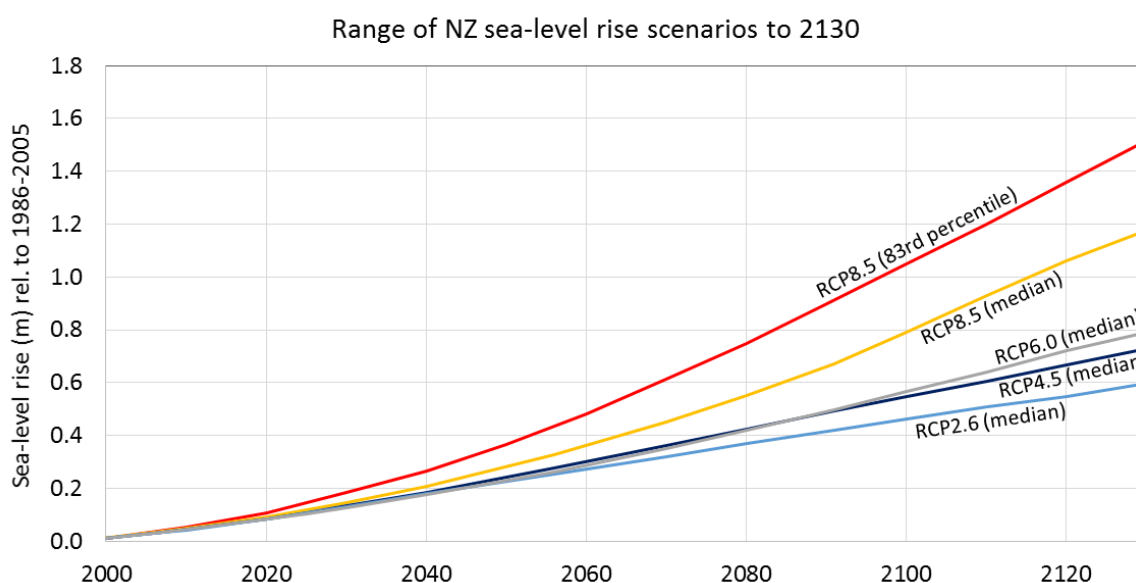


**Figure 8-8:** SLR scenarios for New Zealand seas, based on a set of median projections for all four RCPs (based on Church et al., 2013b) plus a higher 83rd percentile RCP8.5 projection (based on (Kopp et al., 2014)). The M next to the RCP on the plot stands for median. Note: for New Zealand seas, SLR projections will be around 5-10% higher than the global mean SLR published by IPCC, so between 2.5 to 5 cm by 2100 has been added to the median global average projections, and 7.5 cm to the higher scenario.

To assist with adaptive approaches to planning, the bracketed time window (approximate earliest to latest) when various SLR increments will be reached is shown in for all scenarios in Table 8-1 (except for NZ RCP6.0 which is similar to NZ RCP4.5). For example, 0.5 m of SLR for New Zealand is projected to occur by 2060 at the earliest (assuming a RCP8.5 83rd percentile scenario described above) and 2110 at the latest (under the low-emission RCP2.6 scenario). Even earlier exceedance of the specific SLR increment cannot be entirely ruled out (depending on the future emission controls and possible runaway polar ice sheet responses). Exceedance of a 1 m SLR is projected by 2100 for a possible earliest (based on the RCP8.5 83rd percentile scenario) and after 2200 at the latest.

**Table 8-1: Approximate years, from possible earliest to latest, when specific SLR increments (metres above 1986-2005 baseline) could be reached for various projection scenarios of SLR for the wider New Zealand region. From Stephens et al. (2017)**

SLR (metres)	Year achieved for RCP8.5 (83%ile)	Year achieved for RCP8.5 (median)	Year achieved for RCP4.5 (median)	Year achieved for RCP2.6 (median)
0.3	2045	2050	2060	2070
0.4	2055	2065	2075	2090
0.5	2060	2075	2090	2110
0.6	2070	2085	2110	2130
0.7	2075	2090	2125	2155
0.8	2085	2100	2140	2175
0.9	2090	2110	2155	2200
1.0	2100	2115	2170	>2200
1.2	2110	2130	2200	>2200
1.5	2130	2160	>2200	>2200
1.8	2145	2180	>2200	>2200
1.9	2150	2195	>2200	>2200

## 8.2 Bay of Plenty sea-level rise, coastal erosion and inundation

The Bay of Plenty Region’s coastline is exposed to extreme storm tide events, and this exposure will increase further with sea-level rise. A number of coastal hazard and sea level reports have recently been completed by NIWA for Bay of Plenty Regional Council and Tauranga City Council. The reader is directed to those reports for detailed findings rather than reporting them again here.

- Storm-tide and wave hazards in the Bay of Plenty (Stephens et al., 2018)
- Tauranga Harbour extreme sea level analysis (Stephens, 2017)
- Coastal inundation mapping at Te Tumu, Bay of Plenty (for Tauranga City Council) (Stephens and Wadwha, 2017)
- Estimation of 2, 10 and 20-year average recurrence interval storm-tide + wave-setup elevations within Tauranga Harbour (Stephens, 2019)
- Tauranga Harbour inundation modelling (Reeve et al., 2019)

### 8.2.1 Stephens (2017) Bay of Plenty sea-level rise projections

Stephens (2017) tailored the New Zealand sea-level rise projections presented in Figure 8-8 for Bay of Plenty. The information below is summarised from that report.

To use the projections locally requires that the 1986–2005 mean sea level (MSL) be added, relative to a local vertical datum. MSL at the Moturiki tide gauge was 0.07 m above Moturiki Vertical Datum 1953 (MVD–53) for the 1986–2005 baseline period. The projected SLR relative to MVD–53 are shown in Table 8-3.

There are local differences in MSL (of a few centimetres) throughout the Bay of Plenty region including estuaries, relative to the Moturiki tide gauge, some of which may be due to datum or gauge issues.

From the perspective of a specific location on land, such as a human dwelling, intertidal habitat, or water level (tide) gauge, vertical land motion (VLM) also contributes to changes in sea level, and it is this relative sea level rise (RSLR) that is of interest to coastal infrastructure and its inhabitants (Sweet and Park, 2014). The rate of VLM in the Pāpāmoa hills was +0.5 mm/yr, measured over approximately 9 years (Houlie and Stern, 2017, Beavan and Litchfield, 2012). Thus, the land around Tauranga can be considered relatively stable or slightly rising, although rates of VLM can change significantly over 10's of kilometres, so these may not be accurate when extrapolated to the sedimentary features at the coast. Given the relatively low VLM rates, the distance of the measurement location from the coast, and the relatively short VLM record, we recommend that the SLR values in Table 8-3 be used for the Tauranga coastline, with no additional allowance for VLM. Measurements of VLM are proposed to be collected at the Moturiki sea-level gauge location in the future.

The SLR projections in Table 8-3 apply to the Tauranga region and surrounds, but could differ over the wider Bay of Plenty region due to regional differences in MSL and VLM. However, the projections presented here are considered to be broadly representative of the Bay of Plenty Region (S. Stephens, pers. comm., August 2019). Note that current research under the NZSeaRise project aims to develop regional sea-level rise projections for New Zealand that will account for land deformation.

**Table 8-2: SLR projections (metres above 1986–2005 baseline MSL) in 2070 and 2130 for the wider New Zealand region.**

Year	NZ RCP2.6 M (median)	NZ RCP4.5 M (median)	NZ RCP8.5 M (median)	NZ RCP8.5 (83rd percentile)
1986–2005	0	0	0	0
2070	0.32	0.36	0.45	0.61
2130	0.60	0.74	1.18	1.52

**Table 8-3: SLR projections (metres above MVD–53) in 2070 and 2130 for the Bay of Plenty region.**

Year	NZ RCP2.6 M (median)	NZ RCP4.5 M (median)	NZ RCP8.5 M (median)	NZ RCP8.5 H <sup>+</sup> (83rd percentile)
1986–2005	0.07	0.07	0.07	0.07
2070	0.39	0.43	0.52	0.68
2130	0.67	0.81	1.25	1.59

### 8.2.2 Bay of Plenty coastal sensitivity

NIWA completed a study on the sensitivity of New Zealand's coasts to the effects of coastal climate change (Goodhue et al., 2012). The assessment does not include present issues (e.g., with present or historic coastal erosion), but focuses on the sensitivity of coastal margins for any further change. In conjunction with available geomorphic and oceanographic information, Coastal Sensitivity Indices (CSI) were developed for coastal inundation and coastal erosion for New Zealand's soft shore coastline. These indices were created by combining four geomorphic (exposure, hinterland, sediment type and landform type) and three oceanographic (high tide range and change in storm surge and wave height) variables. Relative scores and weightings were then applied to these variables based on

how likely they are to be affected by climate change. For more information on the methodology used to produce the CSI, the reader is directed to Goodhue et al. (2012).

Two national maps were produced, which can be used to identify coastal areas which are more sensitive than others to the potential impacts of climate change-induced coastal erosion and inundation. These have been provided here for the Bay of Plenty Region in Figure 8-9 for erosion and Figure 8-10 for inundation.

Figure 8-9 shows that the Bay of Plenty coastline has moderate-high sensitivity to erosion. The areas with the highest sensitivity are Ōhope, Whakatāne, Maketu, Matakana Island, and the coastline east of Ōpōtiki. The least sensitive area to climate-change related coastal erosion is around Matatā.

Figure 8-10 shows a similar pattern, in that the most sensitive areas to erosion are also the most sensitive to inundation. The least sensitive areas to inundation are around Matatā, and between Ōhope and Ōpōtiki.

The CSI is not an absolute measure of potential risk of future inundation or erosion under climate change, and consequently it should not be used as a replacement for local (beach scale) risk assessments. Rather the CSI has been designed to provide a high-level scoping index and comparison of the relative (higher or lower) sensitivity to climate change of one part of the coast compared to another.

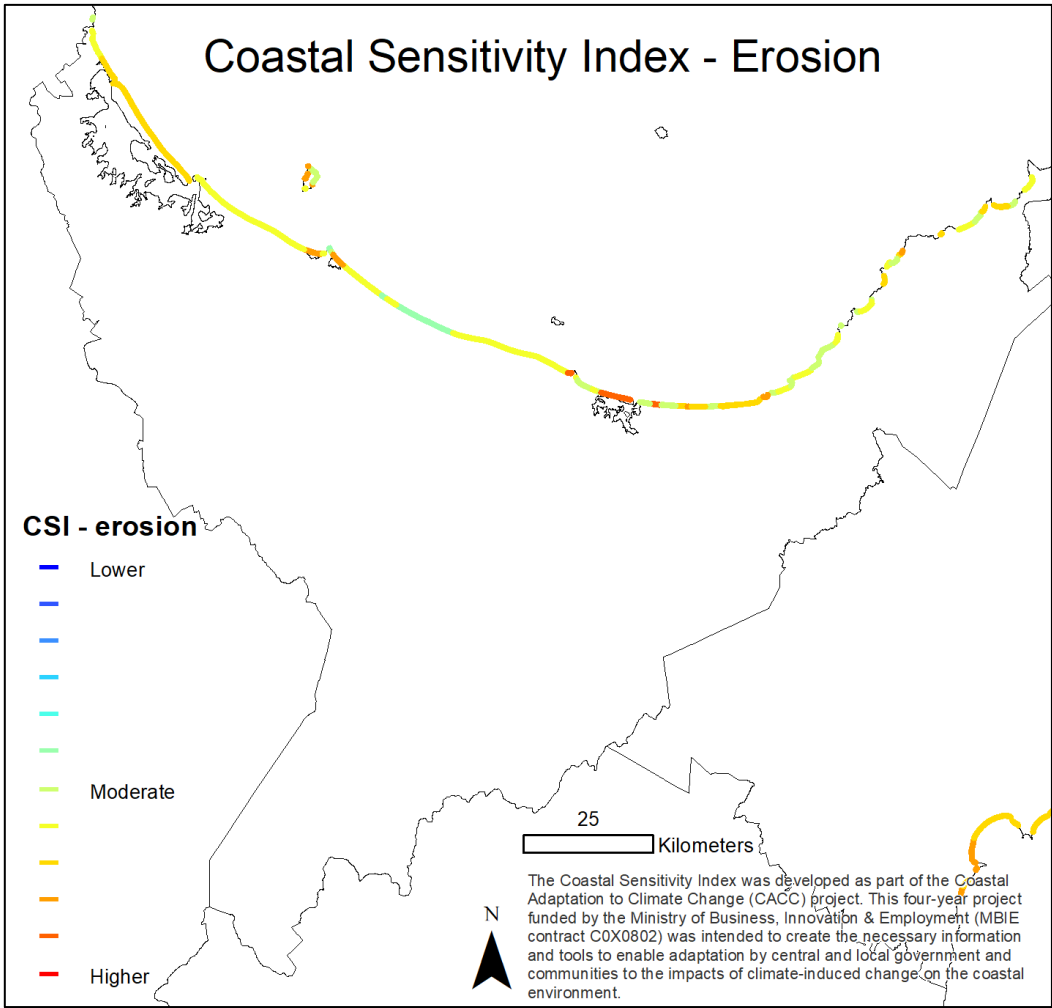


Figure 8-9: Coastal sensitivity index for erosion for the Bay of Plenty Region. After Goodhue et al. (2012).

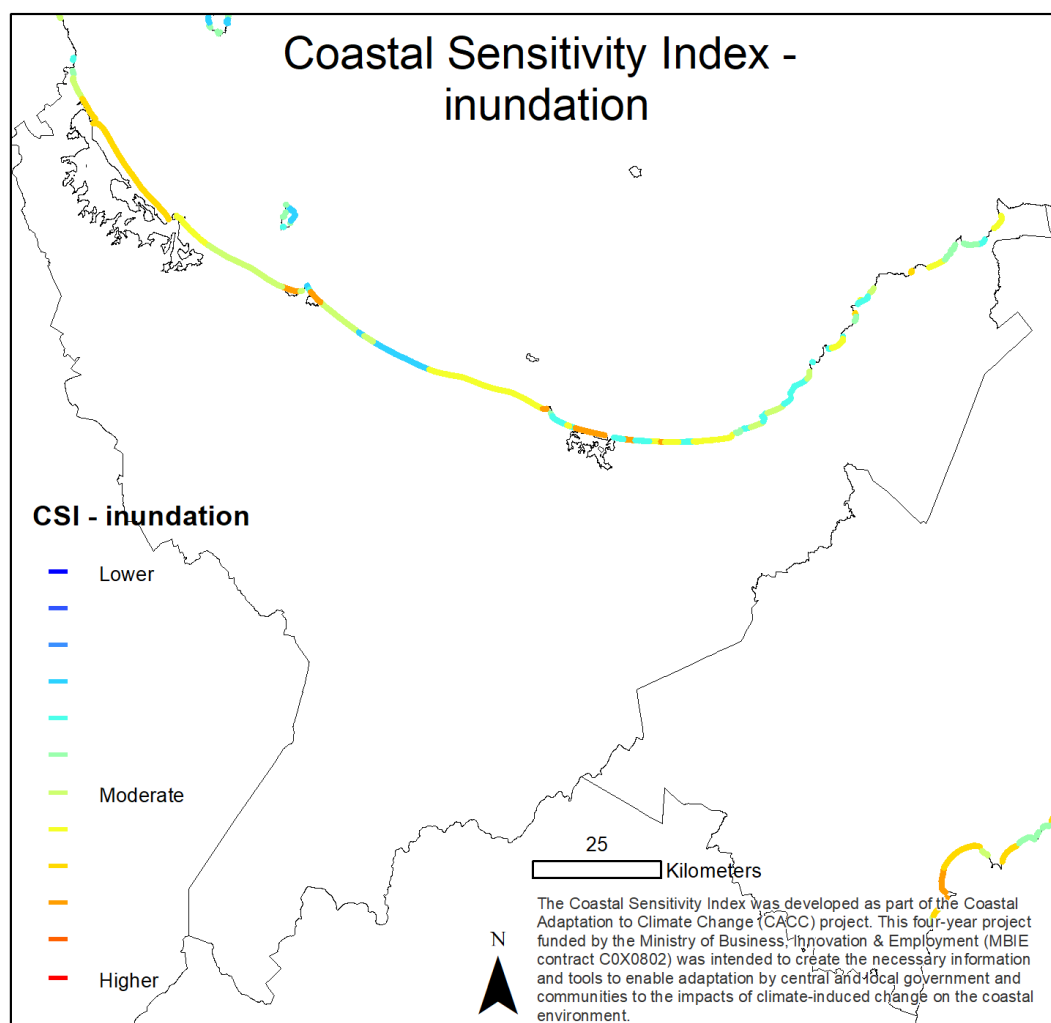


Figure 8-10: Coastal sensitivity index for climate change-induced inundation (flooding by the sea) for the Bay of Plenty Region. After Goodhue et al. (2012).

### 8.3 More extreme SLR projections - Hansen et al. (2016)

James Hansen and co-authors published the 2016 paper *“Ice melt, sea level rise and superstorms: evidence from paleoclimate data, climate modelling, and modern observations that 2°C global warming could be dangerous”*. This paper argues that non-linear processes will apply to polar ice sheet melting, as shown already by recent rapid increase in ice loss from Greenland and Antarctica (see Figure 30 in their paper). However, these non-linear trends in observations of decreasing ice loss are over a relatively short period of the last decade. Invariably, variability due to climate cycles such as ENSO and IPO and other polar-region climate cycles, are likely to substantially influence the trend over such short time periods.

Hansen et al. (2016) conclude that empirical and observational data are too brief to imply a characteristic time for ice sheet mass loss or to confirm their hypothesis that continued high fossil fuel emissions leading to CO<sub>2</sub> concentrations in the atmosphere of approximately 600–900 ppm will cause exponential ice mass loss equivalent of up to several metres of sea level. The empirical data

are consistent with a doubling time of the order of a decade, but slower responses cannot be excluded.

Sea level reached 6–9 m above present levels in the Eemian interglacial<sup>7</sup>, a time that Hansen et al. (2016) concluded was probably less than 1°C warmer than today on a global scale. For the present-day period, Hansen et al. (2016) observe accelerating mass losses from the Greenland and Antarctic ice sheets, and identified amplifying feedbacks that will increase the rates of change. The modelling (especially the effect of increasing freshwater in the oceans from meltwater), palaeoclimate evidence from past geological eras, and trends in ongoing observations together imply that 2°C global warming above the pre-industrial level is dangerous (Hansen et al., 2016). They conclude that continued high fossil fuel emissions this century are predicted to yield nonlinearly growing SLR, reaching several metres over a timescale of 50–150 years.

The Hansen et al. (2016) paper confirms the consensus that Antarctic and Greenland ice sheets are melting and causing oceans to rise and will be the dominant factor for sea level rise especially next century. But the critical question is around how fast? The spectre of a multi-metre SLR in the next 50–150 years is seen by many experts as being hypothetical and the study is seen as not detailed enough. The conclusion is not in line with other recent sea-level projections, with plausible rises that could reach up to 1.0–1.4 m by 2100 for an upper-range RCP 8.5 scenario that includes contributions from polar ice sheets (Kopp et al., 2014, Mengel et al., 2016, Golledge et al., 2015, DeConto and Pollard, 2016). On the other hand, Ritz et al. (2015) concluded a more constrained contribution would occur from West Antarctica by 2100, plus increasing efforts globally to reduce global emissions (e.g. the 2015 COP21 Paris Agreement) may mean a high-emissions baseline scenario RCP 8.5 is not maintained through more mitigation of greenhouse gases. In any case, SLR scenarios covering a range that is not implausible for different planning timeframes should be used in adaptive approaches to stress test climate-change and hazard reduction response options at the coast (see next section).

## 9 Impacts on biosecurity and pests

### 9.1 Terrestrial biosecurity

Climate change is widely regarded as one of the greatest challenges facing indigenous ecosystems in the coming century. As New Zealand (and much of the Bay of Plenty Region) has an economy based on very efficient primary production systems, the risk of exotic pests and diseases affecting the primary industries also needs to be minimised. Climate change will create new biosecurity challenges by allowing establishment of new exotic pest animals, weeds and diseases which are currently prevented by New Zealand's climate. The potential establishment of subtropical pests and current seasonal immigrants are of greatest concern, along with species that are already recognised as high risk (Kean et al., 2015). Tauranga is a point of entry for many high-profile pest species in New Zealand because it has the largest sea port.

Although climate change may affect organisms and ecosystems in a range of ways, the most important driver of pest invasion is likely to be temperature, modified by rainfall, humidity and carbon dioxide (Kean et al., 2015). In addition, changes in large-scale weather patterns will influence the frequency and intensity of extreme weather events (e.g. flooding, drought, damaging wind). Regional winds and currents may affect the ability of potential invaders to reach New Zealand and

---

<sup>7</sup> Warmest recent period prior to the Holocene (current interglacial) approximately 115,000–125,000 years ago before the last Ice Age



establish. The recent (2017) arrival of the fungal plant disease myrtle rust<sup>8</sup> (*Austropuccinia psidii*) in New Zealand is likely to have resulted from wind-blown spores from Australia. Myrtle rust (*Austropuccinia psidii*) is a fungus that has been recently (in 2017) found in northern New Zealand. It attacks plants belonging to the Myrtaceae family, including pohutukawa, manuka, rata, and feijoa. There is concern that myrtle rust may spread further in New Zealand as the climate warms and other fungi that are spread by wind may become established in the country in the future with changes to atmospheric circulation, temperature, wind patterns, and storminess.

Big headed (*Pheidole megacephala*) and Argentine (*Linepithema humile*) ants are some of the worst invasive pest species in the world, as they have the capacity to wreak havoc on the native arthropod fauna, and they are already present in New Zealand. Continued warming and drying eastern climates are likely to encourage their spread. Wasps are highly responsive to climate conditions; wet winters with flooding do not favour nest survival and can lower populations, while warm, dry conditions are ideal for explosive population growth (McGlone and Walker, 2011). Subtropical fruit flies are already considered major threats to the New Zealand horticulture industry. A modelling exercise done for 17 different fruit fly species (Figure 9-1) showed that the Bay of Plenty is one of the regions with the greatest potential for increase in fruit fly establishment (in terms of climate suitability) in the late 21<sup>st</sup> century (along with most of the rest of the North Island) (Kean et al., 2015).

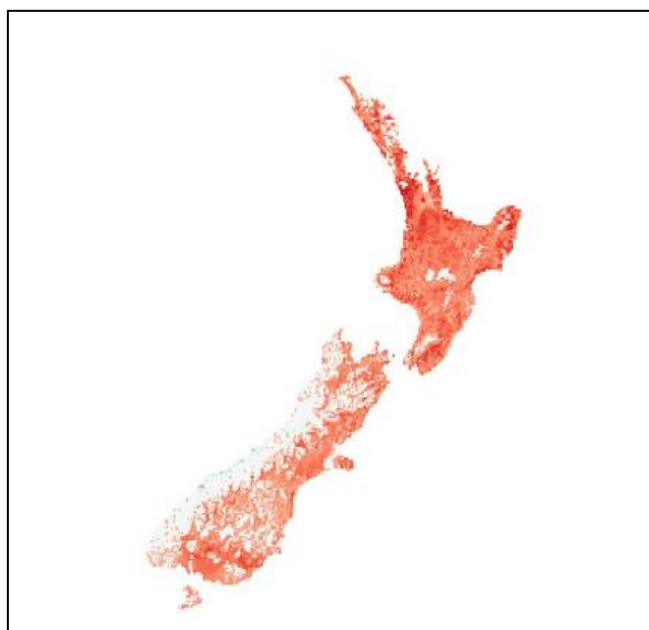


**Figure 9-1: Change in climate suitability from 2015 to 2090 for 17 different fruit fly species.** Darker shades of red indicate the greatest increase in the number of species that might establish. From Kean et al. (2015).

The arrival of new pest plants and the increased invasiveness of existing weeds is one of the most significant likely consequences of climate change. More plant species are present in warmer regions, so as frost declines in frequency, winters warm, and more insect pollinator species are able to survive in warmer temperatures, a much larger range of weed species will be able to compete with local species (McGlone and Walker, 2011). It is expected that farmers and growers in the Bay of Plenty will increase their usage and dependence on existing subtropical plant species and introduce new commercial species. This increased use of subtropical plants may make the Bay of Plenty more

<sup>8</sup> <http://www.mpi.govt.nz/protection-and-response/responding/alerts/myrtle-rust/>

susceptible to invasion by subtropical pests and diseases and new host-pest associations (Kean et al., 2015). Ornamental plants may escape cultivation when climatic constraints (such as frosts) are reduced and subsequently may naturalise and become invasive (Sheppard et al., 2016). Sheppard (2013) modelled the potential distribution of recently naturalised plant species in New Zealand with future climate change (*Archontophoenix cunninghamiana* (bangalow palm), *Psidium guajava* (common guava), and *Schefflera actinophylla* (Queensland umbrella tree)). All three species, which are currently only present in northern New Zealand (Northland and Auckland), have the potential to significantly increase their range further southward in the future, particularly into coastal areas around the country (including the Bay of Plenty).

The shift towards reliance on drought and heat tolerant plants (in particular, pasture grasses) may cause new pest species to spread and for new host/pest associations to develop (Kean et al., 2015). The 2014 emergence of two native moths (*Epyaxa rosearia* and *Scopula rubraria*) as major plantain (a variety of pasture grass) pests demonstrates how a large increase in usage elevated these previously harmless species to pest status. In addition, as kikuyu grass (*Cenchrus clandestinus*) is likely to become the most prevalent forage grass with increasing temperatures, pests that affect kikuyu grass are likely to be important. Some pest species from Australia (e.g. the *Sphenophorus venatus vestitus* weevil) has already been recorded on kikuyu in Northland and pests such as this are likely to spread further in New Zealand as the climate warms. However, the projected reduction in rainfall and humidity in some areas may actually reduce certain fungal disease pressures that require a wetter environment (Coakley et al., 1999).

It is important to note that although much of the biosecurity risk with climate change will come from beyond New Zealand's borders, many of the future's pest, disease and weed problems are currently dormant in New Zealand, awaiting some perturbation, such as climate change, to allow them to spread and flourish. These types of pests are often weeds but may also be invertebrates. A few examples of sleeper invertebrate pests that are affected by temperature include (after Kean et al. (2015)):

- Migratory locust *Locusta migratoria*, found in grassland from Christchurch northwards. Because existing temperatures are not usually high enough to trigger swarming behaviour, the insect currently is not regarded as a pest. However, the locusts have retained the capacity to swarm with a small swarm observed near Ahipara, Northland in the 1980s.
- Tropical armyworm *Spodoptera litura*. While this pest can be found through many lowland North Island districts, epidemic outbreak populations, when caterpillars move 'like an army' through crops and pastures, are rare. However, the combination of events that cause outbreaks will be more common under projected climate change scenarios and include above average summer and autumn temperatures, allowing for additional generations to develop.

The reader is directed to Kean et al. (2015) for more detailed information about the potential effects of climate change on current and potential terrestrial biosecurity pests and diseases in New Zealand.

## 9.2 Aquatic biosecurity

The primary source of entry for aquatic biosecurity risk organisms into New Zealand is and will continue to be through international shipping. These risk organisms are contained within ballast water or attached to the hulls of ships. However, changes in water temperature and ocean currents into the future, because of climate change, may result in species (including pests and pathogens) not usually seen in New Zealand waters to arrive and establish. Sea temperatures are projected to

increase around New Zealand, particularly to the west of the country, and seawater is likely to decrease in pH (i.e. become more acidic) (Law et al., 2018).

Long-term changes in marine environmental variables, such as seawater temperature, may lead to new ecological compatibilities and may alter existing host-pathogen interactions. It is commonly accepted that warmer sea and fresh water temperatures modify host-pathogen interactions by increasing host susceptibility to disease. Such changes could contribute to the emergence of aquatic diseases in new regions (Castinel et al., 2014). Of concern for the Bay of Plenty is a strengthening East Auckland Current off the east coast of the northern North Island. This strengthening current is expected to promote establishment of tropical or subtropical species that currently occur as vagrants in warm La Niña years (Willis et al., 2007). The establishment of these species may have negative impacts on wild fisheries and aquaculture operations.

In terms of freshwater biosecurity, increased water temperatures are likely to favour the expansion of warm water species such as koi carp, goldfish, tench, rudd, and catfish (Office of the Prime Minister's Chief Science Advisor, 2017). These fish can cause water quality degradation and reduced indigenous biodiversity. Increased water temperatures may also facilitate the establishment of tropical fish that are sold in the New Zealand aquarium trade and intentionally or accidentally released. Increasing water temperatures will also favour warm-climate invasive aquatic plant species such as water hyacinth (*Eichhornia crassipes*) and water fern (*Salvinia molesta*).

As is discussed in Section 9.1 for terrestrial biosecurity, aquatic organisms already established within the New Zealand region that are not currently pests may become problematic under changed environmental conditions with climate change – these are called “sleeper pests”.

## 10 Impacts of drought and future pasture growth

It is likely that much of the Bay of Plenty will experience more drought conditions in the future than at present, with larger potential evapotranspiration deficit accumulations and more days of soil moisture deficit (discussed in Section 4.9). Drought has significant impacts on primary industries in the Bay of Plenty.

For primary production, rainfall is one of the most important climate drivers, as there are limits (both too much and not enough water) where plants cease to grow or experience harm. When other climatic factors are not limiting, precipitation levels within these limits can have a direct and proportional relationship to productivity (Clark et al., 2012). Changes in rainfall patterns are important when considering future yield variability of crops and pasture grass. This is because crops respond to both amounts and timing of water supply in relation to demand.

Low rainfall (and therefore drought) can limit crop and grass growth in different ways. When water supply is less than demand, crop and grass yield is mainly reduced by limited canopy expansion and increased leaf aging, thereby decreasing sunlight interception, and reduced photosynthesis rates due to stomatal closure (Clark et al., 2012). In pasture grasses, legumes, and maize, reductions in plant growth are manifested by reduced leaf appearance and extension rates, as well as increased tiller (shoot) and plant mortality. The extent of reduction in growth depends on factors such as the severity and duration of the water deficit as well as the plant species, as some species are more sensitive to water deficits than others.

A plant's demand for water and its sensitivity to water stress varies throughout the plant's annual cycle. Therefore, timing of drought is critical: drought in late summer when plants have largely

completed growth does not have the devastating impact of late winter/early spring drought that prevents achievement of full productive potential (McGlone et al., 2010).

For fruit, rainfall can have positive or negative effects. Girona et al. (2006) found that for grapes, the best fruit-quality parameters were obtained when plants were well watered for the first part of the growing seasons, but then deficit irrigated until harvest to avoid excess vegetative growth. While rainfall in spring and early summer provides needed water and reduces irrigation costs, rainfall later in the season can reduce fruit (and therefore wine) quality. In other fruit crops, similar principles apply. Miller et al. (1998) found that the main effect of early-season water stress on kiwifruit was to reduce vine yields, so rainfall early in the season has demonstrable benefits. Deficit irrigation late in the season had little impact on yield, but did improve fruit quality.

Orwin et al. (2015) considered the impacts of drought on soil processes in four primary sector systems (annual cropping, intensive grazing, extensive grazing, and mature plantation forest). For the cropping industry, drought has a significant negative effect on aboveground crop biomass, leaching, and denitrification (loss of soil fertility). For intensive grazing, drought also has a negative effect on nitrogen fixation in addition to those effects stated for cropping. In extensive grazing systems, drought causes increased erosion.

Farmers may turn towards increased irrigation as a method for dealing with increased incidence of drought (Clark et al., 2012). However, this approach may not be suitable depending on the future changes to rainfall and availability of water for irrigation.

The effect of increased CO<sub>2</sub> levels on plants under limited water supply may help with the effects of drought. Under limited water supply conditions, the effect of CO<sub>2</sub> fertilisation is more evident. Higher CO<sub>2</sub> concentrations reduce the loss of water vapour through leaf transpiration and, therefore, improve the water use of crops (Leakey et al., 2009, Clark et al., 2012). The faster growth of plants due to CO<sub>2</sub> fertilisation may enable plants to avoid exposure to late-season droughts. However, extreme heat and severe drought (deficits of around two to three weeks in duration) override the effect of CO<sub>2</sub> fertilisation in pastures and crops (Clark et al., 2012).

Temperature will also influence the seasonality of pasture growth in the Bay of Plenty. Warmer winter and spring periods will allow for increased seasonal growth rates, however growth during summer may be suppressed due to temperatures being too hot and water availability being limited (Clark et al., 2012).

## 11 Impacts on horticulture

Climate change will likely impact the horticulture industry in the Bay of Plenty, particularly through changes to temperature and rainfall.

Tait et al. (2017) studied the potential impacts of climate change on the “Hayward” kiwifruit variety (*Actinidia chinensis* var. *deliciosa*). The Bay of Plenty region is New Zealand’s largest kiwifruit-producing region; over 90% of New Zealand’s kiwifruit is grown in the region (Cradock-Henry, 2017). It is recognised that climate change effects on winter temperature is an emerging risk to fruit crops, particularly those grown in warm regions, such as kiwifruit. Presently, the coastal Bay of Plenty area has an ideal temperature regime for growing kiwifruit, with good winter chilling, warm springs, and mild summers and autumns. This is combined with high sunshine hours and evenly distributed rainfall on deep free-draining volcanic soils.

Hayward kiwifruit is particularly dependent on temperatures during the May-July period. The ‘coldness’ of this period has a very strong influence on the quantity of flowers per winter bud as well as the number of flowers and the timing of flowering. ‘Winter chilling’ is the term used to refer to how effective the cold of winter has been. For instance, a year of high winter chilling will generally mean more kiwifruit flowers, an earlier flowering period, and often a more compacted flowering period.

Currently, kiwifruit productivity is artificially increased by the late winter application of a dormancy breaking chemical, hydrogen cyanamide (H<sub>2</sub>NC). Spraying this chemical on the vines gives an average of about 2°C of winter chilling benefit, thereby increasing the level of flower development in warmer years to the level of development seen in cooler years. However, H<sub>2</sub>NC use is becoming more restricted or banned in some parts of the world due to toxicity concerns.

As air temperatures in New Zealand continue to rise, the potential for years with marginal or poor winter chilling conditions steadily increases. This could make kiwifruit production marginal or unviable in parts of the Bay of Plenty, particularly if the use of H<sub>2</sub>NC is banned. Tait et al. (2017) created a web-based application which can be accessed at <https://well-shny-vp.shinyapps.io/CCII/>. Figure 11-1 shows a screen shot of the application. The application has a menu where the user can select with or without hydrogen cyanamide (HC), a particular RCP, a particular climate model, and either the Bay of Plenty region or the whole country. The slider can then be dragged to a specific year, or the ‘play’ button can be pressed to start a map animation sequence (and ‘paused’ to stop it). The resultant map shows the Hayward kiwifruit production viability map associated with the particular options selected.

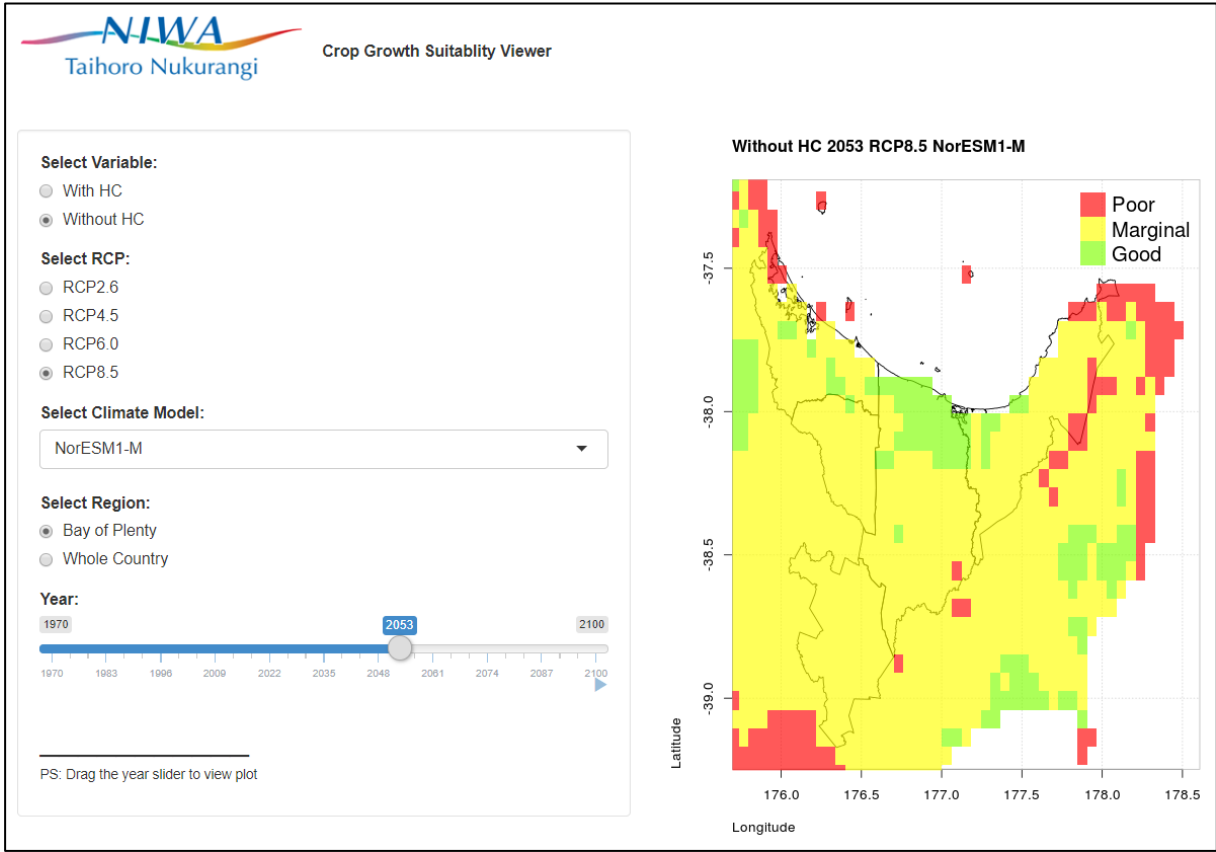


**Figure 11-1: Screenshot of Kiwifruit climate suitability web application.** Source: <https://well-shny-vp.shinyapps.io/CCII/>.

Increasing temperatures will impact all types of crops, as plant phenological development may occur at a faster rate. Different stages of plant growth (e.g. bud burst, flowering, and fruit development) may happen at different times, which may affect the harvested crop. For example, the hottest summer on record for New Zealand in 2017/18 saw wine grapes in multiple New Zealand regions ripen faster than usual (Salinger et al., 2019). In Central Otago, this resulted in the earliest start to harvest of Pinot Noir grapes on record (almost a month earlier than usual). In Wairarapa, the period from flowering to harvest for wine grapes was about 10 days shorter than usual<sup>9</sup>.

Extreme heat affects the rate of evapotranspiration, or the uptake of water by plants. Therefore, increases to extreme heat may affect water availability, as under hot conditions plants use more water than usual. Extreme heat may also result in current varieties of crops and pasture becoming unsustainable if they are not suited to growing in hot conditions.

Reductions in cold conditions may have positive impacts for diversification of new crop varieties that are not able to currently be grown in the Bay of Plenty Region. For example, certain crops (e.g. kumara) are currently grown in warmer parts of New Zealand such as Northland, and other crop species are currently not grown in New Zealand at all. However, in the future with a warmer climate there may be opportunities for growers in the Bay of Plenty to take advantage of the overall warmer climate to diversify their crops.

However, future warmer temperatures may create issues for horticulture in the Bay of Plenty. Increasing risk from pests (plants and animals) and diseases is a concern. Currently, many pests are limited by cold conditions, so that they cannot survive low winter temperatures, and therefore their spread is limited (Kean et al., 2015). Under a warmer climate, these pests may not be limited by cold conditions and therefore cause a larger problem for farmers and growers in the Bay of Plenty. See Section 9.1 for more information about terrestrial pests.

Increases in extreme rainfall event magnitudes may impact horticulture in several different ways. Slips on hill country land may become more prevalent during these events, and soil erosion may also be exacerbated by increasing drought conditions (Basher et al., 2012). This has impacts on the quality of soil for horticulture, the area of land available for production, and other impacts such as sedimentation of waterways (which can impact flooding and water quality). Slips may also impact transport infrastructure (e.g. roads, farm tracks) which may in turn affect connectivity of farms and orchards to markets.

High rainfall will impact soil moisture, and saturated soils may be detrimental for horticulture. Wet soils may cause issues for vegetable growers in particular, as crops may get washed away or the lack of oxygen around the plants reduces their growth rate. Heavy rain at harvest times for fruit may cause a decline in fruit quality, with skins splitting and increased prevalence of diseases.

Increased prevalence of drought and longer dry spells in the Bay of Plenty will likely have impacts on water availability for irrigation and other horticultural uses. Low river flows are likely to decline in the Bay of Plenty, with reduced flow reliability (the time period where river water abstraction is unconstrained) (Collins and Zammit, 2016). In addition, soils are generally projected to be drier in the low elevations of the Bay of Plenty, which may further impact plant growth and increase the need for irrigation.

---

<sup>9</sup> <https://michaelcooper.co.nz/2018-regional-vintage-overview-report/>

## 12 Impacts on forestry

Climate change will have varying impacts on the forestry sector. Growth rates will likely be enhanced through CO<sub>2</sub> fertilisation, particularly of *Pinus radiata*. However, the forestry industry is susceptible to indirect impacts of climate change, related to fire, extreme rainfall, and pests. Watt et al. (2018) provides a synthesis of potential climate change impacts on the plantation forestry sector in New Zealand.

Increases to temperature and changing rainfall patterns which might negatively influence *P. radiata* productivity, but the effect of increased CO<sub>2</sub> fertilisation is modelled to outweigh these negative impacts, significantly increasing *P. radiata* productivity by 2040 and 2090 of 19% and 37%, respectively. However, the extra growth caused by CO<sub>2</sub> fertilisation may make trees more susceptible to wind damage.

Fire risk is projected to increase in the future in New Zealand, due to the following conditions (Pearce et al., 2011):

- Warmer temperatures, stronger winds, lower rainfall and more drought for some areas will exacerbate fire risk (note that winds are generally projected to decline in Bay of Plenty);
- The fire season will probably be longer through starting earlier and finishing later;
- More thunderstorms and lightning will increase ignitions;
- Fuel will be easier to ignite (because of drying); and
- Drier (and possibly windier periods) conditions will result in faster fire spread and greater areas burned.

The following projections for fire risk are based on the IPCC Fourth Assessment Report (Pearce et al., 2011). For Seasonal Severity Rating (SSR)<sup>10</sup>, the 17-model average projection shows a 10-20% increase for the Bay of Plenty by the 2050s (2040-2059) compared to the 1980-1999 historical period. Similar patterns were observed for the 2080s (2070-2089), with the 17-model average projection showing a 10-30% increase in SSR for the Bay of Plenty compared with the historical period. The average SSR over fire season months (October-April) for Tauranga is projected to increase from 1.72 over the historical period to 2.03 in the 2050s and 2.05 in the 2080s.

The number of days of Very High and Extreme (VH+E) forest fire danger is projected to increase by 50-100% for the central part of the Bay of Plenty, for the 2050s and the 2080s compared to 1980-1999. The historical number of VH+E forest fire danger days for Tauranga is 7.7 days, and this is projected to increase to 10.1 days in the 2050s and 10.2 days in the 2080s.

Note that some individual models project a higher increase in Very High and Extreme forest fire danger days, as noted by Reisinger et al. (2014). The reader is directed to Pearce et al. (2011) for more information on the projections of Seasonal Severity Rating and Very High and Extreme forest fire danger days in New Zealand.

Pest species are likely to shift to new habitat areas due to climate change (Section 9.1). Existing tree pathogens causing dothistroma needle blight and cyclaneusma needle cast are likely to decline in

---

<sup>10</sup> Seasonal Severity Rating (SSR) is a seasonal average of the Daily Severity Rating (DSR), which captures the effects of both wind and fuel dryness on potential fire intensity, and therefore control difficulty and the amount of work required to suppress a fire. It allows for comparison of the severity of fire weather from one year to another. Source: [http://www.nrfa.org.nz/OperationalFireManagement/ResourceLibraries/AlertsAndNotices/Documents/Seasonal%20Fire%20Danger%20Outlook\\_North%20Island.pdf](http://www.nrfa.org.nz/OperationalFireManagement/ResourceLibraries/AlertsAndNotices/Documents/Seasonal%20Fire%20Danger%20Outlook_North%20Island.pdf)

severity throughout the 21<sup>st</sup> century in North Island plantations (Watt et al., 2018). However, increasing average temperatures and changing rainfall patterns across the country may make conditions more suitable for climate-limited tree pathogens such as pitch canker (currently present in northern coastal areas). Insect pests may become more of an issue for forestry plantations with climate change, as the major limiting factor for most insect pests is cold stress. Therefore, subtropical insect pests may be able to establish in a warmer New Zealand in the future, and existing insect pests may increase their distribution within New Zealand. Climate change may also affect the severity of damage from existing insect pests because warmer temperatures can be expected to accelerate insect development and therefore lead to an increase in population levels, especially in species that can complete more than one generation per year (e.g. the Monterey pine aphid *Essigella californica*).

Increasing competition with weeds is also a concern for the forestry industry. New Zealand's future climate may become more suitable for some weeds which are already established in some parts of New Zealand but have not spread, so-called "sleeper weeds". An example of this is *Melaleuca quinquenervia*, an exotic tree that is currently established in Auckland and Northland. If the species' thermal requirement for reproduction is reached with a warming climate, this could become quite invasive and difficult to control. Also, woody tree species that are native to Australia (e.g. *Acacia* spp.) have very high growth rates and vigorously compete with *P. radiata* seedlings. As tree species, they can compete further into the plantation rotation than other weed species which are predominantly shrubs.

## 13 Impacts on health

Most of the information in this section is summarised from Royal Society of New Zealand (2017) – a report titled *Human health impacts of climate change for New Zealand*.

Around the world, climate change has already contributed to increased levels of ill health, particularly in connection with summer heatwaves. Approximately 250,000 additional deaths per year globally are forecast by 2030 as a result of heat exposure, diarrhoeal disease, malaria and childhood undernutrition alone. A further 500,000 climate-related deaths per year are forecast worldwide by 2050 due to reductions in global food availability (particularly fruit and vegetable consumption).

Climate change affects human health in a number of ways. The ideal healthy human has complete physical, mental and social wellbeing, and not merely the absence of disease or infirmity. Changes to the climate can impact on these:

- Directly via air and sea temperature, flooding or storms;
- Indirectly due to changes to the environment and ecosystems; and
- Indirectly due to social and economic changes, such as migration stresses, health inequality and socioeconomic deprivation.

In New Zealand, children, the elderly, people with disabilities and chronic disease, and low-income groups are particularly vulnerable to climate change-related health impacts. Maori are also particularly vulnerable due to existing health inequalities, having an economic base invested in primary industries, housing and economic inequalities, and a greater likelihood of having low-income housing in areas vulnerable to flooding and sea-level rise.



## 13.1 Direct health impacts

### Increased flooding, fires and infrastructure damage

Increased frequency and magnitude of fires, floods, storm tides and extreme rainfall events will affect public health directly through injury (e.g. being burnt by fire or swept away by floods or landslides). These extreme events may also have negative effects on wellbeing through disease outbreaks, toxic contamination, effects of damp buildings, mental health issues, disruption to healthcare access and damage to homes (lasting from weeks to months after the initial event).

### Displacement

Sea-level rise and coastal erosion, as well as river flooding, may require people to leave their homes. This can cause uncertainty and lead to mental health issues from the trauma of leaving familiar surroundings, the breaking of social ties, and the difficulty of resettlement.

### Extreme heat

Hot days have well-established negative impacts on the levels of illness and death, and diabetes and cardiovascular disease increase sensitivity to heat stress. Heat stress is particularly significant when hot spells occur at the beginning of the hot season, before people have become acclimatised to hotter weather. The increasing numbers of hot days, extreme hot days and heatwave days in the Bay of Plenty (Section 3) will likely cause detrimental impacts on health.

Heat also poses health risks for people who work outdoors, including heat stroke and renal (kidney) impairment. Increased heat is also associated with increased incidences of aggressive behaviour, violence, and suicide. Individuals with mental health conditions are especially vulnerable to high temperatures or heat waves, primarily due to not drinking enough fluids, getting access to cool places, or recognising symptoms of heat exposure.

## 13.2 Indirect health impacts

### Harmful algal blooms

Increasing temperatures will increase the likelihood of blooms of harmful algae, including blue-green algae (cyanobacteria). These algae produce toxins that can, by either contact or ingestion, cause liver damage, skin disorders, and gastrointestinal, respiratory and neurological symptoms. These blooms can be widespread and long-lasting and can have impacts on commercial seafood harvesting and people reliant on non-commercial harvesting (particularly Maori and Pasifika people), as well as drinking water supplies and recreational water use.

### Microbial contamination

Changing weather patterns, including more extreme rainfall events, flooding, and higher temperatures, are likely to interact with agricultural runoff, and affect the incidence of diseases transmitted through infectious drinking and recreational water. Conditions may also be more suitable for bacterial growth – extreme rainfall may be a key climatic factor influencing the incidence of waterborne diseases like *Norovirus*. *Vibrio* marine bacteria are highly responsive to rising sea temperatures, and may cause infected wounds, diarrhoea and septicæmia.

### Food availability, quality and safety

Climate change-induced changes to weather patterns and sea-level rise have direct effects on food production, which can affect food affordability and availability, locally and globally. Changes in air

and water temperatures, rainfall patterns and extreme events can also shift the seasonal and geographic occurrence of bacteria, viruses, parasites, fungi and other pests and chemical contaminants. This can lead to reduced food safety prior to, during and after harvest, and during transport, storage, preparation and consumption. For example, higher temperatures can increase the number of microorganisms already present on fruit and vegetables, and flooding is a factor in the contamination of irrigation water and farm produce and the *E. coli* contamination of shellfish.

### **Mental health and wellbeing**

Increased temperatures, extreme weather events, and displacement of people from homes and communities will have significant mental health and wellbeing consequences. These range from minimal stress and distress symptoms to clinical disorders such as anxiety, depression, post-traumatic stress and suicidal thoughts. For New Zealanders, the natural environment is at the heart of the nation's identity. Disruption of bonds with the natural environment (e.g. through relocation of communities) can cause grief, loss and anxiety.

### **Outdoor air quality**

Changes in temperature, rainfall, and air stagnation<sup>11</sup> can affect air pollution levels and human health. Chronic health conditions such as asthma and chronic obstructive pulmonary disease are particularly affected by outdoor air quality. Climate change is expected to increase the risk of fire, which may cause more particulate emissions (PM10 and PM2.5) as well as ozone. Particulate matter smaller than 2.5 µm in diameter (PM2.5) is associated with serious chronic and acute health effects, including lung cancer, chronic obstructive pulmonary disease, cardiovascular disease, and asthma development and exacerbation. The amount of soil-derived PM10 dust in the air may also increase in areas more frequently affected by drought. Due to extended growing seasons with climate change (due to higher CO2 and higher temperatures), allergenic pollen may become more abundant in the atmosphere (seasonally, spatially and at higher volumes).

### **Carriers of new diseases**

There are a number of organisms, including mosquitoes, ticks, and fleas that can transmit infectious diseases between humans or from animals to humans. The seasonality, distribution and common occurrence of diseases spread by these carriers are largely influenced by climatic factors, particularly high and low temperature extremes and rainfall patterns. Therefore, climate change may create favourable conditions and increase the risk of infectious disease transmission in some areas. Increased temperature, in particular, heightens the risk for mosquito-borne diseases which are currently absent from New Zealand because the mosquitoes that carry these diseases (*Aedes aegypti* and *Aedes albopictus*) are not established in our current climate (it is too cold) (Derraik and Slaney, 2015). These diseases include West Nile virus, dengue fever, Murray Valley encephalitis, Japanese encephalitis, Ross River virus, and Barmah Forest virus (most of these are present in Australia). Mosquito-borne diseases like Zika and chikungunya that are already present in the Pacific Islands could become more of a risk for New Zealand if climate change allows important disease-transmitting mosquitoes to become established here. Disease-carrying mosquitoes are often intercepted in New Zealand, particularly at sea ports – this is a particular concern for Tauranga going forward.

---

<sup>11</sup> Air stagnation occurs when an air mass remains over an area for an extended period. Due to light winds and lack of precipitation, pollutants cannot be cleared from the air, either gaseous (like ozone) or particulate (like soot and dust).

## 14 Summary and conclusions

This report presents climate change projections for the Bay of Plenty region. Historic climatic conditions are presented to provide a context for future changes. The future changes discussed in this report consider differences between the historical period 1986-2005 and two future time-slices, 2031-2050, “2040”, and 2081-2100, “2090”. Note, the modelled differences between two time periods should not be attributed solely to climate change, as natural climate variability is also present and may add to or subtract from the climate change effect. The effect of natural variability has been reduced by averaging results from six GCM simulations, but it will still be present.

It is internationally accepted that further climate changes will result from increasing amounts of anthropogenically produced greenhouse gases in the atmosphere. The influence from anthropogenic greenhouse gas contributions to the global atmosphere is the dominant driver of climate change conditions, and it will continue to become more dominant if there is no slowdown in emissions, according to the IPCC. In addition, the climate will vary from year to year and decade to decade owing to natural variability.

Notably, future climate changes depend on the pathway taken by the global community (i.e. through mitigation of greenhouse gas emissions or a ‘business as usual’ approach). The global climate system will respond differently to future pathways of greenhouse gas concentrations. The representative concentration pathway approach taken here reflects this variability through the consideration of multiple scenarios (i.e. RCP4.5, the mid-range scenario, and RCP8.5, the business-as-usual scenario). The six climate models used to project New Zealand’s future climate were chosen by NIWA because they produced the most accurate results when compared to historical climate and circulation patterns in the New Zealand and southwest Pacific region. They were as varied as possible to span the likely range of model sensitivity. The average of outputs from all six models (known as the ‘ensemble average’), is presented in the climate change projection maps in this report. The ensemble-average was presented as this usually performs better in climate simulations than any individual model (the errors in different models are compensated).

Changes to Bay of Plenty’s future climate are likely to be significant. An increase in extreme hot days, a reduction in frost days and larger extreme rainfall events are some of the main impacts. The following list summarises the projections of different climate variables in Bay of Plenty:

- The projected Bay of Plenty temperature changes increase with time and emission scenario. Future annual average warming spans a wide range: 0.5-1.0°C by 2040, and 1.0-3.5°C by 2090. Diurnal temperature range (i.e., difference between minimum and maximum temperature of a given day) is expected to increase with time and emission scenarios.
- The area closest to East Cape warms the least (e.g. annual warming of 1.5-2.0°C compared with 2.5-3.5°C for most of the region under RCP8.5 by 2090). This is an area with complex topography close to the coastline with changes modulated by maritime influences. As such, the magnitude of temperature and precipitation changes are more uncertain.
- Changes in extreme temperatures reflect the changes in the average annual signal. The average number of hot days and extreme hot days is expected to increase with time and scenario, with the largest increases in the central part of the region and the least in the eastern hill country. For example, the area between Maketu, Whakatāne, and Murupara may observe 20-25 more hot days per year by 2040 (both scenarios) and 70-80 more hot days per year by 2090 (RCP8.5). Extreme hot days for this area may increase by 1-2 days per year by

2040 (both scenarios), and 10-14 more days per year by 2090 (RCP8.5). This area is also expected to observe the largest increase in heatwave days – 70-80 more heatwave days by 2090 under RCP8.5.

- As expected, the number of frost days is expected to decrease throughout the region. The largest decreases are expected in inland areas; 6-10 fewer frost days per year by 2040 (both scenarios), and 15-25 fewer frost days per year by 2090 (RCP8.5). The number of growing degree days is expected to increase across the region, with the largest increases for the coastal western Bay of Plenty.
- Projected changes in rainfall show variability across the Bay of Plenty region. By 2040 under both scenarios, annual rainfall is not expected to change much, but the seasonality of rainfall is expected to change with spring and summer generally becoming drier (up to 8-15%) and winter and autumn becoming wetter (up to 10-15%) than the historic period. By 2090, annual rainfall totals are projected to decline under both scenarios. Similar to 2040, summer and spring rainfall is projected to decline, and winter and autumn rainfall is projected to increase. However, these patterns of change are not uniform across the region. The numbers of wet days (i.e., days where the total precipitation is more than 1 mm) generally declines across the region under both scenarios at both 2040 and 2090 for spring, summer, and autumn, and increases in winter.
- The number of heavy rain days (i.e., days where the total precipitation exceeds 25 mm) is projected to see little change for most of the Bay of Plenty region by 2040. By 2090, reductions in heavy rain days are projected for the Raukumara Ranges in particular, with small reductions across most of the region.
- The annual 99<sup>th</sup> percentile of daily rainfall (approximately the wettest day of the year) is generally projected to increase, with larger increases by 2090 under RCP8.5 (10-15% increase for central areas). In general, the maximum 1-day rainfall and maximum 5-day rainfall are projected to increase with time and increasing greenhouse gas concentrations.
- Extreme, rare rainfall events are projected to become more severe in the future. Short duration rainfall events have the largest relative increases compared with longer duration rainfall events. The depth currently projected for a 1-in-100-year rainfall event (e.g. 248 mm in Tauranga) is projected to become a 1-in-34-year event by 2090 under RCP8.5, i.e. a rainfall event of this magnitude may occur three times as often under this scenario.
- By mid-century the number of dry days per year (i.e., number of days with < 1 mm of precipitation) is expected to decrease near the coast and increase further inland. This pattern is amplified by the end of the century.
- Drought potential is projected to increase across the Bay of Plenty, with increasing accumulated Potential Evapotranspiration Deficit totals with time and increasing greenhouse gas concentrations. The coastal areas around Tauranga and Te Puke are expected to observe the largest increases in PED, and the hill country areas of the Urewera and Raukumara Ranges the smallest increases in PED. The number of days of soil moisture deficit is projected to generally reduce near the coast and increase further inland.
- Annual mean wind speed is projected to slightly decrease in the Bay of Plenty, but there is a mixed direction of change for different seasons. Generally, summer is projected to observe

reductions in wind speed through time under both scenarios. By 2090 under RCP8.5, summer is projected to experience 4-8% lower mean wind speeds and winter is projected to experience increases of 4-6% in mean wind speed for Rotorua Lakes. Small reductions in the number of windy days per year are projected for most of the region.

- The future magnitude of the 99<sup>th</sup> percentile daily mean wind speed is projected to decrease in all parts of the Bay of Plenty region, under both time periods and scenarios. The magnitude of change is generally amplified with time and RCP.
- Surface solar radiation is projected to decline for low elevation areas and increase for high elevation areas, albeit by small amounts. Spring is projected to observe the largest increases in surface solar radiation. Relative humidity is generally projected to decline in the future in the Bay of Plenty.
- There is good evidence that storms originating from the sub-tropics in the summer that impact on the Bay of Plenty have more intense circulation that is likely to lead to stronger winds, greater storm surge and higher rainfall accumulations. Evidence for such changes in other seasons is less clear. However, there is also good evidence that heavy rainfall intensity associated with storms increases in all seasons with global warming, particularly in winter, likely associated with the increased moisture carrying capacity of a warmer atmosphere.

A changing climate will have impacts on different sectors and environments in the Bay of Plenty.

- Sea-level rise information from Ministry for the Environment (2017) is presented above, as well as sea-level rise projections for the Bay of Plenty, which is rising slightly faster than the New Zealand average. The NZSeaRise project is in the process of developing regional sea-level rise projections for New Zealand that will account for land deformation. Overall, the Bay of Plenty coastline has moderate-high sensitivity to erosion and inundation.
- Increasing temperatures are likely to result in higher biosecurity risks in the Bay of Plenty, through pest incursions (both animal and plant pests). This is because pests that cannot survive in the region over winter currently (because it is too cold) may be able to survive year-round in the future. This may have implications for the primary sector and the natural environment.
- It is likely that the region will experience more drought conditions in the future, with implications for pasture growth and crops. Increased CO<sub>2</sub> in the atmosphere will act as a fertiliser for plants which may enable faster growth. However, if water availability is limited then this may override the effect of CO<sub>2</sub> fertilisation. Low river flows are likely to decline in the Bay of Plenty, with reduced flow reliability – this may affect water available for irrigation and other uses.
- Presently, the coastal Bay of Plenty has an ideal temperature regime for growing kiwifruit, with good winter chilling, warm springs, and mild summers and autumns. Hayward kiwifruit is particularly dependent on winter chilling to influence the quantity of flowers and the timing of flowering. As air temperatures in the region continue to rise, the potential for years with marginal or poor winter chilling conditions steadily increases. This could make kiwifruit production marginal or unviable in parts of the Bay of Plenty (this is assuming no use of chemical agents to break dormancy).

- There may be opportunities for diversification of crop type in the Bay of Plenty, where new varieties that are unviable in the current climate may be able to be grown in the region in the future.
- Exotic forestry (*Pinus radiata*) is projected to increase in productivity in the future due to increasing temperatures and increased CO<sub>2</sub>. However, increased fire risk may cause issues in the forestry industry.
- Human health is likely to be impacted by a changing climate, through both direct and indirect impacts. Direct impacts include injury from floods, extreme heat, and storms, and indirect effects include microbial contamination, mosquito-borne diseases, algal blooms, mental health, and air quality.

## 15 Glossary of abbreviations and terms

Term	Definition
Anthropogenic	Human-induced; man-made. Resulting from or produced by human activities.
Bias correction	Procedures designed to remove systematic climate model errors.
Clausius-Clapyeron relationship	The thermodynamic relationship between small changes in temperature and vapour pressure in an equilibrium system with condensed phases present. For trace gases such as water vapour, this relation gives the increase in equilibrium (or saturation) water vapour pressure per unit change in air temperature.
Climate model	A numerical representation of the climate system based on the physical, chemical and biological properties of its components, their interactions and feedback processes, and accounting for some of its known properties. The climate system can be represented by models of varying complexity, that is, for any one component or combination of components a spectrum or hierarchy of models can be identified, differing in such aspects as the number of spatial dimensions, the extent to which physical, chemical or biological processes are explicitly represented or the level at which empirical parametrizations are involved. Coupled Atmosphere–Ocean General Circulation Models (AOGCMs) provide a representation of the climate system that is near or at the most comprehensive end of the spectrum currently available. There is an evolution towards more complex models with interactive chemistry and biology. Climate models are applied as a research tool to study and simulate the climate, and for operational purposes, including monthly, seasonal and inter-annual climate predictions.
Downscaling	Deriving local climate information (at the 5-kilometre grid-scale in this report) from larger-scale model or observational data. Two main methods exist – statistical and dynamical. Statistical methods develop statistical relationships between large-scale atmospheric variables (e.g., circulation and moisture variations) and local climate variables (e.g., rainfall variations). Dynamical methods use the output of a regional climate/weather model driven by a larger-scale global model.
Emission scenario	A plausible representation of the future development of emissions of substances that act as radiative forcing factors (e.g., greenhouse gases, aerosols) based on a coherent and internally consistent set of assumptions about driving forces (such as demographic and socioeconomic development, technological change) and their key relationships.
Ensemble	A collection of model simulations characterizing a climate prediction or projection. Differences in initial conditions and model formulation result in different evolutions of the modelled system and may give information on uncertainty associated with model error and error in initial conditions in the case of climate forecasts and on uncertainty associated with model error and with internally generated climate variability in the case of climate projections.
Greenhouse gas	Greenhouse gases are those gaseous constituents of the atmosphere, both natural and anthropogenic, that absorb and emit radiation at specific wavelengths within the spectrum of terrestrial radiation emitted by the Earth’s surface, the atmosphere itself, and by clouds. This property causes the greenhouse effect. Water vapour (H <sub>2</sub> O), carbon dioxide (CO <sub>2</sub> ), nitrous oxide (N <sub>2</sub> O), methane (CH <sub>4</sub> ) and ozone (O <sub>3</sub> ) are the primary greenhouse gases

	in the Earth's atmosphere. Moreover, there are many entirely human-made greenhouse gases in the atmosphere, such as the halocarbons and other chlorine- and bromine-containing substances, dealt with under the Montreal Protocol. Beside CO <sub>2</sub> , N <sub>2</sub> O and CH <sub>4</sub> , the Kyoto Protocol deals with the greenhouse gases sulphur hexafluoride (SF <sub>6</sub> ), hydrofluorocarbons (HFCs) and perfluorocarbons (PFCs).
Heatwave days	A period of three or more consecutive days where the maximum daily temperature (T <sub>max</sub> ) exceeds a given threshold, either 25°C or 30°C.
High Intensity Rainfall Design System (HIRDS)	High Intensity Rainfall Design System ( <a href="http://hirds.niwa.co.nz">http://hirds.niwa.co.nz</a> ). HIRDS uses a regionalized index-frequency method to predict rainfall intensities at ungauged locations and returns depth-duration-frequency tables for rainfall at any location in New Zealand. Temperature increases can be inserted and corresponding increases in rainfall for each duration and frequency are calculated
Mitigation	A human intervention to reduce the sources or enhance the sinks of greenhouse gases.
Paris climate change agreement	The Paris Agreement aims to respond to the global climate change threat by keeping a global temperature rise this century well below 2°C above pre-industrial levels and to pursue efforts to limit the temperature increase even further to 1.5°C.
Potential evapotranspiration deficit	PED can be thought of as the amount of water needed to be added as irrigation, or replenished by rainfall, to keep pastures growing at levels that are not constrained by a shortage of water. The unit of PED is millimetres.
Projections	A numerical simulation (representation) of future conditions. Differs from a forecast; whereas a forecast aims to predict the exact time-dependent conditions in the immediate future, such as a weather forecast a future cast aims to simulate a time-series of conditions that would be typical of the future (from which statistical properties can be calculated) but does not predict future individual events.
Radiative forcing	A measure of the energy absorbed and retained in the lower atmosphere. More technically, radiative forcing is the change in the net (downward minus upward) irradiance (expressed in W/m <sup>2</sup> , and including both short-wave energy from the sun, and long-wave energy from greenhouse gases) at the tropopause, due to a change in an external driver of climate change, such as, for example, a change in the concentration of carbon dioxide or the output of the sun
Regional climate model	A numerical climate prediction model run over a limited geographic domain (here around New Zealand), and driven along its lateral atmospheric boundary and oceanic boundary with conditions simulated by a global climate model (GCM). The RCM thus downscales the coarse resolution GCM, accounting for higher resolution topographical data, land-sea contrasts, and surface characteristics. RCMs can cater for relatively small-scale features such as New Zealand's Southern Alps
Representative Concentration Pathway	They describe four possible climate futures, all of which are considered possible depending on how much greenhouse gases are emitted in the years to come. The four RCPs, RCP2.6, RCP4.5, RCP6, and RCP8.5, are named after a possible range of radiative forcing values in the year 2100 relative to pre-industrial values (+2.6, +4.5, +6.0, and +8.5 W/m <sup>2</sup> , respectively)
Sea-level rise	Sea level can change, both globally and locally due to (1) changes in the shape of the ocean basins, (2) a change in ocean volume as a result of a



	change in the mass of water in the ocean, and (3) changes in ocean volume as a result of changes in ocean water density.
Storm tide	Storm tide refers to the total observed sea level during a storm, which is the combination of storm surge (caused by low atmospheric pressure and by high winds pushing water onshore) and normal high tide
Uncertainty	A state of incomplete knowledge that can result from a lack of information or from disagreement about what is known or even knowable. It may have many types of sources, from imprecision in the data to ambiguously defined concepts or terminology, or uncertain projections of human behaviour. Uncertainty can therefore be represented by quantitative measures (e.g., a probability density function) or by qualitative statements (e.g., reflecting the judgment of a team of experts).
Virtual climate station network (VCSN)	Made up of observational datasets of a range of climate variables: maximum and minimum temperature, rainfall, relative humidity, solar radiation, and wind. Daily data are interpolated onto a 0.05° longitude by 0.05° latitude grid (approximately 4 kilometres longitude by 5 kilometres latitude), covering all New Zealand (11,491 points). Primary reference to the spline interpolation methodology is Tait et al (2006).

## Appendix A Climate modelling methodology

### Key messages

- Climate model simulation data from the IPCC Fifth Assessment has been used to produce climate projections for New Zealand.
- Six climate models were chosen by NIWA for dynamical downscaling. These models were chosen because they produced the most accurate results when compared to historical climate and circulation patterns in the New Zealand and southwest Pacific region.
- Downscaled climate change projections are at a 5 km x 5 km resolution over New Zealand.
- Climate projection and historic baseline maps and tables present the average of the six downscaled models.
- Climate projections are presented as a 20-year average for two future periods: 2031-2050 (termed '2040') and 2081-2100 (termed '2090'). All maps show changes relative to the baseline climate of 1986-2005 (termed '1995').

NIWA has used climate model simulation data from the IPCC Fifth Assessment to update climate change scenarios for New Zealand through both regional climate model (dynamical) and statistical downscaling processes. The downscaling processes are described in detail in a climate guidance manual prepared for the Ministry for the Environment (2018), but a short explanation is provided below. Dynamical downscaling results are presented for all variables in this report.

Global climate models (GCMs) are used to make future climate change projections for each future scenario, and results from these models are available through the Fifth Coupled Model Inter-comparison Project (CMIP5) archive (Taylor et al., 2012). Six GCMs were selected by NIWA for dynamical downscaling, and the sea surface temperatures (SSTs) from these six CMIP5 models used to drive an atmospheric global model, which in turn drives a higher resolution regional climate model (RCM) nested over New Zealand. These CMIP5 models were chosen because they produced the most accurate results when compared to historical climate and circulation patterns in the New Zealand and southwest Pacific region. In addition, they were chosen because they were as varied as possible in the parent global model to span the likely range of model sensitivity. For climate simulations, dynamical downscaling utilises a high-resolution climate model to obtain finer scale detail over a limited area based on a coarser global model simulation.

The six GCMs chosen for dynamical downscaling were BCC-CSM1.1, CESM1-CAM5, GFDL-CM3, GISS-E2-R, HadGEM2-ES and NorESM1-M. The NIWA downscaling (GCM then RCM) produced simulations that contained hourly precipitation results from 1970 through to 2100. The native resolution of the regional climate model is 27 km and there are known biases in the precipitation fields derived from this model. The daily precipitation projections, as well as daily maximum and minimum temperatures, have been bias-corrected so that their statistical distributions from the RCM matches those from the Virtual Climate Station Network (VCSN) when the RCM is driven by the observed sequence of weather patterns across New Zealand (known as 're-analysis' data). When the RCM is driven from the free-running GCM, forced only by CMIP5 SSTs, there can be an additional bias in the distribution of weather patterns affecting New Zealand, and the RCM output data for the historical climate will therefore not match the observed distributions exactly.

The RCM output is then downscaled statistically (by interpolation from the model 27 km grid) to a ~5 km x ~5 km resolution with a daily time-step. The ~5 km grid corresponds to the VCSN grid<sup>12</sup>. Figure 15-1 shows a schematic for the dynamical downscaling method used in this report.

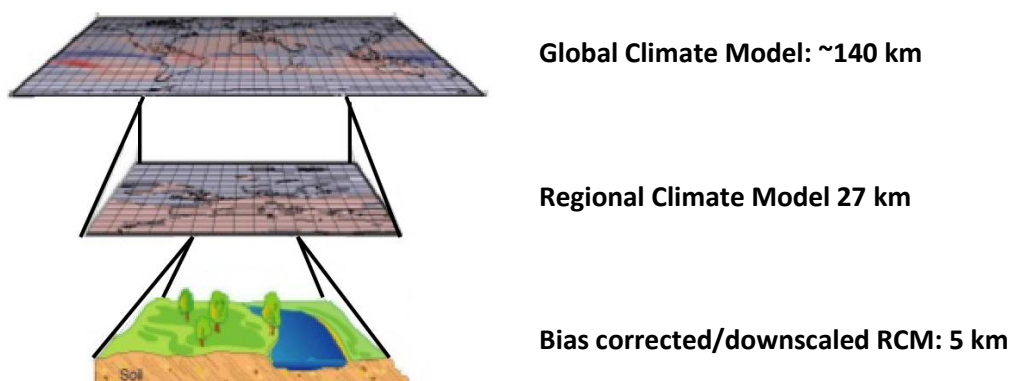


**Figure 15-1: Schematic showing dynamical downscaling method used in this report.**

The climate change projections from each of the six dynamical models are averaged together, creating what is called an ensemble-average. The ensemble-average is mapped in this report, because the models were chosen to cover a wide range of potential future climate conditions. The ensemble-average was presented as this usually performs better in climate simulations than any individual model (the errors in different models are compensated).

Climate projections are presented as a 20-year average for two future periods: 2031-2050 (termed '2040') and 2081-2100 (termed '2090'). All maps show changes relative to the baseline climate of 1986-2005 (termed '1995'), as used by IPCC. Hence the projected changes by 2040 and 2090 should be thought of as 45-year and 95-year projected trends. Note that the projected changes use 20-year averages, which will not entirely remove effects of natural variability. The baseline maps (1986-2005) show modelled historic climate conditions from the same six models as the future climate change projection maps.

---

<sup>12</sup> Virtual Climate Station Network, a set of New Zealand climate data based on a 5 km by 5 km grid across the country. Data have been interpolated from 'real' climate station records (TAIT, A., HENDERSON, R., TURNER, R. & ZHENG, X. G. 2006. Thin plate smoothing spline interpolation of daily rainfall for New Zealand using a climatological rainfall surface. *International Journal of Climatology*, 26, 2097-2115.)

## 16 References

- ACKERLEY, D., BELL, R. G., MULLAN, A. B. & MCMILLAN, H. 2013. Estimation of regional departures from global-average sea-level rise around New Zealand from AOGCM simulations. *Weather and Climate*, 33, 2-22.
- BASHER, L., ELLIOTT, S., HUGHES, A., TAIT, A., PAGE, M., ROSSER, B., MCIVOR, I., DOUGLAS, G. & JONES, H. 2012. Impacts of climate change on erosion and erosion control methods - A critical review. MPI Technical Paper No: 2012/45, 216pp.
- BEAVAN, R. J. & LITCHFIELD, N. J. 2012. Vertical land movement around the New Zealand coastline: implications for sea-level rise. GNS Science report, retrieved from [www.kapiticoast.govt.nz/contentassets/a933446e8c094de8a946d20b9f36a1de/vertical-land-movement-around-the-nz-coastline.pdf](http://www.kapiticoast.govt.nz/contentassets/a933446e8c094de8a946d20b9f36a1de/vertical-land-movement-around-the-nz-coastline.pdf).
- BELL, S. S., CHAND, S. S., TORY, K. J., DOWDY, A. J., TURVILLE, C. & YE, H. 2019. Projections of southern hemisphere tropical cyclone track density using CMIP5 models. *Climate Dynamics*, 52, 6065-6079, doi:10.1007/S00382-018-4497-4.
- BENDER, F. A.-M., RAMANATHAN, V. & TSELIODIS, G. 2012. Changes in extratropical storm track cloudiness 1983-2008: observational support for a poleward shift. *Climate Dynamics*, 38, 2037-2054, doi:10.1007/s00382-011-1065-6.
- CAREY-SMITH, T., HENDERSON, R. & SINGH, S. 2018. High Intensity Rainfall Design System Version 4, NIWA Client Report 2018022CH.
- CASTINEL, A., FORREST, B. & HOPKINS, G. 2014. Review of disease risks for New Zealand shellfish aquaculture: perspectives for management. Prepared for Ministry of Business, Innovation and Employment. Cawthron Institute Report No. 2297, 31p.
- CHANG, E. K. M., GUO, Y. & XIA, X. 2012. CMIP5 multimodel ensemble projection of storm track change under global warming. *Journal of Geophysical Research: Atmospheres*, 117.
- CHAPPELL, P. R. 2013. The climate and weather of Bay of Plenty. 3rd edition. NIWA Science and Technology Series, Number 62. 38 p. Accessed at: <https://www.niwa.co.nz/our-science/climate/publications/regional-climatologies/bay-of-plenty>.
- CHURCH, J. A., CLARK, P. U., CAZENAVE, A., GREGORY, J. M., JEVREJEVA, S., LEVERMANN, A., MERRIFIELD, M. A., MILNE, G. A., NEREM, R. S., NUNN, P. D., PAYNE, A. J., PFEFFER, W. T., STAMMER, D. & UNNIKRIISHNAN, A. S. 2013a. Sea-level rise by 2100. *Science*, 342, 1445.
- CHURCH, J. A., CLARK, P. U., CAZENAVE, A., GREGORY, J. M., JEVREJEVA, S., LEVERMANN, A., MERRIFIELD, M. A., MILNE, G. A., NEREM, R. S., NUNN, P. D., PAYNE, A. J., PFEFFER, W. T., STAMMER, D. & UNNIKRIISHNAN, A. S. 2013b. Sea Level Change. In: STOCKER, T. F., QIN, D., PLATTNER, G.-K., TIGNOR, M., ALLEN, S., BOSCHUNG, J., NAUELS, A., XIA, Y., BEX, V. & MIDGLEY, P. M. (eds.) *Climate Change 2013: The Physical Science Basis. Contribution of Working Group I to the Fifth Assessment Report of the Intergovernmental Panel on Climate Change*. Cambridge, United Kingdom and New York, NY, USA: Cambridge University Press.
- CHURCH, J. A. & WHITE, N. J. 2011. Sea-level rise from the late 19th to the early 21st century. *Surveys in Geophysics*, 32, 585-602.
- CLARK, A., NOTTAGE, R., WILCOCKS, L., LEE, J. M., BURKE, C., KALAUGHER, E., ROCHE, J., BEUKES, P., LIEFFERING, M., NEWTON, P. C. D., LI, F. Y., VIBART, R., TEIXEIRA, E. I., BROWN, H. E., FLETCHER, A. L., HERNANDEZ-RAMIREZ, G., SOLTANI, A., VILJANEN-ROLLINSON, S., HORROCKS, A., JOHNSTONE, P., CLOTHIER, B., HALL, A., GREEN, S., DUNNINGHAM, A., KIRSCHBAUM, M., MEASON, D., PAYN, T., COLLINS, D., WOODS, R., ROUSE, H. L., DUNCAN, M., SNELDER, T. & COWIE, B. 2012. *Impacts of climate change on land-based sectors and adaptation options. Technical report to the Sustainable Land Management and Climate Change Adaptation Technical Working Group*, Wellington, Ministry for Primary Industries.
- CLARK, P. U., SHANKUN, J. D., MARCOTT, S. A., MIX, A. C., EBY, M., KULP, S., LEVERMANN, A., MILNE, G. A., PFISTER, P. L., SANTER, B. D., SCHRAG, D. P., SOLOMON, S., STOCKER, T. F., STRAUSS, B.

- H., WEAVER, A. J., WINKELMANN, R., ARCHER, D., BARD, E., GOLDNER, A., LAMBECK, K., PIERREHUMBERT, R. T. & PLATTNER, G.-K. 2016. Consequences of twenty-first-century policy for multi-millennial climate and sea-level change. *Nature Climate Change*, 6, 360-369.
- COAKLEY, S. M., SCHERM, H. & CHAKRABORTY, S. 1999. Climate change and plant disease management. *Annual Review of Phytopathology*, 37, 399-426.
- COLLINS, D. & ZAMMIT, C. 2016. Climate change impacts on agricultural water resources and flooding. NIWA Client Report for the Ministry of Primary Industries, 2016144CH, 70p.
- CRADOCK-HENRY, N. A. 2017. New Zealand kiwifruit growers' vulnerability to climate and other stressors. *Regional Environmental Change*, 17, 245-259.
- DEAN, S., ROSIER, S., CAREY-SMITH, T. & STOTT, P. A. 2013. The role of climate change in the two-day extreme rainfall in Golden Bay, New Zealand, December 2011. *Bulletin of the American Meteorological Society*, 94, 561-563.
- DECONTO, R. M. & POLLARD, D. 2016. Contribution of Antarctica to past and future sea-level rise. *Nature*, 531, 591-597.
- DERRAIK, J. G. & SLANEY, D. 2015. Notes on Zika virus – an emerging pathogen now present in the South Pacific. *Australian and New Zealand Journal of Public Health*, 39, 5-7.
- DOWDY, A. J., MILLS, G. A., TIMBAL, B. & WANG, Y. 2013. Changes in the risk of extra-tropical cyclones in eastern Australia. *Journal of Climate*, 26, 1403-1417.
- EICHLER, T. P., GAGGINI, N. & PAN, Z. 2013. Impacts of global warming on Northern Hemisphere winter storm tracks in the CMIP5 model suite. *Journal of Geophysical Research Atmospheres*, 118, doi:10.1002/jgrd.50286.
- FISCHER, E. M. & KNUTTI, R. 2016. Observed heavy precipitation increase confirms theory and early models. *Nature Clim. Change*, 6, 986-911, doi:10.1038/nclimate3110.
- GIRONA, J., MATA, M., DEL CAMPO, J., ARBONES, A., BARTA, R. & MARSAL, J. 2006. The use of midday leaf water potential for scheduling deficit irrigation in vineyards. *Irrigation Science*, 24, 115-127.
- GOLLEDGE, N. R., KOWALEWSKI, D. E., NAISH, T. R., LEVY, R. H., FOGWILL, C. J. & GASSON, E. G. W. 2015. The multi-millennial Antarctic commitment to future sea-level rise. *Nature*, 526, 421-425.
- GOODHUE, N. G., ROUSE, H. L., RAMSAY, D., BELL, R. G., HUME, R. M. & HICKS, D. M. 2012. Coastal adaptation to climate change: mapping a New Zealand coastal sensitivity index. A report prepared as part of the Coastal Adaptation to Climate Change Project under contract (CO1XO802) to MBIE, NIWA, Hamilton, New Zealand. 43p.
- HANNAH, J. & BELL, R. G. 2012. Regional Sea Level Trends in New Zealand. *Journal of Geophysical Research: Oceans*, 117, 1-7.
- HANSEN, J., SATO, M., HEARTY, P. & ET AL. 2016. Ice melt, sea level rise and superstorms: evidence from paleoclimate data, climate modelling, and modern observations that 2C global warming could be dangerous. *Atmospheric Chemistry and Physics*, 16, 3761-3812.
- HOULIE, N. & STERN, T. A. 2017. Vertical tectonics at an active continental margin. *Earth and Planetary Science Letters*, 457, 292-301.
- IPCC (ed.) 2013. *Climate Change 2013: The Physical Science Basis. Contribution of Working Group I to the Fifth Assessment Report of the Intergovernmental Panel on Climate Change*, Cambridge, United Kingdom and New York, NY, USA: Cambridge University Press.
- IPCC (ed.) 2014a. *Climate Change 2014: Impacts, Adaptation, and Vulnerability. Part A: Global and Sectoral Aspects. Contribution of Working Group II to the Fifth Assessment Report of the Intergovernmental Panel on Climate Change*, Cambridge, United Kingdom and New York, USA: Cambridge University Press.
- IPCC (ed.) 2014b. *Climate Change 2014: Impacts, Adaptation, and Vulnerability. Part B: Regional Aspects. Contribution of Working Group II to the Fifth Assessment Report of the Intergovernmental Panel on Climate Change*, Cambridge, United Kingdom and New York, USA: Cambridge University Press.

- IPCC 2014c. Climate change 2014: Mitigation of climate change. Contribution of Working Group III to the Fifth Assessment Report of the Intergovernmental Panel on Climate Change. *In*: EDENHOFER, O., PICHES-MADRUGA, R., SOKONA, Y., FARAHANI, E., KADNER, S., SEYBOTH, K., ADLER, A., BAUM, I., BRUNNER, S., EICKEMEIER, P., KRIEMANN, B., SAVOLAINEN, J., SCHLÖMER, S., VON STECHOW, C., ZWICKEL, T. & MINX, J. C. (eds.). Cambridge University Press.
- IPCC 2018. Global warming of 1.5C: An IPCC Special Report on the impacts of global warming of 1.5C above pre-industrial levels and related global greenhouse gas emission pathways, in the context of strengthening the global response to the threat of climate change, sustainable development, and efforts to eradicate poverty, Accessed on 8/10/2018 from <http://ipcc.ch>.
- KEAN, J. M., BROCKERHOFF, E. G., FOWLER, S. V., GERARD, P. J., LOGAN, D. P., MULLAN, A. B., SOOD, A., TOMPKINS, D. M. & WARD, D. F. 2015. Effects of climate change on current and potential biosecurity pests and diseases in New Zealand. Prepared for Ministry for Primary Industries, MPI Technical Paper No: 2015/25. 100p.
- KOPP, R. E., HORTON, R. M., C.M., L., MITROVICA, J. X., OPPENHEIMER, M., RASUMUSSEN, D. J., STRAUSS, B. H. & TEBALDI, C. 2014. Probabilistic 21st and 22nd century sea-level projections at a global network of tide-gauge sites. *Earth's Future*, 2, 383-406.
- KOPP, R. E., KEMP, A. C., BITTERMANN, K., HORTON, B. P., DONNELLY, J. P., GEHRELS, W. R., HAY, C. C., MITROVICA, J. X., MORROW, E. D. & RAHMSTOR, S. 2016. Temperature-driven global sea-level variability in the Common Era. *Proceedings of the National Academy of Sciences*, 113, E1434-E1441.
- LAW, C. S., RICKARD, G. J., MIKALOFF-FLETCHER, S. E., PINKERTON, M. H., BEHRENS, E., CHISWELL, S. M. & CURRIE, K. 2018. Climate change projections for the surface ocean around New Zealand. *New Zealand Journal of Marine and Freshwater Research*, 52, 309-335.
- LEAKEY, A. D. B., AINSWORTH, E. A., BERNACCHI, C. J., ROGERS, A., LONG, S. P. & ORT, D. R. 2009. Elevated CO<sub>2</sub> effects on plant carbon, nitrogen, and water relations: six important lessons from FACE. *Journal of Experimental Botany*, 60, 2859-2876.
- LORREY, A. M., GRIFFITHS, G. M., FAUCHEREAU, N., DIAMOND, H. J., CHAPPELL, P. R. & RENWICK, J. A. 2014. An ex-tropical cyclone climatology for Auckland, New Zealand. *International Journal of Climatology*, 34, 1157-1168.
- MCGLONE, M. & WALKER, S. 2011. Potential effects of climate change on New Zealand's terrestrial biodiversity and policy recommendations for mitigation, adaptation and research. *Science for Conservation*, 312, 1-80.
- MCGLONE, M., WALKER, S., HAY, R. & CHRISTIE, J. E. 2010. Climate change, natural systems and their conservation in New Zealand. *In*: NOTTAGE, R., WRATT, D., BORNMAN, J. F. & JONES, K. (eds.) *Climate change adaptation in New Zealand: future scenarios and some sectoral perspectives*. Wellington: New Zealand Climate Change Centre.
- MENGEL, M., LEVERMANN, A., FRIELER, K., ROBINSON, A., MARZEION, B. & WINKELMANN, R. 2016. Future sea level rise constrained by observations and long term commitment. *Proceedings of the National Academy of Sciences*, 113, 2597-2602.
- MILLER, S. A., SMITH, G. S., BOLDINGH, H. L. & JOHANSSON, A. 1998. Effects of water stress on fruit quality attributes of kiwifruit. *Annals of Botany*, 81, 73-81.
- MINISTRY FOR THE ENVIRONMENT 2008. Climate Change Effects and Impacts Assessment. A Guidance Manual for Local Government in New Zealand. *In*: MULLAN, B., WRATT, D., DEAN, S., HOLLIS, M., ALLAN, S., WILLIAMS, T., KENNY, G. & MFE (eds.). Wellington: Ministry for the Environment.
- MINISTRY FOR THE ENVIRONMENT 2017. Coastal hazards and climate change: Guidance for local government. Lead authors: Bell, R.; Lawrence, J.; Allan, S.; Blackett, P.; Stephens, S. Ministry for the Environment Publication ME-1292. Accessed at: <http://www.mfe.govt.nz/publications/climate-change/preparing-coastal-change-summary-of-coastal-hazards-and-climate-change>.

- MINISTRY FOR THE ENVIRONMENT 2018. Climate change projections for New Zealand: atmospheric projections based on simulations undertaken for the IPCC 5th Assessment, 2nd edition. Accessed at: <https://www.mfe.govt.nz/node/21990>.
- MULLAN, A. B., PORTEOUS, A., WRATT, D. & HOLLIS, M. 2005. Changes in drought risk with climate change. NIWA report WLG2005-23 for Ministry for the Environment and Ministry of Agriculture and Fisheries, Wellington.
- OFFICE OF THE PRIME MINISTER'S CHIEF SCIENCE ADVISOR 2017. New Zealand's fresh waters: Values, state, trends and human impacts. Wellington: Office of the Prime Minister's Chief Science Advisor. Retrieved from: <http://www.pmcsa.org.nz/wp-content/uploads/PMCSA-Freshwater-Report.pdf>.
- PEARCE, H. G., KERR, J., CLARK, A., MULLAN, A. B., ACKERLEY, D., CAREY-SMITH, T. & YANG, E. 2011. Improved estimates of the effect of climate change on NZ fire danger, Prepared for Ministry of Agriculture and Fisheries by Scion and NIWA, Scion Report No. 18087. 83p.
- REEVE, G., STEPHENS, S. & WADSWH, S. 2019. Tauranga Harbour inundation modelling. NIWA Client Report prepared for Bay of Plenty Regional Council 2018269HN, 127p.
- REISINGER, A., KITCHING, R. L., CHIEW, F., HUGHES, L., NEWTON, P. C. D., SCHUSTER, S. S., TAIT, A. & WHETTON, P. 2014. Australasia. In: BARROS, V. R., FIELD, C. B., DOKKEN, D. J., MASTRANDREA, M. D., MACH, K. J., BILIR, T. E., CHATTERJEE, M., EBI, K. L., ESTRADA, Y. O., GENOVA, R. C., GIRMA, B., KISSEL, E. S., LEVY, A. N., MACCRACKEN, S., MASTRANDREA, P. R. & WHITE, L. L. (eds.) *Climate Change 2014: Impacts, Adaptation, and Vulnerability. Part B: Regional Aspects. Contribution of Working Group II to the Fifth Assessment Report of the Intergovernmental Panel on Climate Change*. Cambridge, UK, and New York, NY, USA: Cambridge University Press.
- RENWICK, J. A. & THOMPSON, D. 2006. The Southern Annular Mode and New Zealand climate. *Water & Atmosphere*, 14, 24-25.
- REVELL, C. G. & WARD, G. F. A. 1982. Tropical Storm 'Bernie', 1-14 April 1982. *Weather and Climate*, 2, 31-32.
- REVELL, M. J. & GORMAN, R. M. 2003. The "Wahine storm": Evaluation of a numerical forecast of a severe wind and wave event for the New Zealand coast. *New Zealand Journal of Marine and Freshwater Research*, 32, 251-266.
- RITZ, C., EDWARDS, T. L., DURAND, G., PAYNE, A. J., PEYAUD, V. & HINDMARSH, R. C. A. 2015. Potential sea-level rise from Antarctic ice sheet instability constrained by observations. *Nature*, 528, 115-118.
- ROYAL SOCIETY OF NEW ZEALAND 2016. Climate change implications for New Zealand, 72 pp. Available from: <http://www.royalsociety.org.nz/expert-advice/papers/yr2016/climate-change-implications-for-new-zealand/>.
- ROYAL SOCIETY OF NEW ZEALAND 2017. Human health impacts of climate change for New Zealand: Evidence summary. 18 pp. Available from: <https://royalsociety.org.nz/assets/documents/Report-Human-Health-Impacts-of-Climate-Change-for-New-Zealand-Oct-2017.pdf>.
- SALINGER, M. J. & MULLAN, A. B. 1999. New Zealand climate: temperature and precipitation variations and their links with atmospheric circulation 1930–1994. *International Journal of Climatology*, 19, 1049-1071.
- SALINGER, M. J., RENWICK, J., BEHRENS, E., MULLAN, A. B., DIAMOND, H. J., SIRGUEY, P., SMITH, R. O., TROUGHT, M. C. T., ALEXANDER, L., CULLEN, N., FITZHARRIS, B. B., HEPBURN, C. D., PARKER, A. K. & SUTTON, P. J. H. 2019. The unprecedented coupled ocean-atmosphere summer heatwave in the New Zealand region 2017/18: drivers, mechanisms and impacts. *Environmental Research Letters*, 14.
- SALINGER, M. J., RENWICK, J. A. & MULLAN, A. B. 2001. Interdecadal Pacific Oscillation and South Pacific climate. *International Journal of Climatology*, 21, 1705-1721.

- SHEPPARD, C. S. 2013. Potential spread of recently naturalised plants in New Zealand under climate change. *Climatic Change*, 117, 919-931.
- SHEPPARD, C. S., BURNS, B. R. & STANLEY, M. C. 2016. Future-proofing weed management for the effects of climate change: is New Zealand underestimating the risk of increased plant invasions? *New Zealand Journal of Ecology*, 40, 398-405.
- SIMMONS, A. J., WILLETT, K. M., JONES, P. D., THORNE, P. W. & DEE, D. P. 2010. Low-frequency variations in surface atmospheric humidity, temperature, and precipitation: Inferences from reanalyses and monthly gridded observational data sets. *Journal of Geophysical Research: Atmospheres*, 115.
- SLANGEN, A. B. A., CHURCH, J. A., AGOSTA, C., FETTWEIS, X., MARZEION, B. & RICHTER, K. 2016. Anthropogenic forcing dominates global mean sea-level rise since 1970. *Nature Climate Change*, 6, 701-705.
- STEPHENS, S. 2017. Tauranga Harbour extreme sea level analysis. NIWA Client Report prepared for Bay of Plenty Regional Council 2017035HN, 50p.
- STEPHENS, S. 2019. Estimation of 2, 10 and 20-year average recurrence interval storm-tide + wave-setup elevations within Tauranga Harbour, NIWA Letter provided to Bay of Plenty Regional Council, 13p.
- STEPHENS, S., ALLIS, M., GORMAN, R. G., ROBINSON, B. & GOODHUE, N. G. 2018. Storm-tide and wave hazards in the Bay of Plenty - revised and updated September 2018. NIWA Client Report prepared for Bay of Plenty Regional Council 2018136HN, 125p.
- STEPHENS, S., BELL, R. G. & LAWRENCE, J. 2017. Applying principles of uncertainty within coastal hazard assessments to better support coastal adaptation. *Journal of Marine Science and Engineering*, 5, 40, <http://www.mdpi.com/2077-1312/5/3/40>.
- STEPHENS, S. & WADSWHA, S. 2017. Coastal inundation mapping at Te Tumu, Bay of Plenty. NIWA Client Report prepared for Tauranga City Council 2017275HN, 16p.
- STRAUSS, B. H., KULP, S. & LEVERMANN, A. 2015. Carbon choices determine US cities committed to futures below sea level. *Proceedings of the National Academy of Sciences*, 112, 13508-13513.
- SWEET, W. V. & PARK, J. 2014. From the extreme to the mean: Acceleration and tipping points of coastal inundation from sea level rise. *Earths Future*, 2, 579-600.
- TAIT, A., HENDERSON, R., TURNER, R. & ZHENG, X. G. 2006. Thin plate smoothing spline interpolation of daily rainfall for New Zealand using a climatological rainfall surface. *International Journal of Climatology*, 26, 2097-2115.
- TAIT, A., PAUL, V., SOOD, A. & MOWAT, A. 2017. Potential impact of climate change on Hayward kiwifruit production viability in New Zealand. *New Zealand Journal of Crop and Horticultural Science*, <https://doi.org/10.1080/01140671.2017.1368672>.
- TAYLOR, K. E., STOUFFER, R. J. & MEEHL, G. A. 2012. An Overview of CMIP5 and the Experiment Design. *Bulletin of the American Meteorological Society*, 93, 485-498.
- TRENBERTH, K. E. 1999. Conceptual framework for changes of extremes of the hydrological cycle with climate change. *Climatic Change*, 42, 327-339, doi:10.1023/A:1005488920935.
- WANG, X., SWAIL, V. & ZWIERS, F. 2006. Climatology and changes in extratropical cyclone activity: Comparison of ERA-40 with NCEP-NCAR reanalysis for 1958-2001. *Journal of Climate*, 19, 3145-3166.
- WATT, M. S., KIRSCHBAUM, M., MOORE, J. R., PEARCE, H. G., BULMAN, L. S., BROCKERHOFF, E. G. & MELIA, N. 2018. Assessment of multiple climate change effects on plantation forests in New Zealand. *Forestry*, 92.
- WILLEIT, M., GANOPOLSKI, A., CALOV, R. & BROVKIN, V. 2019. Mid-Pleistocene transition in glacial cycles explained by declining CO<sub>2</sub> and regolith removal. *Science Advances*, 5, eaav7337.
- WILLIS, T. J., HANDLEY, S. J., CHANG, F. H., LAW, C. S., MORRISEY, D. J., MULLAN, A. B., PINKERTON, M., RODGERS, K. L., SUTTON, P. J. H. & TAIT, A. 2007. Climate change and the New Zealand



Marine Environment. NIWA Client Report NEL2007-025 for the Department of Conservation.  
76 pp.

YIN, J. H. 2005. A consistent poleward shift of the storm tracks in simulations of 21st century climate.  
*Geophysical Research Letters*, 32, doi:10.1029.2005GL023684.